Northwest Geology

The Journal of The Tobacco Root Geological Society

Volume 51, July 2022

47th Annual Field Conference

Geology of Wenatchee, Washington

July 29–31, 2022

Published by The Tobacco Root Geological Society, Inc.

P.O. Box 118
Butte, Montana 59703

http://trgs.org

Edited by: Kelsay Stanton and Katie McDonald

Cover photo: Eocene igneous rocks make up the pinnacles of Saddle Rock, a regionally well-known feature near Wenatchee, WA. Photo by Ben Stanton.

NORTHWEST GEOLOGY

The Journal of The Tobacco Root Geological Society

Volume 51, July 2022

47th Annual Field Conference

Geology of Wenatchee, Washington

July 29–31, 2022

Published by The Tobacco Root Geological Society, Inc.

P.O. Box 118
Butte, Montana 59703

http://trgs.org

Edited by: Kelsay Stanton and Katie McDonald

The Tobacco Root Geological Society, Inc.

P.O. Box 118
Butte, Montana 59703

2022 Conference Organizers:

Kelsay Stanton, Washington Geological Survey

Editors: Kelsay Stanton, Washington Geological Survey, and Katie McDonald, Montana Bureau of Mines and Geology

Layout and Editing: Susan Barth (MBMG)

Printed by Insty-Prints, Butte, Montana

ISSN: 0096-7769

http://trgs.org

DEDICATION

Rowland W. Tabor
b. 1932; d. 2022, Portola Valley, CA

Rowland Tabor was raised in Denver, went to Stanford to study engineering, and discovered geology. He received his PhD from the University of Washington. He was then hired by the USGS, where he worked for more than 60 years, including 25 productive years after nominal retirement. He loved the mountains. As a teenager he skied and climbed. At Stanford he was active in the Alpine Club. While at the University of Washington, he became associated with The Mountaineers, and he chose to work almost entirely in mountainous regions.

Rowland helped us learn how the Earth works, with significant technical papers on arc magmatism, the core of the Olympic Mountains as an exposed subduction complex, low-grade metamorphism in the Olympic Mountains, systematics of K-Ar dating, gravitational collapse of mountainous landscapes, the challenges of reactor siting amidst evolving geologic knowledge, and accreted terranes in the North Cascades. He also wrote for the layperson: the geology chapter for the first edition of *Freedom of the Hills* (a mountaineering manual); the delightful *Routes and Rocks: Hiker's Guide to the North Cascades from Glacier Peak to Lake Chelan* (with Dwight Crowder); *Guide to the Geology of Olympic National Park*; and *Geology of the North Cascades: A Mountain Mosaic*.

Rowland taught. Despite his never holding a faculty position, at least seven professional geologists count him as mentor. And he sang: "Mapping faults is not a sin," "My father killed a kangaroo. He gave me the gristly part to chew."

Most of all, Rowland made geologic maps: of the Moon, Kentucky, Nevada, and—especially—the Olympic Mountains and North Cascade Range of northwest Washington. This field conference, situated amidst the Wenatchee (USGS I-1311, 1982) and Chelan (USGS I-1661, 1987) 30' x 60' quadrangles that were comprehensively mapped by Rowland and colleagues at 1:100,000 scale, is a fitting tribute.

Northwest Geology

The Journal of The Tobacco Root Geological Society

Volume 51, July 22

Geology of Wenatchee, Washington

TABLE OF CONTENTS

TRGS CHARTER MEMBERS

Stanley W. Anderson
Clyde Cody
William S. Cordua
Lanny H. Fisk
Richard I. Gibson†
Thomas Hanley
Stephen W. Henderson
Thomas E. Hendrix
Mac R. Hooton
Inda Immega
Steven W. Koehler
Marian Millen Lankston†
Robert W. Lankston†
J. David Lazor
Joe J. Liteheiser, Jr.
Judson Mead*
Marvin R. Miller
Vicki M. Miller*
Allen H. Nelson
Alfred H. Pekarek
Patricia Price*
Donald L. Rasmussen
Raymond M. Rene

TRGS LIFETIME MEMBERS

John Childs
Rob Foster
Joan (Mrs. Jack) Harrison*
Karen Keefer
Layaka Mann
Chris Pool

† = co-founder
* = deceased

TRGS HAMMER AWARD RECIPIENTS

Awarded for distinguished achievement in the study of the geology of the Northern Rocky Mountains

1993: Ed Ruppel*
1994: Dick Berg
2003: Don Winston*
2004: Dean Kleinkopf*
2009: Betty Skipp
2010: Jim Sears
2011: John Childs
2012: J. Michael O'Neill
2013: Paul Karl Link
2014: Reed Lewis
2015: Jeff Lonn
2016: Bruce Cox
2019: Susan Vuke
2021: Katie McDonald

TRGS HONORARY MEMBERS

1980: Charles J. Vitaliano*
2008: Elizabeth Younggren*
(also honorary Board member)
2010: Dick Berg
2010: Bruce Cox
2010: Dean Kleinkopf*
2010: Dave Lageson
2011: Marie Marshall Garsjo
2011: Paul Link
2011: Rob Thomas
2012: Jeff Lonn
2012: Mitch Reynolds
2013: Reed Lewis
2015: Don Winston*
2020: Ted Antonioli, Larry Smith, Mike Stickney

TRGS 2022 SCHOLARSHIP AWARD WINNERS

- Mikelia Heberer (TRGS), University of Utah:
  An Investigation into Ontogenetic Shell Shape and Ornamentation Variation among Juvenile Western Interior Seaway Scaphite Ammonoids in Eastern Montana and Central South Dakota
- Kayla Irizarry (Skipp), Penn State University:
  Did Persistently Low Oxygen Conditions Slow Diversification during the Cambrian?
- Ashlesha Khatiwada (Kleinkopf), University of Montana:
  Analyzing the Multipath of GNSS Time Series to Study Snow Properties
- Jon Lever (Belt Association), Idaho State University:
  Tightening the Belt: New Age and Provenance Constraints on Proterozoic Strata in East-Central Idaho
- Anna Marshall (TRGS), Colorado State University:
  Sources and Functions of Spatial Heterogeneity in Determining Channel Evolution of Large Mountain River
- Carlos Montejo (TRGS), University of Idaho:
  Quantifying Exhumation Related to the Approach of the Yellowstone Hotspot Using Detrital Thermo chronology on mid-Miocene to Present Sediments in the Gallatin Valley, Gallatin County, Montana
- Sarah Morse (Harrison), University of Arkansas:
  Constraining the Regional Impact of the Mesoproterozoic Picuris Orogen Using High Temperature Deformation and Metamorphism in the Wet Mountains, Colorado, USA
- Emma Palko (TRGS), Norther Arizona University:
  High-resolution Lacustrine and Geochronologic Investigation into the Tectonic and Paleogeographic Origins of the Wagon Bed Formation, Central Wyoming
- Sarah Risedorf (Foster), Montana Tech:
  Evaluation of Carbonatite Hosted Rare Earth Elements Deposit in Sheep Creek, Southern Ravalli County, Montana
- Mia Wafer (Skipp), Montana State University:
  Exploring the Relationships between Faulting and Geothermal Systems: Structural Controls on the Norris Hot Spring, Southwest Montana

TRGS thanks Sibanye Stillwater and Wheaton Precious Metals for their generous contributions to our scholarship program.

ABSTRACT

PETROLOGY, GEOCHRONOLOGY, AND CHANGING TECTONIC SETTING OF EOCENE–MIOCENE MAGMATISM NEAR WENATCHEE, CENTRAL CASCADES, WASHINGTON

Jeffrey H. Tepper,[1] Audrey V. White,[1] and Ralph L. Dawes[2]

[1]University of Puget Sound, Tacoma, Washington
[2]Wenatchee Valley College, Wenatchee, Washington

Lava flows and shallow intrusions on the eastern flanks of the central Washington Cascades document a >40-million-year history of discontinuous and compositionally diverse igneous activity. These rocks, which range in age from 52 to 11 Ma, are of particular interest for two reasons. First, they represent magmatism in five distinct tectonic settings: early Tertiary subduction, slab rollback, slab breakoff, Cascadia subduction, and a hot spot. Second, the subduction-related rocks occur farther inland than most other exposures of Cascade arc rocks (fig. 1), and thus provide an opportunity to examine what causes variations in arc width and to look for cross-arc compositional trends such as have been recognized in other arcs. We present new U-Pb dates, whole-rock chemical analyses, and Sr-Nd isotopic data for nine map units (fig. 1); these results are organized on the basis of age and tectonic setting. Because no new data are presented on rocks associated with slab breakoff (Kant and others, 2018) or with hot spot activity (Columbia River Basalts), units representing these settings are not discussed here.

CRETACEOUS–EARLY TERTIARY SUBDUCTION

Plutonic and volcanic rocks related to subduction of the Farallon Plate are widespread across northern Washington, spanning from the North Cascades eastward into Idaho. Among units that range in age from ~113 to 53 Ma, there are no spatiotemporal patterns. Based on a U-Pb age of 52.4 Ma, the Andesite of Peoh Point (Tabor and others, 1982) is among the youngest units associated with this activity. Chemically this unit is a dacite (67 wt.% SiO_2) with some adakite affinities (Sr/Y = 25, Yb = 1.2 ppm).

SLAB BREAKOFF AND ROLLBACK MAGMATISM

Accretion of the Siletzia terrane (Wells and others, 2014) led to breakoff and rollback of the Farallon slab (Kant and others, 2018). Magmatism associated with rollback began at 52 Ma in Idaho and migrated southwestward across northeastern Washington over the next ~8 Ma (Tepper, 2016). Based on their age and location, we interpret the 44 Ma Wenatchee Pinnacles

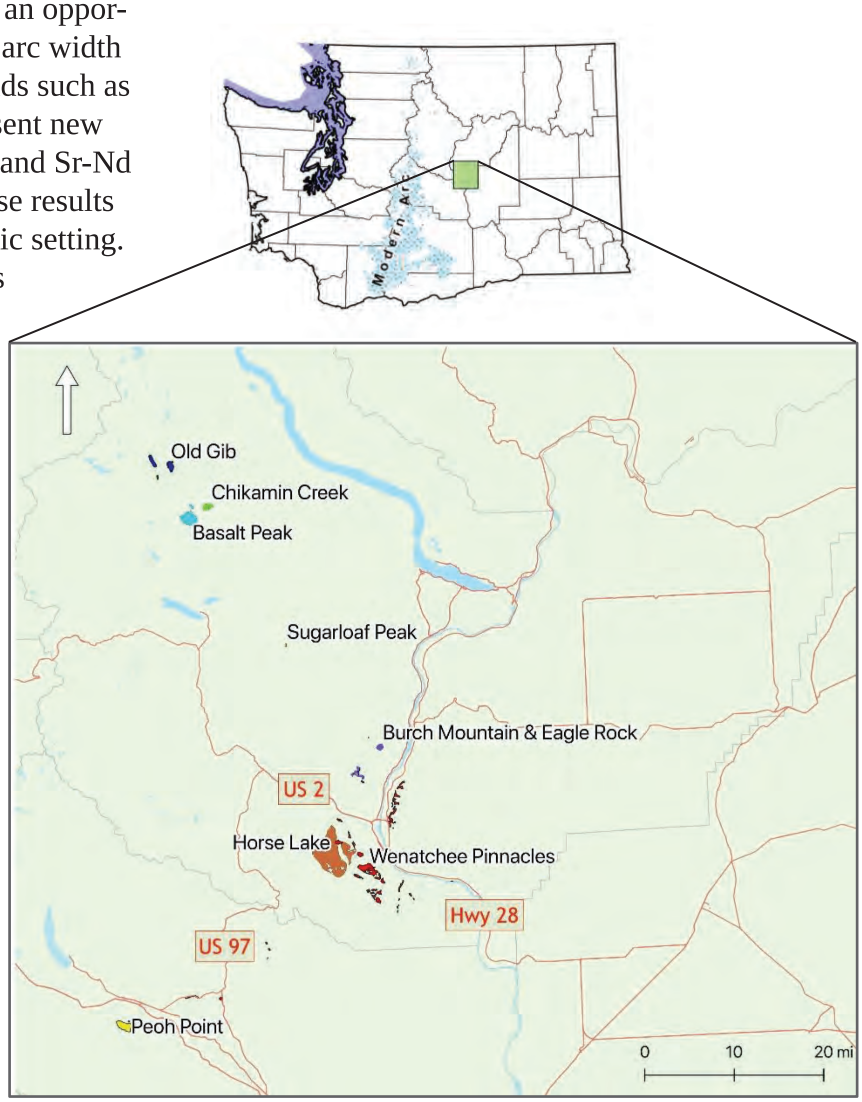

Figure 1. Locations of the nine units included in this study and their position to the east of the main Cascade arc.

(Gresens, 1983; Dawes and Tepper, this volume) as the youngest expression of this rollback event. They are a northwest-trending ~7-km-long belt of hypabyssal intrusions and dikes, which from south to north are Rooster Comb (RC), Wenatchee Dome (WD), Saddle Rock (SR), Old Butte, and Castle Rock (CR). U-Pb ages of WD, SR, and CR cluster between 44.45 and 44.96 Ma (Gilmour, 2012; this study), suggesting all Pinnacles bodies are part of a single episode. SR and CR are dacites, accompanied by minor basaltic dikes, whereas WD and RC are rhyolites. Trace element data indicate the associated basalts were not parental to the felsic rocks, but modeling indicates the dacites and rhyolites can be related by fractional crystallization (plag + amph). Isotopic data ($^{87}Sr/^{86}Sr_i$ = 0.7049, e_{Nd} = +4.29, T_{DM} = 590 Ma) and trace element characteristics (Ta-Nb depletions, $Dy/Yb_n < 1$) suggest the Pinnacles originated by partial melting of an amphibole-bearing lower crustal source with arc affinities that probably formed by underplating during Paleozoic or Mesozoic subduction. Mafic dikes associated with the Pinnacles may be representative of basalts that drove the Eocene melting.

CASCADIA SUBDUCTION

Following breakoff of the Farallon slab, subduction resumed by ~45 Ma and resulted in establishment of the modern north–south-trending Cascade arc. Five units included in this study that are related to Cascadia subduction include the rhyolite of Old Gib (Cater and Crowder, 1967; 27.5 Ma U-Pb; this study), the porphyritic dacite of Basalt Peak (Tabor and others, 1987; 27.8 Ma U-Pb; Gilmour, 2012), the pyroxene-bearing andesite of Sugarloaf Peak (Tabor and others, 1987; 36.85 Ma U-Pb; Gilmour, 2012), rhyolite from Chikamin Creek (23–28 Ma FT; Tabor and others, 1987), and the Horse Lake Complex (25.2 Ma FT; Gresens, 1983). Whole-rock analyses (12) of these units range from 59 to 72 wt.% SiO_2 and on variation diagrams overlap with data from elsewhere in the Cascade arc. Comparisons with Cascade lavas farther west but at similar latitude (e.g., Allen and others, 2017; Dragovich and others, 2011, 2012) reveal no cross-arc geochemical trends. There is also no indication that the emplacement of these units to the east of the main arc is the result of an unusual event (e.g., change in slab dip). Along-strike variations in width of the Cascade arc may be more related to erosion and burial by younger rocks than to tectonic processes.

MIOCENE ADAKITES

The youngest igneous rocks in the Wenatchee area are a cluster of small stocks at Burch Mountain and adjacent Eagle Rock that have been K-Ar dated at 11–10 Ma (Tabor and others, 1987). These pyroxene-hornblende andesites are low-silica adakites (LSA), characterized by high Sr (1,430–1,730 ppm), Sr/Y (131–212), La/Yb (16–24), and Cr (119–152 ppm) and are notable in having the least radiogenic Sr and Nd isotopic compositions measured to date in the Cascade arc ($^{87}Sr/^{86}Sr_i$ = 0.70229 – 0.70246, e_{Nd} = +9.2 to +10.3). LSA form by interaction between slab melts and peridotite in the mantle wedge (Martin and others, 2005), but the initial slab melting event can significantly predate the subsequent wedge melting event that produces the LSA. A model for generation of the Burch Mountain LSA must account for their highly depleted Sr-Nd isotopic compositions and rear-arc location. We suggest they formed by decompression melting of mantle, previously infiltrated by slab melts, that was entrained in the upwelling, rear arc portion of wedge flow.

REFERENCES CITED

Allen, M.D., Mavor, S.P., Tepper, J.H., Nesbitt, E.A., Mahan, S.A., Cakir, R., Stoker, B.A., and Anderson, M.L., 2017, Geologic map of the Maltby 7.5-minute quadrangle, Snohomish and King Counties, Washington: Washington Geological Survey Map Series 2017-02, 1 sheet, scale 1:24,000.

Dragovich, J.D., Anderson, M.L., Mahan, S.A., Koger, C.J., Saltonstall, J.H., MacDonald, J.H. Jr., Wessel, G.R., Stoker, B.A., Bethel, J.P., Labadie, J.E., Cakir, R., Bowman, J.D., and DuFrane, S.A., 2011, Geologic map of the Monroe 7.5-minute quadrangle, King and Snohomish Counties, Washington Open File Report 2011-1, scale:1:24,000.

Dragovich, J.D., Anderson, M.L., Mahan, S.A.; MacDonald, J.H. Jr., McCabe, C.P., Cakir, R., Stoker, B.A., Villeneuve, N.M., Smith, D.T., and Bethel, J.P., 2012, Geologic map of the Lake Joy 7.5-minute quadrangle, King County, Washington Map Series 2012-01, scale:1:24,000.

Cater, F.W., and Crowder, D.F., 1967, Geologic map of the Holden quadrangle, Snohomish and Chelan counties, Washington: U.S. Geological Survey Map GQ-646, 1:62500.

Gilmour, L.A., 2012, U/Pb ages of Eocene and younger rocks on the eastern flank of the central Cascade Range, Washington, USA: unpublished M.S. thesis, University of Washington, 48 p.

Gresens, R.L., 1983, Geology of the Wenatchee and Monitor quadrangles, Chelan and Douglas counties, Washington: Washington Department of Natural Resources Bulletin 75, State of Washington Department of Natural Resources, Division of Geology and Earth Resources, Olympia, WA.

Kant, L.B., Tepper, J.H., Eddy, M.P., and Nelson, B.K., 2018, Eocene basalt of Summit Creek: Slab breakoff magmatism in the Central Washington Cascades, USA: Lithosphere v. 10, no. 6, p. 792–805.

Martin, H., Smithies, R.H., Rapp, R., Moyen, J.F., and Champion, D., 2005, An overview of adakite, tonalite–trondhjemite–granodiorite (TTG) and sanukitoid: Relationships and some implications for crustal evolution: Lithos, v. 79, p. 1–24.

Tabor, R.W., Waitt, R.W. Jr., Frizzell, V.A. Jr., Swanson, D.A., Byerly, G.R., and Bentley, R.D., 1982, Geologic map of the Wenatchee 1:100,000 quadrangle, central Washington: U.S. Geological Survey Miscellaneous Investigations Series Map I-1311, 1:100,000.

Tabor, R.W., Frizzell, V.A. Jr, Whetten, J.T., Waitt, R.B., Swanson, D.A., Byerly, G.R., Booth, D.B., Hetherington, M.J., and Zartman, R.E., 1987, Geologic map of the Chelan 30-minute by 60-minute quadrangle, Washington: U.S. Geological Survey Miscellaneous Investigations Series Map I-1661, 1:100,000.

Tepper, J.H., 2016, Eocene breakoff and rollback of the Farallon slab—An explanation for the “Challis Event”?: Geological Society of America Abstracts with Programs, v. 48, no. 4.

Wells, R., Bukry, D., Friedman, R.F., Pyle, D., Duncan, R., Haeussler, P., and Wooden, J., 2014, Geologic history of Siletzia, a large igneous province in the Oregon and Washington Coast Range: Correlation to the geomagnetic polarity time scale and implications for a long-lived Yellowstone hotspot: Geosphere, v. 10, p. 692–719.

PAPER

GEOLOGIC HISTORY, ROCKS, AND DEPOSITS OF THE WENATCHEE AREA, WASHINGTON

Ralph A. Haugerud[1] and Kelsay M. Stanton[2]

[1]U.S. Geological Survey, Seattle, Washington
[2]Washington Geological Survey, Olympia, Washington

INTRODUCTION

The city of Wenatchee is located at the confluence of the Wenatchee and Columbia Rivers. The name is from a Yakama word meaning "river issuing from a canyon" (Hodge, 1910, p. 932). David Thompson of the Northwest Company passed through by canoe in 1811, encountering residents whose descendants include the Wenatchi Band of the Confederated Tribes of the Colville Reservation. First Euro-American settlement was in 1871, the railroad arrived in 1892, and in 1904 the Highline Canal was completed to irrigate orchard land (Arksey, 2008). Salmon were abundant before Euro-American development (e.g., Taylor 2009); their decline was hastened by damming of the Columbia starting in 1930 (Dougherty, 2021). Now, along with tree fruit, significant economic drivers include hydropower and health care (https://www.wenatchee-wa.gov/government/economic-development).

At Wenatchee, older rocks of the North Cascade Range emerge from beneath Miocene flood basalt of the Columbia Plateau farther east (fig. 1). The older rocks are divided by northwest-striking faults into blocks with differing depths of burial, ages of metamorphism, and cooling ages. In the Wenatchee block, Late Cretaceous plutonic and metamorphic rocks are overlain on the south by Paleocene and Eocene continental strata. In the deep-seated Chelan block, metamorphism and ductile deformation extended into Eocene time and Eocene cooling ages are evident. Between the Wenatchee and Chelan blocks lies the Chiwaukum structural low (or Chiwaukum graben, or Chumstick basin), underlain by folded Eocene sandstone and separated from the Chelan and Wenatchee blocks by the Entiat and Leavenworth faults, respectively. The depositional record after eruption of Miocene basalt is sparse. Landforms—and some deposits—speak of uplift, fluvial incision, glaciation, and catastrophic flooding.

Early geologic mapping in and near Wenatchee was varied and focused on specific locations or rock types (e.g., Russell, 1893, 1900; Waters, 1930, 1932; Page, 1939a,b; Willis, 1950). Rowland Tabor and others (1982, 1987) produced comprehensive 1:100,000-scale geologic maps for the Wenatchee and Chelan 30′ x 60′ quadrangles, which include the Wenatchee River Valley, Lake Wenatchee, the southern part of Lake Chelan, Blewitt Pass, Cle Elum, and parts of the Ellensburg area. These maps remain an important resource and stand as a framework for many models of the regional geologic history. This outline draws heavily from these maps and the 1:200,000-scale compilation by Haugerud and Tabor (2009).

Geologic history of the Wenatchee area is conveniently summarized in four chapters: underlying terranes; Late Cretaceous–Paleogene orogeny; Paleocene–Eocene deposition, magmatism, and deformation; and the Cascadia subduction regime. Our intent is to outline geologic history, rocks, and deposits and direct readers to relevant recent literature.

UNDERLYING TERRANES

In the Paleozoic era, the west edge of North America was east of Wenatchee. Wenatchee and environs are underlain by terranes accreted late in the Mesozoic era (Coney and others, 1980; Monger and others, 1982; Brown and Dragovich, 2003). From southwest to northeast, recognized terranes near Wenatchee are the Ingalls, Nason, Swakane, and Chelan Mountains. With the exception of the Ingalls terrane, metamorphism has largely erased the early history of these rocks. McDonald and others (this volume) explore inliers of other Mesozoic terranes southwest of figure 1 that illustrate some of the complexity of the Cascades.

Ingalls terrane consists largely of the Ingalls Tectonic Complex, a disrupted late Jurassic ophiolite (Tabor and others, 1982, 1987; Miller, 1985; Mac-

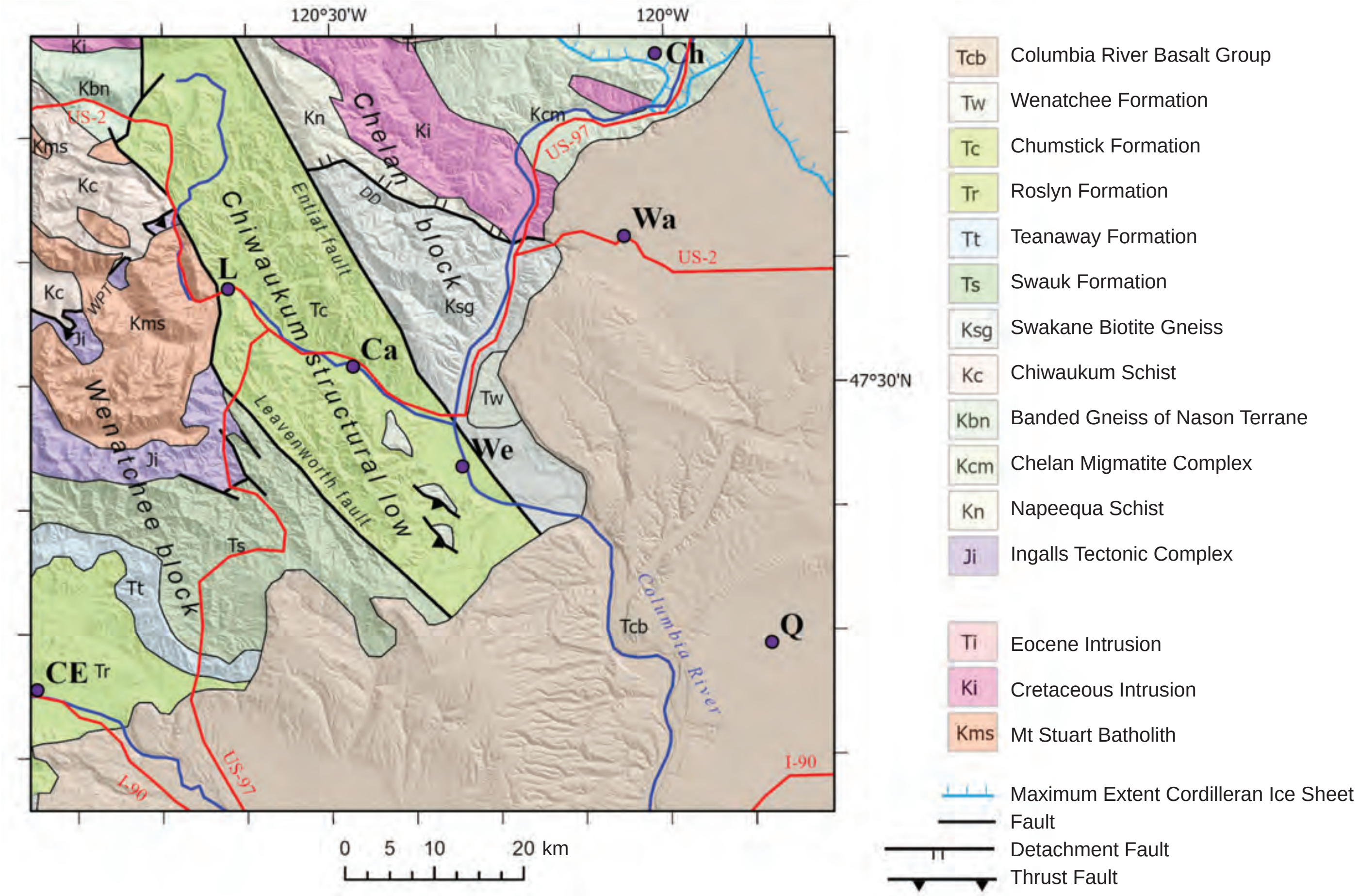

Figure 1. Geologic map of the Wenatchee area. Modified from Haugerud and Tabor (2009) and Washington Geological Survey 1:250,000 digital compilation. Quaternary deposits omitted. Ca, Cashmere; Ch, Chelan; CE, Cle Elum; L, Leavenworth; Q, Quincy; Wa, Waterville; We, Wenatchee; DD, Dinkelman decollement; WPT, Windy Pass thrust. Base image calculated from USGS 1/3 arc-second DEMs.

Donald and others, 2008) that likely formed in a large marginal basin or ocean with little input of arc-derived sediment (Miller, 1985). The Ingalls complex is intricately faulted, with serpentinized ultramafic rock surrounding lenses of basalt, gabbro, and sedimentary rock.

Nason terrane is largely metamorphosed to Chiwaukum Schist, which comprises garnet and staurolite bearing graphite–biotite–quartz schist with minor muscovite gneiss, amphibolite, hornblende schist, calc–silicate schist, and marble (Tabor and others, 1982, 1987). A sedimentary protolith is indicated. Brown and Gehrels (2007) documented a maximum depositional age (MDA) for the Chiwaukum protolith of 125 Ma.

Swakane terrane is composed solely of the Swakane Biotite Gneiss: biotite quartzofeldspathic gneiss with rare layers of hornblende schist, marble, and amphibolite (Tabor and others, 1987). The protolith was likely clastic sediment or silicic volcanic rock (e.g., Waters, 1932; Tabor and others, 1987b). Swakane protolith was long considered to be Precambrian because of ~1.6 Ga upper-intercept U-Pb zircon dates (Mattinson, 1972). However, Matzel and others (2004) obtained U-Pb dates on zircons they thought detrital that indicated an MDA of 73 Ma, younger than metamorphism and intrusion of other rocks in the North Cascades crystalline core. This interpretation has not been universally accepted: Gatewood and Stowell (2012) dated metamorphic recrystallization in the Swakane at 75–63 Ma and concluded that zircon dates younger than ~75 Ma represent metamorphic ages. Sauer and others (2018) analyzed zircons from additional Swakane samples, concluded that zoning patterns and U/Th ratios indicate that the youngest ages are indeed metamorphic, and proposed MDAs of ~93–81 Ma. In any case the Swakane protolith is surprisingly young. Matzel and others (2004) and Sauer and others (2018) noted similarities between Swakane Biotite Gneiss and the Pelona, Orocopia, and Rand Schists of southern California.

Chelan Mountains terrane includes, near Wenatchee, the protolith of the Napeequa Schist. The Napeequa comprises micaceous quartzite, mica schist, garnet–biotite schist, gneissic amphibolite, metagabbro, metadiorite, and metaperidotite (Tabor and others, 1987). Sauer and others (2017) reported Late Triassic protolith ages for Napeequa amphibolite and schist. The assemblage suggests a protolith similar to the Hozomeen Group (Tabor and others, 2003) and the Cache Creek terrane of British Columbia (Monger and others, 1982); all are likely remnants of late Paleozoic–early Mesozoic Pacific Ocean floor.

LATE CRETACEOUS–PALEOGENE OROGENY

Accreted terranes in the core of the North Cascades were buried and metamorphosed during mid- to Late Cretaceous orogeny. General absence of surface-deposited strata of post-Turonian age suggests that this part of the Cordillera was an upland after about 90 Ma. Extensive Late Cretaceous plutons suggest deformation and metamorphism happened within an Andean-style magmatic arc (e.g., Miller and others, 2009), but hypotheses of terrane collision (Monger and others, 1982) and plate-margin transpression (Irving and others, 1985) are also viable. Parts of the North Cascades remained deeply buried and ductilely deforming until Eocene time (Haugerud and others, 1991); thus Tabor and others (2003) and Haugerud and Tabor (2009) considered orogeny to span these periods.

Cretaceous crustal thickening in the North Cascades was a consequence of both thrusting and pluton intrusion. Thrusting is best recorded in less-metamorphosed areas north and northwest of Wenatchee (e.g., Misch, 1966; McGroder, 1991; Haugerud and Tabor, 2009; Brown, 2012). In the southern Wenatchee block, the Windy Pass thrust placed Ingalls terrane over Nason terrane (Miller, 1985; Tabor and others, 1982, 1987). In the southern Chelan block, a major thrust must have slid Swakane terrane beneath Napeequa terrane but has since been excised by slip on the Dinkelman decollement (Paterson and others, 2004). Thickening by intrusion (Brown, 2020) is evident at the margin of the Mount Stuart batholith, where the Chiwaukum Schist shows contact-metamorphic andalusite overprinted by regional kyanite (Evans and Berti, 1986).

Swakane Biotite Gneiss and *Napeequa Schist* both reached peak metamorphic conditions of ~640–750°C and 9–12 kbar (Valley and others, 2003). Matzel and others (2004) suggested peak metamorphism of the Swakane occurred at 68 Ma. High U/Th rims on Napeequa zircons have ages of 130–72 Ma (Paterson, 2014) that may reflect the age of metamorphism.

Chiwaukum Schist reached ~640°C and 6–8 kbar at 91–86 Ma (Stowell and others, 2011; Baker and others, 2019; Duggan and Brown, 1994). Near the northwest corner of figure 1, Chiwaukum Schist grades into banded gneiss of the Nason terrane.

Mount Stuart batholith, composed of granodiorite, tonalite, and lesser diorite and gabbro, underlies Mt Stuart, the second highest nonvolcanic peak in Washington at 2,870 m. U-Pb zircon ages show various parts of the batholith crystallized in the interval 96.2 to 90.7 Ma (Matzel and others, 2006). The batholith was the locale of early paleomagnetic observations of post-mid-Cretaceous northwards translation of the western Cordillera (Beck and Noson, 1972). Housen and others (2003) collected new paleomagnetic data and—after accounting for observed tilting, magnetic mineralogy, and cooling history—again found ~3,000 km of post-90 Ma northwards translation.

Chelan Migmatite Complex of Hopson and Mattinson (1994) is a "huge migmatitic metaplutonic mass, derived from partial melting of tonalitic basement and emplaced at approximately 25–30 km depth" (Hopson and others, 2001). Remelting and emplacement occurred at ~90–117 Ma and cross-cutting relationships suggest multiple intrusions and melt evolution from mafic to felsic, as would be expected with the evolution from a mantle-derived magma source to a felsic crust contribution (Mattinson and others, 2014; Kjelland and others, 2019). See Mattinson and others (this volume) for more discussion on thermobarometry and geochronology.

PALEOCENE–EOCENE DEPOSITION, MAGMATISM, AND DEFORMATION

Widespread early Cenozoic magmatism, basin development, extensional unroofing of mid-crustal rocks, and transcurrent faulting in the northern Cordillera have been hypothesized to record low-angle subduction (Lipman and others, 1972), a transform plate margin (Ewing, 1980) perhaps consequent upon death of the Resurrection plate (Haeussler and others, 2003), passage of a slab window (Thorkelson and Taylor, 1989), gravitational collapse of the late Cretaceous orogen (e.g., Bao and others, 2014), accretion of Siletzia (Eddy and others, 2016), and initiation of the Yellowstone hotspot (Stern and Dumitru, 2019). These hypotheses are not all mutually exclusive.

Swauk Formation is restricted to the Wenatchee block south and west of the Mount Stuart batholith. It includes feldspathic sandstone, conglomerate, mudstone, associated volcanic rocks, and—where it overlies the Ingalls Tectonic Complex—a basal ironstone. Leaf fossils are common and Swauk strata appear to be entirely terrestrial. Taylor (1985) reports 2.5 km of Swauk section. The Swauk is strongly folded and its internal structure has not been worked out. Eddy and others (2016) report eruptive ages of 51.5–51.4 Ma from interbedded volcanic rocks, an MDA of 59.9 Ma, and an eruptive age of 59.9 Ma from tuff in the correlative Chuckanut Formation near Bellingham.

Teanaway Formation unconformably overlies Swauk Formation at the south end of the Wenatchee block. It is mostly basalt flows, basaltic tuff, and breccia with minor andesite, dacite, and rhyolite. Rhyolite has an age of 49.341 ± 0.033 Ma (Eddy and others, 2016). Tabor and others (1982) show the Teanaway to be about 1 km thick. Numerous northeast-striking basalt dikes considered feeders for the Teanaway intrude the underlying Swauk Formation. Smith's (1904) map of these dikes is gorgeous, though rather schematic. Miller and others (2022) quantified the distribution of Teanaway dikes and speculated on the regional stress field that they record.

Roslyn Formation conformably overlies Teanaway Formation. It comprises light-colored fluvial feldpathic sandstone with lesser siltstone, conglomerate, and coal. Roslyn coal was mined starting in 1886, when it began powering the Northern Pacific Railroad over the Cascade Range (Kershner, 2009). The last mines closed in 1963. The Roslyn is about 2.7 km thick, is younger than 49.34 Ma, and has MDAs of 48.80 and 47.58 Ma (Eddy and others, 2016).

Chumstick Formation is coeval with and lithologically similar to the Roslyn Formation. Chumstick differs from Roslyn by the presence of mappable tuff beds, absence of economic coal seams, estimated 9–13 km thickness, steeper dips, and occurrence on the northeast side of the Leavenworth fault. Ages of Chumstick tuffs are 49.12 to 47.98 Ma and MDAs calculated from sandstone detrital zircon populations are 47.8 to 45.9 Ma (Eddy and others, 2016). The Chumstick has been interpreted to have been either deposited in a narrow fault-bounded basin or deposited as a regional blanket coextensive with the Roslyn Formation. Haugerud and Stanton (this volume) assess lithology and structures in the Chumstick and its role in regional tectonism.

Hydrothermal alteration of the Chumstick Formation occurred during the late Eocene, while the sediments were still being deposited in the Chiwaukum/Chumstick basin and after widespread regional folding of the Chumstick (Margolis, 1989). Mineralization resulting from the alteration hosted historical gold mining (Patton and Cheney, 1971; Margolis, 1989; Ott and others, 1986). See Stanton (this volume) for additional discussion of the mineralization.

Numerous small igneous bodies are associated with the Chumstick Formation near Wenatchee. Most have been mapped as intrusions, an interpretation favored by Dawes and Tepper (this volume), though Margolis (1989) reports flows, ash flows, and eruption breccia. Tepper and others (this volume) report ages of 44.45–44.96 Ma for rocks of the Wenatchee Pinnacles (Rooster Comb, Wenatchee Dome, Saddle Rock, Old Butte, and Castle Rock). Based on isotopic and trace element data, they suggest that the Pinnacles originated from partial melting of a lower crustal source that may have been underplated during Paleozoic or Mesozoic subduction.

Swauk Formation and correlative Chuckanut Formation near Bellingham were deposited before accretion of Siletzia at 51–50 Ma (Eddy and others, 2016). Teanaway, Roslyn, and Chumstick Formations postdate accretion and are generally correlative with the Kamloops Group (e.g., Ewing, 1981) and Challis Volcanic Group to the north and east. The northern part of the Chelan block—outside the area of figure 1—shows Eocene ductile deformation and rapid unroofing of mid-crustal rocks (Haugerud and others, 1991) like that in Eocene core complexes of the central and eastern parts of the northern Cordillera. Detachment faulting has not been identified in association with the northern Chelan block, though significant low-angle normal faults are evident in little-metamorphosed rocks to the west (Tabor and others, 2003) and east (Haugerud and Tabor, 2009; Tabor and Haugerud, 2016). Unlike areas farther east, mid- to late Eocene deformation in the North Cascades is widely considered to be dominated by dextral strike slip on north- to northwest-striking faults (e.g., Haugerud and others, 1991; Miller and others, 2022).

CASCADIA SUBDUCTION REGIME

With northward migration of the Kula–Farallon ridge, the west margin of the North American plate changed from a largely transcurrent boundary to a subduction boundary with arc magmatism. Earliest Cascade arc magmas date to ~35 Ma at 49°N (Mullen and others, 2018); in Oregon the earliest arc volcanic rocks date to ~40 Ma (Sherrod and Smith, 2000). Near Wenatchee, Tepper and others (this volume) interpret geochemistry and ages of rocks of the Wenatchee Pinnacles (above) to suggest that arc magmatism here began by ~45 Ma.

Wenatchee Formation of latest Eocene to Oligocene age consists of fluvial and lacustrine quartzose sandstone, conglomerate with felsic volcanic clasts and vein quartz, and tuffaceous shale that unconformably overlie the Chumstick Formation (Gresens and others, 1981a,b; Tabor and others, 1982; Hauptman, 1983). Tuffaceous beds yield zircon fission track ages of ~34 Ma (Gresens and others, 1981b). Locally abundant volcanic debris is consistent with derivation from the nearby Cascade magmatic arc. The general character of the Wenatchee is reminiscent of the John Day Formation of north-central Oregon.

Wenatchee Formation overlaps the south end of the Entiat fault, indicating little significant slip on the Entiat fault after Wenatchee time. Significant post-Wenatchee contraction is shown by northwest-striking faults south of Wenatchee that place Chumstick Formation over Wenatchee Formation (Gresens, 1983; Tabor and others, 1982; Stanton, this volume).

Columbia River Basalt Group (CRBG) erupted from vents in eastern Oregon and Washington and flooded the northern Cascadia backarc. Rapidly erupted 16.5–16.066 Ma Grand Ronde Basalt constitutes almost three-fourths of CRBG lavas (Reidel and others, 2013; ages from Kasbohm and Schoene, 2018) and forms the skyline east and south of Wenatchee. Wanapum Basalt,16.066–15.895 Ma, is preserved in structural lows northeast (Waterville) and southeast (Quincy) of Wenatchee. Saddle Mountains Basalt, which trickled out from 13 to 6 Ma, is not known north of I-90, ~50 km southeast of Wenatchee.

Grande Ronde Basalt flowed across a pre-basalt surface northeast of Wenatchee with at least 240 m of relief (Swanson and Byerly, in Tabor and others, 1987). Northwestward thinning of flows, southeast-directed paleocurrents in interbedded sandstones, and lava flow directions observed from foresets in lava deltas indicate flow of lavas upslope towards a proto-Cascades highland. Lava ponded drainage off the Cascades, which ran along the gutter between the west-sloping lava flows and the Cascades and created the late Neogene course of the Columbia River (Waitt, in Tabor and others, 1987).

CRBG is deformed by the Yakima fold belt, which in the northern Columbia Plateau mostly comprises narrow, fault-cored east–west anticlines (Saddle Mountains, Frenchman Hills, Badger Mountain) that separate broad, flat-floored synclines. Structure appears to be in part controlled by flats and ramps within the CRBG (e.g., Staisch and others, 2018b). The much broader, more north-striking Hog Ranch–Naneum Ridge anticline may reflect a larger, deeper ramp through the Eocene section. Shortening in the Saddle Mountains anticline postdates 10 Ma and accelerated sixfold after 6.8 Ma (Staisch and others, 2018a). Wells and others (1998) explained north–south shortening in the Yakima fold belt as an indirect consequence of translation of the Sierra Nevada block northwards relative to southern British Columbia. GPS observations (for example, McCaffrey and others, 2016) demonstrate that deformation in the Yakima fold belt is ongoing. Recent shortening was also demonstrated by the M_I 6.8 1872 earthquake that ruptured the surface in Spencer Canyon south of Entiat (Bakun and others, 2002; Sherrod and others, 2021).

Age of uplift of the Cascades is not well constrained. Methner and others (2016) used stable isotope compositions of carbonate from the Chumstick Formation to infer there was no Cascade rain shadow at 35–45 Ma. Mustoe and Leopold (2014) compared late Miocene floras from both sides of the Cascades and concluded there was no rain shadow at ~8–6 Ma; however, their evidence is mostly from south of Mt. Rainier and Yakima. Reiners and others (2002) reported low-temperature cooling ages that indicate rapid exhumation of parts of the range at 8–12 Ma and assumed exhumation reflects uplift. As noted above, there is evidence of at least some elevation during eruption of Grande Ronde Basalt (16 Ma). Although the relationship between shortening on the Yakima fold belt and the rise of the Cascades is unclear, westward rise of flows at Jumpoff Ridge south of Wenatchee, on the flank of the Hog Ranch–Naneum Ridge anticline, nicely demonstrates significant post-16 Ma uplift. Cooley (this volume) looks at calcretes, or dryland paleosols, south and east of the Wenatchee area that formed on Pliocene–Pleistocene deposits. Besides providing stratigraphic markers for relative timing of incision, local tectonism, and outburst flooding, these calcretes are evidence of an arid environment in the Pliocene resulting from the Cascade rain shadow.

Ridge-capping deposits at several elevations (Tabor and others, 1982, 1987) document downcutting of the Columbia River and tributaries after eruption of the CRBG. Thick landslide deposits that cap ridges south of Wenatchee are a hiccup in this history. On the northeast end of Wheeler Ridge (aka Wenatchee Heights), these are as much as 130 m thick. Thickness and the presence of interbedded gravel indicate an episode of aggradation.

During the last, Fraser glaciation (dated to ~31–10 cal kyr BP; Cosma and others, 2008) alpine (locally sourced, valley-bound) glaciation in the eastern North Cascades peaked at about 25 cal kyr BP (Porter and Swanson, 2008), when the Icicle glacier built a conspicuous moraine at Leavenworth (Stanton, this volume). Subsequently the Cordilleran ice sheet flooded the North Cascades north of Glacier Peak (Haugerud and Tabor, 2009), the Chelan trough, Waterville Plateau, and areas farther east with maximum extent at about 15.5 cal kyr BP (Balbas and others, 2017). Lateral moraines evident in lidar topography indicate Cordilleran ice reached its limit in the Columbia valley about 5 km south of Chelan. Earlier alpine glaciation is known in the Leavenworth area (Porter and Swanson, 2008; Stanton and others, 2019). Earlier instances of the Cordilleran ice sheet are yet to be documented in north-central Washington (but see Waitt, 2021).

The Purcell Trench lobe of the Cordilleran ice sheet blocked the Clark Fork River northeast of Spokane, flooded much of northwest Montana, and intermittently released scores of catastrophic floods (Bretz, 1923; O'Connor and others, 2020). Flood routing around and across the Columbia Plateau reflected the combined effects of Okanogan lobe ice blocking the Columbia valley—and sometimes Grand Coulee—near Grand Coulee Dam, progressive erosion of Grand Coulee and other passageways by floodwaters, and glacio-isostatic adjustment. Some studies have also suggested a large subglacial flood from the Okanogan lobe of the ice sheet (e.g., Shaw and others, 1999; Lesemann and Brennand, 2009). Dawes (this volume) assesses the evidence for this hypothesis in the southern Okanogan lobe.

Early down-Columbia floods reached a water-surface elevation of 500 m at Wenatchee, 315 m above the present Columbia River, and built the large Pangborn bar (Waitt, 2016). Subsequent floods passed through coulees to the east and bypassed Wenatchee. Cunderla (this volume) looks at evidence of these outburst floods in Moses Coulee and at Dry Falls in Grand Coulee. After retreat of the Okanogan lobe opened the Columbia Valley below Grand Coulee, a late flood left a conspicuous bouldery surface that is present at low elevations from Pateras to south of Wenatchee. People likely saw the last outburst flood(s) (Waitt, 2016).

REFERENCES

Arksey, L., 2008, Wenatchee—Thumbnail history, available at https://www.historylink.org/File/8634 [Accessed 30 April 2022].

Baker, P.L., Mulcahy, S.R., and Vervoort, J.D., 2019, Age of metamorphism in the Cascades crystalline core from garnet Lu-Hf and Sm-Nd geochronology: Geological Society of America Abstracts with Programs, v. 51, abstract 21-7.

Bakun, W.H., Haugerud, R.A., Hopper, M.G., and Ludwin, R.S., 2002, The December 1872 Washington State earthquake: Bulletin of the Seismological Society of America, v. 92, p. 3239–3258, doi: https://doi.org/10.1785/0120010274.

Balbas, A.M., Barth, A.M., Clark, P.U., Clark, J., Caffee, M., O'Connor, J., Baker, V.R., Konrad, K., Bjornstad, B., O'Connor, J., Baker, V.R., Konrad, K., and Bjornstad, B., 2017, ^{10}Be dating of late Pleistocene megafloods and Cordilleran Ice Sheet retreat in the northwestern United States: Geology, v. 45, p. 583–586, doi: https://doi.org/10.1130/G38956.1.

Bao, X., Eaton, D.W., and Guest, B., 2014, Plateau uplift in western Canada caused by lithospheric delamination along a craton edge: Nature

Geoscience, v. 7, doi: https://doi.org/10.1038/NGEO2270

Beck, M.E. Jr., and Noson, L., 1972, Anomalous paleolatitudes in Cretaceous granitic rocks: Nature Physical Science, 235, p. 11–13.

Bretz, J.H., 1923, The channeled scablands of the Columbia Plateau: Journal of Geology, v. 31, p. 617–649, doi: https://doi.org/10.1086/623053.

Brown, E.H., 2012, Obducted nappe sequence in the San Juan Islands–northwest Cascades thrust system, Washington and British Columbia: Canadian Journal of Earth Sciences, v. 49, p. 796–817, doi: https://doi.org/10.1139/E2012-026.

Brown, E.H., 2020, Magma loading in the southern Coast Plutonic Complex, British Columbia and Washington: Lithosphere, v. 2020, article ID 8856566, 17 p., doi: https://doi.org/10.2113/2020/8856566.

Brown, E.H., and Dragovich, J.D., 2003, Tectonic elements and evolution of northwest Washington: Washington Division of Geology and Earth Resources Geologic Map GM-52, 1 sheet, 12 p.

Brown, E.H., and Gehrels, G.E., 2007, Detrital zircon constraints on terrane ages and affinities and timing of orogenic events in the San Juan Islands and North Cascades, Washington: Canadian Journal of Earth Sciences, v. 44, pp. 1375–1396.

Coney, P.J., Jones, D.L., and Monger, J.W.H., 1980, Cordilleran suspect terranes: Nature, v. 288, p. 329–333.

Cosma, T.N., Hendy, I.L., and Chang, A.S., 2008, Chronological constraints on Cordilleran Ice Sheet glaciomarine sedimentation from core MD02-2496 off Vancouver Island (western Canada): Quaternary Science Reviews, v. 27, p. 941–955, doi: https://doi.org/10.1016/j.quascirev.2008.01.013.

Dougherty, P., 2021, Construction of Rock Island Dam on the Columbia River begins on January 27, 1930: available at https://www.historylink.org/File/21173 [Accessed May 12, 2022].

Duggan, K.M., and Brown, E.H., 1994, Correlation of the Tonga Formation and the Chiwaukum Schist, North Cascades, Washington: Implications for Late Cretaceous orogenic mechanisms: Tectonics, v. 13, p. 1411–1424.

Eddy, M.P., Bowring, S.A., Umhoefer, P.J., Miller, R.B., McLean, N.M., and Donaghy, E.E., 2016, High-resolution temporal and stratigraphic record of Siletzia’s accretion and triple junction migration from nonmarine sedimentary basins in central and western Washington: Geological Society of America Bulletin, v. 128, p. 425–441, doi: https://doi.org/10.1130/B31335.1.

Evans, B.W., and Berti, J.W., 1986, Revised metamorphic history for the Chiwaukum Schist, North Cascades, Washington: Geology, v. 14, p. 695–698.

Ewing, T.E., 1980, Paleogene tectonic evolution of the Pacific Northwest: Journal of Geology, v. 88, p. 619–638.

Ewing, T.E., 1981, Regional stratigraphy and structural setting of the Kamloops Group, south-central British Columbia: Canadian Journal of Earth Sciences, v. 18, p. 1464-1477.

Gatewood, M.P., and Stowell, H.H., 2012, Linking zircon U–Pb and garnet Sm–Nd ages to date loading and metamorphism in the lower crust of a Cretaceous magmatic arc, Swakane Gneiss, WA, USA: Lithos, v. 146–147, p. 128–142, doi: https://doi.org/10.1016/j.lithos.2012.04.030.

Gresens, R.L., 1983, Geology of the Wenatchee and Monitor quadrangles, Chelan and Douglas Counties, Washington: Department of Natural Resources, Division of Geology and Earth Resources, Bulletin 75, 90 p.

Gresens, R.L., Naeser, C.W., and Whetten, J.W., 1981a, Stratigraphy and age of the Chumstick and Wenatchee formations: Tertiary fluvial and lacustrine rocks, Chiwaukum graben, Washington: Summary: Geological Society of America Bulletin, v. 92, Part I, p. 233–236, doi: https://doi.org/10.1130/0016-7606(1981)92<233:SAAOTC>2.0.CO;2.

Gresens, R.L., Naeser, C.W., and Whetten, J.W., 1981b, Stratigraphy and age of the Chumstick and Wenatchee formations: Tertiary fluvial and lacustrine rocks, Chiwaukum graben, Washington: Geological Society of America Bulletin, v. 92, Part II, p. 841–876.

Haeussler, P.J., Bradley, D.W., Wells, R.E., and Miller, M.L., 2003, Life and death of the Resurrection plate; evidence for its existence and subduction in the northeastern Pacific in Paleocene–Eocene time: Geological Society of America Bulletin, v. 115, no. 7, p. 867–880, doi: https://doi.org/10.1130/0016-7606(2003)115<0867:LADOTR>2.0.CO;2.

Haugerud, R.A., and Tabor, R.W., 2009, Geologic map of the North Cascade Range, Washington: U.S. Geological Survey Scientific Investigations Map 2940.

Haugerud, R.A., van der Heyden, P., Tabor, R.W., Stacey, J.S., and Zartman, R.E., 1991, Late Cretaceous and early Tertiary plutonism and deformation in the Skagit Gneiss Complex, North Cascades Range, Washington and British Columbia: Geological Society of America Bulletin, v. 103, p. 1297–1307.

Hauptman, J.L., 1983, The sedimentology of the Wenatchee Formation: Late Paleogene fluvial and lacustrine strata of the east-central Cascade Range, Washington State: M.S. thesis, Seattle, University of Washington, 164 p., 24 plates.

Hodge, F.W., ed., 1910, Handbook of American Indians north of Mexico, Part 2: Bureau of American Ethnology, Bulletin 30, 1221 p.

Hopson, C.A., and Mattinson, J.M., 1994, Chelan Migmatite Complex, Washington: Field evidence for mafic magmatism, crustal anatexis, mixing and protodiapiric emplacement, *in* Swanson, D.A., and Haugerud, R.A., eds., Geologic field trips in the Pacific Northwest: 1994 Geological Society of America Annual Meeting, p. 2K-1–2K-21.

Hopson, C.A., Weigand, P.W., Mattinson, J.M., and Mattinson, C.G., 2001, Mid-Cretaceous plutonism in the Chelan Mountains Terrane, North Cascades, Washington; relationship of intrusive plutons to Chelan migmatite complex: Geological Society of America Abstracts with Programs, v. 33, Issue 3, p. 51.

Housen, B.A., Beck, M.E. Jr., Burmester, R.R., Fawcett, T., Petro, G., Sargent, R., Addis, K., Curtis, K., Ladd, J., Liner, N., Molitor, B., Montgomery, T., Mynatt, I., Palmer, B., Tucker, D., and White, I., 2003, Paleomagnetism of the Mount Stuart batholith revisited again: What has been learned since 1972?: American Journal of Science, v. 303, p. 263–299, doi: https://doi.org/10.2475/ajs.303.4.263.

Irving, E., Woodsworth, G.J., Wynne, P.J., and Morrison, A., 1985, Paleomagnetic evidence for displacement from the south of the Coast Plutonic Complex, British Columbia*:* Canadian Journal of Earth Sciences, v. 22, p. 584–598.

Kasbohm, J., and Schoene, B., 2018, Rapid eruption of the Columbia River flood basalt and correlation with the mid-Miocene climate optimum: Science Advances, v. 4, doi: https://doi.org/10.1126/sciadv.aat8223.

Kershner, J., 2009, Roslyn—Thumbnail history, available at https://www.historylink.org/File/9239, [Accessed 16 April 2022].

Kjelland, M., Van Laethem, J.D., Krohn, R., Carney, R., Guthrie, T., Mattinson, C.G., Shea, E.K., and Kylander-Clark, A.R., 2019, The growth of new crust: Tracing the chemical and textural evolution of magma through multiple stages of magmatism, Chelan Migmatite Complex, North Cascades, Washington: American Geophysical Union Fall Meeting 2019 abstract #V43F-0158.

Lesemann, J.E., and Brennand, T.A., 2009, Regional reconstruction of subglacial hydrology and glaciodynamic behaviour along the southern margin of the Cordilleran Ice Sheet in British Columbia, Canada and northern Washington State, USA: Quaternary Science Reviews, v. 28, p. 2420–2444.

Lipman, P.W., Prostka, H.J., and Christiansen, R.L., 1972, Cenozoic volcanism and plate-tectonic evolution of the western United States; early and middle Cenozoic: Philosophical Transactions of the Royal Society of London, v. 271, p. 217–248.

MacDonald, J.H. Jr., Harper, G.D., Miller, R.B., Miller, J.S., Mlinarevic, A.N., and Schultz, C.E., 2008, The Ingalls ophiolite complex, central Cascades, Washington: Geochemistry, tectonic setting, and regional correlations, *in* Wright, J.E., and Shervais, J.W., eds., Ophiolites, arcs, and batholiths: A tribute to Cliff Hopson: Geological Society of America Special Paper 438, p. 133–159, doi: https://doi:.org/10.1130/2008.2438(04).

Margolis, J., 1989, Arkose-hosted, aquifer-controlled, epithermal Au-Ag mineralization, Wenatchee, Washington: Economic Geology, v. 84, p. 1891–1902.

Mattinson, J.M., 1972, Ages of zircons from the northern Cascade Mountains, Washington: Geological Society of America Bulletin, v. 83, p. 3769–3784, https://doi.org/10.1130/0016-7606(1972)83%5B3769:AOZFTN%5D2.0.CO;2.

Mattinson, C.G., Mattinson, J.M., Rioux, M., and Hopson, C.A., 2014, A ~30 million year history of mafic magmatism and partial melting in the Chelan Migmatite Complex, North Cascade Range, Washington, USA: Geological Society of America Abstracts with Programs, v. 46, no. 6, p. 33.

Matzel, J.E.P., Bowring, S.A., and Miller, R.B., 2004, Protolith age of the Swakane Gneiss, North Cascades, Washington: Evidence of rapid underthrusting of sediments beneath an arc: Tectonics, v. 23, TC6009, doi: https://doi.org/10.1029/2003TC001577.

Matzel, J.E.P., Bowring, S.A., and Miller, R.B., 2006, Time scales of pluton construction at differing crustal levels: Examples from the Mount Stuart and Tenpeak intrusions, North Cascades, Washington: Geological Society of America Bulletin, v. 118, p. 1412–1430, doi: https://doi.org/10.1130/B25923.1.

McCaffrey, R., King, R.W., Wells, R.E., Lancaster, M., and Miller, M.M., 2016, Contemporary deformation in the Yakima fold and thrust belt estimated with GPS: Geophysical Journal International, v. 207, p. 1–11, doi: https://doi.org/10.1093/gji/ggw252.

McGroder, M.F., 1991, Reconciliation of two-sided thrusting, burial metamorphism, and diachronous uplift in the Cascades of Washington and British Columbia: Geological Society of America Bulletin, v. 103, p. 189–209.

Methner, K., Fiebig, J., Wacker, U., Umhoefer, P., Chamberlain, C.P., and Mulch, A., 2016, Eocene-Oligocene proto-Cascades topography revealed by clumped (Δ_{47}) and oxygen isotope ($\delta^{18}O$) geochemistry (Chumstick Basin, WA, USA): Tectonics, v. 35, p. 546–564, doi: https://doi.org/10.1002/2015TC003984.

Miller, R.B., 1985, The ophiolitic Ingalls Complex, north-central Cascade Mountains, Washington: Geological Society of America Bulletin, v. 96, p. 189–209.

Miller, R.B., Paterson, S.R., and Matzel, J.E.P., 2009, Plutonism at different crustal levels: Insights from the ~5–40 km (paleodepth) North Cascades crustal section, Washington, *in* Miller, R.B., and Snoke, A., eds., Crustal cross sections from the Western North American Cordillera and Elsewhere: Implications for Tectonic and Petrologic Processes: Geological Society of America Special Paper 456, p. 1–26.

Miller, R.B., Bryant, K.I., Doran, B., Eddy, M.P., Raviola, F.P., Sylva, N., and Umhoefer, P.J., 2022, Eocene dike orientations across the Washington Cascades in response to a major strike-slip faulting episode and ridge-trench interaction: Geosphere, v. 18, p. 1–29, doi: https://doi.org/10.1130/GES02387.1.

Misch, P., 1966, Tectonic evolution of the northern Cascades of Washington, *in* A symposium on the tectonic history and mineral deposits of the western Cordillera in British Columbia and neighboring parts of the United States: Canadian Institute of Mining and Metallurgy Special Volume 8, p. 101–148.

Monger, J.W.H., Price, R.A., and Tempelman-Kluit, D.J., 1982, Tectonic accretion and the origin of the two major metamorphic and plutonic welts in the Canadian Cordillera: Geology, v. 10, p. 70–75.

Mullen, E.K., Paquette, J.-L., Tepper, J.H., and McCallum, I.S., 2018, Temporal and spatial evolution of Northern Cascade Arc magmatism revealed by LA-ICP-MS U-Pb zircon dating: Canadian Journal of Earth Sciences, v. 55, p. 442–446, doi: https://doi.org/10.1139/cjes-2017-0167

Mustoe, G.E., and Leopold, E.B., 2014, Paleobotanical evidence for the post-Miocene uplift of the Cascade Range: Canadian Journal of Earth Sciences, v. 51, p. 809–824, doi:10.1139/cjes-2013-0223.

O'Connor, J.E., Baker, V.R., Waitt, R.B., Smith, L.N., Cannon, C.M., George, D.L., and Denlinger, R.P, 2020, The Missoula and Bonneville floods—A review of ice-age megafloods in the Columbia River basin: Earth-Science Reviews, v. 208, 103181, doi: http://dx.doi.org/10.1016/j.earscirev.2020.103181.

Ott, L.E., Groody, D., Follis, E.L., and Siems, R.L., 1986, Stratigraphy, structural geology, ore mineralogy, and hydrothermal alteration at the Cannon mine, Chelan County, Washington, *in* Macdonald, A.J., ed.: Gold ’86, Willowdale, Ontario, Konsult International Inc., p. 425–435.

Page, B.M., 1939a, Geology of part of the Chiwaukum quadrangle, Washington: Ph.D. thesis, Stanford University, 203 p.

Page, B.M., 1939b, Multiple glaciation in the Leavenworth area, Washington: Journal of Geology, v. 47, p. 787–815.

Paterson, S.R., 2014, Protolith and deformation ages of Mesozoic host rock units in the Cascades Core, WA; implication for crustal amalgamation and Mesozoic orogenesis: Geological Society of America Abstracts with Programs, v. 46, issue 6, p. 32.

Paterson, S.R., Miller, R.B., Alsleben, H., Whitney, D.L., Valley, P.M., and Hurlow, H., 2004, Driving mechanism for >40 km of exhumation during contraction and extension in a continental arc, Cascade core, Washington: Tectonics, v. 23, TC3005, doi: https://doi.org/10.1029/2002TC001440.

Patton, T.C., and Cheney, E.S., 1971, L-D gold mine, Wenatchee, Wash: New structural interpretation and its utilization in the future exploration: Transactions of the Society of Mining Engineers, v. 250, p. 6–11.

Porter, S.C., and Swanson, T.W., 2008, ^{36}Cl dating of the classic Pleistocene glacial record in the northeastern Cascade Range, Washington: American Journal of Science v. 308, p. 130–166.

Reidel, S.P., Camp, V.E., Tolan, T.L., and Martin, B.S., 2013, The Columbia River flood basalt province: Stratigraphy, areal extent, volume, and physical volcanology, *in* Reidel, S.P., Camp, V.E., Ross, M.E., Wolff, J.A., Martin, B.S., Tolan, T.L., and Wells, R.E., eds, The Columbia River Flood Basalt Province: Geological Society of America Special Paper 497, p. 1–43.

Reiners, P.W., Ehlers, T.A., Garver, J.I., Mitchell, S.G., Montgomery, D.R., Vance, J.A., and Nicolescu, S., 2002, Late Miocene exhumation and uplift of the Washington Cascade Range: Geology, v. 30, p. 767–770.

Russell, I.C., 1893, A geological reconnaissance in central Washington: U.S. Geological Survey Bulletin, v. 108, 108 p.

Russell, I.C., 1900, A preliminary paper on the geology of the Cascade Mountains of northern Washington: U.S. Geological Survey, Annual Report 20, pt. 2, p. 83–210.

Sauer, K.B., Gordon, S.M., Miller, R.B., Vervoort, J.D., and Fisher, C.M., 2017, Transfer of metasupracrustal rocks to midcrustal depths in the North Cascades continental magmatic arc, Skagit Gneiss Complex, Washington: Tectonics, v. 36, p. 3254–3276, doi: https://doi.org/10.1002/2017TC004728.

Sauer, K.B., Gordon, S.M., Miller, R.B., Vervoort, J.D., and Fisher, C.M., 2018, Provenance and metamorphism of the Swakane Gneiss: Implications for incorporation of sediment into the deep levels of the North Cascades continental magmatic arc, Washington: Lithosphere, v. 10, p. 460–477, doi: https://doi.org/10.1130/L712.1.

Shaw, J., Munro-Stasiuk, M., Sawyer, B., Beaney, C., Lesemann, J.E., Musacchio, A., Rains, B., and Young, R.R., 1999, The channeled scabland: Back to Bretz?: Geology, v. 27, p. 605–608.

Sherrod, B.L., Blakely, R.J., and Weaver, C.S., 2021, LiDAR and paleoseismology solve earthquake mystery in the Pacific Northwest, USA: Geophysical Research Letters, v. 48, e2021GL093318, doi: https://doi.org/10.1029/2021GL093318.

Sherrod, D.R., and Smith, J.G., 2000, Geologic map of upper Eocene to Holocene volcanic and related rocks of the Cascade Range, Oregon: U.S. Geological Survey Miscellaneous Investigations Series Map I-2569, scale 1:500,000, 17 p.

Smith, G.O., 1904, Mount Stuart folio, Washington: U.S. Geological Survey, Geologic Atlas of the United States Folio GF-106, 4 sheets, scale 1:125,000.

Staisch, L.M., Kelsey, H.M., Sherrod, B.L., Möller, A., Paces, J.B., Blakely, R.J., and Styron, R.H., 2018a, Miocene–Pleistocene deformation of the Saddle Mountains: Implications for seismic hazard in central Washington, USA: Geological Society of America Bulletin, v. 130, p. 411–437, doi: https://doi.org/10.1130/B31783.1.

Staisch, L., Blakely, R., Kelsey, H., Styron, R., and Sherrod, B., 2018b, Crustal structure and Quaternary acceleration of deformation rates in central Washington revealed by stream profile inversion, potential field geophysics, and structural geology of the Yakima folds: Tectonics, v. 37, p. 1750–1770, doi: https://doi.org/10.1029/2017TC004916.

Stern, R.J., and Dumitru, T.A., 2019, Eocene initiation of the Cascadia subduction zone: A second example of plume-induced subduction initiation?: Geosphere, v. 15, no. 3, p. 659–681, doi: https://doi.org/10.1130 /GES02050.1.

Stanton, K.M., Waitt, R.B., and Long, W.A., 2019, Pre-late Wisconsin valley-glacier erratics between Leavenworth and Peshastin, Wenatchee Valley, Washington: Northwest Science, v. 92, p. 311–317.

Stowell, H., Bulman, G., Tinkam, D., and Zuluaga, C., 2011, Garnet growth during crustal thickening in the Cascades Crystalline Core, Washington, USA: Journal of Metamorphic Geology, v. 29, p. 627–647.

Tabor, R.W., and Haugerud, R.A., 2016, Geology of the North Cascades: Summary and enigmas, *in* Cheney, E.S., ed., The geology of Washington and beyond: Washington Division of Geology and Earth Resources and University of Washington Press, p. 131–155.

Tabor, R.W., Waitt, R.B., Frizzell, V.A., Swanson, D.A., Byerly, G.R., and Bentley, R.D., 1982, Geologic map of the Wenatchee 1:100,000 quadrangle, central Washington: U.S. Geological Survey Miscellaneous Investigations Series, 1–1311, 26 p., 3 sheets, scale 1:100,000.

Tabor, R.W., Frizzell, V.A. Jr., Whetten, J.R., Waitt, R.B., Swanson, D.A., Byerly, G.R., Booth, D.B., Hetherington, M.J., and Zartman, R.E., 1987, Geologic map of the Chelan 30-minute by 60-minute quadrangle, Washington: U.S. Geological Survey Miscellaneous Investigations Series I-1661, 29 p., 1 sheet, scale 1:100,000.

Tabor, R.W., Haugerud, R.A., Hildreth, W., and Brown, E.H., 2003, Geologic map of the Mount Baker 30- by 60-minute quadrangle: U.S. Geological Survey Geologic Investigations Series I-2660, 73 p., 2 sheets, scale 1:100,000, available at https://pubs.usgs.gov/imap/i2660/ [Accessed June 2022].

Taylor, J.E. III, 2009, Making salmon: An environmental history of the northwest fisheries crisis: University of Washington Press, 488 p.

Taylor, S.B., 1985, Stratigraphy, sedimentology, and paleogeography of the Swauk Formation in the Liberty area, central Cascades, Washington: M.S. thesis, Pullman, Washington State University, 199 p., 2 plates.

Thorkelson, D.J., and Taylor, R.P., 1989, Cordilleran slab windows: Geology, v. 17, p. 833–836.

Valley, P.M., Whitney, D.L., Paterson, S.R., Miller, R.B., and Alsleben, H., 2003, Metamorphism of deepest exposed rocks in the Cretaceous and Paleogene Cascades belt, Washington: Evidence for large-scale vertical motion in a continental margin arc: Journal of Metamorphic Geology, v. 21, p. 203–220.

Waitt, R.B., 2016, Megafloods and Clovis cache at Wenatchee, Washington: Quaternary Research, v. 85, p. 430–444, doi: https://doi.org/10.1016/j.yqres.2016.02.007.

Waitt, R.B., 2021, Roads less travelled by—Pleistocene piracy in Washington's northwestern Channeled Scabland, *in* Waitt, R.B., Thackray, G.D., and Gillespie, A.R., eds., Untangling the Quaternary period—A legacy of Stephen C. Porter: Geological Society of America Special Paper 548, p. 351–384, doi: https://doi.org/10.1130/2021.2548(18).

Waters, A.C., 1930, Geology of the southern half of the Chelan quadrangle, Washington: Ph.D. thesis, Yale University, 256 p.

Waters, A.C., 1932, A petrographic and structural study of the Swakane gneiss, Entiat Mountains, Washington: Journal of Geology, v. 40, p. 604–633.

Wells, R.E., Weaver, C.S., and Blakely, R.J., 1998, Fore-arc migration in Cascadia and its neotectonic significance: Geology, v. 26, p. 759–762.

Willis, C.L., 1950, Geology of the northeastern quarter of Chiwaukum quadrangle, Washington: Ph.D. thesis, University of Washington.

FIELD GUIDES

GEOLOGY OF THE WENATCHEE PINNACLES

Ralph L. Dawes[1] and Jeffrey H. Tepper[2]

[1]*Wenatchee Valley College , Wenatchee, Washington*
[2]*University of Puget Sound, Tacoma, Washington*

INTRODUCTION

The Wenatchee Pinnacles (Gresens, 1983) are promontories of igneous rock visible on ridge tops and hillsides west and south of the city of Wenatchee. From south to north the five named Pinnacles are Rooster Comb, Wenatchee Dome, Saddle Rock, Old Butte, and Castle Rock (fig. 1). They are aligned southeast–northwest along an Eocene structural trend known as the Eagle Creek fault zone (Evans, 1994), also called the Eagle Creek anticline (Willis, 1953). The Eagle Creek structural zone is ~40 km long. Only at its southern end, adjacent to Wenatchee, do igneous bodies like the Wenatchee Pinnacles and gold-bearing ore bodies occur.

The Eagle Creek fault zone is in a tectonic structure called the Chiwaukum graben (Willis, 1953). The Chiwaukum graben may be a strike-slip basin formed by a combination of extension between the Leavenworth and Entiat fault zones and right-lateral strike-slip offset along the faults, starting at 49 Ma (Eddy and others, 2016, 2017; Donaghy and others, 2021). However, interpretation of the Leavenworth,

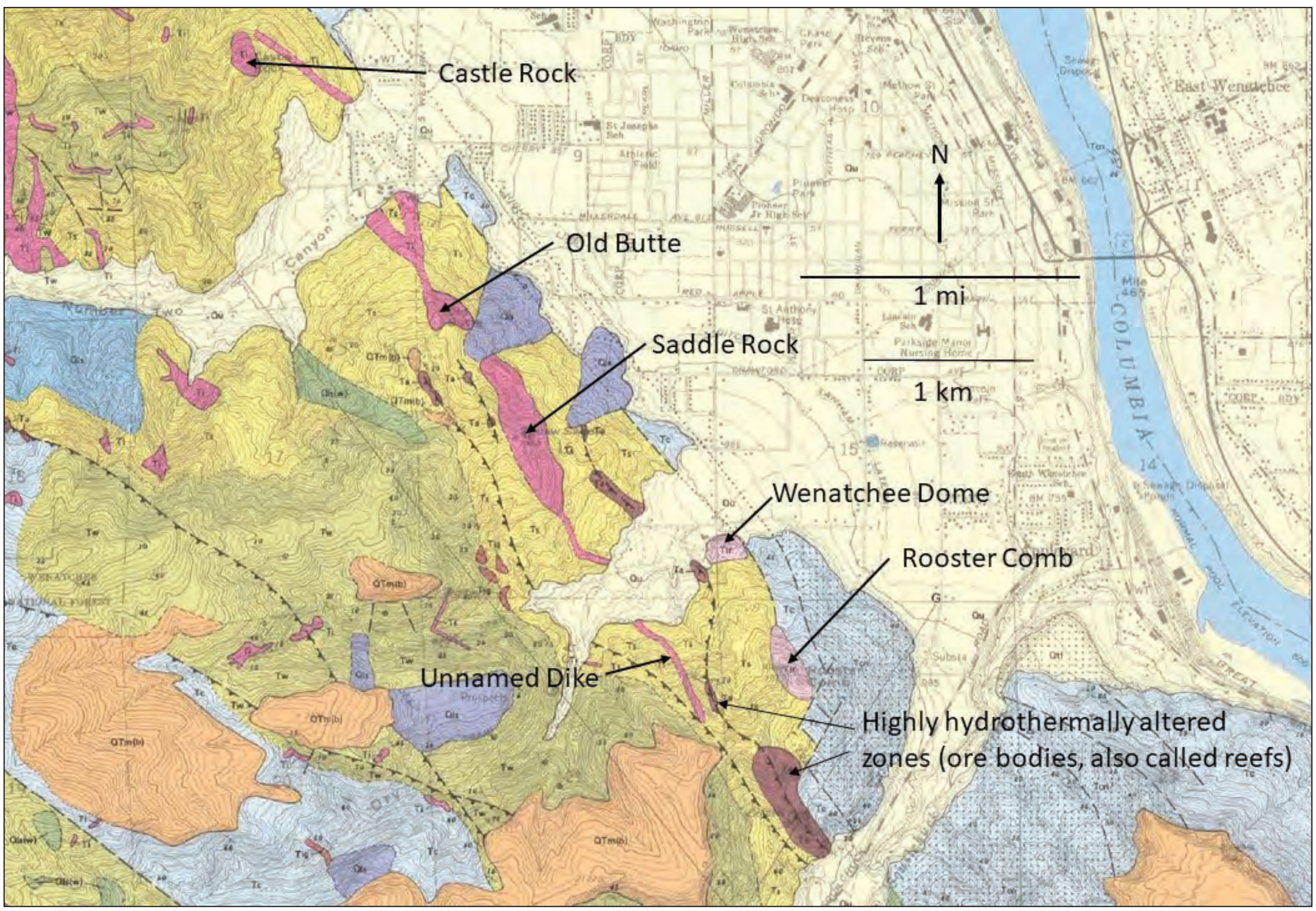

Figure 1. Map of Wenatchee Pinnacles taken from Gresens (1983). What the map shows as Ts, Swauk Formation, is now considered part of Tc, the Eocene (~45–49 Ma) Chumstick Formation. Tw is Oligocene (28–35? Ma) Wenatchee Formation. Ti is Castle Rock, Old Butte, Saddle Rock, and the unnamed dike is described in the map key as Tertiary "hornblende andesite, possibly with minor amounts of dacite." From chemical analysis, we have determined it to be dacite. Tir of Wenatchee Dome and Rooster Comb is listed as "biotitic rhyodacite porphyry." We have found it to be rhyolite.

Eagle Creek, and Entiat faults, and the depositional and structural history of the geological formations that occur within what Willis labeled the Chiwaukum graben, is debated (e.g., Cheney and Hayman, 2009, 2010; Haugerud and Stanton, this volume). We use the term Chiwaukum graben for convenience. Eddy and others (2016, 2017) presented what they saw as evidence of ~30 km of right-lateral strike-slip on the Leaven fault zone, which is about 10 km southwest of the Wenatchee Pinnacles. The Eagle Creek fault zone parallels the sides of the Chiwaukum graben and likely formed as part of the same sequence of tectonic events. The Wenatchee Dome is interpreted by several studies to have intruded a main strand of the Eagle Creek fault (Evans, 1994; Gilmour, 2013; Eddy and others, 2016, 2017). The age of the dome (44.447 ± 0.059 Ma; Gilmour, 2013) may thus constrain the end of motion on the Eagle Creek fault.

The Chumstick Formation (Gresens and others, 1980) surrounds the Wenatchee Pinnacles. The Chumstick Formation is interpreted as either syntectonic sedimentary infill of the Chiwaukum graben structural basins (Gresens and others, 1980; Tabor and others, 1982; Johnson, 1985; Evans, 1988, 1994; Eddy and others, 2016, 2017; Donaghy and others, 2021), or as a regional deposit that extends beyond the Chiwaukum graben and precedes it in age (Cheney and Hayman, 2009). The Chumstick Formation was deposited in stream channels, floodplains, alluvial fans, and lakes, and consists largely of arkosic (feldspathic arenite) sandstone, along with mudstone and conglomerate. Leaf fossils and carbon from decomposed plants are common and several layers of distally deposited tuff occur within the Chumstick sequence. Ages of the tuff, detrital zircon maximum depositional ages, and the age of the Wenatchee Dome have been interpreted as constraining deposition of the Chumstick Formation to 49–45 Ma (Evans, 1994; Gilmour, 2013; Eddy and others, 2016, 2017; Donaghy and others, 2021).

Along the Eagle Creek fault zone, uplifted structures, which include the Eagle Creek anticline and what might be a horst of gneissic basement rock, split the Chiwaukum graben into eastern and western basins (Evans, 1994). The Nahahum Canyon member of the Chumstick Formation (Gresens and others, 1980; Tabor and others, 1982) was deposited in the eastern basin, apparently while it was tectonically active (Evans, 1994), and is interpreted as unconformably overlying the Clark Canyon member (Evans, 1994; Eddy and others, 2016, 2017; Donaghy and others, 2021). Rooster Comb and the Wenatchee Dome have been mapped as lying along the contact between the Nahahum Canyon and Clark Canyon members of the Chumstick Formation (Tabor and others, 1982; Gresens, 1983). Castle Rock, Old Butte, Saddle Rock, and an unnamed dike on the south side of Dry Gulch approximately on strike with Saddle Rock (fig. 1), are all mapped as within what would now be called the Clark Canyon member of the Chumstick Formation (Tabor and others, 1982; Gresens, 1983).

The Wenatchee Pinnacles are associated with a zone of hydrothermal gold and silver mineralization known as the Wenatchee Gold Belt. The Lovitt Mine operated in Pitcher Canyon, <1 km south of Rooster Comb, from 1949 to 1967 (Patton and Cheney, 1971). The Cannon Mine operated in Dry Gulch near the Wenatchee Dome, at the base of Saddle Rock, from 1985 to 1994 (Price, 2007). The gold and silver occur in mineralized, veined, and brecciated zones (“reefs”) within the Chumstick Formation. Price (2007, p. iv) describes it as “classic low-sulfide-adularia type epithermal gold–silver deposits.” The highest-grade ore is in the most silicified parts of the reefs (Lovitt and Skerl, 1958; Patton and Cheney, 1971; Ott and others, 1986; Ott, 1988; Margolis, 1989; Cameron, 1994). Gangue minerals in the veins are dominantly quartz, adularia, and calcite. Ott (1988) lists the ore minerals as pyrite, electrum, pyrargyrite, tetrahedrite, chalcopyrite, and acanthite. Margolis (1989), based partly on microprobe analyses, lists pyrite, arsenopyrite, marcasite, stibnite, chalcopyrite, hesite, electrum, galena, native silver, and pyrargyrite, with marcasite and sphalerite in lower-grade zones. Margolis (1989) emphasizes that the ore bodies formed in aquifers confined by faults and mudstones.

Despite more than a century of study, questions about the geology of the Wenatchee Pinnacles remain controversial. The igneous rocks in the Wenatchee Pinnacles have been given different descriptions and names in previous studies. What types of rock are they, and how did the magmas form? These questions are addressed in Tepper and others, this volume. The geochemical classification of the rocks informs our interpretation of these rocks in the field, as shown in this field trip.

A long-standing question was whether all the Pinnacles formed at the same time, or at times separated by millions of years. We believe we have answered this question with new zircon U-Pb age measurements, discussed below in the section on ages of the Wenatchee Pinnacles.

Another question is whether the Pinnacles represent intrusions or eruptions. This is discussed below in the section on emplacement of the Wenatchee Pinnacle. Our study of the field evidence and petrology of the Pinnacles, age measurements, and reading of other geologists' maps and papers, leads us to favor all the Pinnacles being hypabyssal intrusions. However, the differing previous interpretations of the relationships between the Pinnacles and the adjacent faults and folds in the sedimentary rocks are not resolved.

Lastly, the extent to which ore-forming fluids were magmatic versus meteoric remains uncertain. We have identified likely hydrothermal features associated with the Wenatchee Dome and Rooster Comb that have not previously been interpreted as such, and we think that the fluids were derived from the magma as it solidified. This does not necessarily imply that magmatic fluids contributed to the formation of the ore deposits, which are in sedimentary rocks adjacent to the igneous rock bodies. The new age measurements, which we interpret as showing that the Wenatchee Pinnacles are all close to the same age, 44-45 Ma (discussed below), strongly support the idea that the circulation of hydrothermal fluid in rocks adjacent to the Pinnacles, which created the gold ore, was driven by heat from the igneous intrusions.

IGNEOUS ROCKS OF THE WENATCHEE PINNACLES

Dacite

The Wenatchee Pinnacles consist of two main rock types, dacite and rhyolite (Tepper and others, this volume). The dacite occurs in Castle Rock, Old Butte, Saddle Rock, and an unnamed dike on the side of Dry Gulch 1 km southeast of Saddle Rock (fig. 1). Previous workers mapped these Pinnacles as (hornblende) andesite (Chappell, 1936; Tabor and others, 1982; Gresens, 1983; Ott and others, 1986; Ott, 1988; Cameron, 1994), although Gresens mentions dacite may be present. The dacite is light gray on fresh surfaces, weathers to tan, and contains phenocrysts of plagioclase, hornblende, and biotite 1-4 mm in size in an aphanitic/microcrystalline groundmass. Previous studies (Smith and Calkins, 1904; Chappell, 1936) report pyroxene in Saddle Rock but seem to be referring to atypical exposures that are more mafic, either on the margin (Smith and Calkins, 1904) or in the middle (Chappell, 1936). In our limited visits we have not observed pyroxene.

The dacite as seen in the unnamed dike varies in color and texture. Although hydrothermal alteration and weathering of the rocks has occurred, the variations in appearance may also be due to different amounts of glass and crystals in the rock. In the unnamed dike in Dry Gulch, the bimodal variation in appearance, from light tan to dark, nearly black, makes it look like two different types of rock are in the dike, but the difference does not appear in chemical analysis, which shows both to be dacite. The dark dacite appears to have a much glassier matrix. Further analyses would be needed to tease out the petrographic and possible chemical differences between these two colors of dacite.

Saddle Rock, Old Butte, and the unnamed dike in Dry Gulch, all consisting of dacite, display near-vertical banding that appears as partings in more weathered outcrops. The layers appear to consist of alternating bands of glassy and microcrystalline rock that vary from 2 mm to several centimeters in thickness and strike northwest–southeast, parallel to the overall trend of the Pinnacles. Locally the layers pinch and swell, and subdued undulations and discrete small folds occur (5–20 cm wavelengths). However, in places the layers turn, for a short interval, to strike approximately east–west across the main outcrop trend. As suggested in previous studies of the Wenatchee Pinnacles, these are probably flow layers. Flow layering can develop during emplacement of high-silica lava flows and hypabyssal intrusions when the solidifying magma is flowing and shear bands form as a result of differential motion between layers with different amounts of melt, crystals, crystal alignment, vesicles, and viscosity (Smith, 2002).

Basalt

Gresens (1983) maps "amygdaloidal basalt" in the vicinity of the Wenatchee Pinnacles and Ott (1988) reports drilling through amygdaloidal basalt east of Wenatchee Dome and obtaining a K-Ar age of 42.9 ± 1.9 Ma on the rock. We have sampled an aphanitic basalt dike intruding Castle Rock and another intruding the Chumstick Formation <100 m from Saddle Rock (Tepper and others, this volume).

Rhyolite

Previous studies have identified Wenatchee Dome and Rooster Comb as either dacite (Patton and Cheney, 1971; Cameron, 1994), rhyodacite (Gresens, 1983; Ott and others, 1986; Ott, 1988), or rhyolite (Smith and Calkins, 1904; Lovitt and Skerl, 1958; Margolis, 1989). Our chemical analyses classify the rock as rhyolite (Tepper and others, this volume; White and others, 2021). The rock has phenocrysts of clear quartz, which vary from subhedral to resorbed-looking, plagioclase, biotite, and hornblende. The phenocrysts range from 1 to 4 mm across. Chappell (1936) and Gresens (1983) report that the groundmass has microcrystals of the same minerals as the phenocrysts, along with a small amount of pyroxene.

The Wenatchee Dome and Rooster Comb rhyolite have pervasive layering, interpreted as flow layering (Smith and Calkins, 2004; Patton and Cheney, 1971; Gresens, 1983; Ott and others, 1986; Ott, 1988). It appears similar to the apparent flow layering in the unnamed dike, Saddle Rock, and Old Butte. The flow layering has been accentuated by weathering, making it appear like a form of sheet jointing where layers are becoming separated parallel to the surfaces of the outcrop. The flow layers alternate from predominantly glass to glassy but with a high proportion of microcrystals. Those in Rooster Comb, like those in Old Butte, tend to be near vertical and mainly strike along the southeast–northwest orientation of the outcrop, following the trend of the Eagle Creek structural zone. In Rooster Comb there are also joints, which might be sheet joints, which cut through the outcrop horizontally to subhorizontally. The joints have similar thickness (centimeter-scale) as the steeply dipping flow layers.

Flow layers in Wenatchee Dome parallel its margins on the south and west side. On top of the dome, the flow layers become horizontal. On the near-vertical north side, where erosion may have removed the dome margin, the generally northward-dipping layers meet the surface at an angle. Gresens (1983) reported that flow layers on the east side of the Wenatchee Dome are truncated by the margin of the dome at a high angle, which indicated to him it may have been faulted.

Jointing on top of the Wenatchee Dome is more closely spaced than that on steep layers near the margins, being millimeter-scale instead of centimeter-scale. Joint surfaces on top of the dome are coated with a very fine-grained, locally vesicular, brown layer, underlain by a blue layer. Preliminary SEM analyses have identified barite, rutile, quartz, a Cu-phase, and possibly alkali feldspar in these layers, which were probably deposited by hydrothermal fluids.

Breccia and Perlite

Associated with the rhyolite are breccias consisting of highly angular clasts of flow-banded white rhyolite surrounded, cross-cut, and veined along narrow fractures by a very fine-grained, dark gray matrix. The breccia forms 1- to 10-cm-scale veins near the western border of the Wenatchee Dome. The veins of breccia cut across coherent flow-layered portions of the rhyolite. On the west side of Rooster Comb there is an extensive outcrop of a similar breccia ~10 m wide.

Perlite occurs on the margins of the two rhyolite bodies. In both, perlite occurs between the breccia on the west side and the flow-layered rhyolite of the interior. The perlite is gray and is easily disaggregated into 0.5- to 3-mm spherulites.

EMPLACEMENT OF THE WENATCHEE PINNACLES

Previous Interpretations

No contacts between the Wenatchee Pinnacles and the Chumstick Formation have been observed by us at the surface, nor explicitly reported in previous studies. Contacts seen in Cannon Mine tunnels or drill cores that crossed contacts of sedimentary rock with Saddle Rock, Wenatchee Dome, and Rooster Comb have been reported (Patton and Cheney, 1971; Ott and others, 1986; Ott, 1988; Cameron, 1994).

The presence of numerous mapped faults on various scales, from tens of meters in mine maps to tens of kilometers in regional maps, with faults on some maps cutting Rooster Comb and/or the Wenatchee Dome, complicates the question of how these bodies of igneous rock were initially emplaced. Previous studies do not agree on the timing and nature of the faults in the area. Some interpret the Eagle Creek fault as being active at the time Wenatchee Dome formed, with the magma channeling through the fault zone before motion either ceased (Gilmour, 2013; Eddy and others, 2016, 2017) or tapered off (Evans, 1994). Some studies map key faults in the zone of ore bodies and adjacent to Wenatchee Dome and Rooster Comb as reverse faults, possibly Oligocene in age, which were active after igneous activity and hydrothermal mineralization had ceased (Patton and Cheney, 1971; Margolis, 1989; Cameron, 1994). The Oligocene age is primarily based on the observation that the Oligocene-age Wenatchee Formation, which sits stratigraphically above the Chumstick Formation less than 1 km from the Pinnacles, has been folded and faulted.

Several previous studies interpreted all the Wenatchee Pinnacles as hypabyssal intrusive bodies (Chappell, 1936; Tabor and others, 1982; Gresens, 1983), but Smith and Calkins (1902) interpreted what is probably Rooster Comb as a “doubtless extrusive” flow breccia, and Margolis (1987, 1989) interpreted Rooster Comb as an ash-flow tuff. Most workers consider the Wenatchee Dome and Rooster Comb lithologically equivalent. Because a number of studies have suggested that the Wenatchee Dome is essentially the same rock as Rooster Comb, the assertion of extrusive for Rooster Comb by Smith and Calkins (1904) and Margolis (1987, 1989) raises the question of extrusive vs. intrusive for the Wenatchee Dome as well.

Ott (1988) and Cameron (1994), based on evidence from drill core, interpreted Saddle Rock as probably a lava flow conformable with bedding of the Chumstick Formation in the northeast-dipping limb of an anticline.

Wenatchee Dome Emplacement

Previous studies have interpreted the Wenatchee Dome as an intrusion (Chappell, 1936; Patton and Cheney, 1971; Tabor and others, 1982; Cameron, 1994). Ott (1988) reports from mine tunnels and drill core that the Wenatchee Dome is mantled by perlite on all sides, consistent with it being an intact igneous body. We interpret the Wenatchee Dome as an intrusion.

The combination of breccia, perlite, flow layering, and mineral deposit relations in the Wenatchee Dome suggest the following sequence may have occurred. The dome was emplaced by magma intruding upward and outward. The flow layer orientations suggest that during emplacement the Wenatchee Dome may have grown by expanding outward on the sides and top and the flow layers formed parallel to the contact aligned with least-stress axes. The expansion process thinned the flow layers across the top. As the magma solidified, it produced hydrothermal fluid, which changed glassy rhyolite near the periphery into perlite and, at the margin of the magma body beyond the perlite, brecciated the flow-layered rhyolite. The hydrothermal fluid formed the dark gray groundmass of the breccia by hydrothermal deposition of quartz. At the top of the dome, a fairly high-temperature hydrothermal fluid deposited the brown and blue mineral coatings on flow jointing surfaces.

Rooster Comb Emplacement

Surface exposures of Rooster Comb and the Wenatchee Dome are separated by ~0.5 km. Gresens (1983) and Patton and Cheney (1971) interpreted the two rhyolite bodies as having originally been connected and then separated by dextral strike-slip faulting (see fig. 1). Cameron (1994) shows faults skirting the west and east edges of the Wenatchee Dome and has two of them continuing south and cutting the full length of the sides of Rooster Comb.

Chappell (1936) and Ott (1988) consider Rooster Comb to be a dike, as have most subsequent mappers (Gresens, 1983, Tabor and others, 1984, Cameron, 1994). However, Smith and Calkins (1904) interpret Rooster Comb as tuff and/or volcanic breccia. Margolis (1987, 1989) viewed it as a possible ash-flow tuff that he suggests is part of a sequence of erupted rhyodacite, volcanic breccia, and tuff reported from drill cores from a site ~1.75 km southeast of Rooster Comb and a site in Wenatchee Heights, ~2 km further south.

We interpret Rooster Comb as a dike formed from rhyolitic magma similar to that of the Wenatchee Dome, and the associated breccia as a hydrothermal feature produced by fluid generated by the solidifying magma.

Saddle Rock Emplacement

Ott (1988) suggested Saddle Rock was either a lava flow or a sill, conformable with bedding of the Chumstick Formation and dipping moderately to steeply (40°–70°) to the east. He describes drill core passing through a sequence of sandstone and siltstone into ~20 m of breccia with clasts of Saddle Rock, then into zones of flow-banded Saddle Rock, another interval of brecciated Saddle Rock and some intervals of sandstone, finally passing completely into sandstone (Ott, 1988). He favored a lava flow origin and suggested that the volcanic breccia could be to the product of a subaqueous eruption.

We question Ott's interpretation on the basis of structure, petrology, and age. A fold limb that conformably includes Saddle Rock and Old Butte would have to run at least 1.5 km with little variation from Dry Gulch nearly to Number Two Canyon. This seems unusual given all the small-scale folds, and various scales of faulting, observed in the immediate vicinity. Drill hole data was interpreted by Ott (1988) as indicating that the contact of Saddle Rock and the Chumstick Formation dipped 40–70 degrees to the east on the east side of Saddle Rock and 70–85 degrees to the east on the west side of Saddle Rock, a high range of variation. The varying contact dip and the occurrence of sandstone within Saddle Rock are consistent with intrusion by a dike. Where we have observed Chumstick Formation bedding in the vicinity of Saddle Rock, it has been shallowly dipping and striking at high angles to Saddle Rock. It thus seems likely that Old Butte and Saddle Rock are dikes, probably closely related, likely contiguous. The unnamed dike across Dry Gulch from Saddle Rock, which is approximately along strike with Saddle Rock and Old Butte, has the same dacite composition and flow layering and is likely of the same age. Shallow intrusion into water-saturated sedimentary rock and possibly hydrothermal processes could account for the volcanic breccia of Saddle Rock observed by Ott (1988). The age of Saddle Rock (44.67 ± 0.76 Ma, Tepper and others, this volume) is younger than the estimated age of the Clark Canyon member of the Chumstick Formation it appears to be in contact with (49.2–46.5 Ma; Donaghy and others, 2021), adding to the likelihood that it is an intrusion.

Castle Rock Emplacement

The apparently steeply dipping margins of Castle Rock and its oval shape in map view are consistent with it being a small intrusion. It likely cuts across bedding in the country rock, though direct contacts were not seen. From traversing it, we agree with Gresens (1983) that there is a southeast-trending dike adjacent to Castle Rock (fig. 1), made of the same type of rock.

Boulders of volcanic breccia bearing clasts of Castle Rock dacite (Ralph Haugerud, oral commun., 2021) occur 100 m to the northeast of Castle Rock, at a saddle between it and the adjacent dike. The boulders, 1–2 m across, appear to be auto-breccia, with subrounded 5- to 50-cm clasts enveloped in a matrix of similar dacite. If the saddle with boulders of volcanic breccia is in a contact zone between the main body of Castle Rock and a separate dike, with intervening sedimentary rock possibly accounting for the ridge being eroded to a low point there, then the volcanic breccia was likely formed along the margin of the Castle Rock intrusion.

Castle Rock contains several joint sets with different orientations visible in its steep ramparts. The jointing includes possible flow layers that approximately parallel the southeast and east walls of the castle, etched out locally by erosion into lamina a few centimeters thick. On top of Castle Rock possible flow layers, up to 0.5 m thick, strike northeast and dip steeply northwest, with pinch-and-swell margins. Whether the layers are defined by variation in rock texture or by orientations of crystals is obscured by alteration and weathering.

In sum, the available evidence suggests that all of the Wenatchee Pinnacles are hypabyssal intrusive bodies. The same conclusion was reached by Chappell (1936), Tabor and others (1982), and Gresens (1983). We also agree with previous studies that the correlation of the Wenatchee Pinnacles with the Eagle Creek fault zone, and their alignment along the south-southeast–north-northwest trend of the fault zone, is not a coincidence, and that channeling of magma along faults likely occurred to some extent.

Ages of the Wenatchee Pinnacles

New U-Pb zircon ages of Castle Rock and Saddle Rock (44.67 ± 0.76 Ma, 44.96 ± 0.65 Ma, respectively; Tepper and others, this volume) and Gilmour's (2012) U-Pb zircon age of Wenatchee Dome (44.447 ± 0.059 Ma) overlap within error, indicating all Pinnacles intrusions were part of a single magmatic episode.

Previous interpretations that the country rock of the Wenatchee Pinnacles was the Swauk Formation rather than the Chumstick Formation were based partly on a 50.9 ± 1.9 Ma K-Ar whole-rock age of Saddle Rock (Ott and others, 1986; Ott, 1988; Cameron, 1994). This 51 Ma age was consistent with a report from Gresens (1983) of volcanic rock with a K-Ar age of 50 Ma interbedded with the upper Swauk Formation. Tabor and others (1982) identified the country rock of the Pinnacles as Chumstick Formation. Along with the Wenatchee Dome age (Gilmour, 2013), the new ages of Castle Rock and Saddle Rock (Tepper and others, this volume) put the Pinnacles after, or else very near the end of, deposition of the Chumstick Formation (Eddy and others, 2016, 2017; Donaghy and others, 2021). The Swauk Formation is >50 Ma in age (Eddy and others, 2016, 2017) and pre-dates the Chumstick Formation.

Gresens (1983) did not have age measurements to determine whether Saddle Rock, Old Butte, and Castle Rock could be correlated with the Oligocene-age Horse Lake Igneous Complex, 0.5–5 km to the northeast, or with the Wenatchee Dome and Rooster Comb, which he referred to as the felsic rocks of the Wenatchee Pinnacles. The association of the Pinnacles with the Eagle Creek structural zone and the zone of hydrothermal mineralization led him to favor all of them being related to the same magmatic event and thus about the same age. Our data confirm that Saddle Rock and Castle Rock are the same age, within error, as the Wenatchee Dome and presumably Rooster Comb as well.

The one age measurement of a mafic intrusion in the area, K-Ar on basalt just east of Wenatchee Dome (42.9 ± 1.9 Ma; Ott, 1988), overlaps within error the ages of the Wenatchee Pinnacles and provides additional confirmation that basaltic magma was intruding the crust in the area at the same time.

The age of mineralization in the ore bodies next to Wenatchee Dome and Saddle Rock has been measured from K-Ar in hydrothermal adularia. Ott (1988) reports an age of 44.2 ± 1.9 Ma from one analysis. Cameron (1994) reports an average of 44.7 Ma from four adularia K-Ar ages from the Cannon Mine. The age of the gold ore is the same age as the Wenatchee Pinnacles, within error, 44–45 Ma.

The ages have important implications for petrogenesis of the magmas and their relation to the gold ore in the vicinity. Mafic magma was present in the system at the same time as the felsic magma formed and could have generated dacitic magma by melting of lower crustal rocks (Tepper and others, this volume). The rhyolitic magma that formed Wenatchee Dome and Rooster Comb may have formed by fractional crystallization of the dacitic magma.

Relation of Wenatchee Pinnacles to Gold Ore

The gold-bearing reefs targeted by the Lovitt Mine and Cannon Mine are west of the trend of the Wenatchee Dome and Rooster Comb rhyolites and east of the trend of the dacite bodies at Castle Rock, Old Butte, Saddle Rock, and the unnamed dike. Close age agreement between the igneous rocks and the ore mineralization suggests a single magmatic event was responsible for the hydrothermal activity that led to the gold deposits. The presence of mafic and felsic magma in the shallow crust probably drove the circulation of hydrothermal fluid in the clastic country rock, leading to the mineralization and the brecciation due to local fluid overpressure during boiling.

The reefs of hydrothermal mineralization occur in the Chumstick Formation and most of the ore is in sandstone, which would have been more permeable before being mineralized (Ott, 1988; Margolis, 1987, 1989). According to mining geology reports, the mineralized zones are bound and “capped” by strata of mudstone that were likely less permeable, and by faults or shear zones that contain sheared mudstone, including one shear zone along the west side of Wenatchee Dome (Patton and Cheney, 1971; Ott and others, 1986; Margolis, 1987; Ott, 1988; Cameron, 1994). Assuming the igneous bodies have not been displaced relative to the wall rock, the zone of Au-Ag mineralization was a narrow envelope, <150 m wide underground in the Cannon Mine (Ott, 1988), bordered on the east by the rhyolitic igneous bodies and on the west by the dacitic igneous bodies. It is not known whether the hydrothermal fluids were magmatic or meteoric. Margolis (1987, 1989) makes the case that the locations of the ore bodies derive from how aquicludes or aquitards—mudstones and faults—controlled circulation of hydrothermal fluid in aquifers in the sandstone beds.

Saddle Rock is described by Gresens (1983) as being partly silicified and more altered than Wenatchee Dome. Ott describes Saddle Rock as being lightly mineralized with zones of brecciation and silicification that contain low-grade amounts of gold. The analytical uncertainty in U-Pb zircon ages of Saddle Rock and Wenatchee Dome allow the possibility that Saddle Rock could be hundreds of thousands of years older than Wenatchee Dome. If so, Saddle Rock could have been subjected to some of the ore-forming hydrothermal fluids but without the permeability required for significant gold deposition. Its position to the side of the main zone of hydrothermal circulation in the clastic sedimentary rocks would also have limited its ore-related mineralization. In agreement with previous researchers, the new U-Pb dates are consistent with the Wenatchee Dome having been emplaced later, after the gold-depositing stage of hydrothermal fluid circulation had finished.

Wenatchee Dome and Rooster Comb Field Guide

This on-foot excursion will visit the southern-most two intrusions of the Wenatchee Pinnacles and a nearby dacite dike. We will consider the origin of these bodies and their role in the adjacent Wenatchee Gold Belt. In addition to structures in the igneous rock bodies that may be related to how they were emplaced, we will examine breccias, perlite zones, and silicified 'reefs' produced by the accompanying hydrothermal activity.

Latitudes and longitudes are taken from Google Maps. Figure 2 is a map that shows the stops on the field trip. The walking distance is 2 mi each way (3.2 km), 4 mi total (6.4 km). The elevation gain is 820 ft (250 m).

ROAD LOG

Directions to the Trailhead

In Wenatchee, follow Miller Street to its southern end, turn right on Circle Street, and park in the large lot that straddles the Saddle Rock and Dry Gulch trailheads, elevation 1,080 ft above sea level. The trail to Rooster Comb starts across from the Dry Gulch trailhead sign, near the southeast corner of the parking lot. On the east side of the main Dry Gulch road/trail is the trail to Rooster Comb. A sign at the gate at the start of the route to Rooster Comb says "No Trespassing," but we have permission to walk on the trail for the TRGS meeting field trip. After walking up the trail for about 1,000 ft (300 m), go left (north) 50 ft (15 m) off the trail to climb onto a horizontal ramp blasted into the side of B reef, a body of hydrothermally altered rock.

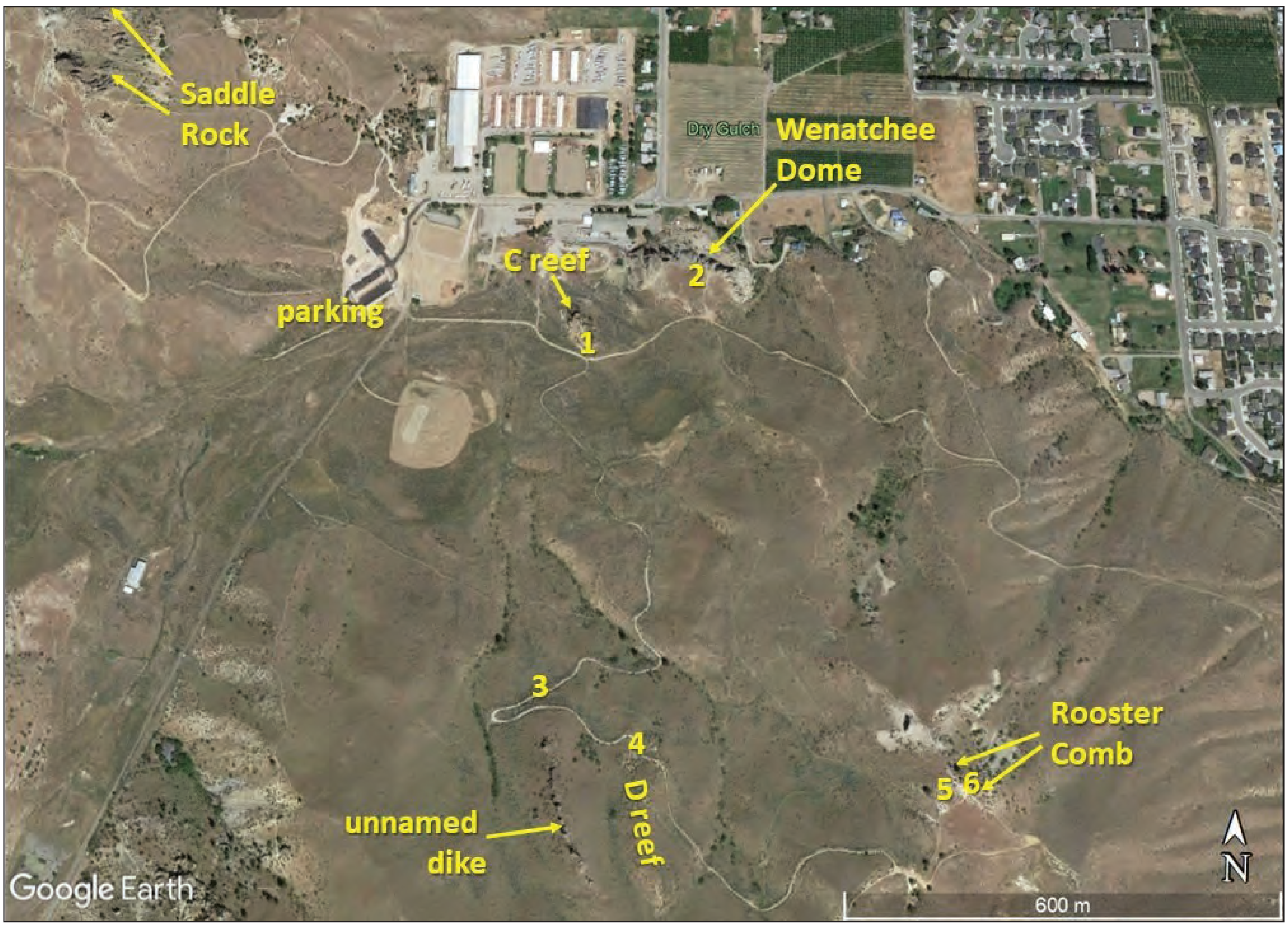

Figure 2. Map showing numbered field trip stops.

STOP 1:
B Reef
+47.39489, -120.32576

This bench exposes mineralized Chumstick Sandstone, and lesser siltstone or mudstone, in beds striking N 40° W and dipping 45° SW. According to Cameron (1994), this outcrop resembles the B and B West underground ore bodies seen in underground mine workings, except that the surface outcrop is oxidized. There are small (centimeter-scale) patches or stringers of limonite on some surfaces. The sedimentary rock is slightly brecciated and to some extent silicified, but veins are absent here and the ore grade is low.

Return to the trail and go east another 600 ft (180 m) to the top of Wenatchee Dome.

STOP 2:
Wenatchee Dome
+47.39600, -120.32332

There is breccia on the west margin of Wenatchee Dome. Between the breccia and the interior of the dome, a small amount of perlite crops out. Chappell (1936) reported a mantle of perlite around the Wenatchee Dome 50 ft (15 m) thick. Coombs (1952) reported a zone of perlite 50 ft thick along the south side of the Wenatchee Dome. Ott (1988), based on views from mine tunnels and drill core, states that perlite surrounds the entire dome, without stating thickness.

The portal and main tunnel and ramp of the Cannon Mine were sited in the Wenatchee Dome because it was competent rock needing little support. The ore was mined from ore bodies (reefs) west and north of Wenatchee Dome. Mining and drilling reached laterally beneath the Appleatchee equestrian facility to the north and beneath Saddle Rock roughly 3,500 ft (1 km) to the northwest. Drilling is interpreted as having encountered an underground extension of Saddle Rock 500 ft (150 m) west of Wenatchee Dome and the ore bodies (Ott, 1988). Wenatchee Dome was found to extend underground to beneath the Appleatchee equestrian facility. The ore bodies are confined to a narrow belt between the Wenatchee Dome and Saddle Rock and their underground extensions.

Wenatchee Dome consists of porphyritic rhyolite with visible crystals of quartz, biotite, feldspar, and hornblende. The matrix varies from microcrystalline with some glass to more thoroughly glassy. It may be of interest to examine the layering that pervades the Wenatchee Dome, which we and previous studies interpret as flow banding, which is largely parallel to the surfaces of the dome. As discussed in the introduction, the apparent flow banding in the Wenatchee Dome, and the assumption that it was parallel to the margin of the body of magma as it solidified, has been used to interpret the faulting and erosional history of the dome.

Across the top of the dome, the subhorizontal layers get thinner and are coated by a sparsely vesicular brown mineral coating with blue underneath. As mentioned earlier in the rhyolite section, preliminary SEM analyses of these layers has identified barite, rutile, quartz, a Cu-phase, and possibly alkali feldspar, which were probably deposited by hydrothermal fluids.

Return on the trail to B Reef. Across from B Reef, turn south on an unmarked trail (old road), which is the path to Rooster Comb. From the turn, go nearly 0.5 mi (0.6 km) to where the unnamed dacite dike on the south side of Dry Gulch crosses the trail.

STOP 3:
Unnamed Dike
+47.39015, -120.32657

The outcrop along the trail is altered, weathered, and largely covered by lichen. It contains both the light-colored dacite with 0.1–0.4 mm plagioclase and hornblende phenocrysts in an aphanitic groundmass and the dark-colored dacite with 0.3–0.6 mm plagioclase and hornblende phenocrysts in a glassy groundmass. The two types of dacite, which are better exposed in the protruding towers of the unnamed dike that can be accessed by scrambling off-trail, apparently differ in appearance due to having different igneous texture, with the dark dacite having more glass in its matrix.

After rounding a hairpin turn, the trail passes close to the unnamed dike, visible above. The lowest spire of the dike is about 150 ft (45 m) south of the trail. Pieces of dark, glassy groundmass dacite can be found in talus along the trail below the dike.

After ~1,300 ft from the first dike outcrop along the trail before the hairpin turn, the trail curves south and passes a prospect pit on the right, elevation ~1,560 ft asl.

STOP 4:
Chumstick Formation
+47.38939, -120.324518

The Chumstick Formation is exposed in the prospect pit. Here it consists of arkosic sandstone and possibly siltstone dipping steeply on the back wall of the pit, with pieces of sandstone decomposing into grus on the floor of the pit. The back wall of the pit can be examined for sedimentary beds and their strike and dip determined. The pit was excavated into the bottom (north) end of C reef, a zone of hydrothermally mineralized Chumstick Formation with gold- and silver-bearing minerals.

Continuing on, the trailside just south of the pit exposes some conglomerate of the Chumstick Formation. Lovitt and Skerl (1958) and Patton and Cheney (1971) report a conglomerate as a marker bed that occurs in the eastern parts of the mines at what they interpreted as the base of the sedimentary sequence. Patton and Cheney (1971) noted that the conglomerate is distinctive for clasts of andesite, plutonic rock, quartz, and biotite gneiss. Though exposure here is limited, this conglomerate contains white quartz pebbles that may have eroded from bodies of pegmatite that are abundant in the Swakane Biotite Gneiss, on the northeast side of the Entiat Fault, 10 km north of here.

Continue another 0.3 mi (500 m) to where the road reaches a saddle in the ridge. From here, turn onto an unmaintained boot path northwest toward the protruding outcrops of Rooster Comb rhyolite at the top of the hill. At the base of Rooster Comb, before the boot path starts steeply up the hill, 250 ft (50 m) from leaving the road, examine the outcrop on the left.

STOP 5:
Hydrothermal Breccia
+47.38879, -120.31898

This breccia contains angular clasts of flow-layered Rooster Comb rhyolite in a dark gray to black matrix. Smith and Calkins (1904) and Margolis (1987, 1989) identified Rooster Comb as tuff, possibly an ash flow from a nearby vent based on volcanic rock in drill cores from 2–4 km south. The clasts are lapilli-size, 2–64 mm, but we think this is part of a dike, rather than erupted pyroclastic rock. Clasts in the breccia consist of angular pieces of what appear to be flow layers of Rooster Comb rhyolite. Broken fragments of the same rhyolite layer can be seen in hand samples and veins of the dark matrix cut across clasts of the layered rhyolite. A pyroclastic breccia would normally contain more disrupted clasts. We interpret this breccia as a hydrothermal feature.

About 75 ft north up the path is a zone of friable gray perlite that weathers into a grus made of spherulites, hydrated glass, and possibly remnants of weathered phenocrysts.

From the perlite, continue northwest on the boot path, stopping to look at outcrops of flow-banded rhyolite near the perlite. Continue another 150 ft northwest to the base of the vertical Rooster Comb promontories and another 150 ft southwest to the base of the highest-elevation promontory.

STOP 6:
Summit of Rooster Comb
+47.38924, -120.318301

Stay back from the steep slopes and chutes between the rock towers that drop precipitously, to the north and west. Features to observe here include near-vertical flow banding, which is cut by more shallowly dipping platy jointing, the weathering and possible alteration of the rock, the chute-like structures between the teeth of the comb, and panoramic views of the region.

See the Rooster Comb section of Emplacement of the Wenatchee Pinnacles, above. Contacts between the Rooster Comb igneous body and the rock bodies next to it are not visible on the surface as far as we know.

Questions to consider include:

- Is Rooster Comb part of a set of erupted volcanics that include volcanic breccia and ash flow tuff (Smith and Calkins, 1904; Margolis, 1989), or a dike (the prevailing opinion)?

- Is flow layering a correct interpretation of the pervasive vertical to subvertical layering? What is the origin of the flow layering? What other joint sets are there?

- How petrologically similar is Rooster Comb to Wenatchee Dome?

REFERENCES

Cameron, D.E., 1994, The Cannon gold mine and its surface outcrop, Wenatchee, Washington, *in* Margolis, J., ed., Epithermal gold mineralization, Wenatchee and Liberty Districts, Central Washington: Society of Economic Geologists, Guidebook Series, v. 20, p. 32–35.

Chappell, W.M., 1936, Geology of the Wenatchee quadrangle, Washington: Doctoral dissertation, Seattle, University of Washington, 250 p.

Cheney, E.S., and Hayman, N.W., 2009, The Chiwaukum Structural Low: Cenozoic shortening of the central Cascade Range, Washington State, USA: Geological Society of America Bulletin, v. 121, p. 1135–1153.

Cheney, E.S., and Hayman, N.W., 2010, The Chiwaukum Structural Low: Cenozoic shortening of the central Cascade Range, Washington State, USA: Reply: Geological Society of America Bulletin, v. 122, p. 2103–2108.

Coombs, H.A., 1952, Spherulitic breccias in a dome near Wenatchee, Washington: American Mineralogist, Journal of Earth and Planetary Materials, v. 37, p. 197–206.

Donaghy, E.E., Umhoefer, P.J., Eddy, M.P., Miller, R.B., and LaCasse, T., 2021, Stratigraphy, age, and provenance of the Eocene Chumstick basin, Washington Cascades: Implications for paleogeography, regional tectonics, and development of strike-slip basins: Geological Society of America Bulletin, v. 133, no. 11–12, p. 2418–2438.

Eddy, M.P., Bowring, S.A., Umhoefer, P.J., Miller, R.B., McLean, N.M., and Donaghy, E.E., 2016, High-resolution temporal and stratigraphic record of Siletzia's accretion and triple junction migration from nonmarine sedimentary basins in central and western Washington: Geological Society of America Bulletin, v. 128, no. 3-4, p. 425–441.

Eddy, M.P., Umhoefer, P.J., Miller, R.B., Donaghy, E.E., Gundersen, M., and Senes, F.I., 2017, Sedimentary, volcanic, and structural processes during triple-junction migration: Insights from the Paleogene record in central Washington, *in* Haugerud, R.A., and Kelsey, H.M., From the Puget Lowland to East of the Cascade Range: Geologic Excursions in the Pacific Northwest, Geological Society of America Field Guides, v. 49, p. 143.

Evans, J.E., 1988, Depositional environments, basin evolution and tectonic significance of the Eocene Chumstick Formation, Cascade Range, Washington: Doctoral dissertation, Seattle, University of Washington, 326 p.

Evans, J.E., 1994, Depositional history of the Eocene Chumstick Formation: Implications of tectonic partitioning for the history of the Leavenworth and Entiat–Eagle Creek fault systems, Washington: Tectonics, v. 13 no. 6, p. 1425–1444.

Gilmour, L.A., 2013, U/Pb ages of Eocene and younger rocks of the eastern flank of the central Cascade Range, Washington, USA: Master's thesis, Seattle, University of Washington, 48 p.

Gresens, R.L., 1983, Geology of the Wenatchee and Monitor quadrangles, Chelan and Douglas Counties, Washington: State of Washington: Department of Natural Resources, Division of Geology and Earth Resources, 75 p. plus maps and cross-sections.

Gresens, R.L., Naeser, C.W., and Whetten, J.W., 1980, Stratigraphy and age of the Chumstick and Wenatchee Formations: Tertiary fluvial and lacustrine rocks, Chiwaukum Graben, Washington: GSA Bulletin 1981, v. 92, p. 841–876.

Haugerud, R., and Stanton, K., 2022, Chumstick Formation: Northwest Geology, Tobacco Root Geological Society, this volume.

Johnson, S.Y., 1985, Eocene strike-slip faulting and nonmarine basin formation in Washington, *in* Biddle, K.T., and Christie-Blick, N., eds., Strike slip deformation, basin formation, and sedimentology: Society of Economic Paleontologists and Mineralogists, Special Publication 37, p. 283–302.

Lovitt, E.H., and Skerl, A.C., 1958, Geology of the Lovitt Gold Mine, Wenatchee, Washington: Mining Engineering, September 1958, p. 63–66.

Margolis, J., 1987, Structure and hydrothermal alteration associated with epithermal Au-Ag mineralization, Wenatchee Heights, Washington: Master's thesis, Seattle, University of Washington, 90 p.

Margolis, J., 1989, Arkose-hosted, aquifer-controlled, epithermal Au-Ag mineralization, Wenatchee, Washington: Economic Geology, v. 84, no. 7, p. 1891–1902.

Ott, L.E., 1988, Economic geology of the Wenatchee mining district, Chelan County, Washington: Doctoral dissertation, Boise, University of Idaho, 270 p.

Ott, L.E., Groody, D., Follis, E.L., Siems, R.L., and Macdonald, A.J., 1986, Stratigraphy, structural geology, ore mineralogy, and hydrothermal alteration at the Cannon Mine, Chelan County, Washington, *in* McDonald, J., ed., Gold '86: An International Symposium of the Geology of Gold Deposits, Toronto, Ontario, v. 86, p. 22–31.

Patton, T.C., and Cheney, E.S., 1971, L-D gold mine, Wenatchee, Washington: New structural interpretation and its utilization in future exploration: Society of Mining Engineers Transactions, v. 250, p. 6–11.

Price, B.J., 2007, Technical report on Compton & Matthews Gold Properties, Wenatchee Area, Washington State, USA, for Kimberly Gold Mines.

Smith, J.V., 2002, Structural analysis of flow-related textures in lavas: Earth-Science Reviews 57, no. 3–4, 279–297.

Smith, G.O., and Calkins, F.C., 1904, A geologic reconnaissance across the Cascade Range near the forty-ninth parallel: U.S. Geological Survey, Bulletin 235, 103 p.

Tabor, R.W., Waitt, R.B., Frizzell, V.A., Swanson, D.A., Byerly, G.R., and Bentley, R.D., 1982, Geologic map of the Wenatchee 1:100,000 quadrangle, central Washington: U.S. Geological Survey, Miscellaneous Geologic Investigations Map I-1331.

Tepper, J.H., White, A.V., and Dawes, R.L., 2022, Petrology, geochronology, and changing tectonic setting of Eocene–Miocene magmatism near Wenatchee, Central Cascades, Washington: Northwest Geology, Tobacco Root Geological Society, this volume.

White, A.V., Tepper, J.H., and Dawes, R.L., 2021, Geochemistry and petrology of Eocene to Miocene rocks in a rear-arc setting, central Cascades, Washington: Geological Society of America Abstracts with Programs, v. 53, no. 6.

Willis, C.L., 1953, The Chiwaukum graben, a major structure of central Washington: American Journal of Science, v. 251, p. 789–797.

CHELAN MIGMATITE COMPLEX, WASHINGTON: MAFIC MAGMATISM AND CRUSTAL RECYCLING AT THE DEEP LEVELS OF A CONTINENTAL MAGMATIC ARC

Chris G. Mattinson,[1] Megan Kjelland,[1,2] and Erin K. Shea[3]

[1]*Geological Sciences, Central Washington University, Ellensburg, Washington*
[2]*Washington Geological Survey, Olympia, Washington*
[3]*Bishop, California*

INTRODUCTION

This field trip investigates the Chelan Migmatite Complex (CMC), which we interpret to represent one of the few localities in the world where the deep crustal melt processing zone of a continental magmatic arc is exposed for study. We will visit localities that preserve different parts of the CMC's history, discuss our new field, age, and isotopic data, and consider potential relationships between the CMC and the adjacent Okanogan Range batholith. All field trip stops are easily accessed roadcuts that are within a short walk of where we will park.

GEOLOGIC BACKGROUND

The North Cascades crystalline core (Cascades core) is located at the southern end of the Coast Plutonic Complex, the remnants of a Cretaceous and Paleogene magmatic arc, and records a history of mid-Cretaceous shortening, metamorphism, and plutonism, and Eocene transtension and plutonism (fig. 1; Haugerud and Tabor, 2009; Miller and others, 2009). Together, the Coast Plutonic Complex and the Cascades core form a plutonic and metamorphic belt that extends over 1,500 km from southeast Alaska to northern Washington. In southern British Columbia and Washington, this belt is expressed as arc plutons intruding Upper Paleozoic to Cretaceous oceanic and arc terranes of the Coast belt, which bridges the

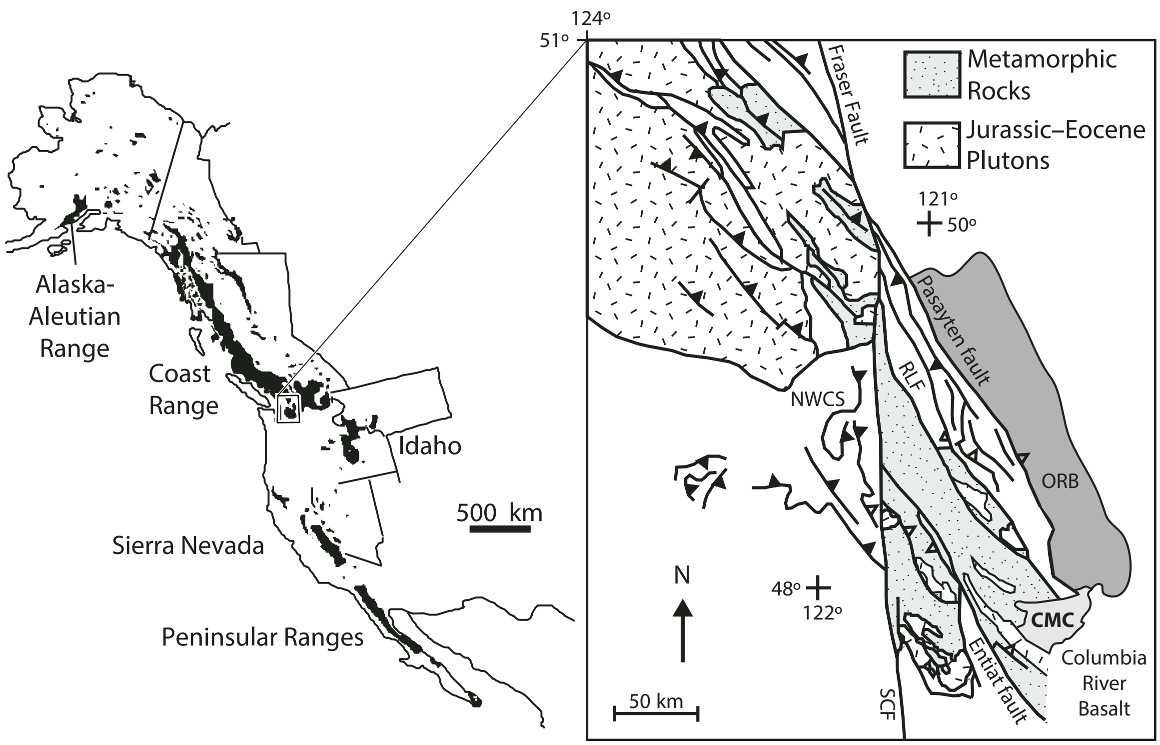

Figure 1. Generalized map of Mesozoic and Paleogene Cordilleran arc plutons adapted from Miller and others (2009). Inset illustrates the location of the Chelan Migmatite Complex (CMC) and Okanogan Range batholith (ORB) relative to metamorphic rocks and plutons in the Cascades core and the southern Coast belt. Locations of the Northwest Cascades thrust system (NWCS), Fraser–Straight Creek fault (SCF), Ross Lake fault zone (RLF), and Pasayten fault are shown.

boundary between the Insular and Intermontane superterranes (Journeay and Friedman, 1993).

The tectonic history of the North Cascades has resulted in the exposure of a variety of crustal levels, making the region ideal for the study of both deep- and shallow-crustal processes. The southern part of the Cascades core exposes deeply exhumed metaplutonic migmatites of the CMC (Hopson and Mattinson, 1994) juxtaposed with trondhjemitic plutonic rocks of the Okanogan Range batholith (Stoffel and others, 1991; Hurlow and Nelson, 1993). Both the CMC and the Okanogan Range batholith give Early Cretaceous U-Pb zircon dates (Mattinson, 1972; Hurlow and Nelson, 1993; Mattinson and others, 2014; Busk, 2019; Kjelland and others, 2020), suggesting contemporaneous partial melting and magmatic activity. We are currently investigating the hypothesis that the Okanogan Range batholith was fed by melts derived from the CMC.

THE CHELAN MIGMATITE COMPLEX

The CMC is an assemblage of metatonalite and metaplutonic migmatite with abundant synplutonic mafic dikes, trondhjemitic leucosomes, and metaultramafic rock (peridotite, pyroxenite, hornblendite) that covers ~900 km^2 in north-central Washington (figs. 1, 2). The CMC is bounded to the north by the Triassic metasedimentary/metaigneous Cascade River–Holden–Twentyfive Mile Creek–Alta Lake units. The western margin of the CMC is intruded by the Eocene Duncan Hill pluton and the Late Cretaceous Entiat pluton, and the southern boundary of the complex is covered by the Miocene Columbia River basalt. In the northeast, the CMC is in contact with the Okanogan Range batholith (fig. 2). Preliminary field studies suggest the nature of this contact appears intrusive and highly complex (Busk, 2019).

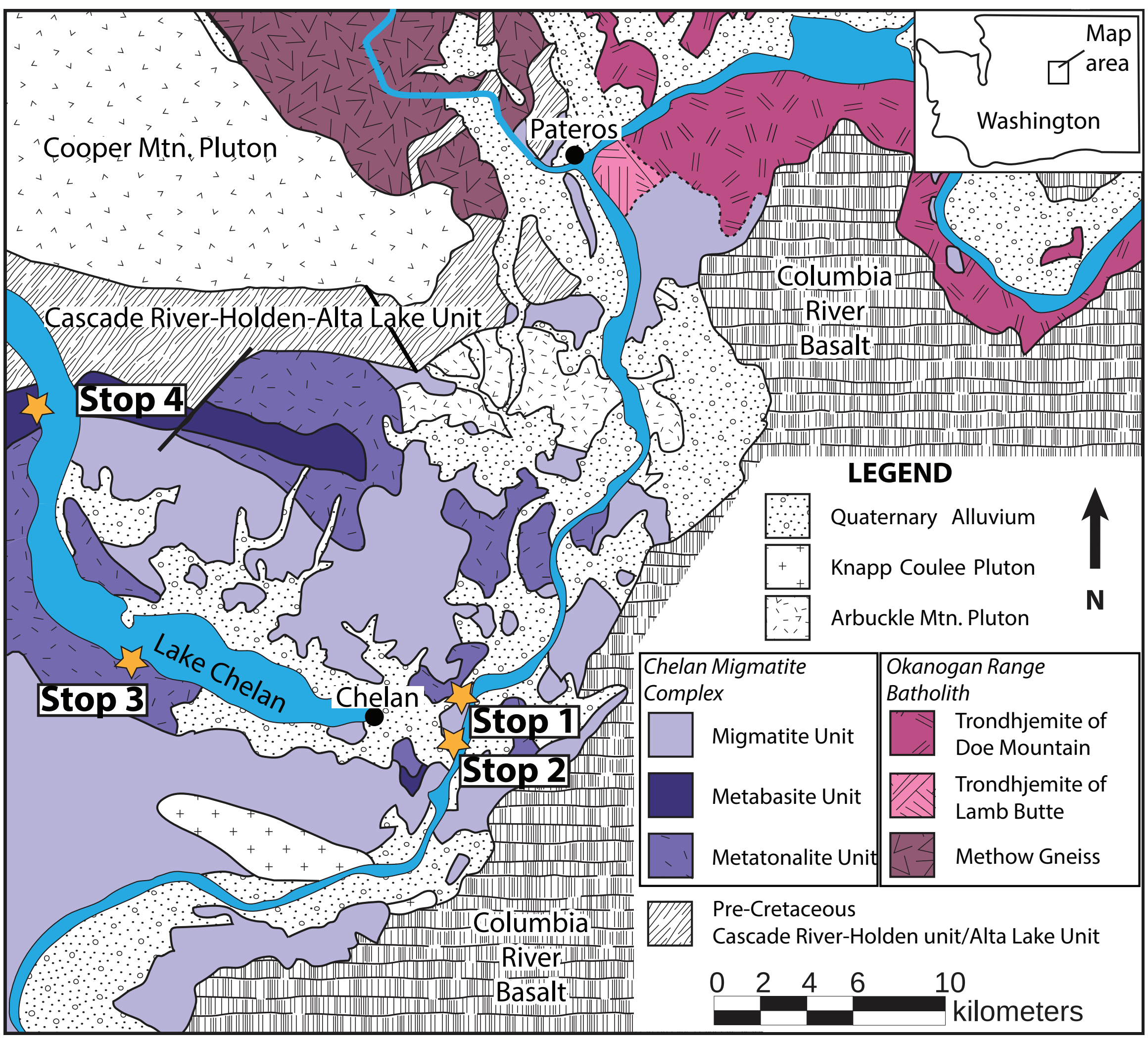

Figure 2. Geologic map emphasizing subdivisions of the Chelan Migmatite Complex (purple shades) and the Okanogan Range batholith (pink shades), showing field trip stops. Towns are indicated by black circles. Modified from Stoffel and others (1991) and Hopson and Mattinson (1994).

Table 1. Chelan Migmatite Complex mafic magma stages (modified from Hopson and Mattinson, 1994).

Stage	Description	Interpretation
MM1	Brittlely disrupted mafic and ultramafic blocks	Pre-anatectic mafic intrusions and associated cumulates, disrupted by later flow of anatectic tonalite
MM2	Layered migmatite and concordant mafic bodies, cut by leucosomes and MM3 dikes	Comingled mafic/intermediate magma, silicic partial melts, and anatectic tonalite
MM3	Mafic to intermediate dikes (cut some leucosomes, cut by others)	Migration of mafic melts (and differentiates) into solidifying tonalite with lower melt fraction, mingling of mafic and silicic melts

Mapping and geochronology of the CMC by Mattinson (1972), Tabor and others (1987), and Hopson and Mattinson (1994) defined the CMC and subdivided it into three map units: metatonalite, metabasite, and migmatite (fig. 2; Hopson and Mattinson, 1994). The widespread metatonalite represents the migmatite's paleosome, which hosts all other related rocks, i.e., the locally abundant mafic intrusive rocks (now amphibolite), and the volumetrically minor but ubiquitous silicic leucosomes. The mafic rocks invade the metatonalite in three main stages (MM1–MM3; table 1), and serve to distinguish the CMC from adjacent units, which lack these multiple stages of mafic magmatism. The leucosomes range from leucotrondhjemite to leucogranite, occur as irregular small bodies (fracture fillings, etc.), and are interpreted to represent the final crystallization of partial melts that were extracted from the metatonalite.

Hopson and Mattinson (1994) and Mattinson and others (2014) have suggested that the CMC formed by a multi-stage process involving the >117 Ma injection of mafic magma beneath and into a Jurassic–Triassic paleosome (the metatonalite unit), causing heating and partial melting of the paleosome to produce the migmatite unit. In contrast, Dessimoz and others (2012) conducted a petrographic and geochemical study of the CMC with particular emphasis on outcrops of the metabasite unit and concluded that the CMC represents the products of amphibole fractionation at the base of the Cretaceous arc, without significant assimilation. While this model can explain geochemical trends, the work of Mattinson and others (2014) suggests that the CMC is an assemblage of intrusions that span over 30 Myr, calling into question the genetic correlations that are assumed by Dessimoz and others (2012). Field observations, the widespread presence of inherited zircon, and zircon trace element data suggest that assimilation of paleosome tonalite, fractional crystallization of intruded mafic melts, and magma mixing all contributed to the formation of the CMC. Further work is needed to integrate geochemical interpretations with geochronology and field observations in order to establish the relationships between different units in the complex.

Thermobarometry on four samples of metatonalite from the CMC and on two samples of garnet amphibolite from the adjacent Twentyfive Mile Creek unit indicate that both equilibrated to conditions of ca. 700–800°C and 7–9 kbar, suggesting depths of ~30 km, interpreted to represent the final juxtaposition of the CMC and Twentyfive Mile Creek units, and solidification of the CMC (fig. 3; Mattinson, 2011). These deep crustal conditions are supported by the presence of kyanite in the Twentyfive Mile Creek unit, rutile in some mafic CMC samples, and magmatic epidote in

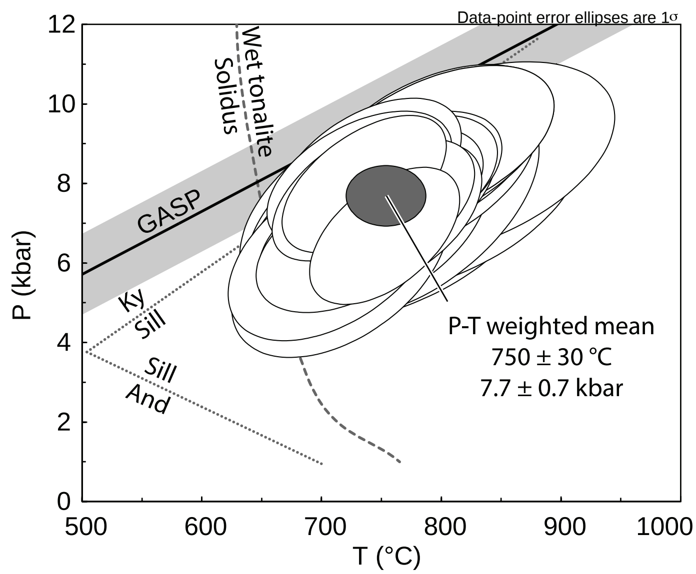

Figure 3. Pressure–temperature calculations from four samples of garnet-bearing metatonalite from the Chelan Migmatite Complex and on two samples of garnet amphibolite from the Twentyfive Mile Creek unit (27 average P-T calculation results shown; Mattinson and others, 2011). GASP, garnet–kyanite–silica–plagioclase barometry of one kyanite-bearing Twentyfive Mile Creek unit sample. Wet tonalite solidus from Lambert and Wyllie (1974), aluminosilicate diagram from Holdaway and Mukhopadhyay (1993). Abbreviations: Ky, kyanite; Sill, sillimanite; And, andalusite.

CMC metatonalite. Field relations suggest domal rise of the CMC into the now-adjacent wall rocks, so CMC textures are interpreted to record processes that occurred at ~30 km and deeper.

CMC GEOCHRONOLOGY AND Hf ISOTOPES

Zircons from the CMC are typified by complex internal zoning visible in cathodoluminescence (CL) images, and our new LA-ICP-MS geochronology for the CMC reveals far more detail than was possible from previous multigrain TIMS analyses (figs. 4, 5). Paleosome ages are dominantly Jurassic (~160–180 Ma) and are represented by entire grains and as resorbed cores overgrown by Cretaceous rims; Triassic zircons (230–250 Ma) are also present in several samples. Cretaceous ages define three peaks that we interpret to record the ~30 Myr timespan when the CMC was partially molten (fig. 5). We infer the 112–117 Ma peak to represent early migmatization, and the number of samples containing these dates suggests that partial melt was widespread by this time. The 112–117 Ma zircon population includes both analyses from oscillatory-zoned whole grains and rims on inherited cores. This early migmatization was likely associated with (undated) MM1 and MM2. We interpret the ~100 Ma peak to represent the intrusion and associated partial melting associated with the quartz diorite

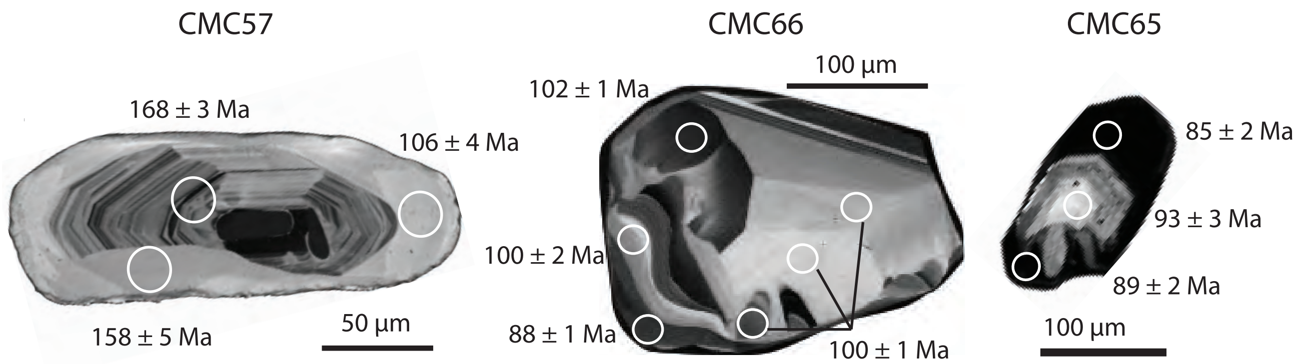

Figure 4. Zircon cathodoluminescence images with LA-ICP-MS spot locations for samples from Stop 1 (Kjelland and others, 2019, 2020).

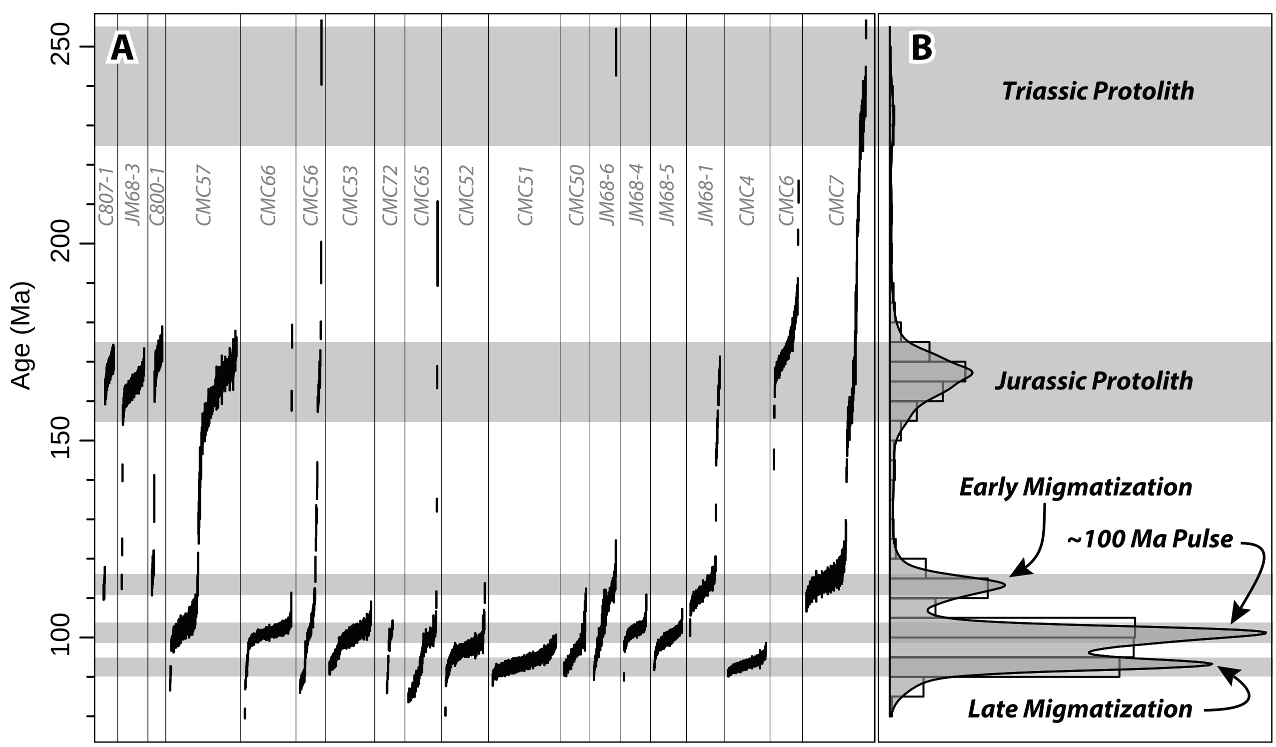

Figure 5. Compiled LA-ICP-MS zircon U-Pb geochronology data from the Chelan Migmatite Complex. (A) Age spectra for each sample; error bars show 2σ uncertainty on individual spot measurements. (B) Kernel density estimate (Vermeesch, 2018) of all analyses (n = 1618). Data from Mattinson and others (2014) and Kjelland and others (2019, 2020).

gneiss bodies observed in the eastern CMC (the area of stops 1 and 2); so far we have not found this age peak in samples from other areas. The quartz diorite gneiss bodies cut MM2 banded migmatite, but are cut by MM3. The ~94 Ma peak is seen in MM3 as well as leucosomes, and we interpret this age to record the last stage of major mafic magma intrusion. The youngest ages recorded in most samples are ~88–90 Ma, which we interpret to record the last stages of melt crystallization and final juxtaposition of the CMC with its wall rocks.

Populations in the Hf isotope data are defined based on age, trace element pattern, CL, and Hf isotope value. Jurassic and Triassic zircons record values in the juvenile to intermediate arc fields, consistent with an origin in a less evolved magmatic arc (fig. 6). Around 100–115 Ma, Hf isotope values drop sharply. The Hf isotope data do not correlate with sample SiO_2, suggesting crustal assimilation does not explain the trend, but introduction of subducted sediments into the melt source region could. The strong ~100 Ma isotopic shift in the CMC may correlate with the major deformation within magmatic arcs and mélange belts up and down the North American Cordillera that has been interpreted to reflect the ~100 Ma collision of the Insular Superterrane with the North America margin (Journeay and Friedman, 1993; Tikoff and others, 2021). Younger CMC analyses show a strong trend towards more juvenile values, suggesting that the CMC system changed back towards the isotopic value of the host metatonalite as the system cooled and crystallized.

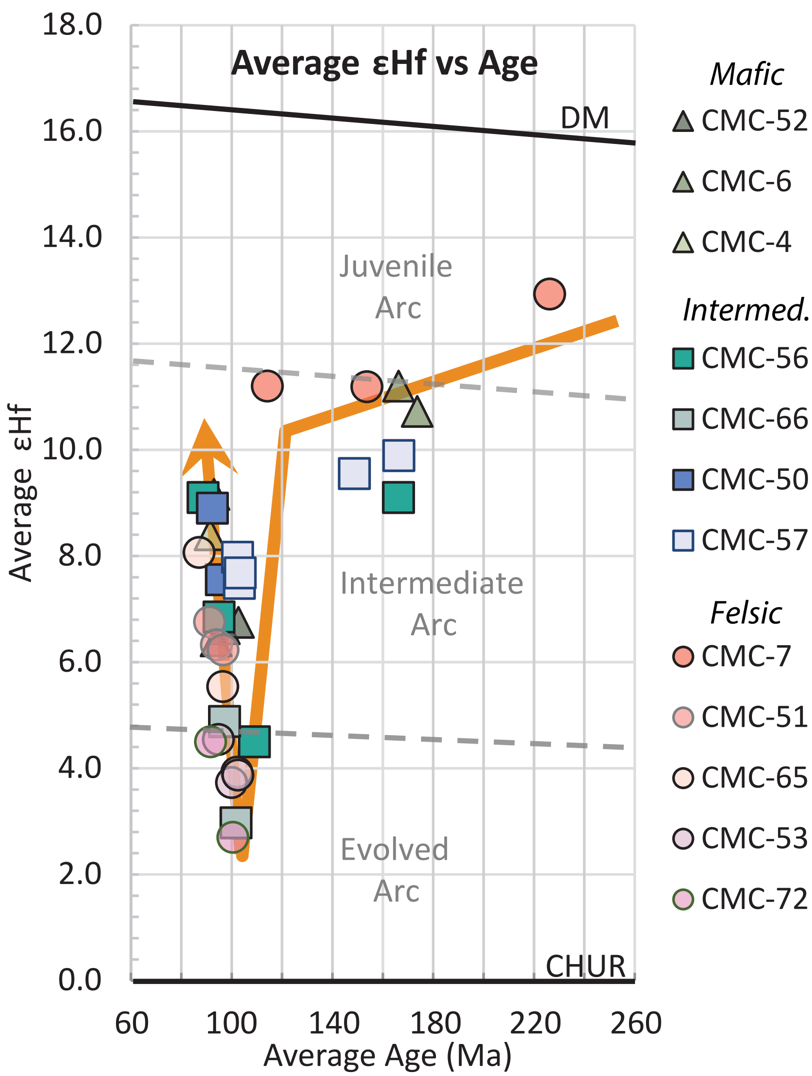

Figure 6. Zircon Hf isotope data from the Chelan Migmatite Complex (Kjelland and others, 2020). Orange trend line shows interpreted isotopic evolution; line slope >120 Ma follows average crustal evolution trend (Gehrels and Pecha, 2014). Values for CHUR (chondritic uniform reservoir), DM (depleted mantle), and boundaries for juvenile, intermediate, and evolved arcs follow Gehrels and Pecha (2014).

POTENTIAL RELATIONSHIP BETWEEN THE CMC AND OKANOGAN RANGE BATHOLITH

The CMC is spatially part of the Cascades Crystalline Core, but is significantly older than other North Cascades Cretaceous plutons (96 Ma and younger; Miller and others, 2009). However, CMC ages do significantly overlap with the Okanogan Range batholith to the northeast. Geochronology from the Okanogan Range batholith indicates crystallization contemporaneous with the major period of melting in the CMC (~118–105 Ma; Busk, 2019). Intriguingly, zircons from the Okanogan Range batholith show similar-age Jurassic cores to those found in CMC samples, possibly indicating a genetic relationship with the CMC. Field observations of the contact region between the CMC and Okanogan Range batholith suggest an intrusive relationship, without a major fault or shear zone separating the two units (Busk, 2019). We therefore suggest that the Okanogan Range batholith may have derived melts from the deep crustal melt processing zone represented by the CMC, but further field, petrologic, and isotopic work is required to test this hypothesis.

ROAD LOG

Figure 7 shows roads and field trip stop locations. Zero odometers at Chelan County Expo Center, drive north on Wescott Dr, then right on Sunset Hwy for 1.3 mi, then left on Division St, then right on Cottage Ave at the traffic circle. Turn right on US 97 north/ US 2 east to Stop 1 (~50 min, 44 mi). At Wenatchee, cross the Columbia and follow US 97 north (first left after the bridge). At the highway interchange, we cross the Entiat Fault, and enter the Swakane Gneiss; outcrops continue for ~8 mi. US 97 re-crosses the Columbia at Beebe bridge; continue 1.2 mi and park at the prominent roadcut on the east side of US 97 (mile marker 236 is at the north end of the pullout).

Optional bathroom stop at Beebe Springs Natural Area, 0.5 mi past Beebe bridge, on right.

STOP 1:
Migmatite of CMC Migmatite Map Unit
Odometer 46.5 mi; N47° 49.76', W119° 58.21'

Examine migmatite at the south end of the roadcut. This outcrop nicely displays metatonalite, quartz diorite gneiss, MM3, and trondhjemitic and granitic leucosomes; Eocene mafic dikes are also present. Note the mottled texture of the MM3 dike, interpreted to represent magma mingling. This outcrop was mapped and sampled in detail (fig. 8; Kjelland and others 2019, 2020), and records most of the major age and Hf isotope relationships of the CMC (figs. 5, 6). Minor sulfides are distributed throughout the outcrop; many are associated with epidote-filled fractures, but some sulfides appear to be magmatic. Bell and others (2021) investigated sulfides in the quartz diorite gneiss, and interpreted

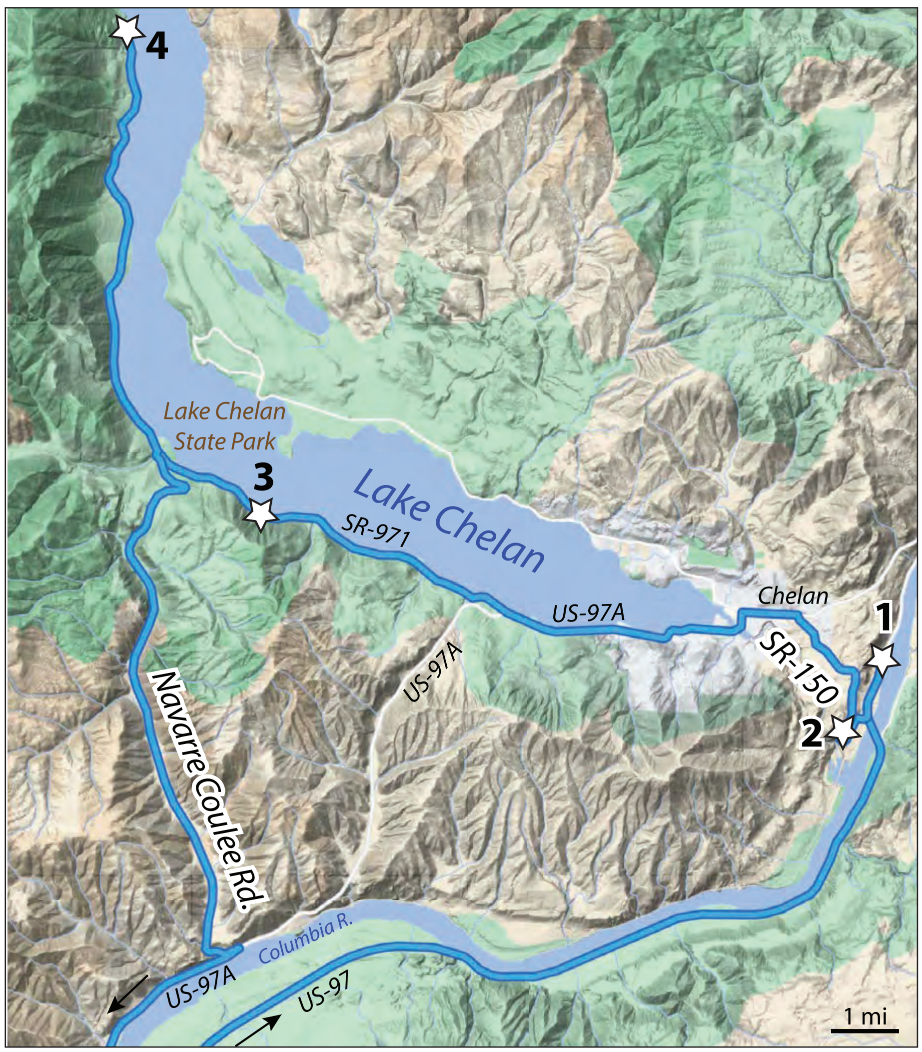

Figure 7. Road map of field trip stops.

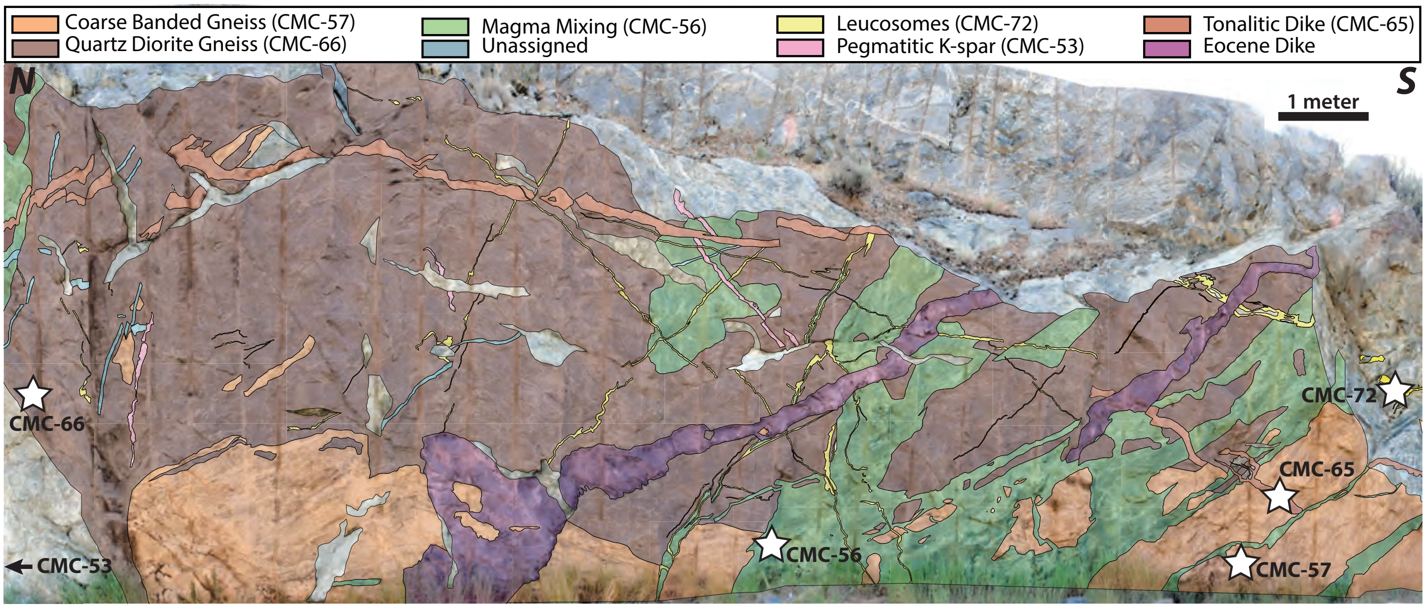

Figure 8. Outcrop map of Stop 1. Uncolored areas within the mapped area are slickensided fault surfaces. The 'unassigned' unit has a texture similar to both the tonalitic dike and magma mixing units. Stars show sample locations; sample CMC-53 was collected north of the mapped outcrop face. Modified from Kjelland and others (2019).

that pyrite crystallized first, followed by minor chalcopyrite that partially replaced pyrite as well as forming small individual grains in the matrix. Both sulfides were subsequently partially replaced by rims of iron oxides (goethite and magnetite), except where sulfides were included within silicate minerals.

Optional bathroom stop at Beebe Springs Natural Area, on left.

Return south on US 97 0.9 mi to SR 150 junction, turn west onto SR 150, cross railroad tracks, and drive up SR 150 to hairpin curve; park on shoulder 0.15 mi above this curve. Watch for traffic when crossing road!

STOP 2:
Layered migmatite of CMC Migmatite Map Unit
Odometer 48.1 mi; N47° 48.87', W119° 58.98'

Examine 200 m of roadcut between the yellow road sign on the west, and the curve beyond prominent Eocene mafic dikes on the east. The outcrop exposes metatonalite, major MM2 layers, minor MM1 and MM3 bodies, and leucosomes. Pay special attention to the cross-cutting relationships among the different rocks, especially the distinctions among MM1–MM3, and the significance of concordant vs. discordant layers. Sample JM68-6 was collected from leucosome at this locality and zircons record ages of 115–90 Ma (fig. 5).

Continue 2.2 mi on SR 150, turn left at junction with US 97A, and follow US 97A signs through Chelan. Turn right at junction with SR 971 (4.7 mi; Pat & Mike store). Continue west on SR 971 4.2 mi, and park just beyond clump of trees at the Bus Memorial. Watch for traffic when crossing road!

STOP 3:
Mafic synplutonic dikes and leucosomes, CMC Metatonalite Map Unit
Odometer 59.2 mi; N47° 51.68', W120° 10.17'

Examine 200 m of roadcut west from the Bus Memorial, containing metatonalite, MM3, and leucosomes. This outcrop contains good examples of the metatonalite unit in addition to mafic to intermediate dikes. Sample JM68-1 was collected from the metatonalite, and sample CMC4 was collected from a MM3 mafic dike. What are the relationships between the leucosomes and the mafic layers and dikes? What do the deformation styles of the mafic rocks suggest about the relative ages?

Carefully recross road to vehicles, and continue west on SR 971, pass junction with Navarre Coulee Rd. just beyond Lake Chelan State Park entrance (1.8 mi), continue on S. Lakeshore Rd. for 6.7 mi, and park on right in wide roadside parking space by prominent roadcuts on both sides of the road.

Optional bathroom stop at Lake Chelan State Park, just past junction with Navarre Coulee Rd., on right.

STOP 4:
Pressure–temperature constraints, CMC Metabasite Map Unit
Odometer 67.7; N47° 57.81', W120° 12.66'

Inspect CMC amphibolite and tonalite gneiss in roadcuts near parking strip. Note concordant amphibolite layers within tonalite, and minor garnet (mainly within tonalite, but locally within amphibolite). Samples CMC6 (amphibolite) and CMC7 (garnet tonalite) were collected from this site. Pressure–temperature estimates based on reactions among garnet, amphibole, plagioclase, and quartz from this locality as well as from the adjacent Twentyfive Mile Creek unit yield 7–9 kbar, ~750 °C (fig. 3). These pressures correspond to ~30 km depth, and calculated temperatures are consistent with experimentally determined tonalite solidus temperatures. Felsic and mafic Eocene dikes cut the outcrop. The contact with the Twentyfive Mile Creek Unit is ~200 m west, but is not well exposed.

Turn around and return 6.7 mi to junction with Navarre Coulee Road (SR 971).

Optional bathroom stop at Lake Chelan State Park, just past junction, on left.

Head up SR 971 (away from the lake); the highest point on SR 971 marks the glacial highstand of Lake Chelan, when Navarre Coulee was the outlet for Glacial Lake Chelan. Continue south on SR 971 for 9 mi, turn right at junction with US 97A, and continue for 23 mi.

Geologic features along the drive: after 4.9 mi, we pass Earthquake Point, where a landslide triggered by the 1872 magnitude ~7.2 earthquake temporarily blocked the Columbia River. This is also a good place to observe features of the 72 Ma Entiat pluton in the boulders at the base of the cliff. About 1 mi after crossing the Entiat River, we cross a poorly exposed strip (~0.2 mi) of the Napeequa unit, then enter outcrops of the Swakane Gneiss. Observe the cross-cutting relationships in the outcrops along the right (W) side of the highway. See Miller and others (2009) for a description of a stop at the viewpoint 1.8 mi before Rocky Reach Dam.

At Wenatchee, follow signs for US 97 south/US 2 west. After 6.7 mi (just past the Cashmere gas station), turn left onto Cotlets Way/Cottage Ave. At the traffic circle, turn south on Division St., then right on Sunset Hwy. Continue for 1.3 mi, then turn left on Wescott Dr. to return to Chelan County Expo Center.

ACKNOWLEDGMENTS

We thank Cliff Hopson and Jim Mattinson for introducing us to the CMC; students Alexandra Busk, Sydney Souza, Kelley Wood, Jared Van Laethem, Rebecca Krohn, Rylynn Carney, Tessa Guthrie, Colton Bell, and Sam Eyassu for assistance in the field and lab; Angela Halfpenny and the Murdock Research Lab for assistance with CL imaging, and Matt Rioux and Andrew Kylander-Clark for assistance with LA-ICP-MS analysis at UC Santa Barbara. This research was supported in part by funding from the School of Graduate Studies and Research at Central Washington University, and the Yakima Rock and Mineral Club.

REFERENCES CITED

Bell, C., Eyassu, S., Mattinson, C.G., Kjelland, M., and Halfpenny, A., 2021, Evaluating the role of deep earth processes in mineral deposit formation, North Cascades, Washington: Geological Society of America Abstracts with Programs, v. 53, no. 6, doi: 10.1130/abs/2021AM-370875.

Busk, A.C., 2019, Petrologic relationship of deeply exhumed magmatic arc bodies on the southeastern edge of the North Cascades crystalline core, Washington: Insights into crustal evolution?: MS Thesis, University of Alaska Anchorage, 116 p.

Dessimoz, M., Müntener, O., and Ulmer, P., 2012, A case for hornblende-dominated fractionation of arc magmas: The Chelan Complex (Washington Cascades): Contributions to Mineralogy and Petrology, v. 163, p. 567–589.

Gehrels, G., and Pecha, M., 2014, Detrital zircon U-Pb geochronology and Hf isotope geochemistry of Paleozoic and Triassic passive margin strata of western North America: Geosphere, v. 10, p. 49–65.

Holdaway, M.J., and Mukhopadhyay, B., 1993, A reevaluation of the stability relations of andalusite: Thermochemical data and phase diagram for the aluminum silicates: American Mineralogist, v. 78, p. 298–315.

Hopson, C.A., and Mattinson, J.M., 1994, Chelan Migmatite Complex, Washington: Field evidence for mafic magmatism, crustal anatexis, mixing and protodiapiric emplacemnt, *in* Swanson, D.A., and Haugerud, R.A., eds., Geologic field trips in the Pacific Northwest: Seattle, Department of Geological Sciences, University of Washington, 1994 Geological Society of America Annual Meeting, p. 2K1–2K21.

Haugerud, R.A., and Tabor, R.W., 2009, Geologic map of the North Cascade Range, Washington: U.S. Geological Survey Scientific Investigations Map 2940, scale 1:200,000.

Hurlow, H.A., and Nelson, B.K., 1993, U-Pb zircon and monazite ages for the Okanogan Range batholith, Washington: Implications for the magmatic and tectonic evolution of the southern Canadian and northern United States Cordillera: Geological Society of America Bulletin, v. 105, p. 231–240.

Journeay, J.M., and Friedman, R.M., 1993, The Coast Belt thrust system: Evidence of Late Cretaceous shortening in southwest British Columbia: Tectonics, v. 12, p. 756–775.

Kjelland, M., Van Laethem, J.D., Krohn, R., Carney, R., Guthrie, T., Mattinson, C.G., Shea, E.K., and Kylander-Clark, A.R., 2019, The growth of new crust: Tracing the chemical and textural evolution of magma through multiple stages of magmatism, Chelan Migmatite Complex, North Cascades, Washington, *in* Proceedings 2019 Fall Meeting, American Geophysical Union, San Francisco, California, abstract V43F-0158.

Kjelland, M., Mattinson, C.G., Van Laethem, J., Krohn, R., Kylander-Clark, A., and Shea, E.K., 2020, Crustal growth at depth: Tracing the evolution of subduction related magmas through multiple stages of magmatism using Hf isotopes and textural relations, Chelan Migmatite Complex, North Cascades, Washington, USA: Geological Society of America Abstracts with Programs, v. 52, no. 6, doi: 10.1130/abs/2020AM-359119.

Lambert, I.B., and Wyllie, P.J., 1974, Melting of tonalite and crystallization of andesite liquid with excess water to 30 kilobars: Journal of Geology, v. 82, p. 88–97.

Mattinson, C.G., 2011, Thermobarometric constraints on the Chelan Migmatite Complex, North Cascades, Washington: Geological Society of America Abstracts with Programs, v. 43, no. 4, p. 77.

Mattinson, C.G., Mattinson, J.M., Rioux, M., and Hopson, C.A., 2014, A ~30 million year history of mafic magmatism and partial melting in the Chelan Migmatite Complex, North Cascade Range, Washington, USA: Geological Society of America Abstracts with Programs, v. 46, no. 6, p. 33.

Mattinson, J.M., 1972, Ages of zircons from the Northern Cascade Mountains, Washington: Geological Society of America Bulletin, v. 83, p. 3769–3784.

Miller, R.B., Gordon, S.M., Bowring, S.A., Doran, B.A., McLean, N.M., Michels, Z.D., Shea, E.K., Whitney, D.L., Wintzer, N.E., and Mendoza, M.K., 2009, Linking deep and shallow crustal processes in an exhumed continental arc, North Cascades, Washington, *in* O'Connor, J.E., Dorsey, R.J., and Madin, I.P., eds., Volcanoes to Vineyards: Geologic field trips through the dynamic landscape of the Pacific Northwest: Geological Society of America Field Guide 15, p. 373–406.

Stoffel, K.L., Joseph, N.L., Zurenko Waggoner, S., Gulick, C.W., Korosec, M.A., and Bunning, B.B., 1991, Geologic map of Washington–Northeast quadrant: Washington Department of Natural Resources, Division of Geology and Earth Resources Geologic Map GM-39.

Tabor, R.W., Frizzell, V.A. Jr., Whetten, J.T., Waitt, R.B., Swanson, D.A., Byerly, G.R., Booth, D.B., Hetherington, M.J., and Zartman, R.E., 1987, Geologic map of the Chelan 30-minute by 60-minute quadrangle, Washington: U.S. Geological Survey Miscellaneous Investigations Series, Map I-1661.

Tikoff, B., Housen, B., Maxson, J., Nelson, E., and Trevino, S.F., 2021, The 100 Ma oblique collision of the Insular terrane along western North America: Geological Society of America Abstracts with Programs, v. 53, no. 6, doi: 10.1130/abs/2021AM-371118.

Vermeesch, P., 2018, IsoplotR: A free and open toolbox for geochronology: Geoscience Frontiers, v. 9, p. 1479–1493.

GLACIAL GEOLOGY OF ICICLE CREEK, WASHINGTON

Kelsay M. Stanton

Washington Geological Survey, Olympia, Washington

This half-day field trip explores the evidence of late Pleistocene glacial episodes of the Icicle Creek valley glacier. This includes a ~3.2-mi moderate hike with approximately 1.5 mi having limited shade, and another approximately 0.5–0.75-mi easy hike, mostly in sun. We will discuss the glacial advances of the last ~300,000 yr as shown by lateral and terminal moraines. We will also look at glacial erosional features.

Table 1. Age of Icicle Creek glacial advances from Porter and Swanson, 2008.

Moraine	Oldest Date (yr)
Leavenworth I	17,000 ± 1,000
Leavenworth II	24,700 ± 1,100
Mountain Home	72,200 ± 1,200
Pre-Mountain Home	94,900 ± 3,100
Peshastin	112,800 ± 1,700
Boundary Butte	160,000+

INTRODUCTION

Icicle Creek drains the central Cascades and joins the Wenatchee River near the town of Leavenworth, Washington (figs. 1, 2). Several authors describe evidence of multiple alpine glacial advances through the late Pleistocene. Page (1939) used lateral and terminal moraines to surmise three stands of the Icicle Creek glacier, with at least one reaching the town of Peshastin, east and downstream of the Icicle Creek–Wenatchee River confluence. Later work further differentiated deposits and surmised several additional advances (Long and Porter, 1968; Porter, 1969; Waitt, 1977). Porter and Swanson (2008) used cosmogenic chlorine-36 (^{36}Cl) exposure dating to determine ages for boulders on Icicle Creek glacier moraines. They constrain the timing of at least five stands of the glacier (fig. 2). Studies mapping the location of erratics associated with the glacier support at least two pre-and-early Wisconsin stands that terminated beyond the confluence of Icicle Creek and Wenatchee River (Stanton and others, 2019; Yokel-Deliduka and Davis-Stanton, 2016).

At least two advances of the Icicle Creek glacier topped the northern end of Boundary Butte, terminating in the Wenatchee River valley near the town of Peshastin or further east: the Boundary Butte advance and the Peshastin advance (Page, 1939; Porter and Swanson, 2008). Boulders from the Boundary Butte advance are thoroughly weathered and cosmogenic dating was inconclusive. Porter and Swanson (2008) estimate the age of this advance to be at least 160,000 yr (table 1). Boulders of the Peshastin advance are also highly weathered, although many show only surface weathering. The oldest dated boulder provides an age of 112,800 ± 1,700 yr (Porter and Swanson, 2008). Two advances have less distinct lateral and end moraines: the pre-Mountain Home advance (oldest boulder 94,900 ± 3,100 yr) and the Mountain Home advance (oldest boulder 72,200 ± 1,400 yr). Both the Leavenworth I (oldest boulder 24,700 ± 1,100 yr) and the Leavenworth II advances (oldest boulder 17,000 ± 1,000 yr) show prominent lateral moraines along Boundary Butte (the topographic feature) with fresh, mostly unweathered boulders. They also have distinct terminal moraines within the town of Leavenworth (fig. 2).

Icicle Creek glacier lateral moraines are well preserved on Boundary Butte, near Leavenworth (fig. 2), where the degree of boulder weathering provides a relative age progression consistent with Porter and Swanson's (2008) dating. Glacial erosional features are prominent where Icicle Creek crosses the Leavenworth fault, likely influenced by changes in lithology across the fault. West of the fault the Icicle Creek drainage is underlain by granodiorite and tonalite of the Cretaceous Mount Stuart batholith and by various Mesozoic metamorphic and ultramafic units, while east of the fault the bedrock consists of sedimentary rocks of the Eocene Chumstick Formation (Tabor and others, 1982). The distinct change in lithology from sedimentary rocks to igneous and metamorphic rocks is marked by steeper topography and greater relief, by a narrower stream valley, and by glacial erosive features rather than depositional features west of the fault.

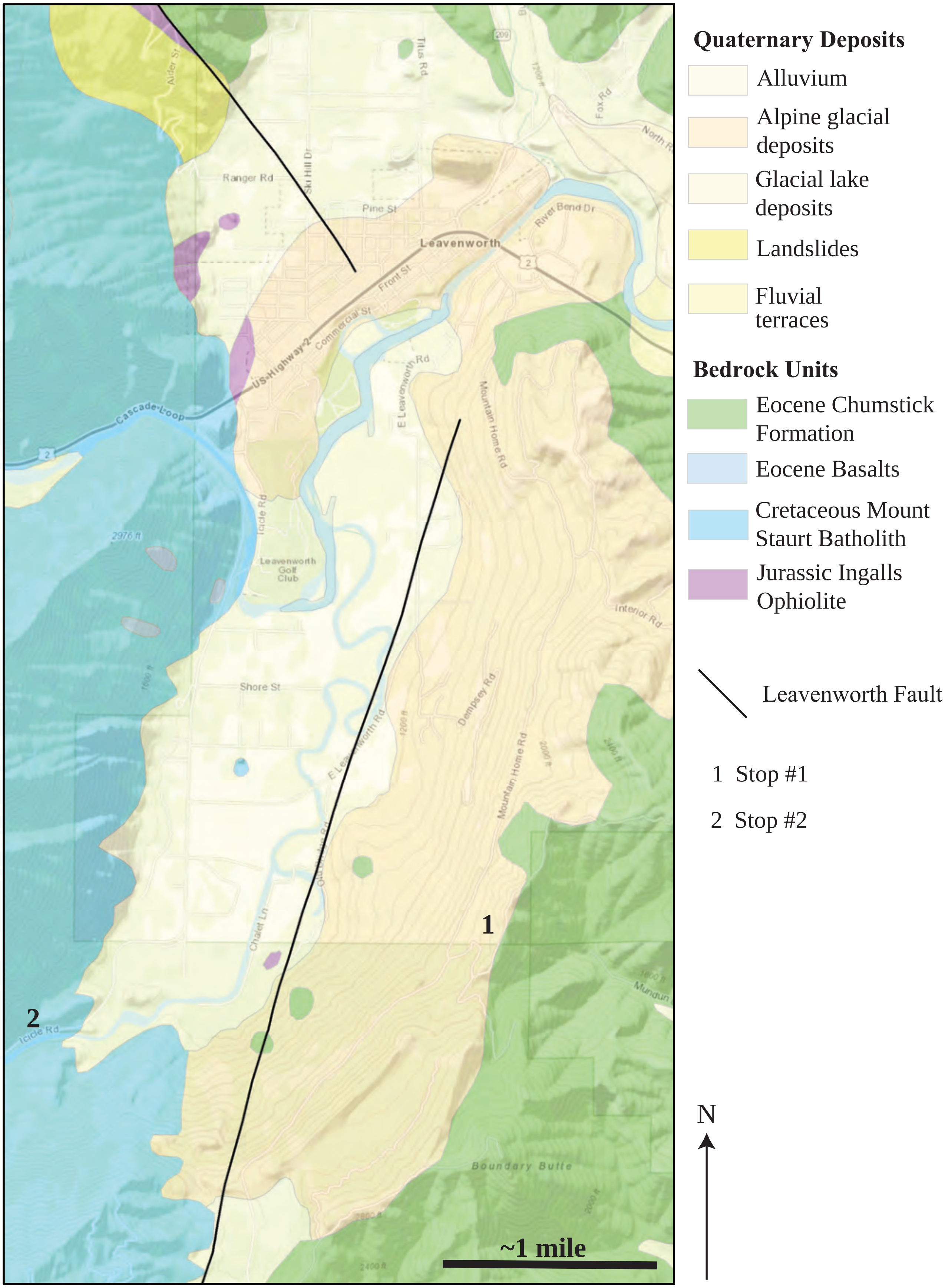

Figure 1. Geologic map of the Leavenworth, WA, area showing field trip stops.

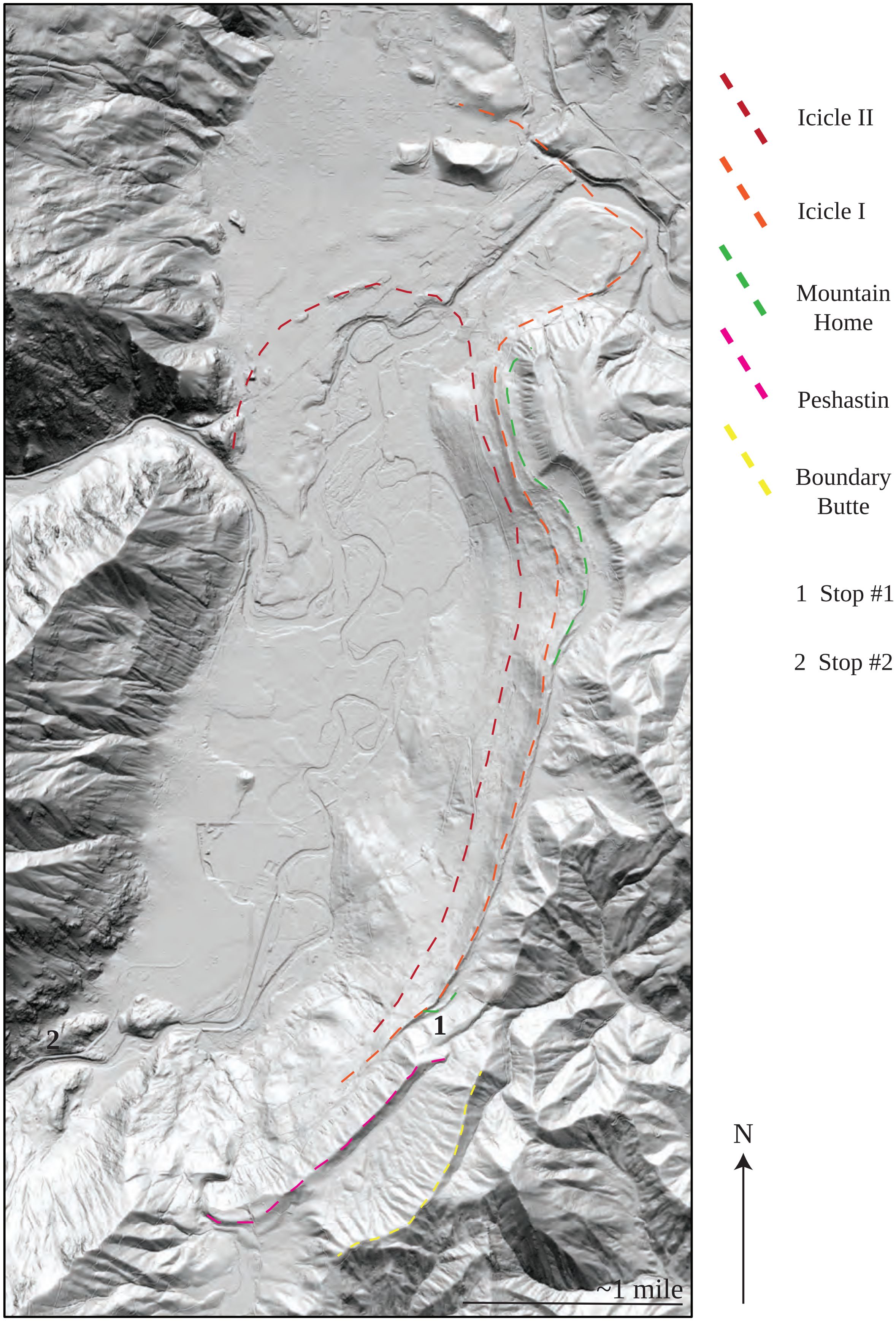

Figure 2. LiDAR imagery with glacial advances from Porter and Swanson (2008). Base map is 2015 and 2018 lidar with same map extent as figure 1.

ROAD AND TRAIL LOG

Mile 0.0 (47.5200, -120.4984)

Start at Chelan County Expo Center in Cashmere, WA. Drive north on Wescott Dr. for approximately 0.3 mi. Turn west (left) on Sunset Hwy briefly and take a slight right onto Stine Hill Rd. for ~3.5 mi. Turn west (left) onto Hwy 2 toward Leavenworth for 6 mi. Turn left on East Leavenworth Rd and take an immediate left on Mountain Home Rd. This road becomes gravel after approximately 1/3 mile. Stay on Mountain Home Rd. for 3.5 mi and use the dirt pullout parking lot just before the end of the county road. The Chelan–Douglas Land Trust Mountain Home Preserve property is southeast, across Mountain Home Rd. from the parking area.

Geology en route

Between Wenatchee and Leavenworth are exposures of the Eocene Chumstick Formation. The Chumstick Formation is comprised of sedimentary rocks, mostly sandstones and siltstones with basal conglomerates. The sedimentary rocks were deposited in river valleys approximately 45–48 million years ago, and since deposition have been tilted and faulted (Gresens and others, 1981; Tabor and others 1982; Evans, 1994).

Mountain Home Road passes through two large sections of boulders, one section where a giant boulder is nearly in the road! These are boulders of the Mount Stuart granodiorites and tonalities, approximately 90–93 million years old (Tabor and others, 1982). However, the underlying bedrock is the Chumstick Formation. Thus, the boulders, moved here by the Icicle Creek glacier from further upstream, are erratics. The road crosses two moraines, which Porter and Swanson (2008) call the Leavenworth II and Leavenworth I moraines (~17 ka and ~24 ka respectively).

STOP 1:
Chelan–Douglas Mountain Home Preserve hike

Mile ~13.3 total, mile 3.5 off Mountain Home Road (47.5529, -120.6556)

Trail Stop 1

Parking lot

The Leavenworth I moraine (~24 ka) is to the west of the parking lot, trending north parallel to the road. Large boulders east of the moraine are fresh, producing a loud ring or ping when hit with the rock hammer. They are likely boulders that rolled off the crest of the Leavenworth I moraine. On the east side of the road just across from the parking area is a small sand borrow pit. The sediments are bedded, fine- to medium-grained sands. These are likely outwash sands from meltwater off the Icicle Creek glacier that flowed north along the Leavenworth I moraine with the gradual slope of Boundary Butte. These outwash sediments have created a small, perched aquifer along the ridge of Boundary Butte, where water-loving plants thrive (aspen grove along the east side of the road seen during the drive; abundant shrubs and grasses east of the road; Wenatchee checker mallow, which is endemic to the Wenatchee Mountains).

Proceed up the road on the Preserve, stopping at the first crossroads.

Trail Stop 2

Mile 0.4 (47.5512, -120.6591)

Weathered boulder at crossroads

In contrast to the boulder at the parking lot that is likely from the ~24 ka Leavenworth I advance, this boulder is highly weathered and decomposing into grus. It is possible this small ridgeline is the lateral moraine for the pre-Mountain Home (~95 ka) or Mountain Home (~72 ka) advances, although the weathering of the boulder suggests it is much older. It is likely an erratic from the ~112 ka Peshastin advance or the >160 ka Boundary Butte advance (Porter and Swanson, 2008). Both these advances topped the northern portion of Boundary Butte Ridge and extended at least as far as Peshastin (the town) on the Wenatchee River (Page, 1939; Stanton and others, 2019).

Continue south along the road. This will follow along the ridge, then curve east and uphill. As the road curves back south there will be a trail on the west side of the road at ~0.7 mi from the trailhead. Take the trail uphill until you reach the ridgeline and stop where the view is clear.

Trail Stop 3

Mile ~0.9 (47.5467, -120.6597)

Overlook from Peshastin lateral moraine

The ridgeline is the lateral moraine for the ~112 ka Peshastin advance. The southern portion of Boundary Butte Ridge burned in the 1994 Rat Creek fire. You will note abundant regrowth, but the view is still open. From here you can look southwest into Icicle Creek drainage and south to Wedge Mountain. The Leavenworth fault runs north of Wedge Mountain (between the viewer and the mountain) and along the western side of the valley west of Boundary Butte Ridge. The difference in topographic relief on either side of the fault is obvious, with the igneous and metamorphic rocks west of the fault creating high relief and steep slopes. Icicle Creek takes a meandering form after crossing the Leavenworth fault, as does the Wenatchee River after crossing the fault further north where it exits Tumwater Canyon. The Wenatchee River "exit drop" is a test piece for area kayakers.

Icicle Ridge is west of Boundary Butte Ridge and has scant evidence of glacial deposits in comparison, although faint trim lines are occasionally visible after a light snow. The lack of glacial deposits may be because Icicle Creek drainage is at an angle to Boundary Butte Ridge, thus directing ice flow there.

East of the Peshastin lateral moraine is the Boundary Butte Ridge line as well as a ridge of the Boundary Butte lateral moraine. This advance is likely 160 ka or more. Porter and Swanson (2008) were unable to obtain a cosmogenic date from the highly weathered boulders, which in road cuts are almost entirely decomposed. Like the Peshastin advance, this advance topped Boundary Butte Ridge further to the north and terminated in the Wenatchee River valley, likely east of the town of Peshastin. Terminal moraines for either advance are no longer visible, even in LiDar. They have been eroded by time and the river, although a faint curve in topography east of the town of Peshastin potentially suggests a terminal moraine.

If the heat is bearable, continue south along the exposed ridgeline to where it curves east and then north back to the road. If not, stick to the shade and retrace your way back to the road, turning south.

Trail Stop 4

Starting at mile 1.7 (47.5390, -120.6681)

Perched aquifer between Peshastin and Boundary Butte Ridge lateral moraines

Between the ~112 ka Peshastin and the 160+ ka Boundary Butte lateral moraines is a north verging "drainage" or perched aquifer that hosts abundant water-loving vegetation and occasionally has standing or gently flowing water. It is likely that outwash sands fill this depression, similar to sands seen at the parking lot between the ~24 ka Leavenworth I and the ~112 ka Peshastin lateral moraines.

This hike ends back at the parking lot (total 3.2 mi roundtrip). Those who wish to end the trip may do so now or continue for the second short hike to look at erosional features left by the Icicle Creek glacier.

Drive back down Mountain Home Rd for 3.5 mi, turn south (left) on East Leavenworth Rd for ~3.3 mi. Turn south (left) on Icicle Rd for ~1.5 mi and park in a gravel pullout on the left side of the road.

STOP 2:
Sam Hill hike

Mile 18.1 total (47.5472, -120.6950)

Cross Icicle Road to the unmarked trail near a large boulder. Continue north–northeast along the trail, avoiding the spur to the west.

Trail Stop 5

Basaltic dike, mile ~0.2

Granodiorite and tonalite make up the Cretaceous Mount Stuart batholith (with minor diorite and more mafic inclusions). Paleomagnetic studies suggest that the batholith formed further south (Housen and others, 2003). The middle Eocene Teanaway basalt intrudes both the Mount Stuart rocks and Eocene sedimentary rocks (Tabor and others, 1982). Near this spot are also exposures of metal piping, likely water pipes related to the small community of Icicle sited near the mouth of the canyon.

Continue up the trail. Where it turns west, continue north–northeast along the ridge to the crest of the rise.

Trail Stop 6

Roche moutonnée, mile ~0.4

This rise, and others nearby, have a long, gentle slope upstream and a sharp, steep face downstream. This feature, formed by glaciers plucking the rock from the downslope face, is called a roche moutonnée ("rock mutton"). They are common near the Leavenworth fault, where the Mount Stuart rocks form steeper slopes and greater relief to the west, and the valley opens and widens in the Chumstick Formation to the east.

Along the crest of the rise are smaller erosional features, such as chatter marks and muschelbruch. Again, these features are common along the bedrock exposures in the center of Icicle valley near the Leavenworth fault. It appears the Icicle glacier eroded the underlying rock differently here than further up valley, away from the fault. This could result from a bend in the valley here, or from moving across the fault from more resistant rock to softer units.

Return to the parking lot.

REFERENCES CITED

Evans, J.E., 1994, Depositional history of the Eocene Chumstick Formation; implications of tectonic partitioning for the history of the Leavenworth and Entiat–Eagle Creek fault systems, Washington: Tectonics, v. 13, no. 6, p. 1425–1444, doi: https://doi.org/10.1029/94TC01321.

Gresens, R.L., Naeser, C.W., and Whetten, J.W., 1981, Stratigraphy and age of the Chumstick and Wenatchee formations: Tertiary fluvial and lacustrine rocks, Chiwaukum graben, Washington: Geological Society of America Bulletin, v. 92, Part II, p. 841–876.

Housen, B.A., Beck, M.E. Jr., Burmester, R.R., Fawcett, T., Petro, G., Sargent, R., Addis, K., Curtis, K., Ladd, J., Liner, N., Molitor, B., Montgomery, T., Mynatt, I., Palmer, B., Tucker, D., and White, I., 2003, Paleomagnetism of the Mount Stuart batholith revisited again: What has been learned since 1972?: American Journal of Science, v. 303, p. 263–299, doi: 10.2475/ajs.303.4.263.

Long, W.A., and Porter, S.C., 1968, Revision of the alpine glacial sequence in the Leavenworth area, Washington: Geological Society of America, Abstracts Special Paper 115, p. 338.

Page, B.M., 1939, Multiple alpine glaciation in the Leavenworth area, Washington: Journal of Geology, v. 47, p. 787–815.

Porter, S.C., 1969, Pleistocene geology of the east-central Cascade Range, Washington: Guidebook for the Third Pacific Coast Friends of the Pleistocene Field Conference, University of Washington, Seattle.

Porter, S.C. and Swanson, T.W., 2008, ^{36}Cl dating of the classic Pleistocene glacial record in the northeastern Cascade Range, Washington: American Journal of Science, v. 308, p.130–166.

Stanton, K.M., Waitt, R.B., and Long, W.A., 2019, Pre-late Wisconsin valley-glacier erratics between Leavenworth and Peshastin, Wenatchee Valley, Washington: Northwest Science, v. 92, p. 311–317.

Tabor, R.W., Waitt, R.B., Frizzell, V.A., Swanson, D.A., Byerly, G.R., and Bentley, R.D., 1982, Geologic map of the Wenatchee 1:100,000 quadrangle, central Washington: U.S. Geological Survey Miscellaneous Investigations Series, 1–1311, 26 p., 3 sheets, scale 1:100,000.

Waitt, R.B., 1977, Guidebook to Quaternary geology of the Columbia, Wenatchee, Peshastin, and upper Yakima valleys, west-central Washington: U.S. Geological Survey Open-File Report 77-753.

Yokel-Deliduka, A., and Davis-Stanton, K.M., 2016, Mapping erratics in the mid-to-upper Wenatchee River valley, Washington State: Geological Society of America Rocky Mountain Section Abstracts with Programs 48.

CALCRETE IN THE CHANNELED SCABLANDS, YAKIMA FOLD BELT, AND PALOUSE HILLS

Skye W. Cooley

Geologist, Mission Valley, Montana

ABSTRACT

This field trip guide explores spectacular calcretes in south-central Washington. The thick, bright white $CaCO_3$-rich paleosols overprint Miocene basalt, Pliocene Ringold Fm, and various Pleistocene sediments, including a pre-Missoula megaflood gravel, early Palouse loess, and basaltic fanglomerates shed from fault-bounded ridges. Their morphology indicates they formed primarily by soil processes (pedogenic) and some influence by the paleo-water table. Thickening was likely accelerated during dry interglacials of the Pleistocene. In south-central Washington, they encrust sediments of a broad, dusty, low-relief alluvial plain fringed by bedrock ridges and the Palouse hills. The calcretes armor a relatively thin interval (<20 m thick) of Pleistocene-age sediments and an underlying Pliocene unconformity formed following an abrupt base level fall along the ancestral Columbia River system around 3 Ma. The calcretes define a long-lived, geomorphically stable lowland surface modified by at least one megaflood–loess cycle and later deformed by the rising Yakima Folds (fig. 1).

Figure 1. A boulder gravel deposited by an ancient glacial outburst flood (pre-Missoula) truncates Pliocene sediments of the uppermost Ringold Fm and is capped by three calcrete ledges (calcium carbonate-rich paleosols) with sandy material between. The calcretes took hundreds of thousands of years to form. The age of the flood gravel may be 500,000 years old or more.

INTRODUCTION

Calcrete is a $CaCO_3$-rich hardpan paleosol commonly found in geomorphically stable desert regions of the world (Lamplugh, 1902; Zamanian and others, 2016). Calcrete is a secondary deposit formed in soil B-horizons, the rooting zone for most plants (fig. 2). The accumulation of pedogenic carbonate results from the interplay of evapotranspiration, pH, microbial activity around roots, the water table, and the partial pressure of CO_2. Calcium is leached from loess (Ca^{2+}) by rainwater or snowmelt. Carbon is supplied by rainwater and root-zone respiration as CO_2 (carbon dioxide) or HCO_3^- (bicarbonate). Calcrete in Eastern Washington is primarily pedogenic, but evidence of lateral throughflow in the vadose zone and influence of groundwater is strongly suspected (Slate, 1996, 2000).

Relict soils are a mark of long-term stability of the ground surface. Meter-thick calcretes indicate persistent stability lasting hundreds of thousands of years. Calcrete paleosols are visually conspicuous marker beds that span all three of the region's geomorphic domains: Palouse Hills (wind-dominated), Channeled Scablands (flood-dominated), and Yakima Fold Belt (uplift-dominated).

Calcrete in Eastern Washington is most abundant in Pleistocene-age sediments (~1.8 Ma and ~50 ka) and commonly appears in outcrops as 1–3 resistant, white ledges with sediments between. Welded (superimposed B-horizons) relationships within some ledges is clear. Carbonate cements of Pliocene age are present in the Ringold Fm too (Lindsey, 1996, appendix A), and calcrete–silcrete crusts are commonly found in sedimentary interbeds between Miocene basalt flows. Weak calcretes (Stage I–II) are encountered in Late Pleistocene sediments, but almost never in sediments younger than 14 kyr.

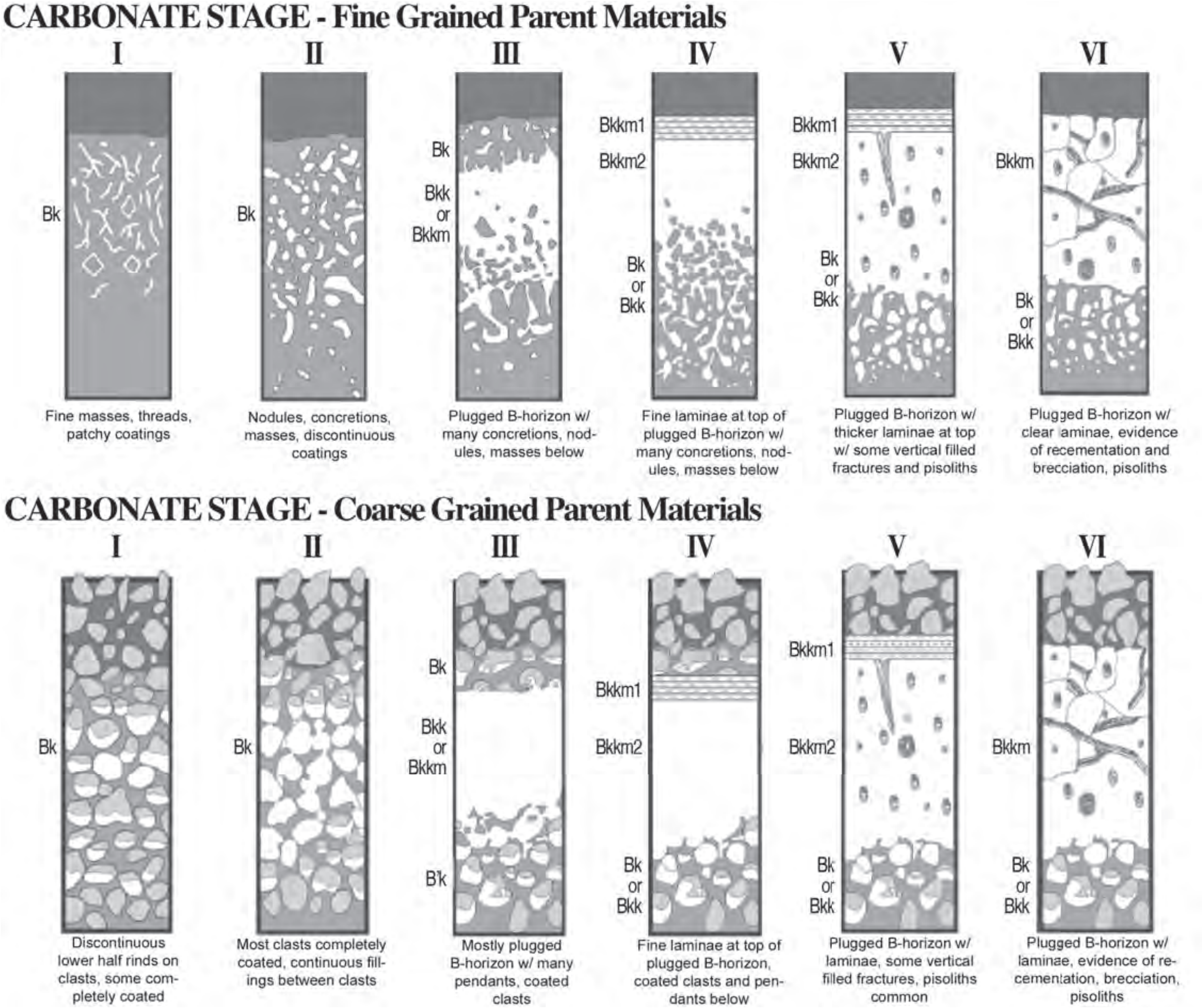

Figure 2. Carbonate stage (calcrete morphology) for fine- and coarse-grained parent materials modified from Schoeneberger and others (2012), Gile and others (1966), Machette (1985), and Birkeland (1999).

GEOLOGIC SETTING

Bedrock in the region is Miocene Columbia River Basalt Group with sedimentary interbeds between certain flows. Terrigenous basin-fill sediments of the Miocene–Pliocene Ellensburg Fm and mostly Pliocene Ringold Fm lie atop the basalt. The Ellensburg is a lithologically diverse wedge of sediment shed east off the Cascades that interfingers with and overlies the basalt. Ellensburg is present, but not abundant in the area covered by this guide. The Ringold Fm is the more abundant and important unit. The Ringold consists of fluvial, lacustrine, and overbank sediments with numerous paleosols deposited across a broad lowland plain by the south-flowing ancestral Columbia River and west-flowing Salmon–Clearwater–Snake system (Fecht and others, 1987). The formation is up to 150 m thick and divided into three informal members based on sedimentological characteristics and facies associations (Lindsey, 1996): Wooded Island (fluvial gravels, <9.5 Ma), Taylor Flat (sandy fluvial, ~5.5–4.5 Ma), and Savage Island (lacustrine-paleosols, ~4.5–3.4 Ma). Tephras, vertebrate fossil evidence (Gustafson, 1978; Smith and others, 2000), plant fossils (Mustoe and Leopold, 2014), and paleomagnetic data (Packer, 1979) have helped constrain the age of the Ringold to ca. 9.5–3.4 Ma (Lindsey, 1996; Staisch and others, 2018). Pliocene deposits other than Ringold are almost entirely absent elsewhere in the Columbia Basin.

The top of the Ringold is truncated by an unconformity that formed following a base level drop on the Columbia River around 3 Ma (Brown, 1959, 1960; Grolier and Bingham, 1978; Lindsey, 1996; USDOE, 2002, 2010; Cheney, 2016a; Staisch and others, 2021). As much as 100 m of Ringold strata has been removed in a few locations; however, the post-Ringold unconformity is commonly observed truncating distinctive laminated siltstones of the uppermost Ringold (Savage Island Member). The unconformity and the calcrete-bearing interval above it are warped across Yakima Fold Belt anticlines and faulted in a few places. Calcretes are encountered in boreholes drilled into synclines adjacent to fold belt anticlines (Riedel, 1988; Bjornstad and others, 2001).

Beginning around 2 Ma, Ice Age megafloods began to inundate the region. The calcrete-bearing interval contains a conspicuous boulder gravel and calcrete rip-up gravels. Vestiges of old scabland channels that are partially filled with sediment (and paleosols) occur in the study area. A flight of broad terrace-like benches in the Othello area pre-date coulees cut by the younger Missoula floods and appear to be flood-formed. Loess, recycled from flood basins to the south and west, occurs between most calcrete ledges, indicating pre-Late Wisconsin flooding and calcrete growth overlapped in time.

PREVIOUS WORK ON CALCRETE IN COLUMBIA BASIN

Reconnaissance geologists assigned various names to calcareous hardpans they encountered in the Channeled Scablands, Yakima Fold Belt, and Palouse Hills (figs. 3, 4). Some of the names include “hard cemented light yellow alkali“ (Russell, 1893), “calcareous strata” (Merriam and Buwalda, 1917),“lime rock

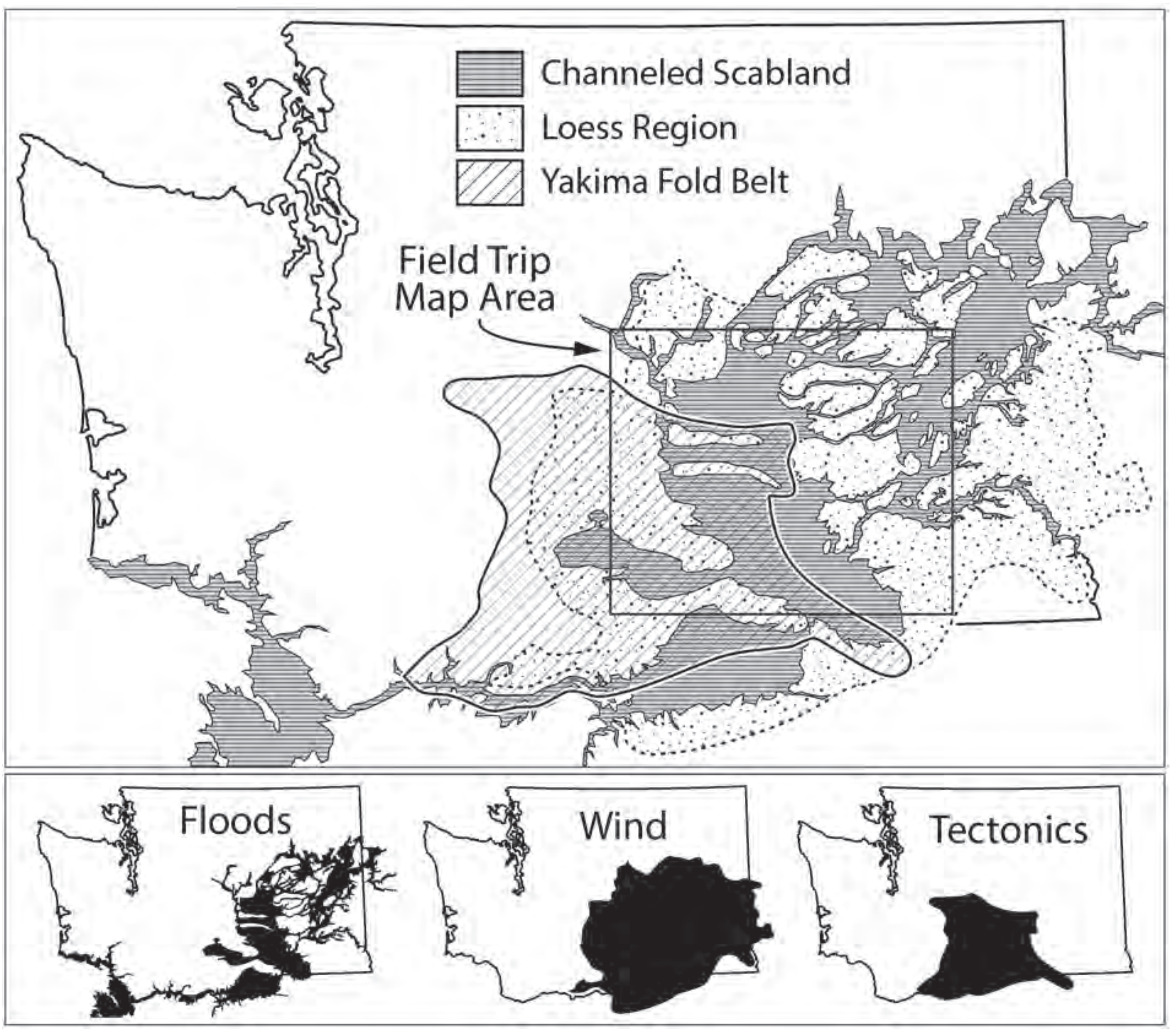

Figure 3. Geomorphic domains of Eastern Washington. Channeled Scablands, and Yakima Fold Belt generalized from digital elevation data. Loess region combines loess polygons in McDonald and others (2012) and Washington’s Level IV Ecoregions Map (Clarke and Bryce, 1997).

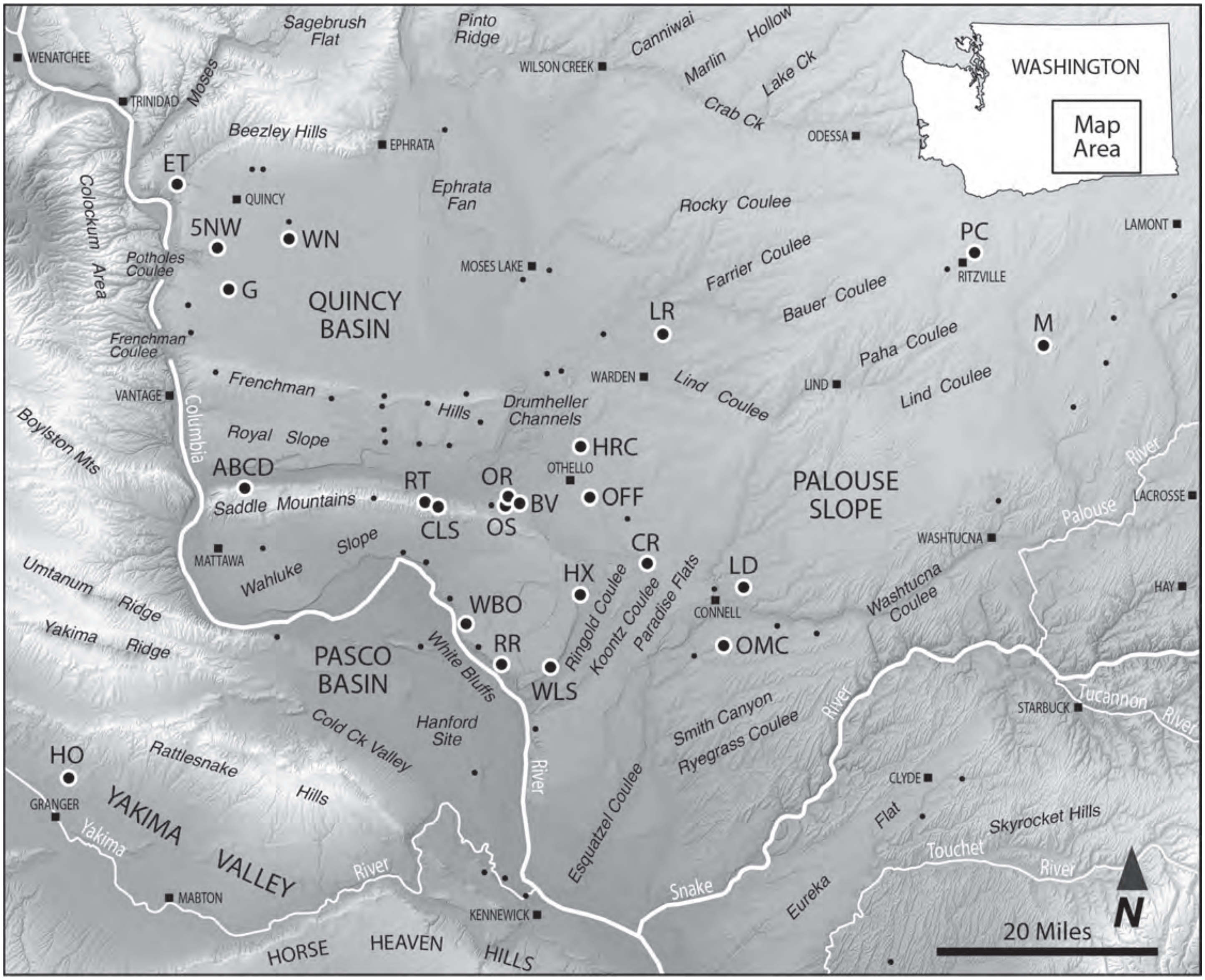

Figure 4. Map of field trip stops (white circles) and other calcrete study sites (small black dots). ABCD, Saddle Mountains Ridge; BV, Benchview Rd.; CLS, Corfu Landslide Overlook; CR, Coyan Rd.; ET, East Trinidad; G, George Landfill; HO, Houghton Rd.; HRC, Herman Railcut; HX, Hendricks Rd.; LD, Lind Rd.; L, Leisle Rd.; M, Marengo; OFF, Offramp; OMC, Old Maid Coulee; OR, O'Brian Rd., Railcut A; OS, Orchard Scarp; PC, Pacific Rd.; RR, Ringold Rd.; RT, Red Tank; WBO, White Bluffs Overlook; WLS, Watt Ln. Landslide; WN, Winchester Canal; 5NW, White Trail Rd/Rd5NW.

zone" (Beck, 1936), "calcareous layer" (Culver, 1937), "caliche cap" (Newcomb, 1958), "caliche cap on the Ringold" (Brown, 1959, 1960), "calcrete cap" on the Ringold (Grolier and Bingham, 1978), or "calcareous sand, silt, and eolian deposits" (Ledgerwood and others, 1978). Calcretes and and the sediments that scaffold them have been lumped with the Ringold on geologic maps (Schuster and others, 1997), mapped separately as pre-late Wisconsin deposits (Stoeffel and others, 1991), and distinguished as a geohydrologic unit at the Hanford Site, their "Plio-Pleistocene unit" (Lindsey, 1992).

Ancient megaflood deposits capped by calcrete are mentioned in numerous articles on scabland geology (Patton and Baker, 1978; Busacca, 1989; Baker and others, 1991; Bjornstad and others, 2001; Spencer and Jaffee, 2002; Bjornstad, 2006; Baker and others, 2016; Waitt, 2017). Calcrete and silcrete horizons are carefully documented in Palouse soils using soil taxonomy (Busacca, 1989; McDonald and Busacca, 1992; McDonald and others, 2012; Sweeney and others, 2017). Detailed measured sections through Ringold at White Bluffs show multiple calcrete horizons (Lindsey, 1996, appendix A). I recently correlated 28 of Lindsey's sections in a single figure, which is available online (www.skyecooley.com/single-post/correlating-kevin-lindsey-s-measured-sections-at-white-bluffs-wa). Slate (1996, 2000) identified pedogenic and groundwater-influenced morphologies in cores collected at the

Hanford Site. In 2021, the Seattle-based Northwest Geological Society toured calcrete exposures in the Othello area, a trip led by the author. An unpublished field trip guide was distributed to trip participants.

One of the most important aspects of calcretes in Eastern Washington—hardly mentioned in previous articles— is their formation in lowland settings. They are closely associated with alluvial sediments; broad, flat landscapes; and low-gradient alluvial fans. Where developed in loess (an upland deposit), alluvial sediments are nearby. Many appear to have developed very near the paleo-water table, possibly within the capillary fringe. The "capping calcretes" atop the Saddle Mountains ridge were formed in a valley and later elevated by faulting.

AGE OF CALCRETES

Fecht and others (1987) used a thermoluminescence (TL) date on a Columbia Basin calcrete to bracket regional incision on the ancestral Columbia River to between 3.4 and 2.0 Ma. More recently, Medley (2012) quantified carbonate content in calcretes of the region using a Chittick apparatus. She found morphologies consistent with Stage III development or greater (>15,000 yr old) at 15 of 25 sites. U-series ages ranging from 44,000 to 669,000 ka have been reported for calcretes in the Pasco Basin and adjacent Saddle Mountains (Bjornstad and others, 2001; Pluhar and others, 2006; Staisch and others, 2018). U-series dating, specifically the uranium-thorium method (U-Th), has generally proven reliable for carbonates up to ~500,000 years old. Older samples are subject to open-system effects. Open-system behavior is inherent to vadose zone soil carbonates and known to diminish the accuracy of U-series results (Alonso-Zarza and Tanner, 2010). Several of the samples analyzed in the aforementioned studies exceeded the 500,000-yr limit. Reported U-series ages are therefore considered to be minimum ages.

More dates are needed, but the oldest calcretes in the Columbia Basin approach 500,000 yr old (early Pleistocene) and some may pre-date the Brunhes–Matuyama magnetic reversal (780 ka). A robust paleomagnetic survey of pre-late Wisconsin deposits and the calcrete-bearing interval would also help provide clarity.

CALCRETE AND RISE OF THE CASCADES

Calcretes in Eastern Washington are dryland paleosols, formed in the rain shadow cast by the Cascade Range. The Cascades began to grow about 42 million yr ago with the establishment of a convergent plate margin along the west coast of North America. The rock record indicates the Cascades in northern Washington achieved a height sufficient to partially block Pacific storms from tracking farther inland between 12 and 6 Ma (Reiners and others, 2002; Takeuchi and Larson, 2005). A strong rain shadow is in place east of the Cascade divide by 5 Ma when a hardwood tree community is replaced by sagebrush-steppe (Mustoe and Leopold, 2014). Establishment of a high-elevation crest and strong orographic divide appears to have lagged behind rock uplift by some 30 million yr, possibly due to high erosion rates through the warm, wet Miocene, which kept mean elevations low. Climate in Eastern and Western Washington diverged quite late in the life of the range, apparently in the Pliocene.

CLIMATE IN A STRUCTURALLY SEGMENTED MOUNTAIN RANGE

Neogene paleoclimate records for central Oregon contrast somewhat with those for central Washington (Hammond, 1979; Kohn, 2002; Retallack, 2007; McLean and Bershaw, 2021). The contrasts confirm the Cascade Range is structurally segmented, that each segment has its own rock uplift and climate history, and that each should be evaluated separately. The Cascade orogeny was not steady. Rock types, topography, and weather patterns differ from segment to segment and varied through time. Cross the North Cascades via Highway 20, then cross the Oregon Cascades via the Santiam Highway and tell me it is the same mountain range.

SUMMARY

Calcretes in south-central Washington are widespread and thick. These resistant and well-preserved soil carbonates have helped constrain the timing of regional incision of the ancestral Columbia River (Fecht and others, 1987), date local tectonism (Staisch and others, 2018), identify pre-Missoula megaflood deposits (Baker, 1973), and refine the stratigraphic framework for the Palouse (McDonald and others, 2012). Pedogenic calcretes highlighted in this field guide constitute an important, but largely ignored sedimentary interval (a marker unit) that spans the region's three geomorphic domains: Palouse Hills, Channeled Scablands, and Yakima Fold Belt (fig. 5). The relict hardpan soils define a formerly low-relief paleosurface that has since been warped and faulted by Yakima Fold Belt structures (figs. 6, 7).

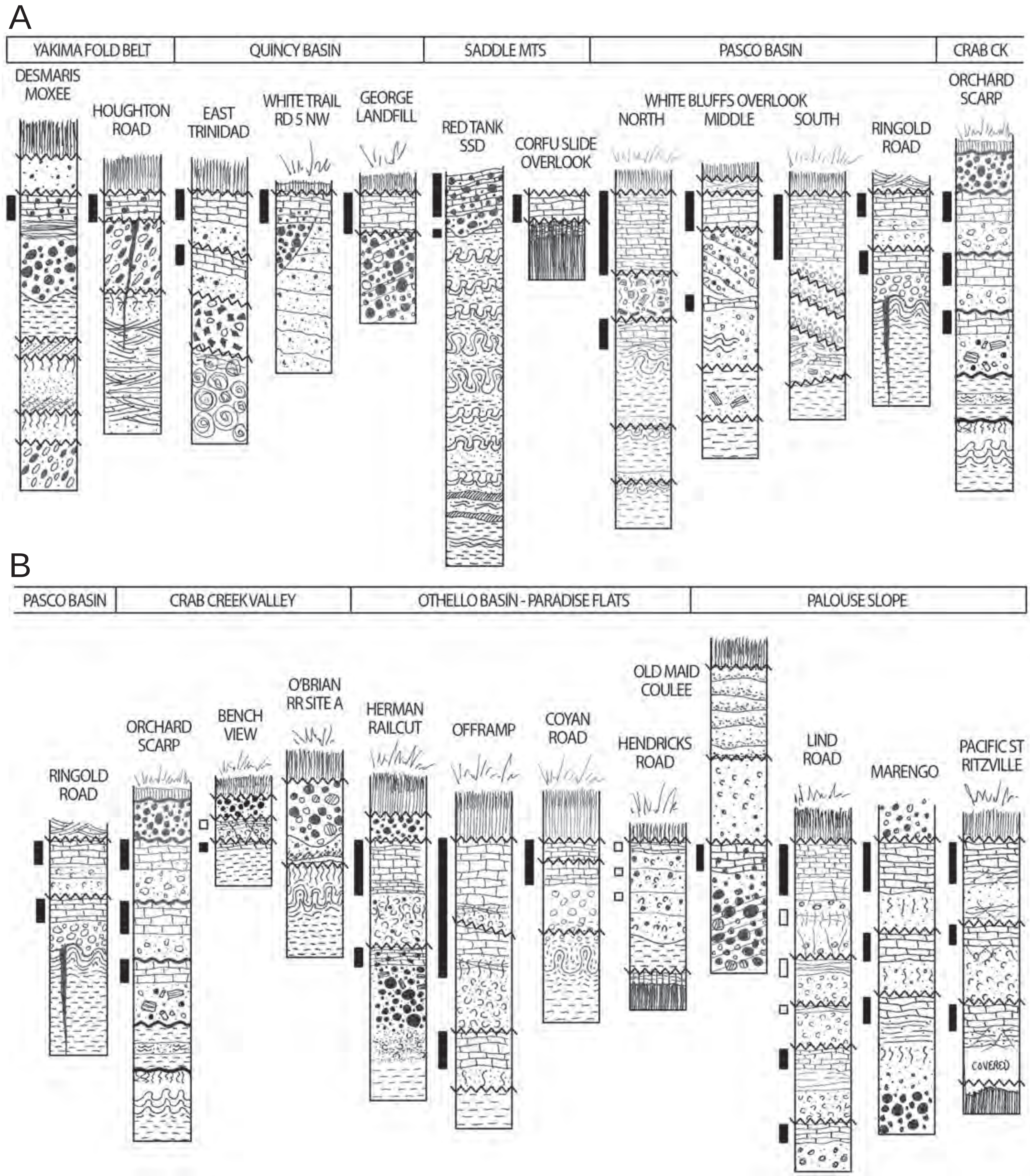

Figure 5. Stratigraphic columns in calcrete-bearing strata in the Channeled Scablands, Yakima Fold Belt, and Palouse Hills. Pedogenic calcretes (black bars) are developed in a variety of parent materials including Palouse loess, Ice Age megaflood deposits, locally derived basaltic fan gravels, Pliocene Ringold Fm, Ringold-equivalent Ellensburg Fm, and weathered Columbia River Basalt. White boxes denote low Stage soil carbonate ("caliche"). The Desmaris Moxee site is located west of the map area in figure 3.

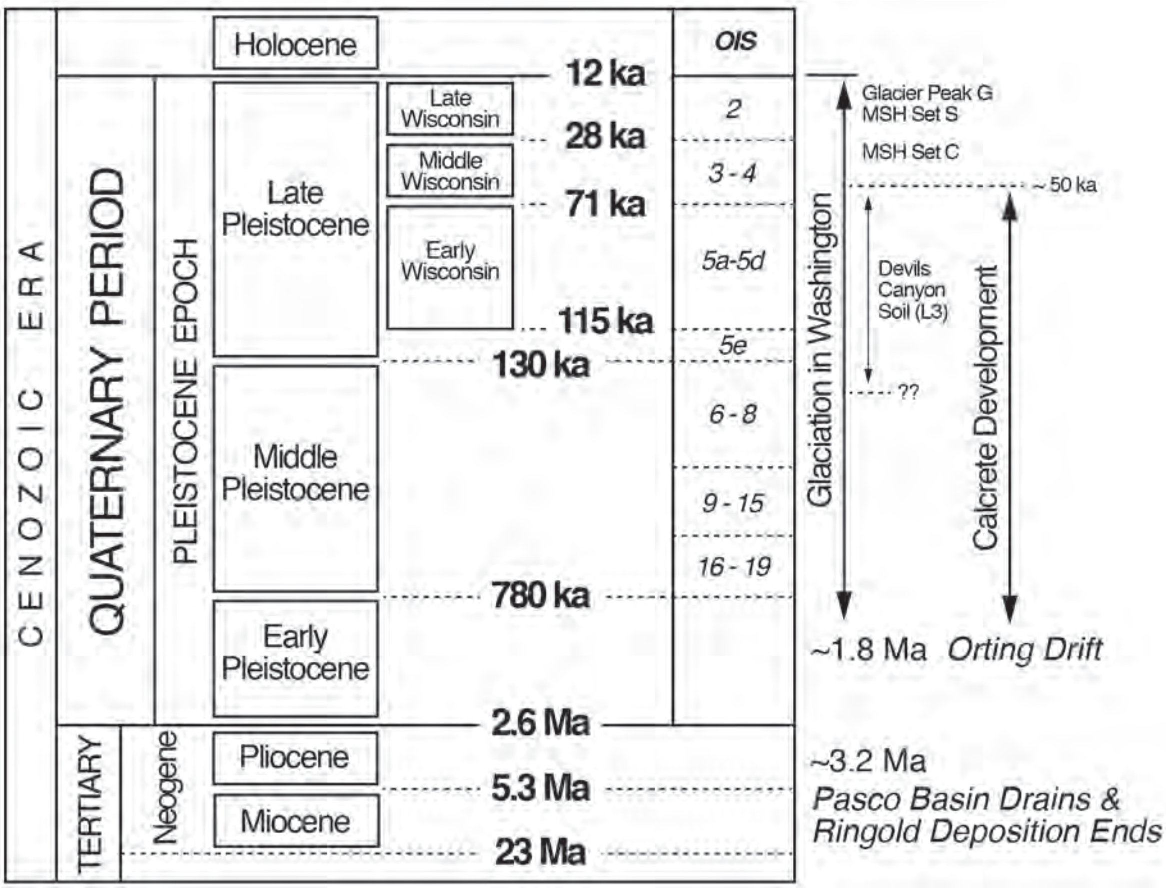

Figure 6. Geologic timescale highlighting the period when most calcretes formed in Eastern Washington (~1.8 Ma to ~50 ka). Older soil and groundwater carbonates occur in the Pliocene Ringold Formation (Lindsey, 1996, appendix A). Cascade tephras have helped establish a chronostratigraphic framework for Palouse loess and scabland deposits. Flood deposits separate the loess into three units (L1, L2, L3). The oldest tephra in the earliest loess (L3) is from Mt. Baker's Kulshan caldera, dated at 1.15 Ma (King and others, 2016). Thermoluminescence (TL) dates for the L3 loess include 116.3 ka (TL method, Winona WIN-1), 74.6 ka (TL method, Washtucna WA-5; Richardson and others, 1997).

A SELF-GUIDED FIELD TRIP

Due to drive time limitations, only 1–2 of the stops in this field guide will be visited during the conference in Cashmere. Readers are encouraged to visit the other stops on their own at a later date. Detailed driving directions and GPS locations are provided to aid navigation to specific locations. Some stops are roadcuts, while others involve half-day hikes over rough ground. I've tried to provide a range of interesting stops that show the range of characteristics commonly observed in Plio–Pleistocene sediments and calcretes of the region.

STOP 1:
East Trinidad at Baird Springs Road

Calcretes overprint colluvium, flood gravel(?), and loess atop corestones of basalt

47.242526, -119.993356

Directions

From Wenatchee, drive 25 mi east on Hwy 28 to Trinidad. Just beyond Smith Brothers Antiques and Espresso, turn left (north) onto Baird Springs Road NW and follow for 0.8 mi. Park on shoulder, cross tracks, and hike a dirt two-track the short distance north to the white outcrop, an old roadcut.

Description

Two calcretes are separated by wedges of loess and brown silty-sandy-gravelly beds. The lower calcrete is 30–50 cm thick with platy to blocky morphology (Stage IV) that becomes fully plugged in its upper 15 cm. The upper calcrete is less advanced, 25 cm thick, with blocky to platy morphology. Both calcretes are developed into silt-sand-gravel parent materials (alluvium) containing trace fossils of plants. Thick colluvium atop the bedrock contains rip-ups of green mudstone

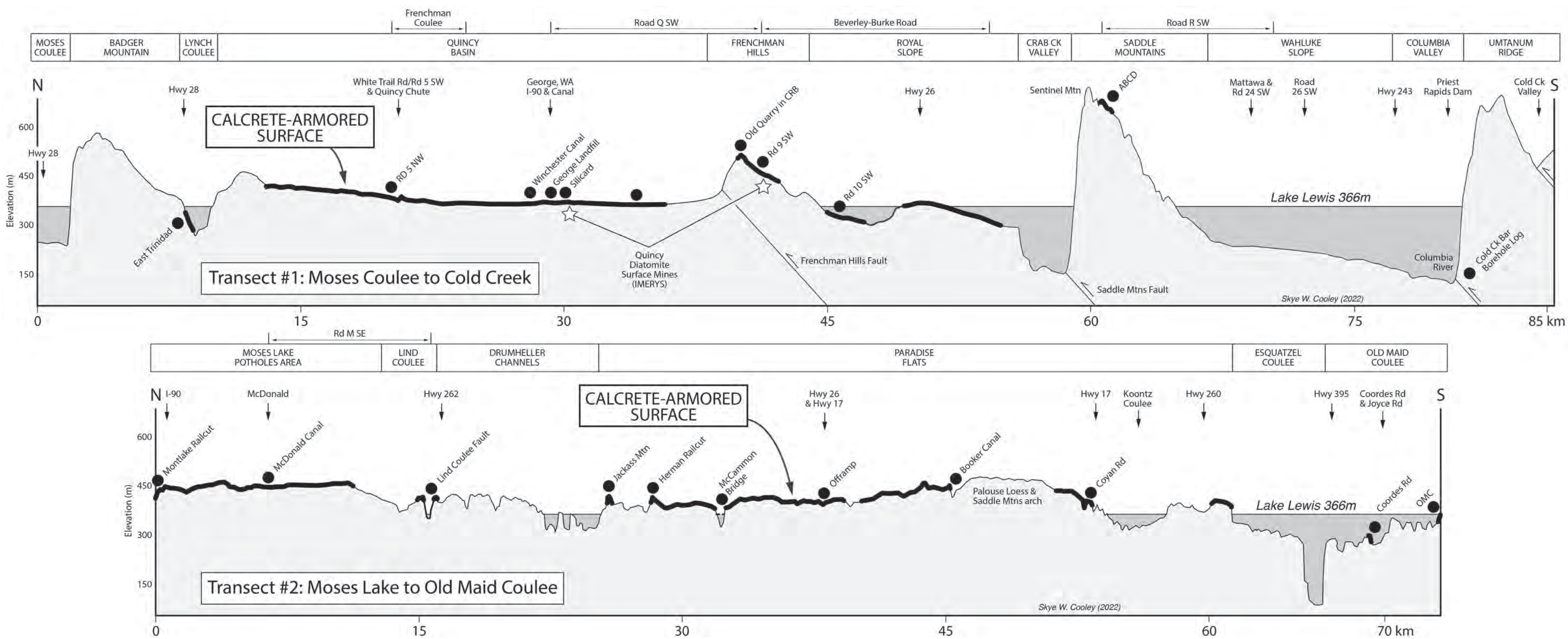

Figure 7. North–south transects through south-central Washington show calcrete-armored surfaces deformed by Yakima Fold Belt structures and eroded by Ice Age floods. Black dots are field stops and other study locations.

and basalt in powdery matrix. White cement fills cracks in the top of the basalt bedrock. Boulder-like corestones of basalt are weathering out of the bedrock nearby. Contacts between the various sedimentary beds reflect both hillslope instability (colluvium, lens-shaped beds, angular relationships) and surface stability (calcic soil profiles, root casts, burrows). Bedding follows the shape of the hillslope, which is curious. Are the sediments (parent materials of calcretes) hillslope deposits or alluvial deposits? Is bedding tilted? If so, by tectonics or mass wasting? Though East Trinidad is located at the western edge of Quincy Basin and the western limit of calcrete distribution (i.e., Pliocene structural basins of Cheney, 2016b), the section contains sediments and calcretes developed in Palouse-like loess and scabland-like gravels, a pattern we will see at several other stops.

STOPS 2 and 3:
Hendricks Road and White Trail/Rd. 5 NW

Two stops with Pleistocene sandstones with calcic soil profiles atop old scabland surfaces

Directions to Hendricks Road

Hendricks Road site is located west of Connell (Pasco Basin) at the south end of the Eagle Lakes scabland. From Connell, drive west on Hwy 260 to intersection with Hwy 17/Hendricks Road. Cross Hwy 17 and continue west for 7.5 mi on Hendricks Road. Roadcut is located where Bailie Creek crosses the road, a short distance past the kiosk and public parking area for Bailie Memorial Youth Ranch and Wildlife Area. An unnamed pond immediately east of the road fills a scabland basin. Park at the kiosk and walk or find a spot along the narrow road shoulder. Do not block gated driveways.

46.674414, -119.151598

Directions to White Trail/Rd. 5 NW

The White Trail site is located south of Quincy (Quincy Basin) at the head of the Potholes Coulee cataract. From Quincy, drive south on Hwy 281 for 5 mi. Turn right (west) onto White Trail/Rd. 5 NW at Colockum Golf Course. Cross the canal at the Quincy Chute Hydroelectric Plant and promptly pull off into one of the orchard driveways on the north side of the road. The low roadcut is located on the south side ~200 m west of the canal at a power pole (#WAN-COL-AL-53-100603). Truck traffic is relentless here. Be careful.

47.1600, -119.9015

Description

The two stops, separated by 50 mi, exhibit nearly identical (and rare) beds of cemented Pleistocene alluvium resting atop flood-scoured basalt. “Brown alluvium” is often mentioned in pre-WWII reconnaissance reports on Eastern Washington’s scabland geology, but has received little attention in the past 80 yr (i.e., Grolier and Bingham, 1978). Roadcuts along Hendricks Road at Bailie Creek expose beds of brown, locally derived sediment resting atop the Eagle Lakes scabland surface. Five gray-brown sandstone beds, each about 30 cm thick, contain deeply weathered basalt cobbles, cicada burrows, and Bk soil profiles (Stage I–II+ caliche). The top bed has the thickest Bk horizon (fig. 8). A lens of lacustrine sediment and a yellow-

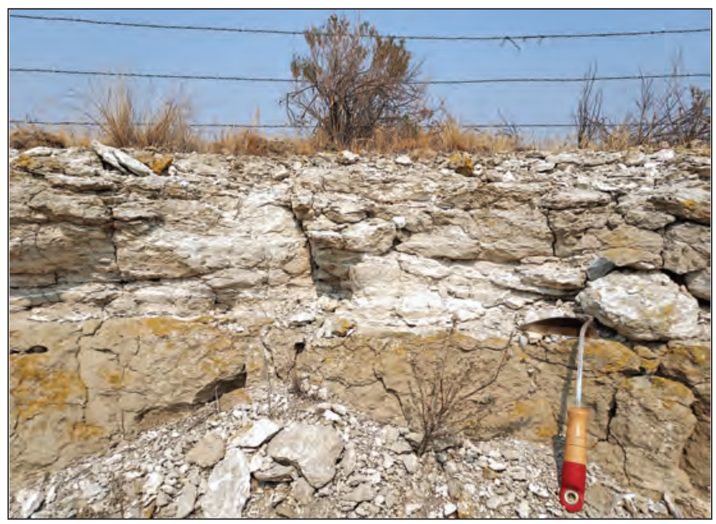

Figure 8. Hendricks Road. Five gray-brown sandstone beds composed of basaltic detritus contain weathered basalt cobbles, fossil cicada burrows, and Bk soil profiles (Stage II+). Cementation is most prominent in the top bed. Calcic soil profiles and cicada burrows suggest time passed between the deposition of each bed. Cicadas burrow above the water table, so the landscape drained between periodic sedimentation events. The beds may be flood rhythmites, but do not resemble Touchet Beds, which are typically light-colored and micaceous. Deeply weathered basalt clasts are either colluvium or gravel. Rounding can be explained by sedimentary transport or weathering. Similar weathered clasts have been used to distinguish pre-Missoula flood deposits elsewhere in the Channeled Scablands. Cross-cutting relationships show the beds (local alluvium or far-traveled flood sediment) were deposited atop a pre-late Wisconsin scabland surface. Each was colonized by insects and developed a soil profile. Most of the material was removed by one or more younger floods through the Eagle Lakes scabland.

ish zone of weathered regolith 20 cm thick occur at the base of the exposure. The fact that bedded sediments exist here, in the heart of a major scabland, is remarkable. At White Trail, a flood-cut, gravel-filled channel is incised into beds of brown, cemented, alluvium(?) nearly identical to those at Hendricks Road (fig. 9). These also contain faint cicada burrows in addition to curious chips and pebbles of dark red opal. Bedding dips gently west into Potholes Coulee. A thick, flat-lying calcrete—much thicker and more advanced than at Hendricks Road—caps both the flood gravel and the older alluvium, making both deposits pre-late Wisconsin in age. This calcrete is at least Stage III and likely the same as at George Landfill and Winchester Wasteway.

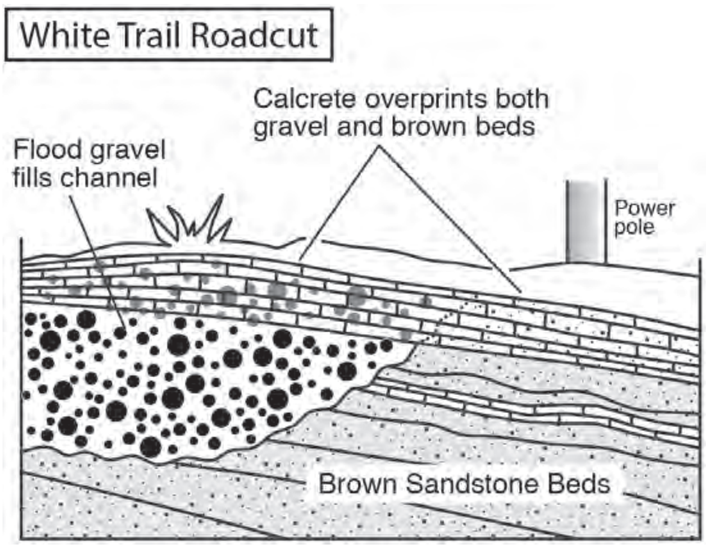

Figure 9. White Trail. A thick calcrete overprints two parent materials: flood gravel and brown sandstone.

STOP 4:
George Landfill

Ancient flood gravels from the Columbia Valley capped by a thick calcrete

47.100418, -119.870179

Directions

George, WA is located on I-90 northeast of Vantage. Exit I-90 at Exit 149 for Hwy 281/Quincy/Wenatchee. Turn left (west) onto Hwy 281, crossing over freeway. Cross canal and turn left onto Beverly-Burke Rd., then right onto Rd. 1 NW. The closed and partially reclaimed George Landfill, which some call the "George Drop Box," is located on the left. Grant County Public Works owns the pit and seems to still use part of it. Please respect any signage they have posted.

Description

The low walls of the pit expose old flood gravels with south- and east-dipping foresets capped by a thick, platy calcrete (fig. 10). The bouldery gravel contains weathered and unweathered basalt clasts, chunks of Vantage sandstone, and green opal from local pillow–palagonite complexes (i.e., Silica Rd offramp of I-90). Baker (1973), following Bretz and others (1956), describe the deposit as "pre-Bull Lake flood gravels." Floods that deposited the gravel at George flowed down the Columbia River, exited into Quincy Basin at Babcock Ridge, and coursed inland. Later floods spilled in a westerly direction across Quincy Basin.

Figure 10. George Landfill. A platy calcrete caps old flood gravels at George.

STOP 5:
Red Tank Hike at Smyrna Bench

Hike to cemented fanglomerate that truncates deformed Ringold lakebeds

46.812059, -119.465638

Directions

This stop involves a 2-mi hike (roundtrip) high on the Saddle Mountains/Smyrna Bench accessed via a semi-rough road. From Vantage, drive 19 mi to Mattawa, then follow Rd. 24 SW (becomes Hwy 24) west for 20 mi to Corfu Rd. From Othello, drive Hwy 24 west 17.5 mi to the White Bluffs Area gate, but do not turn in. Instead, continue west 2.8 mi farther to Corfu Rd. Leave Hwy 24 and turn north onto Corfu Rd., passing a sign that reads, "Saddle Mountains Overlook 5 miles." The gravel road winds up the south flank of Saddle Mountains, crossing the canal at 4.9 mi, after which potholes and washboard increase. At 7.1 mi reach the saddle crest and 4-way intersection (565 m elevation). Turn left and follow the curving road west, staying right at the branch, and downhill for 0.8 mi to the red metal tank. The road is rocky here, so go slow. Higher clearance vehicles only beyond the intersection. Park off the road to the left in sparse sagebrush on a somewhat flat spot just past the tank. Do not block Corfu Rd. Hike north for 1/4 mi downhill to join a worn trail leading west along the scarp and through the "summit graben" toward a conspicuous knob of basalt (fig. 11). Just past the knob a wire fence leads due north. Follow it to the fence corner, then to SSD Outcrop located at the rim of Smyrna Bench. One-way hiking distance is less than 1 mi. Other outcrops are found along the rim nearby. Oil and gas prospecting in Columbia Basin is detailed in McFarland (1979), Campbell and Banning (1985), Brownfield (2008), Wilson and others (2008), Tincher and Reidel (2009), and Czajkowski and others (2012).

GPS Locations for Hike

Red Tank	46.802445, -119.465330
480 m elevation	Along Corfu Rd.
Rock Knob	46.806944, -119.474625
412 m elevation	Scarp/Gully #2–#3
Fence Corner	46.809946, -119.475858
400 m elevation	Between Gully #3–#4
SSD Outcrop	46.812059, -119.465638
350 m elevation	Gully #2
Caprock Outcrop	46.812672, -119.470164
370 m elevation	Gully #3
Pedestal Outcrop	46.813255, -119.476206
360 m elevation	Gully #4

Description

Impressive alluvial fan gravels, or "fanglomerate," more than 3 m thick and heavily cemented with $CaCO_3$, overlie tan lakebeds of the Savage Island Member (upper Ringold Fm; fig. 12). The contact is erosional with several meters of relief. Soft sediment deformation (swirled bedding) occurs repeatedly in the Pliocene lakebeds and is synsedimentary (fig. 13). The deformation occurred

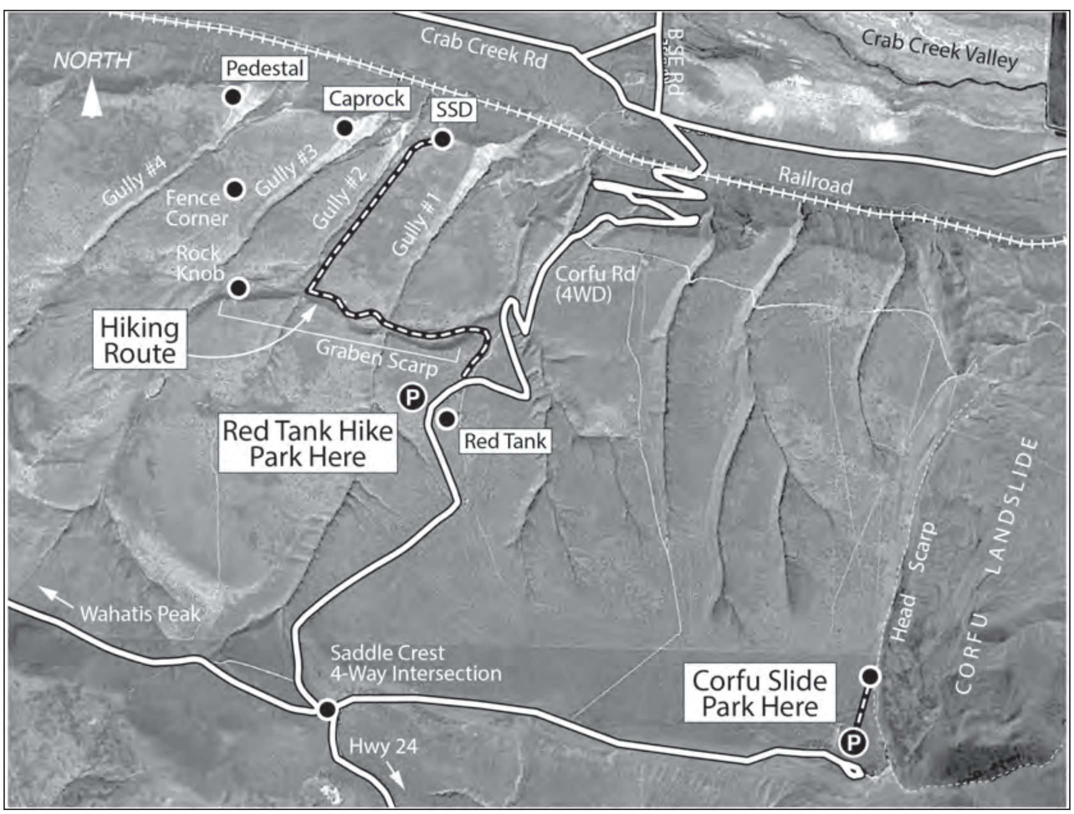

Figure 11. Red Tank hike map. Map showing hiking route to SSD Outcrop and other outcrops on the Smyrna Bench rim.

Figure 12. SSD Outcrop fanglomerates. Heavily cemented basaltic fanglomerate, derived from the rising Saddle Mountains ridge, truncate deformed Savage Island lakebeds (Ringold Fm).

Figure 13. SSD Outcrop soft sediment deformation. Repeated soft sediment deformation in silty and sandy beds of the Savage Island Member formed prior to being overridden by the fanglomerate.

prior to overloading by the Pleistocene fan gravels, when the sediments were wet and on the valley bottom (low ridge or no ridge present). Crab Creek at that time was a low-gradient, meandering, and sediment-choked channel. The Pleistocene-age fanglomerate is composed of angular basaltic colluvium that was shed in sheets and gully fills from near the crest of the Saddle Mountains anticline during uplift. They are syntectonic deposits. A thrust fault is mapped at the upper end of Smyrna Bench and at the range front (Reidel, 1988; Lidke and Haller, 2016; Staisch and others, 2018; Crane and Klimczak, 2019). Fan gravels and other sediments, now perched on Smyrna Bench (fig. 14), originally spilled onto the alluvial floor of Crab Creek Valley. The nearly 600 m of relief on the north flank of the Saddle Mountains is due in part to tectonic uplift and in part to incision by westward-flowing megafloods. Before the floods, the more or less continuous Smyrna Bench surface, which is now tilted north and dissected by landslides and local faults, swept smoothly across Crab Creek Valley to join Royal Slope (south flank of Frenchman Hills). Its profile probably resembled the profile of Saddle Mountains' south flank (Wahluke Slope).

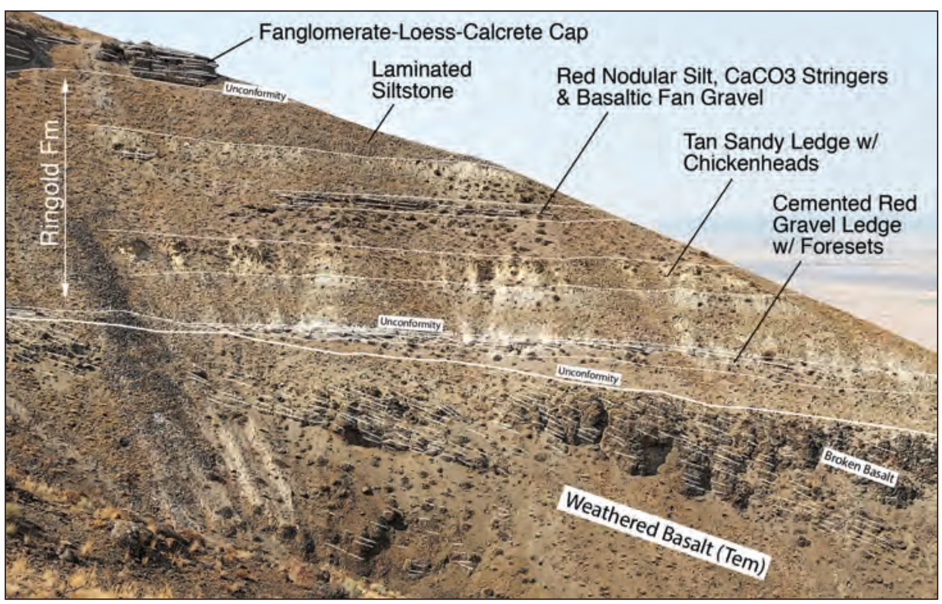

Figure 14. Nearby strata exposed at Smyrna Bench. Other slopes in the vicinity of the SSD Outcrop expose Pliocene Ringold strata. Several beds below the fanglomerate–calcrete cap are carbonate-cemented. The Ringold lies unconformably atop folded, weathered basalt.

Tentative Timing of Events

(a) Miocene–Pliocene. Modest rise of an early Saddle Mts ridge above the Ringold alluvial plain.

(b) Plio–Pleistocene. Weathering of bedrock ridge, accumulation of basaltic regolith, and calcic soil development.

(c) Early–Middle Pleistocene. Renewed activity on Saddle Mts Fault, ridge growth, slope steepening, mobilization and deposition of weathered regolith as fanglomerate atop Ringold sediments, a few early Ice Age floods, and calcic soil development.

(d) Late Pleistocene. Repeated voluminous Ice Age flooding, deep incision of Crab Creek–Drumheller scabland, landslides, creation of Smyrna Bench and Royal Slope escarpments, continued calcic soil development, and continued growth of anticline.

STOP 6:
Corfu Landslide Overlook

Calcrete-silcrete crust on basalt at crest of Saddle Mountains crest

46.791953, -119.446162

Directions

From Othello, drive Hwy 26 west for 17.5 mi to the White Bluffs Area gate. Do not turn. Instead, continue west on the highway 2.8 mi farther. Turn right (north) onto the gravel road (Corfu Rd.) signed "Saddle Mountains Overlook 5 miles." From Vantage, drive 19 mi to Mattawa, then follow Rd. 24 SW (becomes Hwy 24) west for 20 mi to Corfu Rd. Corfu Rd. ascends the south flank of Saddle Mountains, crossing the canal at 4.9 mi, after which potholes and washboards increase. At 7.1 mi reach the saddle crest and 4-way intersection (565 m elevation). Turn right (east) following the sign "Saddle Mts Overlook 1 Mile." Continue up the easy gravel incline to concrete slabs and road's end (fig. 11). Park and walk the short distance to the head scarp of the Corfu Landslide Complex (Lewis, 1985; Baker and others, 2016). Calcrete–silcrete crust is exposed below, a short ramble down the cliff edge.

Description

The 10- to 40-cm-thick crust is developed into cracked and weathered Pomona Member of the Saddle Mountain Basalt (10.5 Ma; fig. 15). Parent material is unclear. It is certainly fine grained, but has been completely cemented. The unit formed when the basalt was flat-lying or nearly so. The crust is possibly the basal portion of the Ringold Fm or that of a sedimentary interbed that previously stood atop the Pomona flow prior to uplift of the anticline. Identical hard, white crust also occurs on the crests of local anticlines and at the contacts between sedimentary interbeds and the underlying basalt exposed elsewhere in the Saddle Mountains.

Figure 15. Corfu landslide overlook. A bright white calcrete–silcrete crust is exposed along the rim below the overlook. Calcrete–silcrete overprints weathered basalt beneath certain Miocene sedimentary interbeds high on the north flank of the Saddle Mountains between Wahatis Peak and Sentinel Peak.

STOP 7:
White Bluffs Overlook

Exotic-bearing calcrete gravel truncates Savage Island lakebeds

46.625799, 119.395588

Directions

From Othello, drive Hwy 26 west for 17.5 mi to the White Bluffs Area gate. Turn left (south) and follow the gravel road for 8 mi to its end at the White Bluffs Overlook parking lot. Continuous outcrops line the Old Ringold Road and a few others are accessible by dropping down from the rim.

Description

There is a lot to see at White Bluffs Overlook. It's a large and diverse set of roadcuts and clifftop exposures through the upper Ringold Fm and its thick calcrete cap (fig. 16).

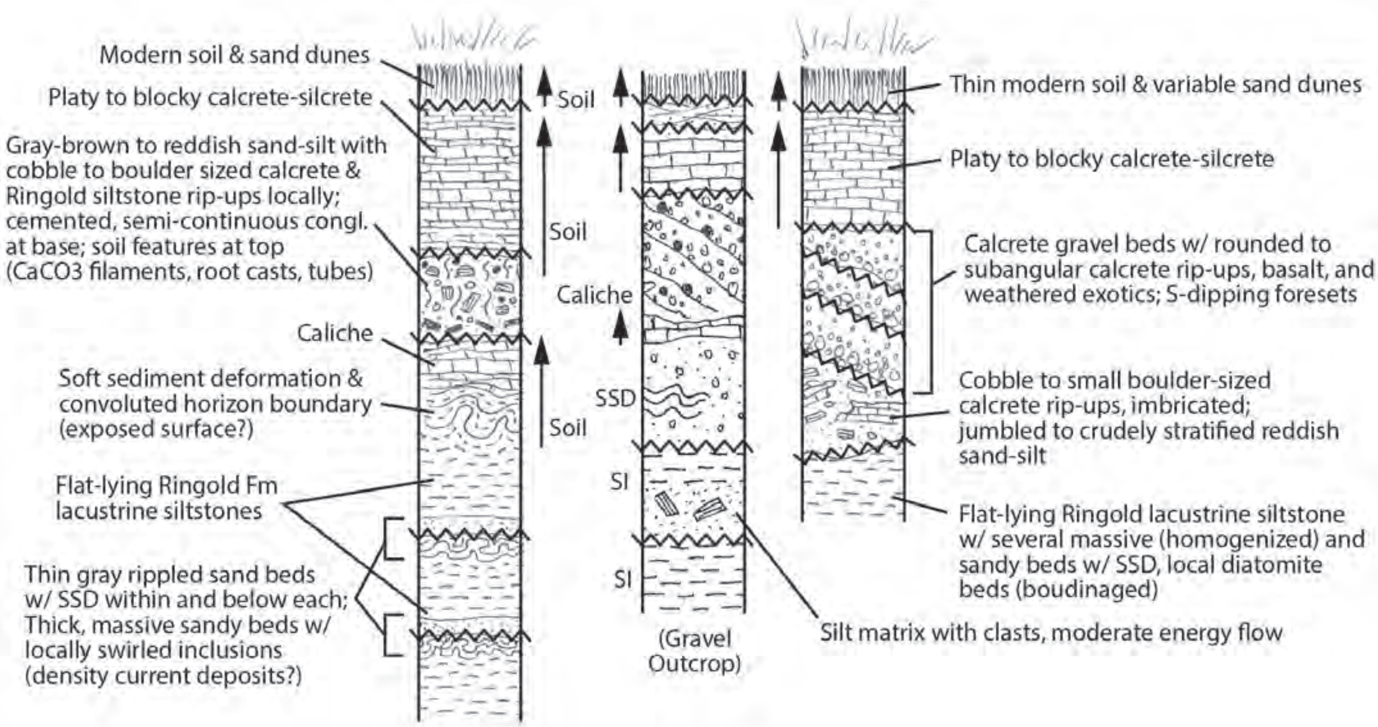

Figure 16. White Bluffs Overlook stratigraphy. White Bluffs is located in the heart of Pasco Basin, which gathered waters from nearly all scabland floods and near the center of Pliocene Lake Ringold. Evidence of energetic overland floods moving west across the abandoned Pliocene surface and into the Columbia Valley dislodged large stratified laths of lacustrine siltstone and transported rip-ups of calcrete and exotic clasts. A zone of soft sediment deformation occurs in laminated siltstone (Pliocene deformation), below the erosional contact with the younger flood-laid sediments.

Savage Island Member siltstones. Laminated lacustrine siltstones of the Pliocene Ringold Fm Savage Island Member, called “buff laminated clay” by Grolier and Bingham (1978), comprise much of the exposure. The Savage Island is tan-green-white-gray siltstone. Some fizzes vigorously in acid (tan silt) or not at all (gray-green clay).

Gray fluvial sands. Beds of gray rippled sand interrupt the lake deposits. Sands are mostly unconsolidated, but can be thoroughly cemented with a lumpy appearance. Convoluted bedding is commonly where sand and lacustrine sediments interfinger.

Massive beds. Two conspicuous, thick, massive beds of muddy sand are found near the lower end of the first yellow guardrail (fig. 17). Their thickness changes across the exposure. They were deposited on the flat lake bottom, but have no coarse bedload. Where thin laminae are highlighted by oxidation, they are internally swirled and thoroughly deformed. Massive sand beds similar to these are common in deep water successions (turbidity flows). Are they gravity flow deposits or something else?

Cemented ribbons of white. Resistant white beds up to about 10 cm thick occur in the Savage Island near the gate at the upper end of Old Ringold Road. The ribbons pinch laterally over tens of meters and slightly thin and thicken (boudins). The white material may be volcanic ash or young silica cements.

Figure 17. Massive(?) beds in the Ringold Fm at White Bluffs Overlook. Curious massive beds of silty sand, when inspected closely, show intense deformation.

Post-Ringold unconformity. The top of the Ringold is truncated by a prominent unconformity that began to form when base level on the Columbia River dropped abruptly around 3.2 Ma. Ice Age floods and local streams have deepened the erosion in places. The surface is commonly deformed and armored by Pleistocene calcrete.

Capping calcretes. Two thick calcretes cap the bluff (fig. 18). The lower calcrete is a blocky, Stage III+ unit 20–40 cm thick. It is partially disaggregated. Above is a reddish, massive to stratified, water-lain silty unit that contains cobble- to boulder-sized rip-up clasts of calcrete and stratified laths of siltstone. The unit exhibits considerable variation in thickness and grainsize. It grades laterally into exotic-bearing calcrete gravels with foresets. A thin, cemented, semi-continuous conglomerate occurs near the base of the unit in places (more to north, less to south). The upper calcrete is a ~3-m-thick, Stage V ledge-former with blocky to platy-laminar morphologies. Based on its thickness, it is probably a stack of welded calcretes, but the ledge is too broken up along the rim to resolve welded contacts. The contact with the underlying unit (calcrete gravels or jumbled red-pink sediment) is well defined and fairly flat.

Figure 18. Capping calcretes at White Bluffs Overlook. Thick Pleistocene calcretes overprint the Ringold Fm and post-Ringold unconformity.

Calcrete rip-up gravels with exotic clasts. The best exposure is had by walking south along the rim for a few hundred meters and dropping a short way down below the ledge. A crude path leads you along the ledges. Calcrete-clast conglomerate more than a meter thick shows west- and south-dipping

Figure 19. Calcrete gravels at White Bluffs Overlook. Clasts of calcrete and exotic constitute a thick, foreset gravel bed that cuts into Pliocene lakebeds of the Savage Island Member.

foresets (fig. 19). Clasts are subangular to rounded, pebble- to cobble-sized. A variety of clasts with exotic lithologies, including felsic volcanic, granite, dark gray schist, vein quartz, a dark intrusive, and weathered basalts. Exotics have carbonate coatings and comprise only a small fraction of gravel. Mafics disintegrate when excavated.

Paleosols. Two colorful paleosol intervals mark the shoaling of the Pliocene Ringold lake (fig. 20).

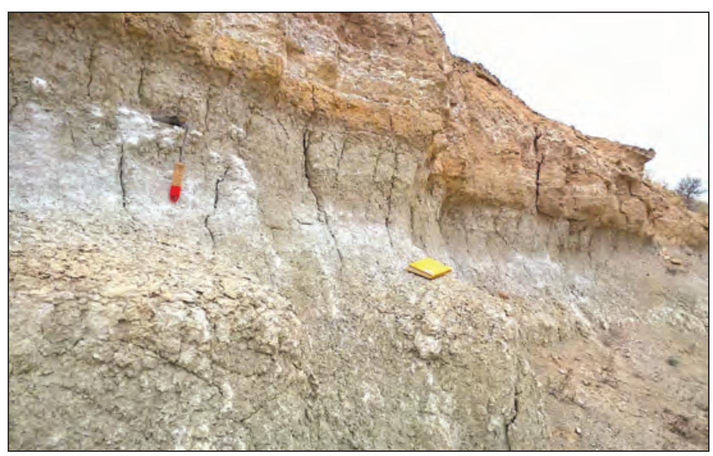

Figure 20. Paleosols at White Bluffs Overlook. Colorful paleosol intervals formed in lowland and upland (loess) settings separate coherent sections of Savage Island lakebeds.

Look for exposures in tumbleweed-filled gullies along the road. Reddish nodular loess is found in both intervals (Pliocene loess).

STOPS 8 and 9:
Ringold Road Bluffs Hike and Coyan Roadcut

Calcrete rip-ups and deformation at the upper and lower ends of Ringold–Koontz Coulee

Directions to Coyan Roadcut in upper Koontz Coulee

From Othello, drive south on Hwy 17 toward Scooteney Reservoir. At 10.4 mi turn left (east) onto Coyan Road. Continue past a house with a large green barn, through an uphill bend, and past the roadcut to the top of the hill. Park along shoulder or in the private farm pullout. Get permission from the farmer at the house with green barn. Alternatively, park vehicles along Hwy 17 at a wide pullout and walk up to the roadcut. Farm trucks move fast here. Stay completely off roadway.

Directions to Ringold Road Hike in lower Koontz Coulee

From Basin City, drive west on Rd. 170. In a little over a mile turn left (south) onto Fairway Rd. (Rd. 170), which becomes W. Klamath Rd., then Rd. 170 again. In a few minutes, turn right (west) onto Ringold Rd., which drops to the Columbia River, then right (north) onto graveled Ringold River Rd. Drive 5.5 mi north and park on road shoulder. This is federal land managed by the U.S. Fish and Wildlife Service. Leave the road and hike NE across open ground, crossing a wire fence, toward a thin path leading up a nose in light-colored Ringold sediments. Active landsliding is occurring along the steep, short path to the rim. Note the network of lateral spread fractures and toppled blocks. Your goal is the white ledge of calcrete near 46.570941, -119.310777. Short traverses in either direction provide excellent views of the 2-m-thick calcrete ledge. Spring and fall are the best times to visit. The White Bluffs are blazing hot in summer.

Description

Coyan Rd. and Ringold Rd. sites are located at the upper and lower ends of Ringold–Koontz Coulee. Though separated by nearly 30 km, their stratigraphy is remarkably similar. Calcrete rip-ups comprise gravel beds that unconformably overlie deformed Ringold lakebeds (Savage Island Member). At Coyan Rd., a contorted zone 40 cm thick is laterally traceable for over 25 m (fig. 21). At Ringold Rd., the same contorted zone occurs at the top of the Savage Island Member lakebeds (fig. 22). Cemented, downward-tapering clastic dikes descend from erosional contact between the calcrete gravel and lakebeds beneath.

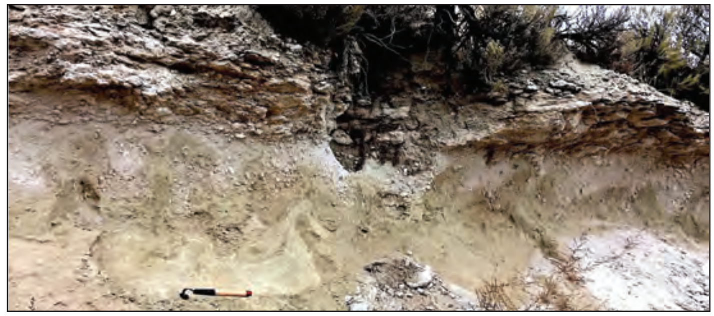

Figure 21. Coyan roadcut in Upper Koontz Coulee. Convoluted bedding beneath a thick calcrete ledge. Nearly identical deformation occurs in the same stratigraphic position at other sites in this field guide (Ringold Rd., Orchard Scarp, White Bluffs Overlook, etc.). A flood-cut trimline at ~330 m elevation is visible to the west on the hill that separates Koontz and Ringold Coulees.

Figure 22. Ringold Road bluffs in Lower Koontz Coulee. Convoluted bedding beneath calcrete rip-up gravel and a thick calcrete ledge. Downward-pinching clastic dikes are truncated by the base of the gravel.

STOP 10:
Watt Lane Landslide Scarp

Hike to the scarp of an active landslide exposing Ringold Fm, paleosols, and flood gravels

46.567908, -119.208250

Directions
From Basin City, drive west on Rd. 170. In a little

over a mile turn left (south) onto Fairway Rd. (Rd. 170), which becomes W. Klamath Rd. As the road descends the slope west through ag land of lower Ringold Coulee, the landslide becomes visible along the edge of the bluff. At 4.5 mi, navigate a 4-way intersection, keeping right on Klamath Hill Rd., then turning quickly right onto Watt Ln. If you miss Watt Ln, continue to the top of the hill where there are safe places to turn around. Park near the end of Watt Ln, which dead ends in a 1/2 mi at the toe of the slide. Hiking trails lead through slide debris and forest cover to scarp. Google Earth will help you locate the trail, as the active toe is constantly being excavated. The higher you hike, the better the view of the exposed strata. Large natural landslides and smaller irrigation-caused slides are numerous along the Hanford Reach of the Columbia River (White Bluffs).

Description

The scarp exposes tens of meters of Pliocene Ringold strata truncated by coarse Pleistocene flood gravels above (fig. 23). Pliocene strata is a mix of tan-green lake beds (Savage Island Member), red fluvial sandstones, oxidized nodular loess that resemble named Palouse paleosols, white ash beds, and a number of colorful paleosols. Cemented and uncemented layers interfinger. Several meters of boulder gravel containing abundant calcrete rip-ups unconformably overlie the Ringold. The section is undeformed except for a wavy, sagged zone in gray, cross-bedded micaceous sand located at the top of the lake beds section, beneath a conspicuous orange paleosol. Flame structures, load casts, and a few small, descending, single-fill clastic dikes are found nearby (fig. 24). This same contorted zone is found throughout the study area in the same stratigraphic position. Is the deformation the result of rapid sedimentation or seismic shaking? A short stack of grayish, slightly-tilted Touchet Beds containing a few sheeted clastic dikes is present at the base of the slide along the road.

STOP 11:
Railway Hike—Danielson Road to Hays Road

Railbed hike to flood-laid boulder gravels, Ringold Fm, and calcrete-bearing sediments

46.803022, -119.334278

Directions

From the South 1st Avenue–Hwy 26 intersection at Othello, drive west on Hwy 26 to Crab Creek Valley. At 7.2 mi, turn left (south) onto Danielson Rd.

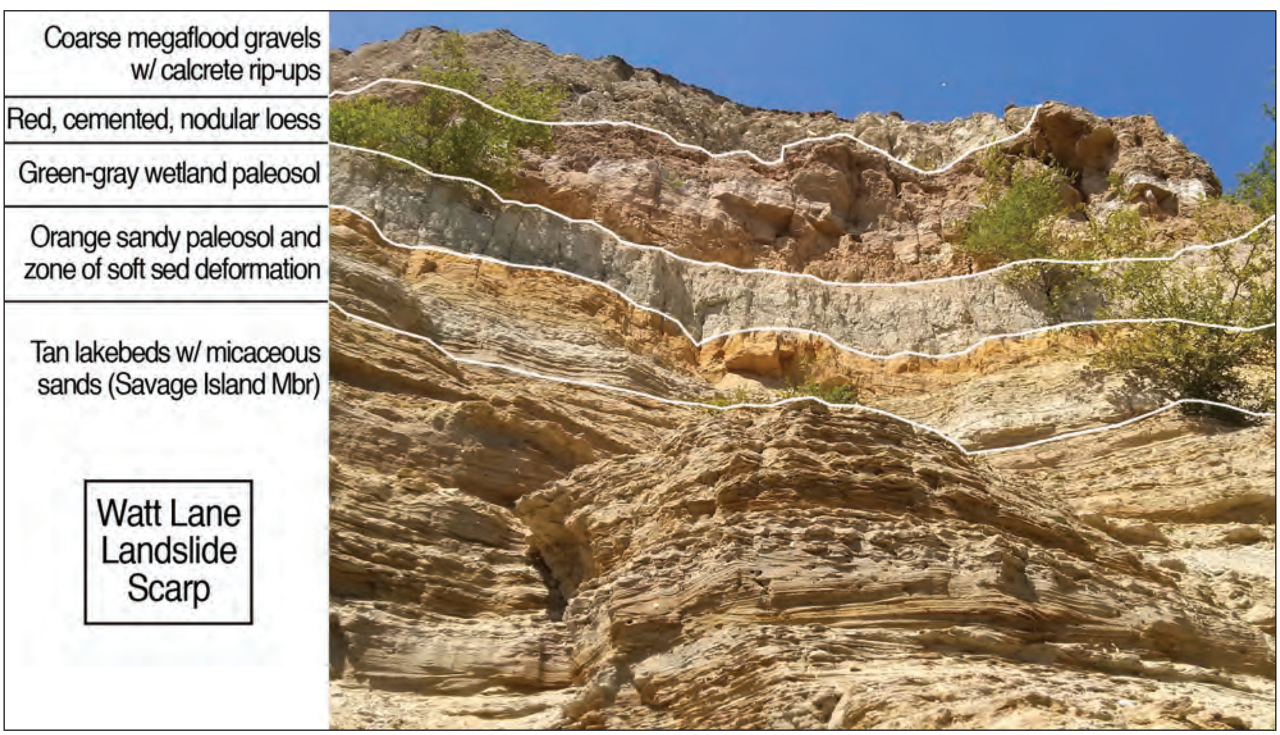

Figure 23. Heterogeneous strata exposed in landslide scarp at Watt Lane. Pliocene Ringold, "Plio–Pleistocene" sediments and paleosols, and coarse flood gravels at Watt Lane. A deformed zone occurs at the top of the Savage Island section.

Figure 24. Soft sediment deformation at Watt Lane. Sags, clastic dikes, mud squirts, and flame structures occur in a single interval near the top of the Savage Island lakebeds. Watt Lane is located at the lower end of the Koontz–Ringold Coulee, where floodwaters exited to the Columbia Valley. The coulee is 75 m deep and perched 60 m above the Columbia plain. Bretz noted that, despite its nearly identical position, no cataract formed at the mouth of the Koontz–Ringold Coulee as was done at Potholes Coulee and Frenchman Coulee.

Figure 25. Deformed bed below paleosols and calcrete ledges. An orange sandy bed below a paleosol with prismatic soil structure occurs at the top of the Pliocene section in a landslide scarp near railroad tracks. Evidence of soft sediment deformation from numerous outcrops in the area agrees with information from measured stratigraphic sections at White Bluffs (Lindsey, 1996, appendix A). There, three distinct zones of soft sediment deformation are associated with flooding surfaces, where the lake deepened and inundated cemented paleosols (lakebeds over paleosols).

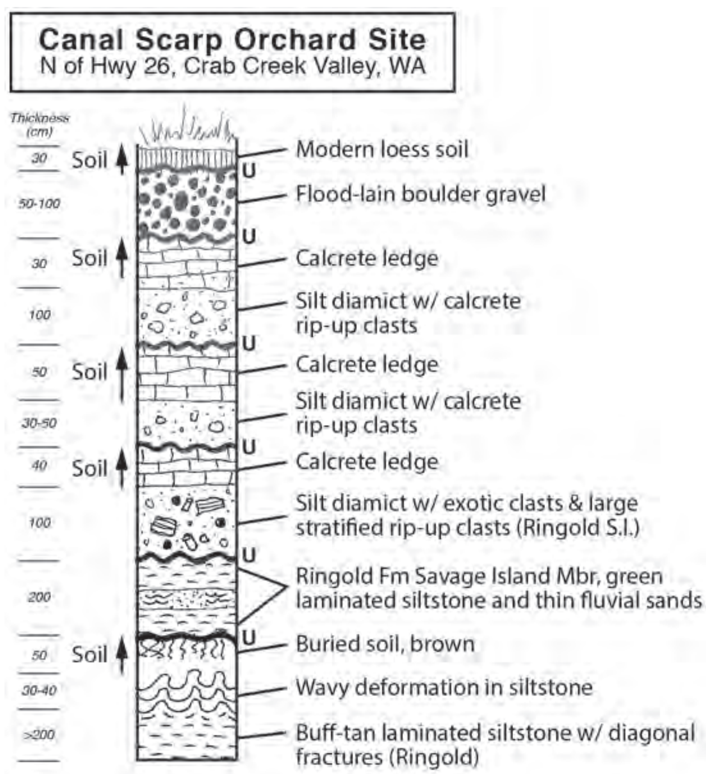

Figure 26. Stratigraphy in the Danielson-Hays Road area. Railcuts in the area expose variations on the stratigraphy of eastern Smyrna Bench. A flight of flood-cut terraces preserves a partial record of incision along Crab Creek Valley.

Gain the slope and park in a pullout at the sharp bend near the Taunton Heights Ln. sign. Hike the abandoned railroad tracks east where several slide scarps and railcuts reveal interesting relationships between upper Ringold sediments and coarse megaflood deposits of Smyrna Bench. Turn around after ~3 mi, when parallel with Hays Rd. (46.808472, -119.273994). If permission from the Wahluke Watermaster Office in Othello is secured, shorten the hike by driving 0.8 mi east on the narrow irrigation canal road and park in a grassy one-car pullout past the second hairpin curve (46.805043, -119.317094). Cross a short stretch of brushy ground to the tracks. A large scarp below a private orchard lies just south of tracks.

Description

The half dozen or so outcrops can be toured on foot over the course of a few hours. The contact between Ringold Fm, stacked calcretes, and megaflood deposits are on the menu for this off-the-beaten-path geology hike (figs. 25, 26).

For a look at Corfu Landslide deposits cutting fluvial-lacustrine sediments of the upper Ringold Fm, drive or hike the short, rough Taunton Heights Ln west 1/2 mi to the old Taunton Power Plant. The substation served the now abandoned Milwaukee Road Railroad, in the process of being converted into the Palouse to Cascades State Park Trail. Good outcrops are found behind the dilapidated brick structure.

STOP 12: Herman Railcut

Two calcrete ledges and pre-Missoula boulder gravels

46.884440, -119.150858

Directions

From Othello, drive 4.5 mi north on Hwy 17. Turn left (west) onto Herman Rd. There is no left turn lane here, so be careful. Drive 1 mi west on Herman Rd., cross tracks, and park at the bottom of hill in a wide pullout. Hike the tracks north for a few hundred meters past a landfill to the railcut. The north cut offers easy, weed-free access, but the south cut contains more dramatic geology. For the south cut, make a gently rising traverse up the sagebrush slope, behind the stack of ties, toward a small tree in the distance. Stay above the wet ditch that parallels the tracks. Drop down to ledges when they appear. South cut outcrops can get weedy and buggy in late summer.

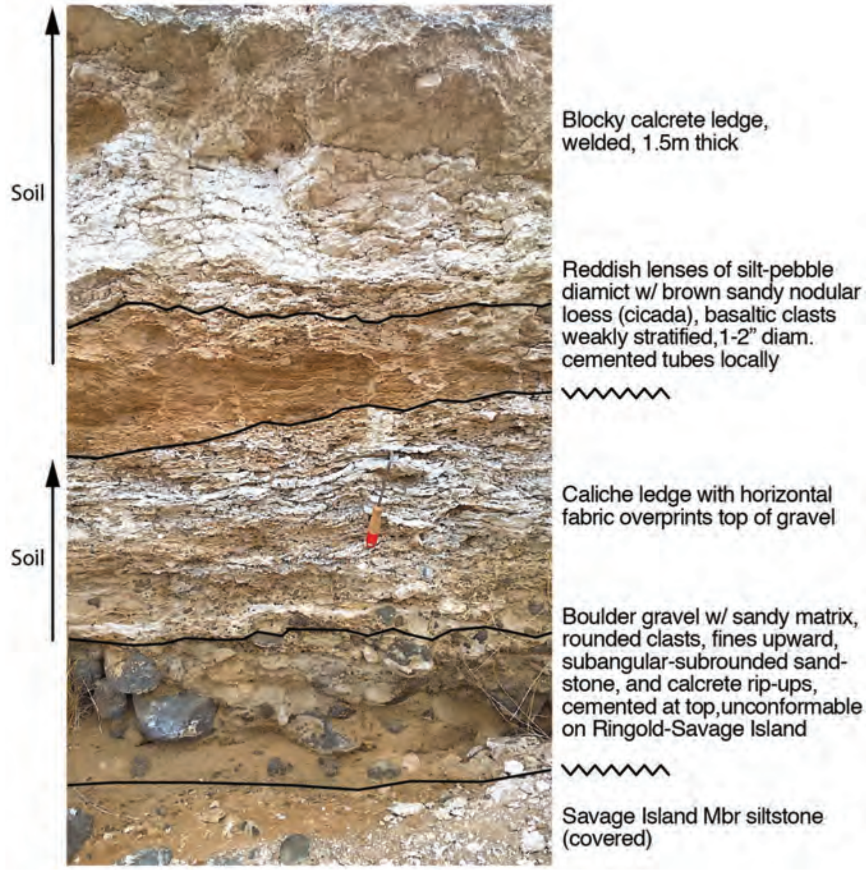

Figure 27. Boulder gravel beneath calcrete at Herman Railcut. Coarse gravel bed lying atop Savage Island lakebeds is cemented by a thick calcrete, which is in turn overlain by a silt-sand diamict and an even thicker calcrete.

Description

The railway runs along an escarpment at the outer bend of the Crab Creek–Drumheller Channels scabland. Butte-and-basin scabland and Columbia National Wildlife Refuge are visible to the NW. We are at the margin of high-energy, erosive flows and far beyond the toes of alluvial fan gravels that spill from the Saddle Mountains and Frenchman Hills ridges.

A boulder gravel, overprinted by calcrete, rests directly atop truncated Pliocene lakebeds (Savage Island Member) and is overlain by two more calcrete ledges (fig. 27). I interpret the gravel as a pre-Late Wisconsin flood deposit. Calcrete overprints the gravel and shows evidence of lateral throughflow. Look for chunks of green-gray Vantage sandstone, white Ringold mudstone, and other non-basalt clasts. The upper two calcrete ledges are separated by beds of nodular loess (upland deposits) and a red-brown, pebbly silt-sand diamict (stream-reworked loess) over variable thickness. The upper calcrete is a fully plugged, Stage V carbonate more than 1 m thick. Its parent material is almost entirely consumed by $CaCO_3$ except for sparse basalt cobbles that appear here and there. The amount of time required to accumulate a meter-thick calcrete is substantial. A conservative estimate for the age of the boulder gravel is 300,000–500,000 years.

Aridity alone does not build thick calcrete. You need a lot of water. These subsoil hardpans formed in a dusty, alluvial lowland setting, where seasonal wetting alternated with longer periods of intense drying. Considerable water, carrying dissolved carbonate, was made available to soils through time. Calcrete ledges show evidence of pedogenic development near the water table, and I suspect their growth has been somewhat accelerated due to their proximity to groundwater. In order to grow thick calcretes, the recipe seems to include a dry climate with periodic intense, soaking rains and a shallow, possibly fluctuating, water table.

STOP 13: Offramp

Two thick calcretes separated by sandy nodular loess overprint Savage Island lakebeds

46.809707, -119.132850

Directions

The Offramp site is a canal cut located behind a hay storage lot just east of the Hwy 26–Hwy 17 interchange SE of Othello. Park along the shoulder of Hwy 26, just east of the overpass, between the hay storage lot and the northbound offramp of Hwy 17. Locate a dusty two-track leading south along the hay lot fence. Walk a few hundred meters south, cross the wire fence, and drop below the rim to canal level on an easy footpath at its north end. Footing can be loose, brushy, and seasonally wet.

Description

Three calcrete ledges are separated by irregular bodies of reddish, fine-grained sediment containing abundant soil features including carbonate stringers, root casts, and cemented burrows (fig. 28). The red sediment appears to be wind deposited, but in places is quite sandy. Either it is Palouse loess with a slightly coarser grainsize similar to proximal loess of Eureka Flat (sand sheet deposit of Sweeney and others, 2017) or it is a combination of wind-deposited silt that has been reworked by flowing water. The first red bed occupies the same stratigraphic position as boulder gravels at Herman Railcut, where the same three calcrete ledges crop out.

Cicada nymph feeding burrows in the red sediment produce a distinctive trace fossil commonly found in Palouse soils (O'Geen and others, 2002). The burrows are A- and B-horizon features that lend a nodular appearance to silty and sandy host sediments ("nodular loess"). Burrows are cylinders typically 1–2 cm in diameter and 3–15 cm long. Sediment inside displays the unmistakable pattern of fine, arcuate ridges. People tend to associate cicada burrows with loess, but they occur in sandy sediment, too; I recently discovered some in coarse sand on the floor of Upper Grand Coulee. Again, cicada are a mark of surface stability.

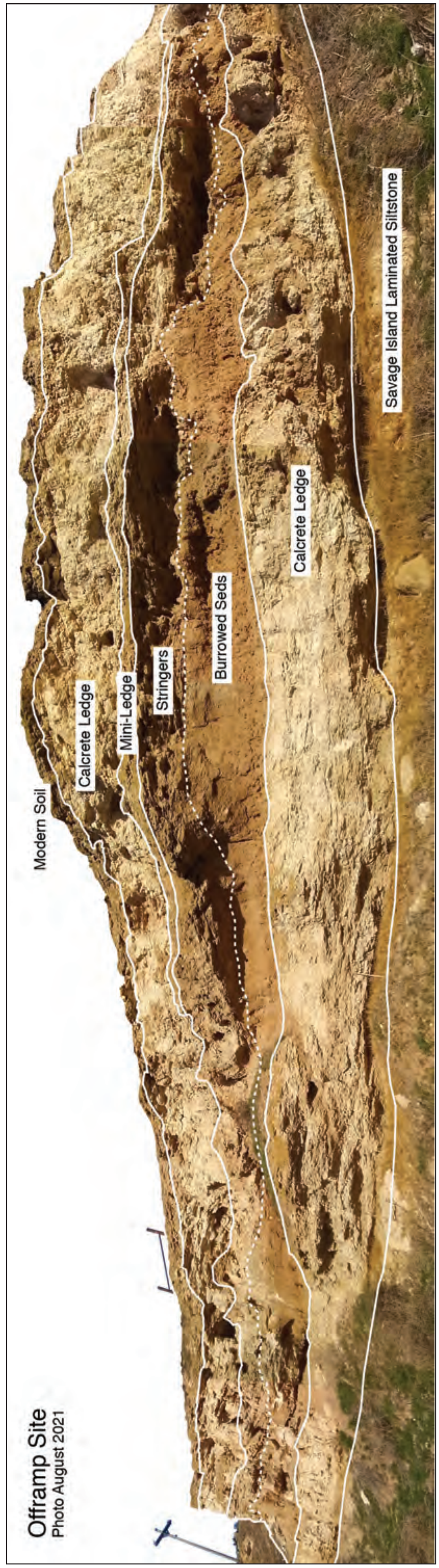

Figure 28. Offramp ledges. Two thick calcretes with sandy, nodular loess are well exposed along a wasteway canal draining Paradise Flats near Othello. Groundwater influence is apparent in the lower calcrete ledge.

The lower calcrete overprints flat-lying Savage Island Member (Ringold Fm) lakebeds and has a hard, blocky top 20 cm thick. The uncemented green-tan lakebeds are visible in small caves at the base of the exposure. The upper ledge is a fully plugged Stage V calcrete more than a meter thick. Its thickness and morphology suggest it formed near the water table (capillary fringe?).

STOP 14: Old Maid Coulee at Blanton Road

A classic site containing calcrete, pre-late Wisconsin flood deposits, and younger sediments

46.604506, -118.859540

Directions

From Connell, drive east on Hwy 260. Shortly after crossing over Hwy 395, look for Blanton Rd. Turn right (south) onto Blanton Rd. and continue south for 3.3 mi. The site is a borrow pit west of the road. Park on the shoulder opposite the pit.

Description

Old Maid Coulee was one of the first sites in the Channeled Scablands to contain evidence of "pre-late Wisconsin" flooding (figs. 29, 30). The site was discovered early in the 20th century (Bryan, 1927) and described by Bretz and others (1956) and Baker (1973). Cobble gravels at the base of the exposure were deposited by ancient floods. They contain south-dipping foresets and a reversed magnetic signature (>780 ka), and are capped by an advanced-stage calcrete that dates to at least 350 ka. A pebbly silt diamict unconformably overlies the calcrete and grades upward into modestly cemented L2 nodular loess. The nodular texture is created by thousands of backfilled feeding burrows

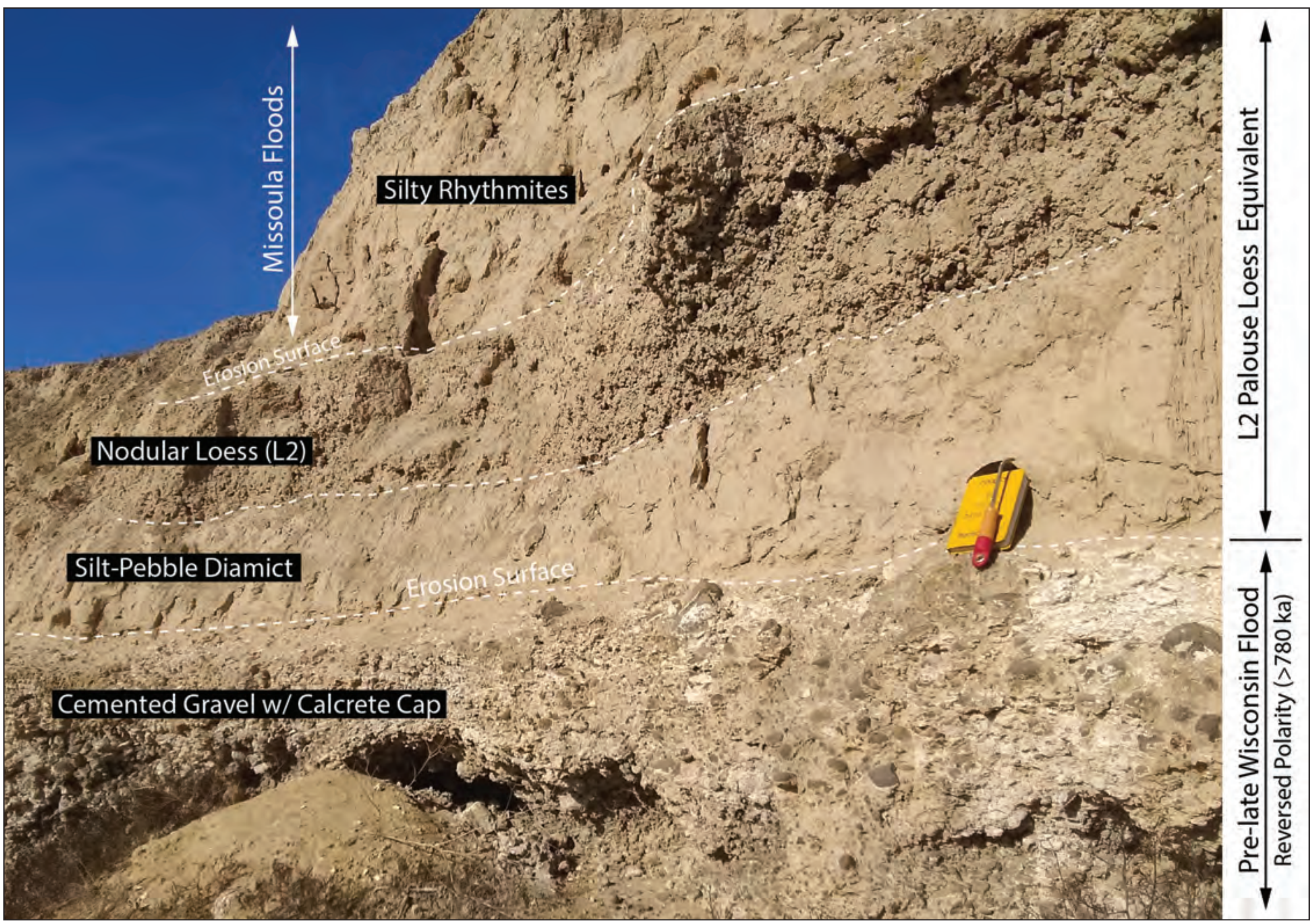

Figure 29. Old Maid Coulee. Ancient cemented flood gravels, nodular loess, and silty rhythmites constitute a long record of megaflooding and loess deposition. Silt diamicts (pebbles floating in a silt matrix) are commonly found with pre-Missoula gravels. Overland floods swept hillslopes of their loess, thus carried mostly silt and a few pebbles. The term silt diamict identifies their bi-modal grainsize distribution and implies transport of silt by flowing water. Diamicts in the Palouse–Scablands region are not loess, but reworked loess. Unlike sands and gravels sediment, silt does a poor job of preserving bedforms.

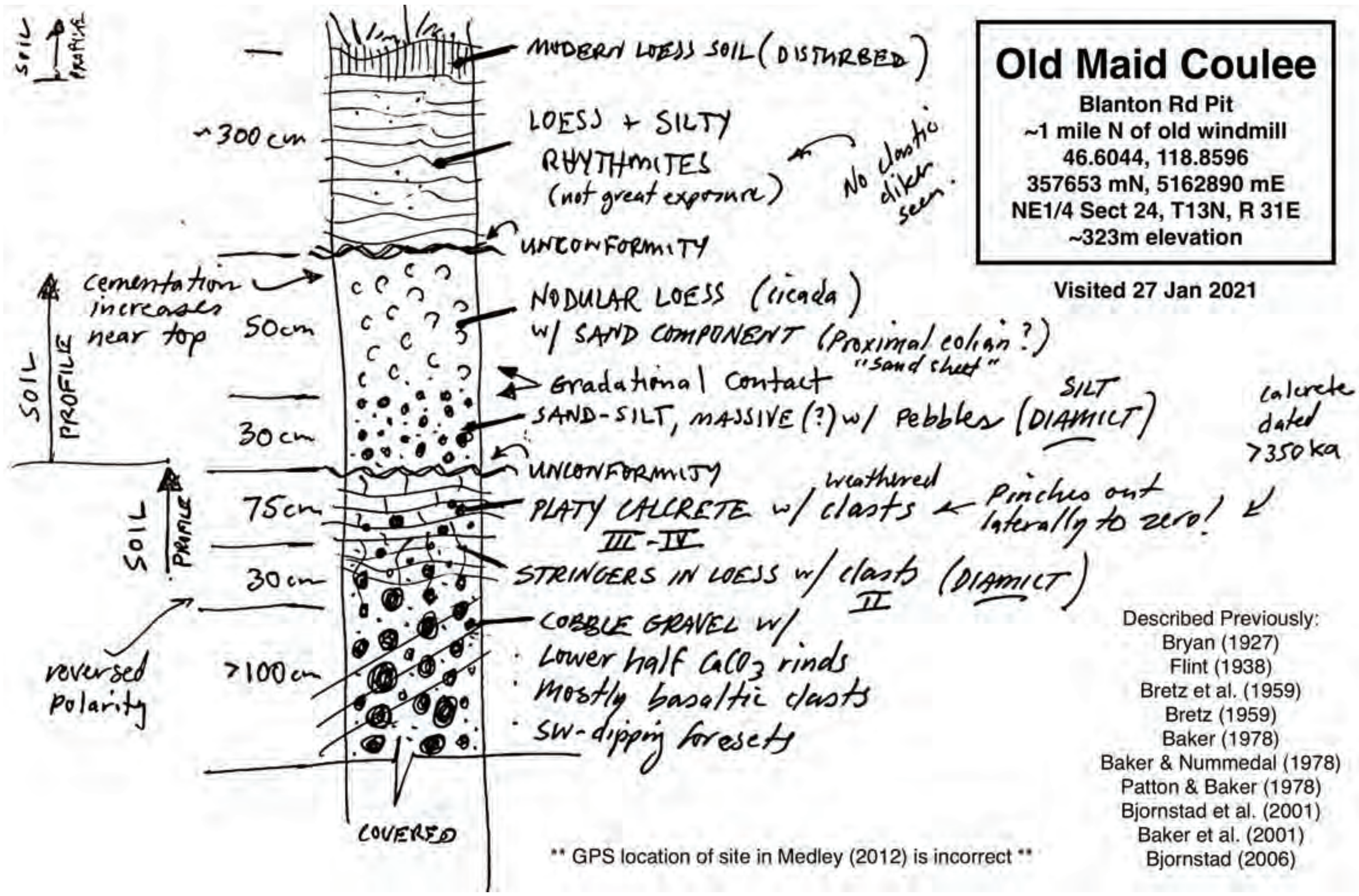

Figure 30. Old Maid Coulee Stratigraphy. Easily accessible pit along Blanton Road provides a good look at diverse stratigraphy.

of cicada nymphs. Several thin, silty, uncemented flood rhythmites (Touchet Beds), above, were deposited by the late Wisconsin Missoula floods (18–14 ka).

Some geologists remain unconvinced by the purported evidence of ancient scabland flooding in Eastern Washington. The detractors attribute the coated exotic clasts, silt diamicts, deep chroma loess, paleosols, sediment-filled coulees, reverse-polarity signatures, and lithified clastic dikes to alluvial processes of local streams. While some of the skepticism is legitimate, the evidence for pre-Missoula overland floods is accumulating. This subtle geology—what Spencer and Jaffee (2002) call the “indirect record”—looks very different from the bombastic landforms and thick deposits left behind by the younger, more voluminous Missoula floods.

STOP 15:
Pacific Road at Ritzville

Thick calcrete overprints loess on the western Palouse Slope

46.130863, -118.372266

Directions

The outcrop, an old excavation, is located in a vacant residential lot at the corner of 1st Street (Danekas Rd.) and Pacific Street in Ritzville about 1/2 misouth of the Top Hat Motel. Park on the street or in the vacant lot.

Description

Pacific Rd. is located in a scabland coulee through the Palouse. Strata exposed here is loess and calcrete (fig. 31). This may be one of Busacca and McDonald’s “Ritzville” sites.

Figure 31. Pacific Street. Stacked calcretes and loess at Ritzville. The site is located on the Palouse Slope in a scabland coulee near the eastern margin of the Ringold lake basin.

STOP 16: Marengo Railcut

Ancient flood deposits and loess in a transitional region between Scablands and Palouse

47.012298, -118.214064

Directions

From Ritzville, drive 5.2 mi east on Wellsand Rd., turn right (south) on Hills Rd. and follow for 4 mi. Turn left (east) on Urquart Rd. for 1.4 mi. Turn right on Marengo Rd. for 3.7 mi. Cross the tracks at the Marengo grain elevators, bearing right on Cow Creek Rd. Follow for 0.8 mi to another crossing. Park here on the shoulder or back at the elevators. The site is a double-sided railcut at a sweeping bend, above Cow Creek Rd. The Old Milwaukee Road railway is now the Palouse to Cascades State Park Trail (John Wayne Trail).

Description

Marengo is a classic scabland site among streamlined islands of Palouse loess (fig 32). Calcrete ledges, flood gravels, and loess with soil features are on display. Some of the loess contains pebbles and small cobbles suggesting the silt was, in part, transported by water (silt diamict).

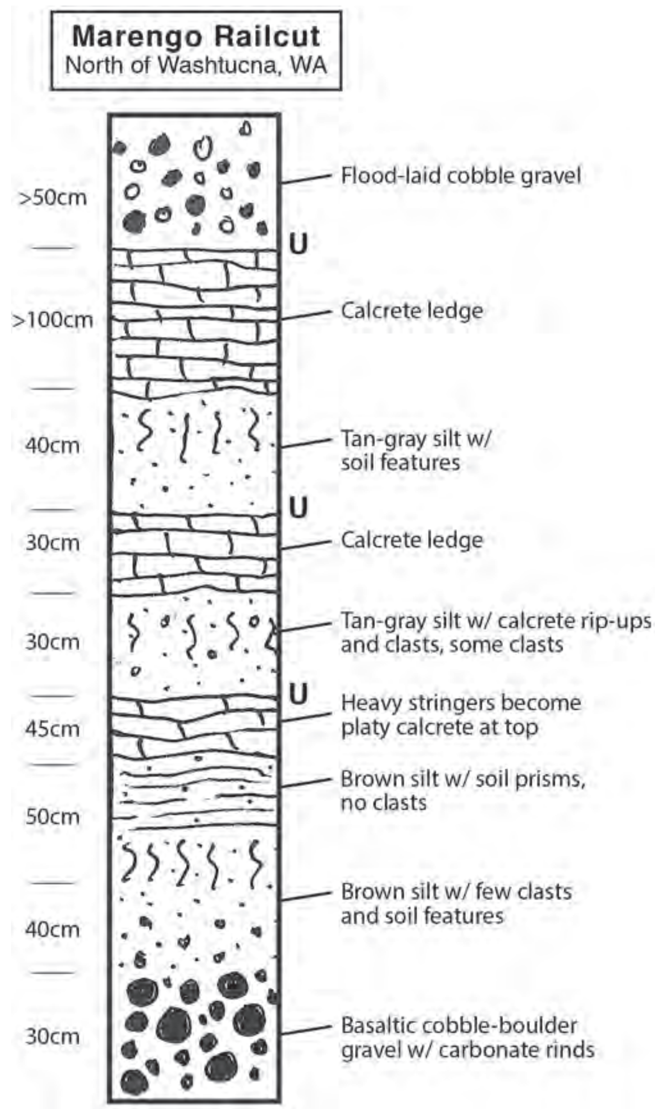

Figure 32. Marengo Railcut. Repeated loess deposition and calcic soil development with flood gravels above and below.

REFERENCES

Alonso-Zarza, A.M., and Tanner, L.H., 2010, Carbonates in Continental Settings, *in* Alonso-Zarza, A.M., and Tanner, L.H., eds., Geochemistry, Diagenesis and Applications 62, p. 1–319.

Baker, V.R., 1973, Paleohydrology and sedimentology of Lake Missoula flooding in eastern Washington: Geological Society of America Special Paper 144.

Baker, V.R., Bjornstad, B.N., Busacca, A.J., Fecht, K.R., Kiver, E.P., Moody, U.L., and Tallman, A.M., 1991, Quaternary geology of the Columbia Plateau, *in* Geology of North America—Quaternary nonglacial geology, Conterminous U.S., v. 2, p. 215–250.

Baker, V.R., Bjornstad, B.N., Gaylord, D.R., Smith, G.A., Meyer, S.E., Alho, P., Breckenridge, R.M., Sweeney, M.R., and Zreda, M., 2016, Pleistocene megaflood landscapes of the Channeled Scabland: Geological Society of America Field Guide, v. 41, p. 1–74.

Beck, G.F., 1936, Limerock zone of Columbia Basin: The Mineralogist, v. 4, p. 12–14.

Bjornstad, B.N., 2006, On the Trail of the Ice Age Floods—A geological field guide to the mid-Columbia Basin: Keokee Publishing, 307 p.

Bjornstad, B.N., Fecht, K.R., and Pluhar, C.J., 2001, Long history of pre-Wisconsin, ice age cataclysmic floods: Evidence from southeastern Washington state: Journal of Geology, v. 109, p. 695–713.

Birkeland, P.W., 1999, Soils and geomorphology: Oxford University Press, 430 p.

Bretz, J.H., Smith, H.U., and Neff, G.E., 1956, Channeled Scabland of Washington: New data and interpretations: Geological Society of America Bulletin, v. 67, p. 957–1049.

Brown, D.J., 1959, Subsurface geology of the Hanford Separation areas, Richland, WA: General Electric Company Report HW-61780, 21 p.

Brown, D.J., 1960, An introduction to the surface of the Ringold Formation beneath Hanford Works area: Richland, Washington: Hanford Atomic Products Operation Report HW-62530, 12 p.

Brownfield, M.E., 2008, Cretaceous–Tertiary composite Total Petroleum System and geologic assessment of undiscovered gas resources of the Eastern Oregon and Washington Province: U.S. Geological Survey Digital Data Series DDS–69–O, 43 p. + CD-ROM.

Bryan, K., 1927, The Palouse soil problem: U.S. Geological Survey Bulletin, v. 790, p. 21–45.

Busacca, A.J., 1989, Long Quaternary record in eastern Washington, USA, interpreted from multiple buried paleosols in loess: Geoderma, v. 45, p. 105–122.

Campbell, N.P., and Banning, D.L., 1985, Stratigraphy and hydrocarbon potential of the northwestern Columbia Basin based on recent drilling activities: Rockwell Hanford Operations Report SD-BWI-TI-265, 54 p.

Cheney, E.S, 2016a, Overview of the Cenozoic unconformity-bounded sequences of Washington, *in* Cheney, E.S., ed., The geology of Washington and beyond: From Laurentia to Cascadia: University of Washington Press, p. 183–190.

Cheney, E.S, 2016b, The Neogene eggcrate of the Pacific Northwest, *in* Cheney, E.S., ed., The geology of Washington and beyond: From Laurentia to Cascadia, University of Washington Press, p. 206–219.

Clarke, S.E., and Bryce, S.A., 1997, Hierarchical subdivisions of the Columbia Plateau & Blue Mountains ecoregions, Oregon & Washington: U.S. Department of Agriculture General Technical Report PNW-GTR-395, 114 p.

Crane, K.T., and Klimczak, C., 2019, A 3-D structural model of the Saddle Mountains, Yakima Fold Province, Washington, USA: Implications for Late Tertiary tectonic evolution of the Columbia River Flood Basalt Province: Tectonophysics, v. 766, p. 1–13.

Culver, H.E., 1937, The geology of Washington I: General features of Washington geology: Washington Department of Conservation and Development Bulletin, v. 32, 70 p.

Czajkowski, J.L., Bowman, J.D., Schuster, J.E., and Wheeler, C.M., 2012, Oil and gas wells in Washington State: Washington Division of Geology and Earth Resources Open-File Report 2012-02 (rev. 2015), 4 p. + CD-ROM.

Fecht, K.R., Reidel, R.P., and Tallman, A.M., 1987, Paleodrainage of the Columbia River System on the Columbia Plateau of Washington State: Washington Division of Geology and Earth Resources Bulletin, v. 77, p. 219–248.

Gile, L.H., Peterson, F.F., and Grossman, R.B., 1966, Morphological and genetic sequences of carbonate accumulation in desert soils: Soil Science, v. 101, p. 347–360.

Grolier, M.J., and Bingham, J.W., 1978, Geology of parts of Grant, Adams, and Franklin Counties, east-central Washington: Washington State Division of Geology and Earth Resources Bulletin, v. 71, 91 p.

Gustafson, E.P., 1978, The vertebrate faunas of the Pliocene Ringold Formation, south-central Washington: Bulletin of the Museum of Natural History (University of Oregon), v. 23, 72 p.

Hammond, P.E., 1979, A tectonic model for evolution of the Cascade Range: SEPM Pacific Coast Paleogeography Symposium 3—Cenozoic paleogeography of the western United States, p. 219–237.

King, G.E., Pearce, N.J., Roberts, H.M., Smith, V.C., Westgate, J.A., Gaylord, D.R., and Sweeney, M.R., 2016, Identification of a Kulshan caldera correlative tephra in the Palouse loess of Washington State, northwest USA: Quaternary Research, v. 86, p. 232–241.

Kohn, M.J., 2002, Oxygen isotope evidence for progressive uplift of the Cascade Range, Oregon: Earth and Planetary Science Letters, v. 204, p. 151–165.

Lamplugh, G.W., 1902, Calcrete: Geological Magazine, v. 9, p. 575–575.

Ledgerwood, R.K., Myers, C.W., and Cross, R.W., 1978, Pasco Basin stratigraphic nomenclature: Rockwell International Report RHO-BWI-LD-1, 10 p.

Lewis, S., 1985, The Corfu landslide: A large-scale prehistoric compound-complex slide in south-central Washington: MS Thesis, University of Arizona, 48 p.

Lidke, D.J., and Haller, K.M., 2016, USGS Quaternary fault and fold database of the United States, available at https://earthquake.usgs.gov/cfusion/qfault/ [Accessed June 2022].

Lindsey, K.A., 1992, Revised stratigraphy for the Ringold Formation, Hanford Site, south-central Washington: Westinghouse Hanford Document WHC-SD-EN-EE-004, 15 p.

Lindsey, K.A., 1996, The Miocene to Pliocene Ringold Formation and associated deposits of the ancestral Columbia River system, south-central Washington and north-central Oregon: Washington Division of Geology and Earth Resources Open-File Report 96-8, 176 p.

Machette, M.N., 1985, Calcic soils of the southwestern United States: Geological Society of America Special Paper, v. 303, p. 1–21.

McDonald, E.V., and Busacca, A.J., 1992, Late Quaternary stratigraphy of loess in the channeled scabland and Palouse of Washington State: Quaternary Research, v. 38, p. 141–156.

McDonald, E.V., Sweeney, M., and Busacca, A., 2012, Glacial outburst floods and loess sedimentation documented during Oxygen Isotope Stage 4 on the Columbia Plateau, Washington State: Quaternary Science Reviews, v. 45, p. 18–30.

McFarland, C.R., 1979, Oil and gas exploration in Washington: Washington Division of Geology and Earth Resources Information Circular, v. 67, p. 1–6.

McLean, A., and Bershaw, J., 2021, Molecules to mountains: A multi-proxy investigation into ancient climate and topography of the Pacific Northwest, USA: Frontiers in Earth Science, v. 9, p. 1–7.

Merriam, J.C., and Buwalda, J.P., 1917, Age of strata referred to the Ellensburg Formation in the White Bluffs of the Columbia River: University of California Bulletin of the Department of Geology, v. 10, p. 255–266.

Medley, E., 2012, Ancient cataclysmic floods in the Pacific Northwest: Ancestors to the Missoula floods: PhD Dissertation, Portland State University, 186 p.

Mustoe, G.E., and Leopold, E.B., 2014, Paleobotanical evidence for the post-Miocene uplift of the Cascade Range: Canadian Journal of Earth Sciences, v. 51, p. 809–824.

Newcomb, R.C., 1958, Ringold Formation of Pleistocene age in the type locality, the White Bluffs, Washington: American Journal of Science, v. 225, p. 328–340.

O'Geen, A.T., McDaniel, P.A., and Busacca, A.J., 2002, Cicada burrows as indicators of paleosols in the inland Pacific Northwest: Soil Science Society of America Journal, v. 66, p. 1584–1586.

Packer, D.R., 1979, Paleomagnetism and age dating of the Ringold Formation and loess deposits in the State of Washington: Oregon Geology, v. 41, p. 119–132.

Patton, P.C., and Baker, V.R., 1978, New evidence for pre-Wisconsin flooding in the channeled scabland of eastern Washington: Geology, v. 6, p. 567–571.

Pluhar, C.J., Bjornstad, B.N., Reidel, S.P., Coe, R.S., and Nelson, P.B., 2006, Magnetostratigraphic evidence from the Cold Creek bar for onset of ice-age cataclysmic floods in eastern Washington during the Early Pleistocene: Quaternary Research, v. 65, p. 123–135.

Reidel, S.P., 1988, Geologic map of the Saddle Mountains, south-central Washington: Washing-ton Division of Geology and Earth Resources, GM-38, scale 1:48,000.

Reiners, P.W., Ehlers, T.A., Garver, J.I., Mitchell, S.G., Montgomery, D.R., Vance, J.A., and Nicolescu, S., 2002, Late Miocene exhumation and uplift of the Washington Cascade Range: Geology, v. 30, p. 767–770.

Retallack, G., 2007, Cenozoic paleoclimate on land in North America: Journal of Geology, v. 115, p. 271–294.

Richardson, C.A., McDonald, E.V., and Busacca, A.J., 1997, Luminescence dating of loess from the northwest United States: Quaternary Science Reviews, v. 16, p. 403–415.

Russell, I.S., 1893, A geological reconnoissance in central Washington, U.S. Geological Survey Bulletin, v. 108, 108 p.

Schoeneberger, P.J., Wysocki, D.A., and Benham, E.C., 2012, Field book for describing and sampling soils (Version 3.0): NRCS National Soil Survey Center, 298 p.

Slate, J.L., 1996, Buried carbonate paleosols developed in Pliocene–Pleistocene deposits of the Pasco Basin, south-central Washington, U.S.A.: Quaternary International, v. 34–36, p. 191–196.

Slate, J.L., 2000, Nature and variability of the Plio–Pleistocene Unit in the 200 West Area of the Hanford Site: Bechtel Hanford Report BHI-01203, unpaginated.

Smith, G.R., Morgan, N., and Gustafson, E., 2000, Fishes of the Mio-Pliocene Ringold Formation, Washington—Pliocene capture of the Snake River by the Columbia River: University of Michigan Museum of Paleontology Papers on Paleontology, v. 32, p. 1–47.

Spencer, P.K., and Jaffee, M.A., 2002, Pre-Late Wisconsinan glacial outburst floods in southeastern Washington—The indirect record: Washington Geology, v. 30, p. 9–16.

Staisch, L.M., Kelsey, H., Sherrod, B., Möller, A., Paces, J., Blakely, R., and Styron, R., 2018, Miocene–Pleistocene deformation of the Saddle Mountains—Implications for seismic hazard in central Washington, USA: Geological Society of America Bulletin, v. 130, p. 411–437.

Staisch, L.M., O'Connor, J.E., Cannon, C.M., Holm-Denoma, C., Link, P.K., Lasher, J., and Alexander, J.A., 2021, Major reorganization of the Snake River modulated by passage of the Yellowstone Hotspot: Geological Society of America Bulletin, doi: https://doi.org/10.1130/B36174.1.

Sweeney, M.R., McDonald, E.V., and Gaylord, D.R., 2017, Generation of the Palouse loess—Exploring the linkages between glaciation, outburst megafloods, and eolian deposition in Washington State, *in* Haugerud, R.A., and Kelsey, H.M., eds., From the Puget Lowland to east of the Cascade Range—Geologic excursions in the Pacific Northwest: Geological Society of America Field Guide, v. 49, 207 p.

Takeuchi, A., and Larson, P.B., 2005, Oxygen isotope evidence for the late Cenozoic development of an orographic rain shadow in eastern Washington, USA: Geology, v. 33, p. 313–316.

Tincher, C.R., and Reidel, S.P., 2009, New evidence for the nature of the Saddle Mountains fault zone: GSA Annual Meeting Abstracts with Programs, v. 41, p. 226.

U.S. Department of Energy, 2002, Standardized stratigraphic nomenclature for the post-Ringold Formation sediments within the central Pasco Basin: Richland Operations Office Report RL-2002-39, 121 p.

U.S. Department of Energy, 2010, Hydrogeologic model for the Gable Gap area, Hanford Site: Pacific Northwest National Laboratory Report PNNL-19702, 115 p.

Waitt, R.B., 2017, Pleistocene glaciers, lakes, and floods in north-central Washington State, *in* Haugerud, R.A., and Kelsey, H.M., eds., From the Puget Lowland to east of the Cascade Range—Geologic excursions in the Pacific Northwest: Geological Society of America Field Guide, v. 49, p. 175–205.

Wilson, M.S., Dyman, T.S., and Condon, S.M., 2008, Chapter 4—Evaluation of well-test results and the potential for basin-center gas in the Columbia Basin, central Washington: U.S. Geological Survey Digital Data Series DDS-69-O, 12 p.

Zamanian, K., Konstantin, P., and Yakov, K., 2016, Pedogenic carbonates—Forms and formation processes: Earth-Science Reviews, v. 157, p. 1–17.

FIELD GUIDE TO THE ICE AGE FLOODS FEATURES OF MOSES COULEE—DRY FALLS AND GLACIAL FEATURES OF THE WATERVILLE PLATEAU

Brent Cunderla

Retired Geologist, Wenatchee, Washington

INTRODUCTION

On this field trip, we will examine ice age flood features predominately in the Moses Coulee and the Dry Falls area. Moses Coulee is second only to the grandeur of Grand Coulee, but is less known or visited due to access and lack of a major state highway though the coulee. Glacial landforms/features (moraines, drumlins, eskers, kames, kettles, kettle lakes, erratics, bedrock striations, and grooves) on the Waterville Plateau are well preserved due to the semi-arid climate of north-central Washington. Figure 1 shows our stops and major roads in the north-central Washington area.

Early authors including Waters (1933), Flint (1935), and Flint and Irwin (1939) first gave an overview of the Cordilleran Ice Sheet (Okanogan Lobe) glacial geology. Waitt and Thorson (1983) examined the relationship between the Okanogan Lobe and flooding down the Columbia River drainage prior to ice blockage, and Atwater (1987) looked at the relationship between the Okanogan Lobe, formation of Glacial Lake Columbia, and how that affected later flooding down Grand Coulee. Weis (1965) and Carrara, Kiver, and Stradling (1996) gave an overview of the Cordilleran Ice Sheet in northern Idaho and Washington with some discussion of the Waterville Plateau area. Hanson (1970), Waitt and Thorson (1983), and more recently Kovanen and Slaymaker (2004) have given more details about Waterville Plateau glaciation.

Waitt (2017) summarizes the timing and megaflood relationships down the Columbia River drainage, Moses Coulee, Grand Coulee, and further eastern high-elevation outlets. Work by Balbas and others (2017) further defines the relationship between Pleistocene ice age floods and Cordilleran Ice Sheet retreat

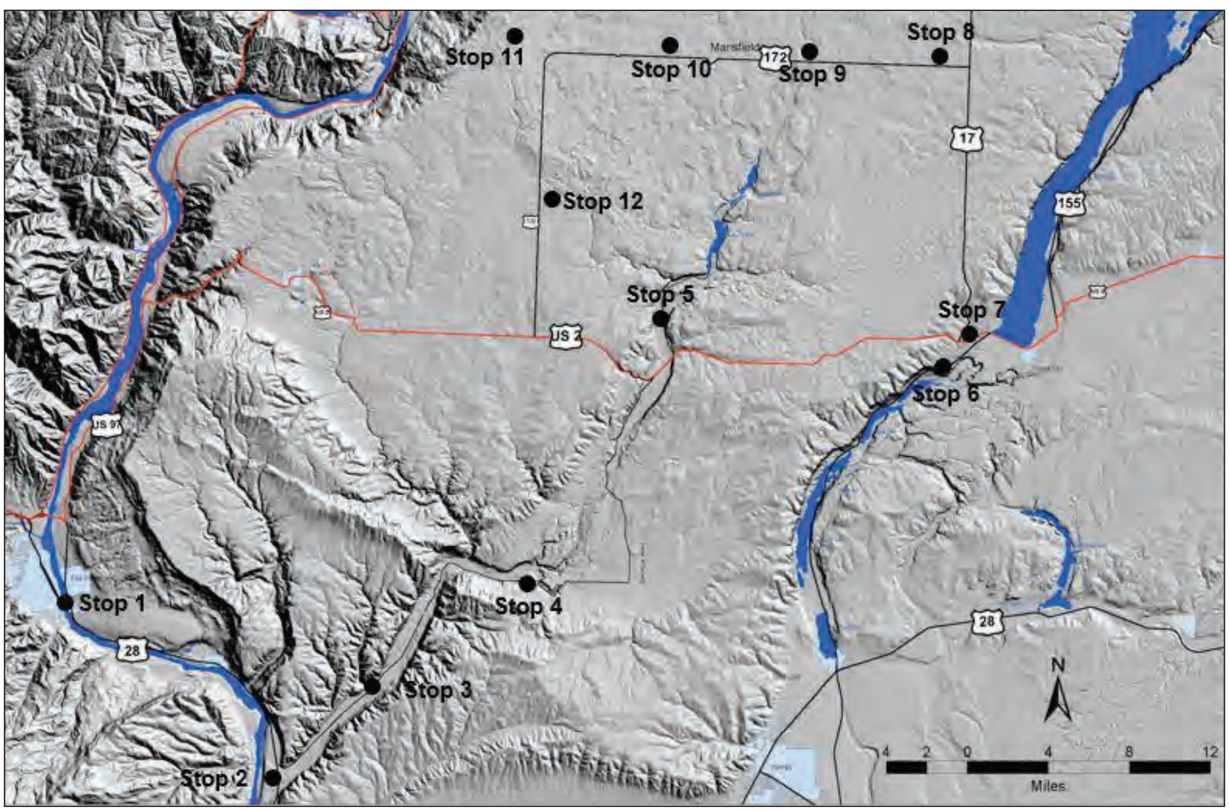

Figure 1. Field trip stops and major roads for the field trip.

using cosmogenic age dating techniques. O'Conner and others (2020) give a comprehensive review of "megafloods" associated with the Channeled Scabland of eastern Washington. Figure 2 shows the regional distribution of Cordilleran ice sheet at maximum stand, glacial lakes, and ice age flood erosional and depositional areas (Waitt, 2017).

ROAD LOG

STOP #:
Mileage between stops/cumulative mileage

From the Chelan County Fairgrounds campground turn right (E) onto Kimber Road. Follow Kimber Road east 0.1 mi to Wescott Drive. Turn left (N) onto Wescott Dr. for 0.2 mi to Sunset Highway. Turn right (E) onto Sunset Hwy and proceed 1.3 mi until Aplets Way. Turn left (N) on Aplets Way and proceed 0.3 mi to U.S. Highway 2/97 (US 2/97). At light turn right (E) onto US 2/97. Proceed east on US 2/97 for 8.0 mi into Wenatchee, WA. Take the exit/off-ramp for US 2/97 and follow US 2 (2.0 mi) across the Columbia River and get into the far right lane. At the light turn right (S) onto SR-28 (Sunset Hwy) for 3.7 mi to Stop 1. Stop 1 is on the right shoulder of SR-28 just past 9th Street (old Wenatchee Bridge).

STOP 1:
Large bedload erratic boulders
13.6/13.6

Large boulders are located at least as high as 120 ft above the Columbia River. Most are Swakane Biotite Gneiss. At least 15 gneiss boulders here have diameters greater than 15 ft, and all are angular despite 4–16 mi of transport (Waitt, 2017). The more rounded boulders of hornblende quartz diorite and as large as 6 ft in diameter were derived from a distinctive rock belt near Entiat 17–23 mi up-valley (Waitt, 2017). The largest gneiss boulder is 40 ft in diameter, so big and angular it looks like a bedrock outcrop. Eocene sandstone near the base of the river bank (water line) is the local bedrock and the crystalline rocks here are all boulders. The well-defined limit of glaciation is about 30 mi north up-valley (near Chelan Falls, WA), well upriver of the limits of the two source bedrock belts; therefore, these boulders are interpreted as bedload flood deposits. Figure 3 shows the bedload boulders.

Pull out onto SR-28 and stay in the right lane (left lane goes to Wenatchee, WA) and proceed south under an overpass and merge back onto SR-28; proceed 15 mi through Rock Island, WA and past Rock Island Dam (1st dam on the Columbia River) to Nelson Siding Road. Turn right (W) onto Nelson Siding Road, which turns south and parallels SR-28. Proceed 0.6 mi to Stop 2.

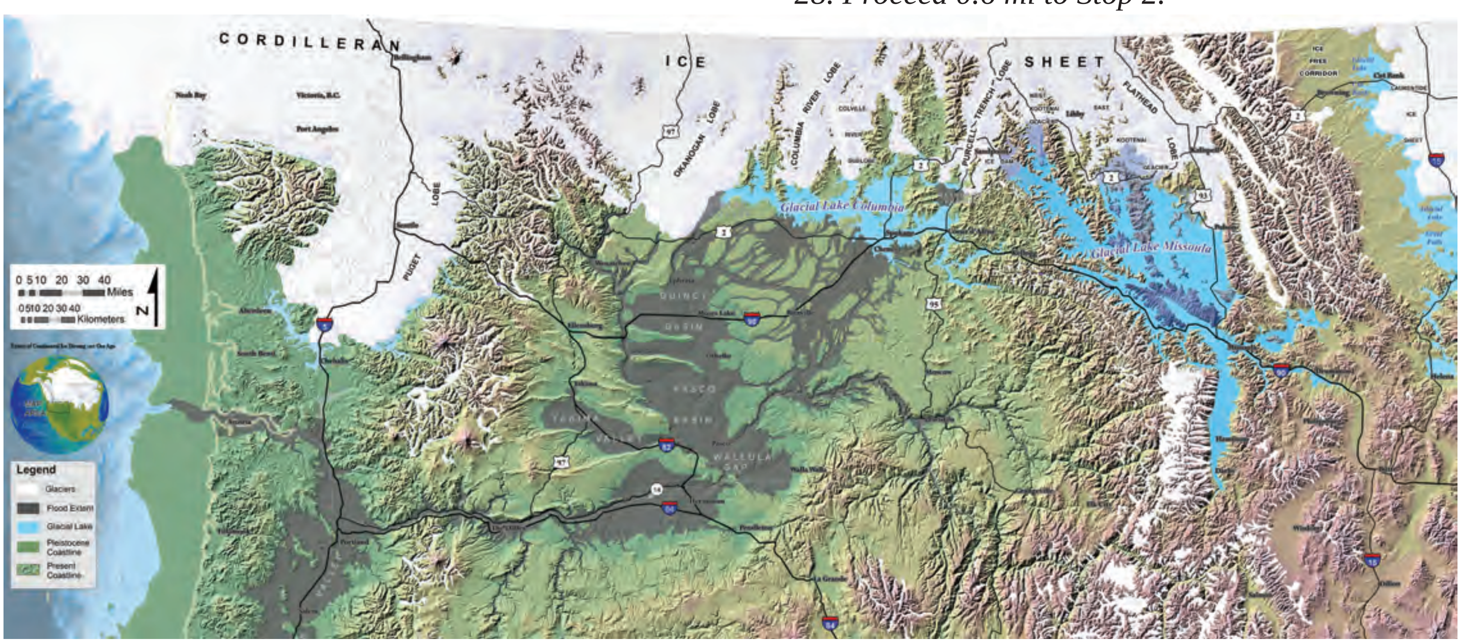

Figure 2. Ice Age Floods of the Pacific Northwest. Map shows Cordilleran ice sheet at maximum stand (white), glacial lakes (light blue), Ice-age flood erosional and depositional areas (brown), and Pleistocene coastline (green; IAFI/EWU, 2010).

STOP 2: Moses Coulee and Moses Coulee Bar 15.6/29.2

The lower end of Moses Coulee, almost 1 mi wide and 750 ft deep, shows magnificently flood-truncated spurs between hanging valleys. The deposit at its mouth is the dissected main remnant of a great fan built by floods out of Moses Coulee (Bretz, 1930, 1969; see fig. 4). The high part of the deposit stands well out into the Columbia River valley. The gravel is almost entirely basalt, evidence of derivation from Moses Coulee, not from the up-valley Columbia. During glacial advance, the Okanogan Lobe blocked the Columbia valley but not yet the upper portion of Moses Coulee. Floodwater could not descend the Columbia during the Moses Coulee floods, so these floods built a great fan across the Columbia River, evidently blocking it. Flood sediments back-flooded up-valley to above Rock Island and south to Trinidad, Washington.

The surface of the bar is marked by giant current dunes whose steeper down-valley slopes indicate down-valley flow (Waitt, 2017). Therefore, this early glacial bar was overtopped in late glacial time by great flood(s) that mainly reworked the basaltic gravel, probably from the final demise of the ice dam holding back Glacial Lake Columbia. This surficial reworked gravel extends into a fan that diverges into and up Moses Coulee, showing that no great flood subsequently came down Moses Coulee.

Proceed ahead about 100 ft to CRO Drive and turn left (E) onto CRO Drive for a short distance (50 ft) to the intersection of SR-28. Turn left (N) onto SR-28 and travel 0.6 mi to Palisades Road (same road we previously turned right on). Turn right (E) onto Palisades Road, which is the main road through lower Moses Coulee, and proceed 7.0 mi to Stop 3. Pull off on right shoulder of Palisades Road.

Figure 3. Large bedload flood boulders located along the southern end of the Apple Capital Loop Trail in East Wenatchee, Washington. View is southeast from bridge across Columbia River.

Figure 4. Digital Elevation Model (DEM) of lower Moses Coulee and gravel bar. Image shows lower portion of Moses Coulee and large gravel bar (fan) emanating from the coulee mouth. The bar expands across the Columbia River valley and both up-valley to Rock Island and downstream about 10 mi to Trinidad, Washington.

STOP 3:
Columbia River Basalt Group (CRBG)
7.6/36.8

The thick sequences of Miocene "flood basalts" that blanket the Columbia Plateau belong to the Columbia River Basalt Group (CRBG). Flood basalt volcanism on the Columbia Plateau occurred between 17.5 and 6 MYBP (Reidel and Hooper, 1989). This sequence of basalts is further subdivided into the Yakima Basalt Subgroup (Reidel and Hooper, 1989) consisting of three formations (from oldest to youngest): Grande Ronde Basalt, Wanapum Basalt, and Saddle Mountains Basalt. The majority of eruptions (85%), known as the Grand Ronde Basalt, occurred between 15.5 and 17.5 MYBP (Reidel and Hooper, 1989). Over 300 individual lava flows have been mapped. The greatest thickness of the basalts occurs in the Tri-Cities area (in excess of 16,000 ft). Basalt flow thickness averages 100 ft but can be much thicker, especially in inter-canyon flows. The CRBG covers about 106,000 mi^2 and has a volume of approximately 39,000 mi^2 (Bjornstad and Kiver, 2012).

The basalt flows visible in the walls here belong to the upper "series or members" with "normal magnetic polarity" associated with the youngest of the Grande Ronde Basalts. Note the formation of large talus slopes that have developed along the coulee walls since the last ice age flood.

A typical basalt flow consists of four different sections (Swanson, 1967). At the bottom of the flow, if the lava came in contact with water (lake, swamp, etc.), a pillow basalt-palagonite layer was formed. A yellow-orange mineral called palagonite develops from weathering on the outside of the pillows and material that fills the voids between pillows. Above the pillow-palagonite section is the colonnade portion of the basalt flow, which depicts polygonal columns or columnar jointing. Above the colonnade is the entablature, which often illustrates shorter, radiating, more slender columns. At the top of the lava flow where hot gases and water vapor were actively escaping, a vesicular crust (numerous holes) forms where the gases were trapped when the basalt solidified.

Continue on Palisades Road (NE) through lower Moses Coulee for 11.8 mi to Stop 4. Northeast of Palisades, WA, Palisades Road turns east and the pavement ends and becomes gravel. Palisades Road eventually turns into 24 NW Road as it enters the Billingsley Ranch. The county road through the Billingsley Ranch turns right (S) after the main farmhouse, and heads up a short hill. Stop 4 is on the left at the top of the hill.

STOP 4:
Three Devils Cataract
11.8/48.6

The cataract is subdivided into three separate and distinct drainages (fig. 5). The "Three Devils" name was given by the locals historically as there was no easy access for the old wagon loads of wheat down off of the Sagebrush Flats area. Basin and butte topography includes basalt mesas or buttes that will be visible to the north. Those features are remains of the "Scabland" topography created by flooding and plucking of younger flows of the Wanapum Basalt. This area is a large "bowl shaped" basin bounded on the south and the east by the Badger Mountain and Three Springs Anticlines. As flood waters entered the wide open expanse, known today as Sagebrush Flats, water velocity decreased, allowing sand and gravels to be deposited, but the velocity increased as Moses Coulee narrowed and formed the Three Devils Cataract, which likely started where the Badger Mountain Anticline bisects the coulee to the west.

Continue east on 24 NW Road/12th Road SE (same roads) for 5.0 mi until the intersection with Sagebrush Flats Road. Turn left (N) onto Sagebrush Flats Road for 11.4 mi to US 2. Turn right (E) onto US 2 and travel 1.2 mi. Turn left (N) onto Jameson Lake Road and travel 2.9 mi to Stop 5, a gravel turnout on the east (right) side of Jameson Lake Road.

STOP 5:
Great Gravel Bar, Dutch Henry Draw, Withrow Moraine, and flood bar(s)
20.5/69.1

As we proceed up Jameson Lake Road, look to the west (left) and note that the Great Gravel Bar of Moses Coulee starts north of US 2 as the coulee makes a gradual southwest bend and extends for 3.5 mi down-coulee (fig. 6). Also note where the

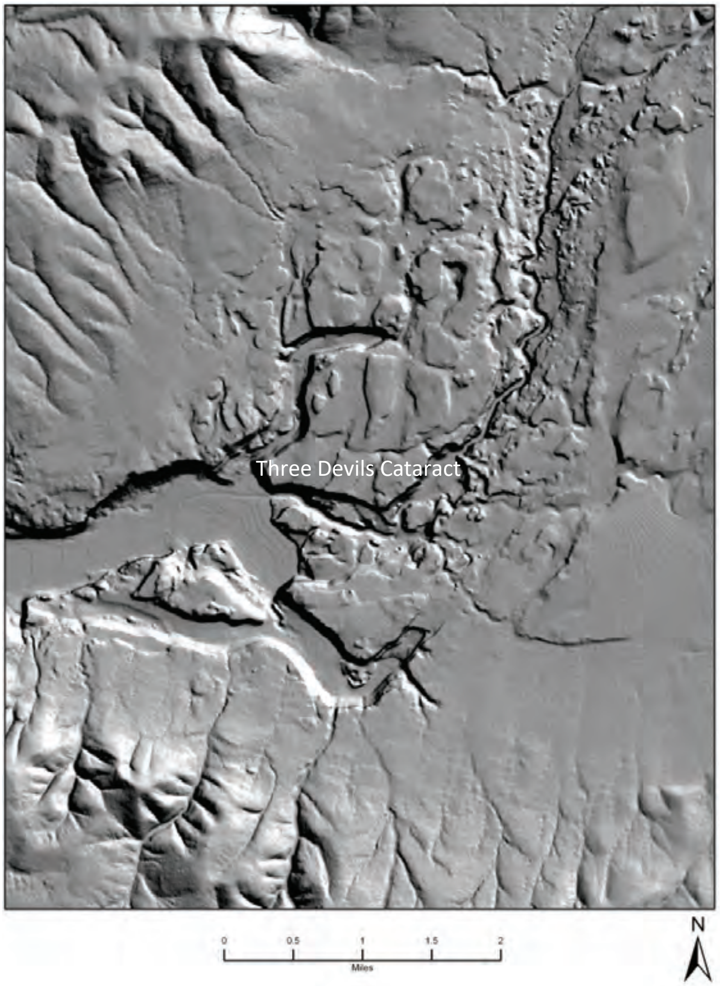

Figure 5. DEM of Three Devils Cataract.

basalt cliff ends and the gravel bar begins. At the northern end of the gravel bar it is about 250 ft high above the coulee floor.

At this stop an older pendant floods bar is visible behind the basalt headland to the northeast. Note the hummocky topography to the north. This is the remnants of the Withrow Moraine as it crossed upper Moses Coulee. Glacial drift is draped over the basalt bedrock in the middle of the coulee. Outwash from the melting Okanogan Lobe occurs on the east and west sides of the basalt bedrock. Figure 6 shows these deposits/features.

Retrace route back to US 2 (2.9 mi). Turn left onto US 2 and travel 16.8 mi to the intersection of SR-17 (south). Turn right onto SR-17 and travel 2.0 mi to Washington State Parks–Dry Falls Visitor Center. Get into the left turn lane and turn left (E) into Dry Falls Interpretive Center (Stop 6).

STOP 6:
Dry Falls Cataract
21.7/90.8

Grand Coulee, the deepest of the great scabland channels, consists of two tandem canyons described by Bretz (1932). Upper Grand Coulee heads at the south wall of the Columbia valley and leads to the lip of the spectacular Dry Falls cataract (fig. 7) that defines the head of lower Grand Coulee. Upper Grand Coulee was the outlet for Glacial Lake Columbia and also the main discharge conduit for invading Ice Age floodwaters flowing from the west end of the lake. The conspicuous Dry Falls twin cataract, 400 ft high and over 1 mi wide, is twice as high as Niagara Falls and a third wider. Lesser cataracts in this group extend 3 mi farther east (Deep Lake). On the coulee floor below Dry Falls, longitudinal bars are studded with huge basalt boulders quarried from the cataract walls.

Turn right (N) onto SR-17 and proceed 2.0 mi back to US 2. Turn left (W) onto US 2 and head uphill for 1.6 mi. Turn left into a large pullout (Stop 7) on the south side of US 2.

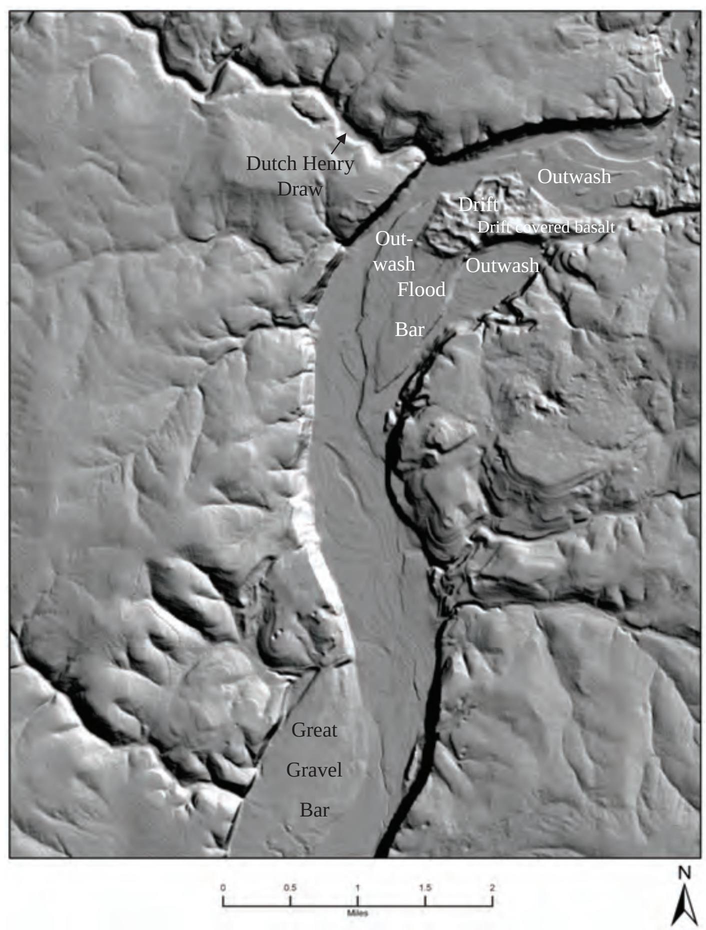

Figure 6. DEM of upper Moses Coulee. Image shows Great Gravel Bar, Dutch Henry Draw, and Withrow glacial moraine.

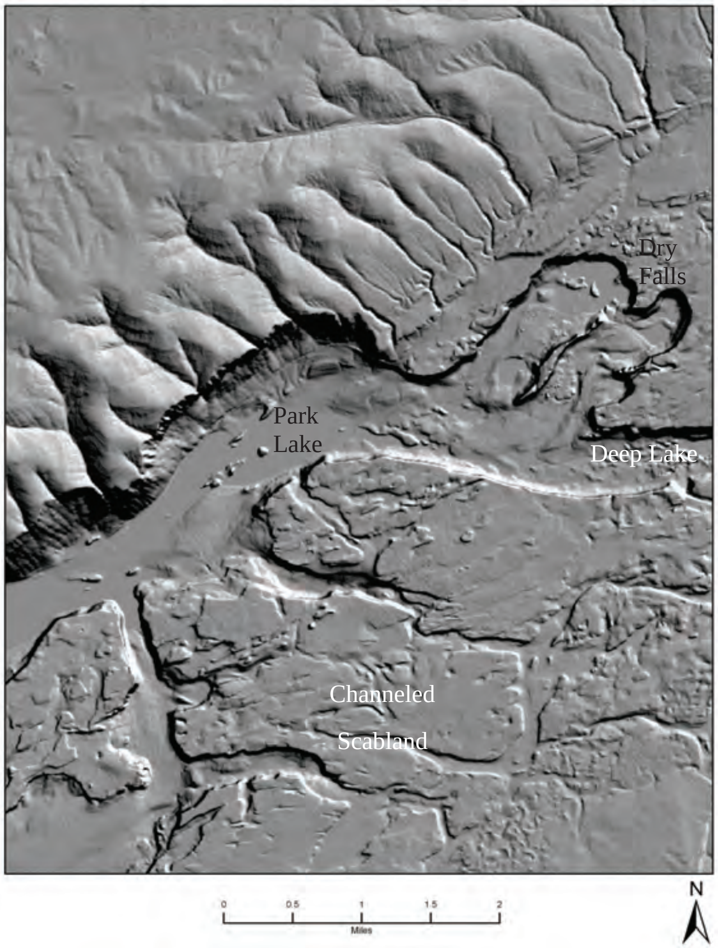

Figure 7. DEM Model of Dry Falls Cataract.

STOP 7:
Dry Falls Overlook–Coulee Monocline–Upper Grand Coulee
3.6/94.4

The sweeping view here is outstanding. The mouth of the Upper Grand Coulee, the Dry Falls Dam, Coulee City, the Hartline Basin, the upper part of Dry Falls, and the Lower Grand Coulee are spread out in a wide panoramic view.

The recessional cataract that cut the Upper Grand Coulee was initiated by floodwaters plunging over the monoclinal fold (Coulee Monocline) that turns eastward across the mouth of the coulee. Bending of rock layers produced more jointing and fracturing along the flexure, which helped initiate cataract recession (fig. 8). The resulting waterfall retreated some 21 mi northward, eventually destroying itself when it breached the divide with the Columbia River valley near the present site of the North Dam of Banks Lake (Electric City, WA). A similar sequence of events occurred in the Lower Grand Coulee. However, in the Lower Grand Coulee cataract recessions ended at Dry Falls before it could retreat into the Hartline Basin or continue into the Upper Grand Coulee. Waitt and others (2021) continue to refine the interrelationship of flooding and timing of flooding down Moses and Upper Grand Coulee.

At the west end of the large pullout (Stop 7) go straight across US 2 onto SR-17.

The glacier left the confines of the Okanogan Valley, filled the Columbia River valley, and spilled up onto the Waterville Plateau as a piedmont glacier (Kiver and Cunderla, 2009). A fascinating array of glacial landforms and features were left in its wake (Kiver and Stradling, 1994). Ice thickness near the mouth of the Okanogan Valley was over 3,500 ft thick (Waitt and Thorson, 1983; Kovanen and Slaymaker, 2004). Ice flowed radially from the mouth of the Okanogan Valley (Kovanen and Slaymaker, 2004) to south of Lake Chelan on the west to the Neal Canyon area upstream of Grand Coulee Dam on the east. The glacier plugged the north end of the Grand Coulee forming Glacial Lake Columbia (fig. 2) and forcing water to drain southward along the edge of the ice sheet and perhaps through low divides near Cheney and elsewhere to the east (Atwater, 1987; Kiver and Cunderla, 2009). At its maximum the piedmont glacier covered over 1000 mi^2 (Kiver and Cunderla, 2009).

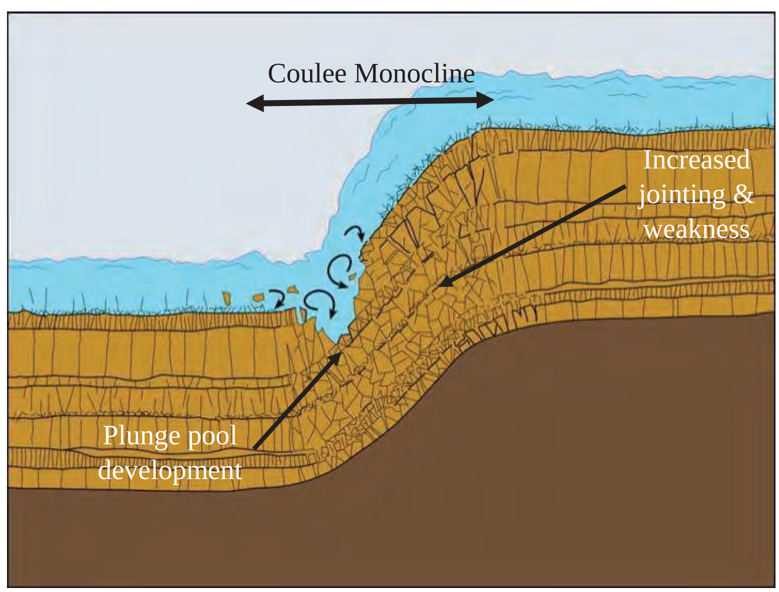

Figure 8. Diagram shows initiation of the Upper Grand Coulee cataract when Missoula floodwaters poured over the Coulee Monocline.

Within several miles there will be evidence of glaciation. Glacial erratics, “haystack rocks,” ground moraine, kettles, and kettle lakes will be evident. Burial of ice blocks by meltwater-derived sediment and later melting produced many of the closed depressions (kettle holes) and shallow lakes and ponds on the Waterville Plateau.

Proceed north on SR-17 for 14.0 mi to Sims Corner and the intersection of SR-172. Turn left onto SR-172. In 2.4 mi there will be a small gravel pit/borrow site on the right. Turn right into the gravel pit access road and park. Walk a short distance northeast into the gravel borrow site which is Stop 8.

STOP 8:
Eskers and Kames near Sims Corner
16.4/110.8

Small gravel pit opening in sinuous ridge exposes well-sorted pebble gravel, mostly of basalt but containing a few diverse igneous and metamorphic stones. Eskers are thought to record a stream at the bed of a glacier too stagnant to obliterate or deform the fluvial deposits. Kames are also visible in this area. A kame is where there was a hole in the glacial ice that was filled with stratified drift. After the ice melts, a steep-sided hill remains. This and other stagnant ice deposits and depositional topography show that as the ice sheet dwindled from the Waterville plain, its margins stagnated. Other glacial landforms on the Waterville Plateau include drumlins, kettles and kettle lakes.

Exit out of the borrow site access and turn right (W) onto SR-172.

The roadcut on SR-172 through the Pot Hills shows only angular basalt—quite different from the nearby eskers and ground moraine. Hanson (1970) interpreted this and other large high areas of this character as great blocks of bedrock basalt transported semi-intact by overriding glacier ice. The underlying sandstone and siltstone interbeds, wetted by water draining from the overlying glacier bed, perhaps provided a low-friction “grease plane” on which the basalt block could glide, impelled by shear stress at the base of the overriding ice.

Heading west on SR 172, bedrock exposures become more abundant. Depositional glacial features including haystack rocks still occur, but local areas of polished and striated bedrock exposures are present. The ice was thicker and more erosive here and produced a distinct northwest–southeast orientation of landforms reflecting the radial movement of ice from its Okanogan Valley source (Kovanen and Slaymaker, 2004).

Continue 6.5 mi on SR-172 to Yeager Rock (Stop 9). A short distance (0.1 mi) west of Yeager Rock (Stop 9) is a gravel road on the right (N) where cars can safely park.

STOP 9:
Yeager Rock
6.6/117.4

As the Okanogan Lobe of the Cordilleran Ice Sheet advanced southward across the Columbia River drainage from the north and rode up over the southern valley lip up onto the Waterville Plateau, vast quantities of basalt were ripped loose by the advancing glacier and transported south. House-sized boulders, such as Yeager Rock (fig. 9) are typically only of the entablature portion of the basalt flow, which can stay intact. Most of the larger “haystack rocks” are split in two, likely due to freeze–thaw cycles, since being deposited by glacial ice. This basalt boulder is not a “true” glacial erratic due to the fact that it is basalt residing on basalt bedrock (not resting on a different type of bedrock).

Turn right (W) back onto SR-172 and proceed (4.6 mi) just west of Mansfield, WA to Stop 10. Pull out on the right (N) side of SR-172. Stop 10 is on the south side of SR-172. PLEASE USE CAUTION CROSSING SR-172!

STOP 10:
Glacial Striations and grooves in basalt bedrock
4.6/122.0

Figure 10 shows basalt bedrock with glacial striations and small grooves oriented in principally a north–south orientation.

Pull back on SR-172 and proceed west on SR-172 for 7.4 mi. Just before SR-172 heads south, turn right (N) onto C Road NW. In 1.3 mi C Road NW turns left (W) onto 15 Road NW. Follow 15 Road NW for 2.2 mi to the intersection of McNeil Can-

Figure 9. "Yeager Rock," a large basalt entablature boulder located east of Mansfield, Washington along the north side of State Highway 172.

yon Road and F Road NW. Turn left (W) onto F Road NW for 0.5 mi to Stop 11. Make a U-turn using the borrow site access and pull onto the wide right shoulder.

STOP 11:
Ice Margin, Glacial Moraine and Boulder Park
11.4/133.4

Exceptionally large glacial erratics here are called haystack rocks (fig. 11). Many of the erratics were derived from bedrock in the mountains to the north, but the huge haystack rocks are entirely Columbia River Basalt (entablature). Plucking or quarrying of large blocks downstream of bedrock buttes accounts for some of the large boulders. The movement of ice into the Columbia River valley and over its southern edge was particularly effective in ripping large bedrock blocks from the canyon rim and incorporating them into the glacier. Thinning ice near the glacier margin and later complete melting left a jumble of materials, including the haystack rocks, strewn across the glaciated landscape (e.g., Boulder Park). Note the difference between the unglaciated (NW) and glaciated (N and NE) areas where all the basalt haystack rocks occur.

Figure 10. Striated and glacial grooves in basalt bedrock located along SR-172 west of Mansfield, Washington.

Figure 11. Upper Withrow Moraine showing large "haystack rocks." Photo shows margin between unglaciated wheat field (left) and glaciated area (right) where basalt boulders occur.

Proceed back the same route back to SR-172 (4.0 mi). Turn right (S) onto SR-172 and proceed 8.0 mi to the intersection of Road B NW just SW of Withrow, WA. Turn left (NE) onto Road B NW and proceed 0.5 mi to the large grain elevators (Stop 12).

STOP 12:
Withrow Moraine
12.5/145.9

Ice is most erosive where it is thickening and moving fastest. Here at its outer margin, the ice was thinning and unable to carry its accumulated debris load, and deposition occurred to form a terminal moraine. The moraine is known as the Withrow Moraine (fig. 12) for its excellent development and accessibility near the town of Withrow, Washington. At Withrow the moraine is about 3 mi wide, hummocky till, boulder-strewn topography that is dramatically in contrast to the low-lying loess hills (wheat fields) to the south (fig. 12). The moraine is about 100 ft thick at the margin and reaches more than 300 ft in thickness just north of Withrow, Washington. To the east the Withrow Moraine is more subdued and typically not more than 50 ft in height.

Retrace route back along Road B NW to SR-172 (0.5 mi). Turn left (S) onto SR-172 and travel 6.1 mi to US 2. Turn right (W) onto US 2 and proceed 23.4 mi to Orondo, WA (through Douglas and Waterville, WA). At Orondo, WA, US 2 merges with US 97. Turn left (S) onto US 2/97 and proceed 12.1 mi to East Wenatchee, WA. At the intersection of US 2/97 and SR-28, get into the right lane and turn right (W) onto US 2/97. Stay in the right lane for 1.8 mi across the Columbia River to the next traffic light. Only the right lane continues straight ahead/west onto US 2/97. Continue 8 mi to Cashmere, WA. Take a left (S) at the second Cashmere exit (light) onto Aplets Way and proceed 0.3 mi to Sunset Highway (just S of RR tracks). Turn right (W) onto Sunset Highway and proceed 1.3 mi to Wescott Drive. Turn left (S) onto Wescott Drive, go 0.2 mi and then right (W) onto Kimber road for 0.1 mi back to Chelan County Fairground campground.

Ending Mileage (53.8/199.7)

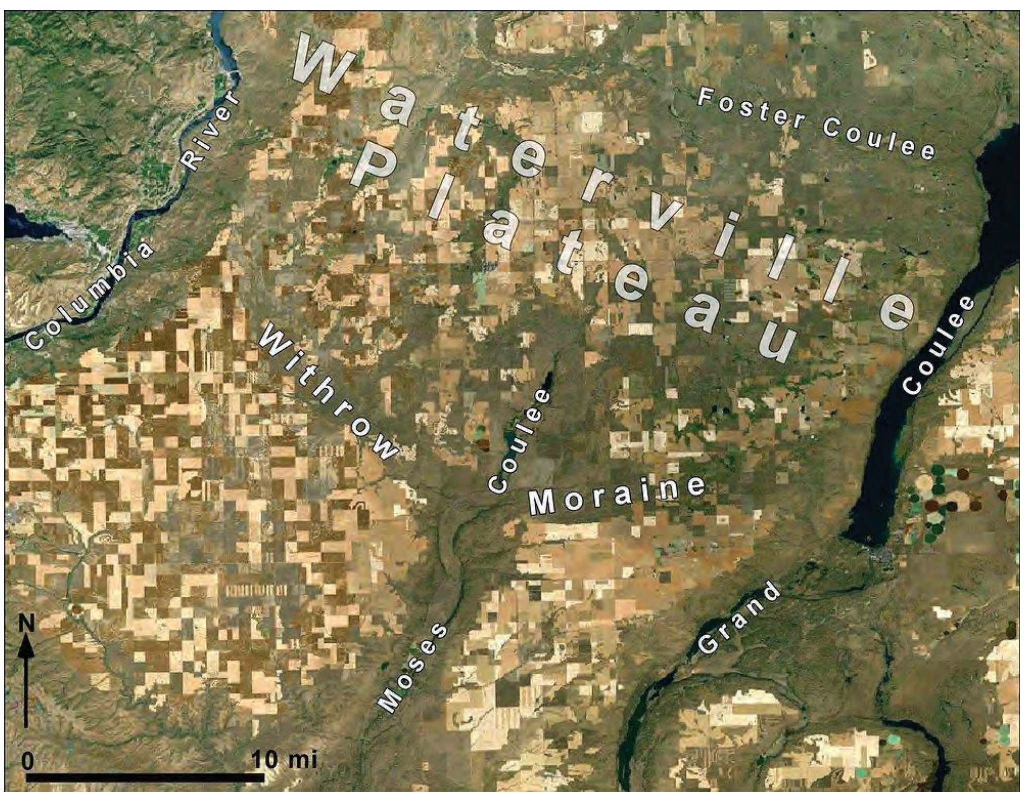

Figure 12. Glacial outburst flood and Okanogan Lobe features on the Waterville Plateau. Moses, Grand, and Foster Coulees are depicted as well as the Okanogan Lobe terminal moraine or "Withrow Moraine." Image from Bjornstad and Kiver (2012), with permission.

REFERENCES

Atwater, B.F., 1987, Status of Glacial Lake Columbia during the last floods from Glacial Lake Missoula: Quaternary Research, v. 27, p. 182–201.

Balbas, A.M., Barth, A.M., Clark, P.U., Clark, J., Caffee, M., O'Conner, J.E., Baker, V.R., Konrad, K., and Bjornstad, B., 2017, ^{10}Be dating of the late Pleistocene megafloods and Cordilleran Ice Sheet retreat in northwestern United States: Geology, v. 45, p. 583–586.

Bjornstad, B., and Kiver, E.P., 2012, On the trail of the Ice-Age Floods—The Northern Reaches—A geological field guide to northern Idaho and the Channeled Scabland: Sandpoint, Idaho: Keokee Company Publishing, 432 p.

Bretz, J.H., 1930, Lake Missoula and the Spokane Flood: Geological Society of America Bulletin, v. 41, p. 92–93.

Bretz, J.H., 1932, The Grand Coulee: American Geographical Society Special Publication 15, p. 1–89.

Bretz, J.H., 1969, The Lake Missoula Floods and the Channeled Scabland: Journal of Geology, v. 77, p. 505–543.

Carrara, P.E., Kiver, E.P., and Stradling, D.F., 1996, The southern limit of Cordilleran ice in the Colville and Pend Oreille alleys of northeastern Washington during the Late Wisconsin glaciation: Canadian Journal of Earth Sciences, v. 33, p. 769–778.

Flint, R.F., 1935, Glacial features of the southern Okanogan region: Geological Society of America Bulletin 46, p. 169–194.

Flint, R.F., and Irwin, W.H., 1939, Glacial geology of Grand Coulee Dam, Washington: Geological Society of America Bulletin 50: p. 661–680.

Hanson, L.G., 1970, The origin and deformation of Moses Coulee and other scabland features of the Waterville Plateau, Washington: Ph.D. thesis, University of Washington, 137 p.

Kiver, E.P., and Cunderla, B.J., 2009, Grand Coulee and Waterville plateau—A field guide for the Ice Age Floods Institute (IAFI) Fall 2009 Regional Field Trip, October 3, 2009, 54 p.

Kiver, E.P., and Stradling, D.F., 1994, Landforms, *in* Ashbaugh, J.G., ed., The Pacific Northwest, geographical perspectives: Chapter 2, Kendall-Hunt Publishing Co., p. 41–75.

Kovanen, D.J., and Slaymaker, O., 2004, Glacial imprints of the Okanogan Lobe, southern margin of the Cordilleran Ice Sheet: Journal of Quaternary Science, v. 19, p. 547–565.

O'Conner, J.E., Baker, V.R., Waitt, R.B., Smith, L.N., Cannon, C.M., George, D.L., and Denlinger, R.P., 2020, The Missoula and Bonneville floods—A review of ice-age megafloods in the Columbia River, *in* Carling, P.A., Baker, V.R., and Herget, J., eds., Megaflooding on Earth—A global perspective: Earth-Science Reviews, v. 208, p. 103–181.

Reidel, S.P., and Hooper, P.R., eds., 1989, Volcanism and tectonism in the Columbia River flood-basalt province: Boulder, Colo., Geological Society of America Special Paper 239, 386 p.

Swanson, D.A., 1967, Yakima Basalt of the Tieton River area, south-central Washington: Geological Society of America Bulletin, v. 78, no. 9, p. 1077–1110.

Waters, A.C., 1933. Terraces and coulees along the Columbia River near Lake Chelan, Washington: Geological Society of America Bulletin 44, p. 783–820.

Waitt, R.B., 2017, Pleistocene glaciers, lakes, and floods in north-central Washington State, *in* Haugerud, R.A., and Kelsay, H.M., eds., From the Puget Sound Lowland to East of the Cascade Range—Geologic excursions in the Pacific Northwest: Geological Society of America Field Guide 49, p. 175–205.

Waitt, R.B., and Thorson, R.M., 1983, The Cordilleran ice sheet in Washington, Idaho, and Montana, *in* Late Quaternary environments of the United States, v. 1, ch. 3: The Late Pleistocene: Minneapolis, Minn., University of Minnesota Press, International Association for Quaternary Research, p. 53–70.

Waitt, R.B., Atwater, B.F., Lehnigk, K., Larsen, I.J., Bjornstad, B.N., Hanson, M.A., and O'Conner, J.E., 2021, Upper Grand Coulee: New views of a channeled scabland megafloods enigma, *in* Booth, A.M., and Grunder, A.L., eds., From terranes to terrains: Geologic field guides on the construction and destruction of the Pacific Northwest:

Geological Society of America Field Guide 62, p. 245–300.

Weis, P.L., and Richmond, G.M., 1965, Maximum extent of late Pleistocene Cordilleran glaciation in northeastern Washington and northern Idaho: U.S. Geological Survey Professional Paper 525-C, p. C128–C132.

THE CHUMSTICK FORMATION: EXPLORING THE SEDIMENTARY AND STRUCTURAL HISTORY

Ralph A. Haugerud[1] and Kelsay M. Stanton[2]

[1]*U.S. Geological Survey, Seattle, Washington*
[2]*Washington Geological Survey, Olympia, Washington*

INTRODUCTION

The Chumstick Formation (Gresens and others, 1981a,b) comprises Eocene (49 to ~45 Ma) fluvial sandstone with lesser conglomerate, mudstone, and tuff currently exposed on the east flank of the North Cascade Range (fig. 1). The unit is restricted to the northwest–southeast-trending region Willis (1953) called the Chiwaukum graben. To the northeast, Chumstick is separated from Swakane Biotite Gneiss and Napeequa Schist by the Entiat fault. To the southwest, the Leavenworth fault juxtaposes Chumstick strata with the 90 Ma Mount Stuart batholith, prebatholith rocks of the Chiwaukum Schist, and the Ingalls Tectonic Complex, and, farther south, ~61–51 Ma fluvial strata of the Swauk Formation. Within the Chiwaukum graben lies a northwest-trending uplift of Swakane Biotite Gneiss termed the Eagle Creek anticline (Willis, 1953) or Eagle Creek fault zone (Evans, 1994).

By most accounts the Chumstick Formation is thick, rapidly deposited, and lithologically rather homogenous. In recent decades the tephrostratigraphy, sedimentology, thermal history, stable-isotope systematics, and geochronology of the unit have been investigated. Yet to be explored is how Chumstick beds were deformed to an average dip of ~40° (figs. 2–4).

Stanton is a long-time observer of the Chumstick Formation with a special interest in how its mineralization relates to regional structures. In 2018 Haugerud began mapping the Chumstick with a particular interest in documenting and interpreting its structural geometry. We caution readers that our understanding is incomplete: our interpretations *will* change with continued work.

This field trip introduces the Chumstick Formation. We hope it encourages discussion of the questions outlined below. Stanton (this volume) describes a second day spent in Dry Gulch and vicinity, with a focus on mineralization and younger deposits.

BACKGROUND

Distribution, structure, and internal stratigraphy of the Chumstick Formation are known from 1:24,000-scale geologic maps by Whetten and Laravie (1976), Whetten and Waitt (1978), Whetten (1980a,b,c), and Gresens (1983). These maps were compiled and extended into 1:100,000-scale maps by Tabor and others (1982, 1987). All these studies mapped various sandy, shaly, and conglomeratic facies within the Chumstick. Where the Chumstick overlies Swakane Biotite Gneiss in the core of the Eagle Creek anticline, they mapped a basal fanglomerate of angular biotite gneiss clasts in a sandy matrix.

There is not agreement on the gross physical stratigraphy or stratigraphic subdivision of the Chumstick Formation (fig. 5). Gresens and others (1981a,b) identified a lacustrine unit near the top of the Chumstick that they designated the Nahahum Canyon Member. Evans (1994) divided the remainder of the Chumstick into his Clark Canyon Member (the bulk of the unit), Tumwater Mountain Member (restricted to a zone along the Leavenworth fault), and Deadhorse Canyon Member (the uppermost part of the unit), which he thought overlies the Nahahum Canyon. He considered the basal fanglomerate (Whetten and Laravie, 1976; Whetten, 1980c) to be entirely younger, perhaps Miocene. Cheney and Hayman (2010) considered the Nahahum Canyon to be younger than the Deadhorse Canyon and excluded it from the Chumstick (which they identified as Roslyn Formation).

The age of the Chumstick Formation is known from high-precision U-Pb analyses of zircons in interbedded tuffs, which give eruptive ages of 49.12 to 47.98 Ma; similar analyses of detrital zircons in sandstone establish maximum depositional ages (MDAs) of 47.8, 46.90, and 45.91 Ma (Eddy and others, 2016).

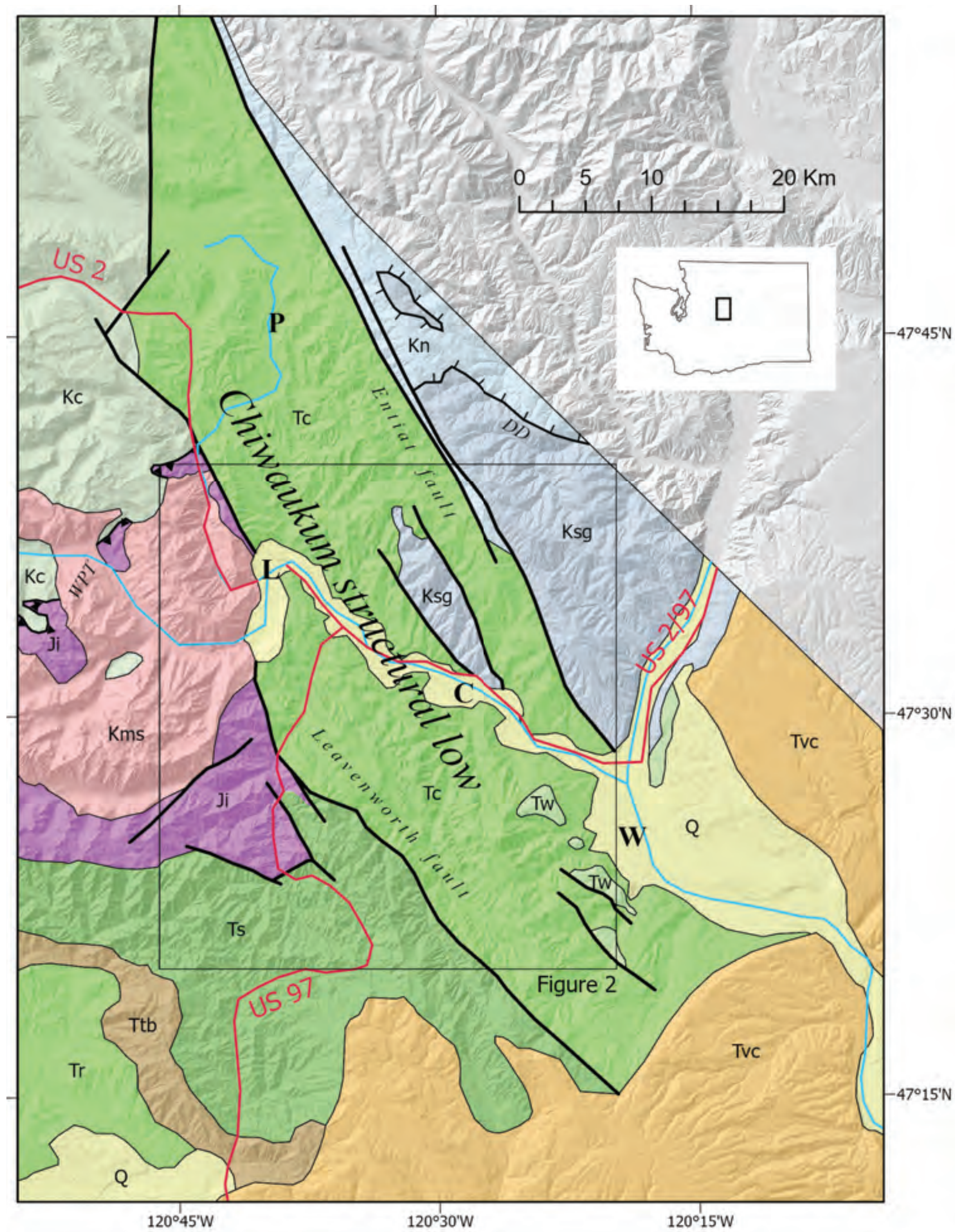

Legend for Figures 1 and 2

Map Units

Q	Unconsolidated deposits (Quaternary)
Tvc	Columbia River Basalt Group (Miocene)
Tw	Wenatchee Formation (Eocene-Oligocene)
Tc	Chumstick Formation (Eocene)
Tcb	Basal conglomerate (only shown on Fig. 2)
Tr	Roslyn Formation (Eocene)
Ttb	Teanaway Basalt (Eocene)
Ts	Swauk Formation (Paleocene and Eocene)
Ksg	Swakane Biotite Gneiss (Cretaceous-Paleogene?)
Kn	Napeequa Schist (Cretaceous)
Kc	Chiwaukum Schist (Cretaceous)
Kms	Mt Stuart batholith (Cretaceous)
Ji	Ingalls Tectonic Complex (Jurassic)

Field trip stop
bedding
cleavage
foliation
Tuff of Eagle Creek
anticline axis
syncline axis
syncline axis, concealed
contact
fault
thrust fault

Figure 1. Geologic setting of the Chiwaukum structural low. Igneous rocks—diabase of Camas Land, Horse Lake intrusions, Saddle Rock, etc.—intrusive into (or interlayered with?) the Chumstick Formation are omitted. Abbreviations for towns: C, Cashmere; L, Leavenworth; P, Plain; W, Wenatchee. Abbreviations for structures: *DD*, Dinkelman decollement; *WPT*, Windy Pass thrust. Modified from Tabor and others (1982, 1987). Shaded relief base calculated from USGS 1/3 arc-second DEMs.

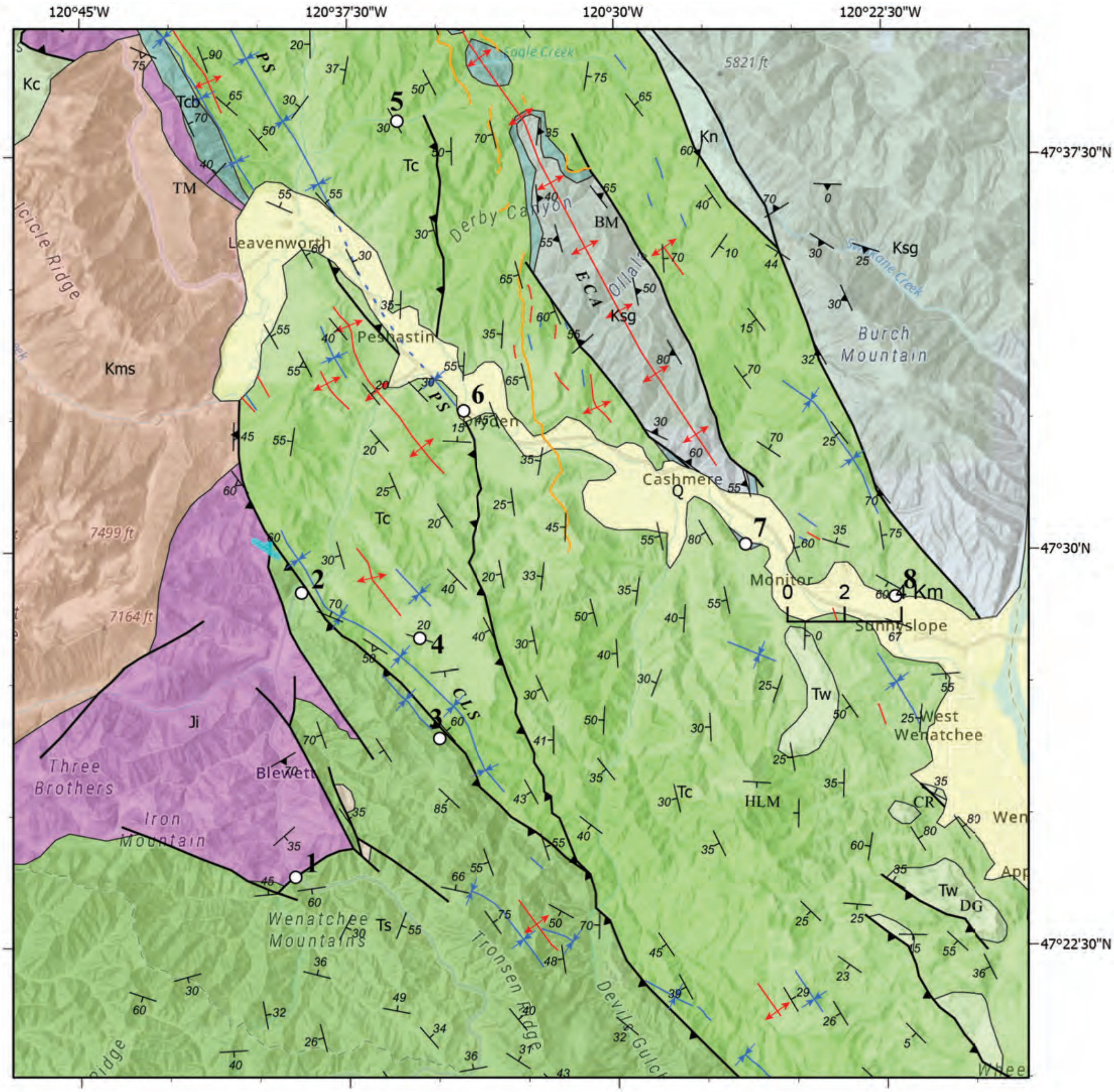

Figure 2. Simplified geologic map with field trip stops. Legend in figure 1, previous page. Map compiled from Whetten and Laravie (1976), Whetten and Waitt (1978), Whetten (1980a,b,c), Tabor and others (1982, 1987), Gresens (1983), Cheney and Hayman (2009), field observations (Ralph Haugerud, U.S. Geological Survey, unpublished data, 2018–2021) and LiDAR (https://lidarportal.dnr.wa.gov/) interpretation (Ralph Haugerud, U.S. Geological Survey, unpublished, 2021–2022). Tuff of Eagle Creek from Whetten and Laravie (1976) and Whetten (1980c). Base from ESRI, BLM, NASA, NGA, USGS. BM, Blag Mountain; DG, Dry Gulch; HLM, Horse Lake Mountain; TM, Tumwater Mountain. CLS, Camas Land syncline; ECA, Eagle Creek anticline; PS, Peshastin syncline.

Figure 3. Steep, locally overturned beds at southwest margin of Swakane Biotite Gneiss in Eagle Creek anticline. Outcrops ~100 m to right of image are basal conglomerate (red-bed fanglomerate of Gresens and others, 1981b) of Chumstick Formation. View northwest from Cashmere. Photograph by Ralph Haugerud, USGS.

Figure 4. Folds in Chumstick Formation. View east from shoulder of US 2/97, 1½ miles east of Cashmere. Selected bedding traces highlighted in yellow. Photographs by Ralph Haugerud, USGS.

Donaghy and others (2021) calculated depositional rates of 2 to 7 mm/yr for different parts of the section; their extrapolation to the oldest recognized Chumstick beds suggested an age of 49.22 Ma. Their data suggest the average depositional rate for much of the unit was ~4.7 mm/yr.

The Chumstick Formation is unconformably overlain by fluvial and lacustrine strata of the Wenatchee Formation of probable late Eocene to early Oligocene age (Gresens and others, 1981a,b; Gresens, 1983; Hauptman, 1983). Gresens and others (1981b) reported zircon fission track ages from tuffs in the Wenatchee Formation of 33–35 Ma, along with substantially older ages that may reflect contamination. We will see Wenatchee strata tomorrow (Stanton, this volume).

The Chumstick Formation has been the subject of several topical studies. McClincy (1986) investigated the tephrostratigraphy of the unit, obtained 60+ instrumental neutron activation analyses of tuff beds, and, on compositional grounds, was able to distinguish tuffs and correlate them along strike. Evans (1994)

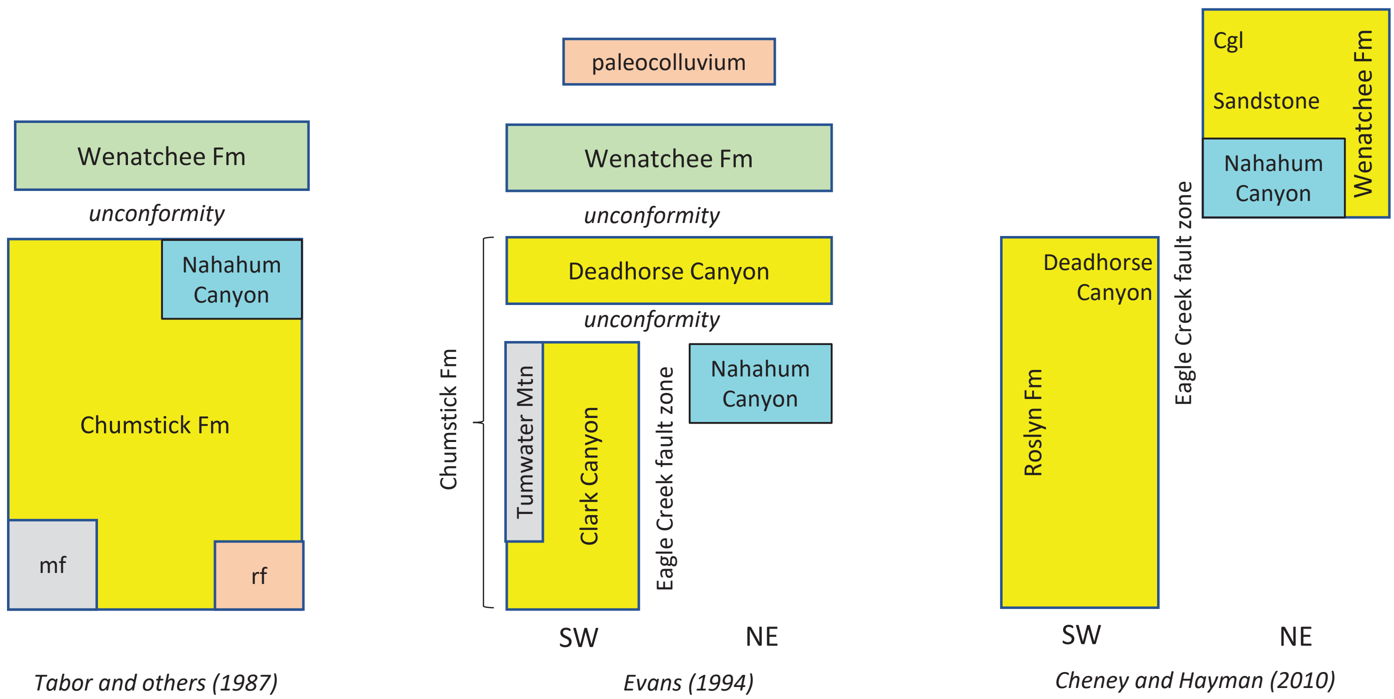

Figure 5. Three views of the stratigraphy of the Chiwaukum structural low. Colors denote equivalent lithosomes. Area mapped by Cheney and Hayman (2010) does not include lithosome mapped as Wenatchee Formation by others. Abbreviations: mf, monolithologic fanglomerate; rf, redbed fanglomerate; Cgl, conglomerate.

studied the sedimentology of the unit and proposed a history of subsidence and basin segmentation driven by motion on bounding faults. Enkelmann and others (2015) used new detrital apatite (U-Th-Sm)/He and fission-track ages and published vitrinite reflectance data to infer that unroofing of the Chumstick largely postdates 17 Ma. Methner and others (2016) measured oxygen isotopes and carbonate clumped isotopes from concretions in the Chumstick Formation and inferred the absence of an Eocene–Oligocene Cascade Range rain shadow, and therefore only limited elevation of the range at that time. Donaghy and others (2021) mapped lithofacies, counted conglomerate clasts, and analyzed detrital zircon ages to explore sediment provenance, routing, and deposition in the Chumstick basin.

High-precision ages generated by Eddy and others (2016) allowed a clearer understanding of the relation between Eocene deposition and the evolving regional tectonic setting in Cascadia. Nonmarine deposition of the Swauk Formation from ~60 to 51 Ma was interrupted by accretion of Siletzia between 51.3 and 49.9 Ma. Immediately following, dextral strike-slip faulting began, or accelerated, and Eddy and others (2016) thus interpreted the Chumstick to have been deposited in a strike-slip basin.

Cheney and Hayman (2009) remapped parts of the Chumstick and Swauk Formations and the Leavenworth fault system that separates them. They observed that the Leavenworth fault (their Camas Creek fault) cuts the Chumstick Formation and thus must be younger, correlated all of the Chumstick with the Roslyn Formation farther southwest, and proposed that (1) the Chumstick and Roslyn were deposited as a regionally extensive blanket of sediment, (2) Eocene and younger history of this region is marked by folding and reverse faulting alternating with periods of strike-slip faulting, and (3) the "Chiwaukum graben" is better known as the Chiwaukum structural low.

QUESTIONS

How does one distinguish Chumstick Formation from Swauk Formation?

Israel Russell (1900, p. 119) wrote:

> About Camas Land, to the east of the Wenache Mountains, and in the valley of the Wenache in the vicinity of Mission [Cashmere], Leavenworth, etc., the Swauk formation consists largely of thick-bedded, nearly white, but still impure sandstone, with minor quantities of sandy shale. These rocks correspond closely with the characteristic white sandstone of the Roslyn formation. To the south of the Wenache Mountains, in the region drained by the North and Middle forks of the Teanaway

> and by Swauk Creek, the Swauk formation consists largely of thin-bedded, yellowish, arkose sandstone and yellowish sandy shale…

However, on his map Russell did not distinguish the white sandstone found near Camas Land, now called Chumstick Formation, from the Swauk Formation found along Swauk Creek, as "Messrs. Willis and Smith…found…them to be the deposits of a single Tertiary lake or estuary."

Gresens and others (1981a, b) confirmed long-standing suspicions and formally identified the Chumstick Formation as distinct from the older Swauk Formation. They did not specify distinguishing characteristics. Tabor and others (1982) described the two units as "relatively dark gray weathering to tan… micaceous feldspathic to lithofeldspathic sandstone" (Swauk Formation) and "white, locally gray, micaceous feldspathic sandstone" (Chumstick Formation).

We find the characteristics listed in table 1 helpful in distinguishing the two units and note that they are similar to those identified by Cheney and Hayman (2009, their table 2).

How one maps these units dictates the geometry of the Leavenworth fault. It also bears on the stratigraphic identity of largely monolithologic fanglomerates near the Leavenworth fault. Evans (1994) assigned these beds to his Tumwater Mountain Member of the Chumstick Formation and, following Tabor and others (1982), suggested they recorded syn-Chumstick uplift along the Leavenworth fault zone. In contrast, Cheney and Hayman (2009) and Haugerud (2021) considered the fanglomerates to be part of the older Swauk Formation, an interpretation that does not require syn-Chumstick motion on the Leavenworth fault.

How thick is the Chumstick Formation?

Gresens and others (1981b) indicated the Chumstick Formation may comprise as much as 9.1 km of section, but cautioned that thicknesses may be extremely variable. Evans (1994) suggested stratigraphic thickness was >12 km. Donaghy and others (2021) revised this to ~10.5 km.

Evans (1994) calculated an elevated paleogeothermal gradient of 60–70°C/km from vitrinite reflectance values in samples from the NORCO-1 exploration well south of Wenatchee. Other data suggested maximum burial temperatures for the Chumstick of 170–225°C. Combining these estimates, he suggested maximum burial of ~3.5 km (Evans, 1994). Evans noted that this estimate is similar to Silling's (1979) interpretation, of a gravity profile in the northern part of the Chiwaukum structural low, that there are only 2 km of sedimentary rock above basement. Evans (1994) suggested that contrasting estimates of stratigraphic and basin-fill thickness could be reconciled by rapid lateral shifting of depocenters.

We note that rapid sedimentation should have depressed the geothermal gradient, not elevated it. However, the area around the NORCO-1 well is rich in igneous rocks and evidence of geothermal activity, which may explain the local high geothermal gradient. Uncertainties in the densities of Chumstick strata and its basement suggest caution in accepting the interpretations of gravity data. Given these caveats, we are troubled by the apparent great thickness and rapid deposition of the Chumstick Formation.

McClincy's (1986) tuff stratigraphy allows thrust repetition of the Chumstick Formation, as the tuffs he analyzed only span the lower 5.5 km (Donaghy and

Table 1. Field criteria for distinguishing Swauk and Chumstick Formations.

	Swauk Formation	Chumstick Formation
Sandstone color	Gray, brown. Darker.	White, creamy. Paler.
Conglomerate clast lithologies	Varied! Granitic rocks, chert, mafic to intermediate volcanic rocks, phyllite, serpentinite, greenstone, gabbro….	Granitic rocks, biotite gneiss, felsic to intermediate volcanic rocks, mudstone. Basal conglomerate reflects subjacent units.
Conglomerate clast roundness	Generally well-rounded.	Breccias near base.
Overall lithology	Heterogeneous assortment of sandstone, conglomerate, mudstone.	Mostly thick-bedded sandstone, locally with conglomeratic layers. Relative scarcity of overbank deposits.
Weathering style	Outcrops fringed with angular rubble.	Decomposes to sand.

others, 2021) of the 10+ km-thick section. Any structural repetition would reduce deposition rate estimates but cannot explain the small thickness (~2 km) inferred from gravity surveys.

Extension on subparallel down-to-the-southeast normal faults with associated block tilting would thin the upper crust, exaggerate apparent stratigraphic thickness of the Chumstick Formation if unrecognized, and explain the prevailing northwest plunge of folds in the Chiwaukum low. But such faulting appears to be ruled out by the continuity of tuff beds as mapped by Whetten and Laravie (1976), Whetten and Waitt (1978), Whetten (1980a,c), and McClincy (1986).

Was the Chumstick Formation deposited in a strike-slip basin or as a regional blanket?

Prevailing opinion is that the Chumstick Formation is a thick prism of sediment deposited in a narrow, strike-slip fault-bounded basin. Gresens (1982), Johnson (1985, 1996), Taylor and others (1988), Eddy and others (2016), and Donaghy and others (2021) interpreted strike-slip fault activity during Chumstick deposition. The interpretation of deposition restricted to a fault-controlled basin is implicit in the stratigraphy adopted by Tabor and others (1982, 1987), who conspicuously did not correlate the Chumstick with the nearby Roslyn Formation of similar age.

In contrast, many workers—starting with Russell (1900)—have correlated part or all of the Chumstick Formation with the Roslyn Formation in the Cle Elum area to the southwest. Evans (1994) correlated the top of the Chumstick (his Deadhorse Canyon Member) with the Roslyn. Cheney and Hayman (2009) considered all of the Chumstick to be Roslyn, though Cheney and Hayman (2010) subsequently mapped the Nahahum Canyon Member of the Chumstick Formation as the younger Wenatchee Formation.

The Roslyn Formation (fig. 1) mostly has gentle bedding dips, is little deformed, and is well known from extensive coal exploration and exploitation. It is ~2.7 km thick and records three major depositional environments: meandering river channels with a floodplain subfacies containing thin, discontinuous coalbeds; fluviolacustrine swamps, where thicker coal seams formed; and lakes (Walker, 1980). The Roslyn overlies 49.34 Ma volcanic rocks and the lower and middle Roslyn have MDAs of 48.80 Ma and 47.58 Ma, respectively (Eddy and others, 2016). Other than the greater thickness and the lack of significant coal seams in the Chumstick, the two units are rather similar.

There is also no agreement that the Entiat and Leavenworth faults were active during Chumstick deposition. Willis (1953) and Cheney and Hayman (2009) thought that the Leavenworth and Entiat faults postdated deposition of what we now call the Chumstick Formation. Evans (1994, 1996, 2010) proposed an intermediate interpretation. He inferred that initial Chumstick deposition was in an extensional half-graben open to the southwest and bounded on the northeast by the then-normal-slip Entiat–Eagle Creek fault, with later strike-slip activation of the Leavenworth fault. He also suggested that his Deadhorse Canyon Member (the top of Chumstick) may have formed a continuous depositional system with the Roslyn.

How were beds of the Chumstick Formation rotated from horizontal?

The average dip of the Chumstick Formation is about 40° (n = 4,005). Major structures (fig. 2) include: (1) The northwest-plunging Eagle Creek anticline, which is well defined northwest of Blag Mtn. At all points the northeast limb is mapped as faulted, and southeast of Blag Mtn the southwest limb also appears to be faulted. (2) A west-dipping homocline—the west limb of the Eagle Creek anticline—that extends west from Cashmere/Wenatchee almost to the Leavenworth fault and may include 7 km of section. (3) The Peshastin syncline, also northwest plunging, which extends northwest from Dryden. Southeast of Dryden the syncline does not exist. See Stop 6 for further discussion.

Lesser structures include a northwest-trending anticline–syncline pair on the east flank of Tumwater Mountain, northwest of Leavenworth; several minor northwest-trending folds between the Leavenworth fault and the Peshastin syncline (PS), south of Peshastin, including the Camas Land syncline that may indicate a duplex between the Leavenworth fault and the sub-PS detachment; north- and northwest-trending folds northwest of Cashmere where the Chumstick abuts Swakane Biotite Gneiss in the west limb of the Eagle Creek anticline (fig. 3); poorly resolved folds and faults northeast of the Eagle Creek anticline; and a fold train southeast of Cashmere (fig. 4).

Existing geologic maps are unrestorable—that is, they do not provide sufficient hints as to how strata were transformed from original horizontality to their present state. Currently we have no significant improvements to offer, but note the following:

Page (1939) was probably correct. The so-called Leavenworth fault on Tumwater Mountain north–northwest of Leavenworth is likely a depositional contact and, in this area, the Tumwater Mountain Member of Evans (1994) is a basal conglomerate.

Down-section disappearance of the Peshastin syncline suggests the presence of a significant detachment at the base of the fold (Haugerud, 2021).

The tuff of Eagle Creek is about 350 m stratigraphically above Swakane Biotite Gneiss in the core of the Eagle Creek anticline at Eagle Creek. In contrast, at the north edge of the Tiptop quad, 16 km farther south, there are at least 3.5 km of Chumstick strata beneath the tuff of Eagle Creek.

The down-to-the-north Dinkelman decollement (fig. 1), which separates Swakane Biotite Gneiss from overlying Napeequa Schist, appears to have been active during deposition of the Chumstick Formation (Paterson and others, 2004).

Deformation of the Chumstick Formation was protracted. West of Wenatchee, on the ridge west of Castle Rock, Wenatchee Formation overlies Chumstick with ~60° angular unconformity. At Dry Gulch (Stanton, this volume, Stops 4, 5), Wenatchee Formation is locally nearly vertical and overthrust by Chumstick Formation.

ROAD LOG

See figure 2 for stop locations on a preliminary geologic map.

Latitude and longitude values below are referenced to WGS84 (Google Earth, Google Maps).

From the Chelan County Expo Grounds in Cashmere, return to US 2/97 and head northwest toward Leavenworth and Seattle. At the Big Y (7 mi NW of Cashmere, junction with US 97 south towards Ellensburg, Seattle), exit right. At stop sign turn left (south) and pass under US 2. Proceed south 12.9 mi, past The Rock (on left, coffee), past historical marker for the Blewett townsite (on left), past right turn for Scotty Creek and the Old Blewett Pass Highway, and 0.4 mi farther to a large pullout on the right.

STOP 1:
Ingalls Tectonic Complex, Swauk Formation, Teanaway dikes
47.5254°N, 120.4868°W

At this stop the Ingalls Tectonic Complex, on the north, is faulted against the Swauk Formation and intruded by northeast-striking basalt dikes of the Teanaway dike swarm. On the southwest side of US 97 is a readily accessible outcrop of greenstone and serpentinite of the Ingalls complex. Please be very careful if you choose to cross US 97 to examine the Swauk and Teanaway outcrop.

The Ingalls Tectonic Complex (or Ingalls ophiolite; Miller, 1985) is a mixture of peridotite, serpentinite, gabbro, basalt, chert, sandstone, and argillite. U-Pb and radiolarian ages from the Ingalls are Jurassic (MacDonald and others, 2008).

Swauk Formation, south of the fault here, is sandstone and conglomerate. Observe the ranges of clast size, clast lithology, and clast roundness. Published CA-ID-TIMS U-Pb zircon ages of volcanic rocks in the Swauk Formation range from 59.9 to 51.4 Ma (Eddy and others, 2016). Detrital zircon U-Pb ages from sandstone collected about 350 m stratigraphically above its depositional contact with Ingalls Tectonic Complex 5.5 km north of here indicate an MDA of 66 ± 2 Ma ($n = 9$, MSWD = 1.3; Alexis Licht, University of Washington, written commun., 2020). Teanaway Formation unconformably overlies the Swauk Formation (fig. 2). Eddy and others (2016) reported an age (CA-ID-TIMS U-Pb zircon, $n = 5$, MSWD = 2.2) of 49.341 ± 0.033 Ma for rhyolite of the Teanaway Formation 12 km southwest of here, 0.5 km north of Red Top Mountain.

Numerous basalt dikes, generally with a northeast strike, thread through the Swauk Formation. They have long been considered feeders for basalt of the overlying Teanaway Formation (e.g., Smith, 1904). The dark brown, rusty-weathering, irregular dikes at this stop are typical. Miller and others (2022) described the Teanaway dike swarm along with other Eocene dike swarms in and near the North Cascades and argued that they reflect transtension associated with dextral strike-slip faulting prior to the onset of the Cascade arc.

Absence of basaltic dikes has been taken as a defining characteristic of the Chumstick Formation (e.g., Gresens and others, 1981b), but this is not so: we will see such dikes (at a distance) at Stop 3, and we have encountered basalt dikes cutting Chumstick sandstone along Mission Creek Rd. a few miles south of Cashmere, along Squilchuck Rd. immediately north of Squilchuck State Park, and in the Castlerock trail west of Wenatchee (pointed out by Ralph Dawes).

On the drive north admire the constriction of the valley bottom, in large part due to extensive landslides in serpentinite of the Ingalls complex.

Turn left onto US 97 northbound, back towards the Big Y. In 6.5 mi, turn right on Old Blewett Rd. Go another 0.6 mi and park on shoulder.

STOP 2:
Fanglomerate of the Swauk Formation
47.4881°N, 120.6452°W

Rock here is well-cemented coarse breccia–conglomerate with mostly granitoid clasts and at least one ultramafic clast. Smith (1904) mapped it as Mount Stuart granodiorite.

Tabor and others (1982) mapped this rock as **Tcf**, fanglomerate and monolithologic fanglomerate of the Chumstick Formation (fig. 5). On their map the north–northwest-trending Leavenworth fault is ill-defined where it crosses US 97 but occurs about a mile southwest of this point. Similar rocks are well exposed along the road to the Mission Ridge ski area south of Wenatchee, 300 m north of the ski area parking lot. All were assigned by Evans (1994) to his Tumwater Mountain Member of the Chumstick Formation.

Cheney and Hayman (2009) mapped this rock as **Tscd**, diamictite of the Swauk Formation, and placed their Camas Creek thrust immediately to the east of this locale, separating Swauk to the southwest from Chumstick Formation to the northeast. We essentially agree with them (fig. 2). The most obvious bedding discordance—a fault—lies to the northeast of Stop 2, and elsewhere fanglomerates such as these are intercalated with texturally mature, but generally lithic, conglomerates, sandstones, and mudstones that are more typical of the Swauk Formation than the Chumstick.

Stratigraphic identity of this rock is germane to (at least) two questions. First, what is the geometry of the Leavenworth fault? Second, is this rock part of Evans' (1994) Tumwater Mountain Member of the Chumstick Formation? If this and similar rocks are instead constituents of the older Swauk Formation, the argument for syn-Chumstick activity on the Leavenworth fault collapses.

Continue N on Old Blewett Rd. In 0.5 mi, turn right onto US 97. In another 0.2 mi, turn right onto Camas Creek Rd. At 2.9 mi from US 97, pass spur road on right to quarry (on private land) with large cliff exposure of gabbro of the Camas Land Diabase of Southwick (1966). At junction with mailboxes, 3.0 mi from US 97, keep right on FS 7200. Pavement ends. At next Y (3.7 mi from US 97), keep right. At 5.7 mi from US 97, park at large pullout on corner.

STOP 3:
Swauk Formation and view to northeast and east
47.4408°N, 120.5837°W

This outcrop was mapped by Tabor and others (1982) as **Tcr**, red conglomerate of the Chumstick Formation. Cheney and Hayman (2009) mapped it as **Ttb**, Teanaway Formation, in which they included "polymict conglomerate with angular to subrounded clasts of basalt." The range of clast lithologies, generally lithic character of the rock, presence of distinct conglomerate beds, and abundance of angular rubble (table 1), lead us to instead map this as Swauk Formation. Conglomerates in the Chumstick Formation are commonly more or less indistinct stringers within thick sandstone beds and, as we will see at the next stop, the Chumstick mostly weathers to sand. Which way do these beds young?

View to northeast is across the Leavenworth fault (Camas Creek fault of Cheney and Hayman, 2009) to a cliff eroded into northeast-dipping beds of white Chumstick sandstone on the southwest limb of the Camas Land syncline, threaded by mafic dikes. To the east are miles and miles of west-dipping Chumstick Formation in the big homocline that is the dominant structure of the Chiwaukum structural low. Skyline summit 11 km east is Twin Peaks (4,621'), also known as Horse Lake Mtn.

Optional: walk ¼ mi north along the road to find outcrops of Chumstick Formation on east side of road. You have crossed the Leavenworth fault.

Retrace route back toward US 97. In 3.2 mi, about 0.5 mi past junction with mailboxes, park on shoulder.

STOP 4:
Thick-bedded sandstone of the Chumstick Formation
47.4727°N, 120.5959°W

The roadcut here exposes typical thick-bedded sandstone of the Chumstick Formation. We interpret these rocks as channel deposits and estimate that more than half of the Chumstick is similar thick-bedded sandstone, locally with conglomerate stringers. Overbank deposits are less abundant than in similar fluvial units (Swauk, Chuckanut, Winthrop, Kootenai) we are familiar with. Why?

Note how the rock has weathered to sandy debris, with a lack of angular rubble (table 1).

Continue downhill (N) towards US 97. In 2.6 mi, turn right on US 97. Travel 5.2 mi to the Big Y and turn left onto US 2 (to Leavenworth). A mile farther, begin outcrops on left of NE-dipping sandstone of the Chumstick Formation. At 3.8 mi from Big Y (stoplight) find coffee, lunch, and bathrooms at large grocery on right. At 4.2 mi from Big Y (stoplight), turn right on Chumstick Hwy. Go 2.1 mi north and turn right on Eagle Creek Rd. 2.4 mi farther, park on right shoulder.

STOP 5:
Tuff in the Chumstick Formation
47.6361°N, 120.6038°W

West-dipping tuff beds in roadcut here are unit **Tt(3**) of Whetten and Laravie (1976), which McClincy (1986) called **Tctc2**. Eddy and others (2016) reported a CA-ID-TIMS U-Pb zircon population age of 47.981 ± 0.019 Ma (n = 6, MSWD = 1.1) for a sample of **Tctc2** collected 9 km north–northwest of here.

The junction of Eagle Creek Road and the Chumstick Highway is on the axis of the Peshastin syncline. From this junction to the Big Y, intermittent outcrops of sandstone dip to the northeast.

Retrace route to US 2 in Leavenworth. At 4.5 mi (stoplight), turn left on US 2. Proceed past Big Y (4.2 mi). Cross bridge over Wenatchee River 1.3 mi past Big Y; 0.3 mi farther turn right on Alice Avenue. Turn right again on Josephine Avenue and proceed 0.2 mi to parking at WDFW Upper Dryden public access point.

STOP 6:
Peshastin syncline
47.5444°N, 120.5720°W

This stop is at the southeast limit of the Peshastin syncline, which plunges 18° northwest. To the northwest of this point there is a well-developed southwest limb; northeast-dipping beds of this limb are exposed in roadcuts between here and Leavenworth and along the Chumstick Highway north of Leavenworth. Southeast of here, there is no southwest limb: beds uniformly dip to the southwest.

Whetten (1980c) and Tabor and others (1987) proposed a short, straight, northeast-striking right-lateral fault which passes through this point to explain the down-section disappearance of the syncline. Their geometry is unrestorable. Cheney and Hayman (2009) did not map this area.

Haugerud (2021) argued that this geometry requires a significant thrust fault near this point. North of this stop, the fault is flat on flat and need not have any stratigraphic throw. To the south, it places a hanging wall cutoff on a footwall flat, with stratigraphic throw increasing to the south. This fault is a younger branch of the Leavenworth fault. An older branch lies farther west in lower Icicle Creek, 8 km west of here, where it places Mount Stuart batholith over Chumstick Formation. The older branch was refolded and carried piggyback in the hanging wall of this younger branch, as sketched in figure 6.

Are there other plausible geometries?

Return to US 2/97 (0.2 mi) and turn right. In 5 mi, at stoplight, turn right onto Aplets Way. Go 0.3 mi to downtown Cashmere roundabout and turn left on Cottage Avenue. In 0.5 mi, immediately before Wenatchee River bridge, turn right on Riverfront Drive. Follow Riverfront 0.9 mi to right turn across railroad tracks (caution!) onto Kelly Rd.

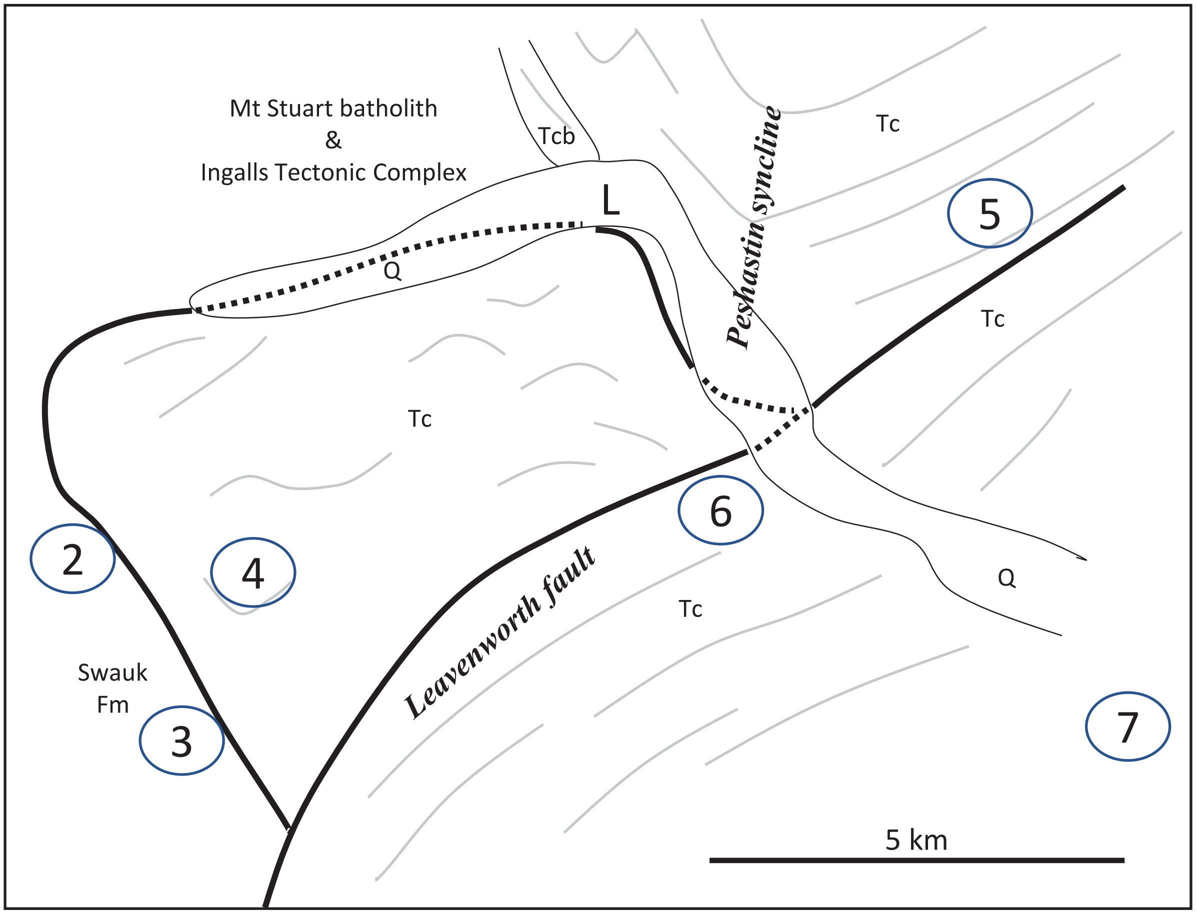

Figure 6. Profile geometry of Peshastin syncline and Leavenworth fault, as inferred by Haugerud (2021). View down projection axis 321°/18°. Heavy lines are faults, gray lines are bedding traces. Circled numbers are approximate locations of Stops 2–7. Abbreviations: L, Leavenworth; Tc, Chumstick Formation; Tcb, Chumstick basal conglomerate on Tumwater Mountain; Q, Quaternary deposits along Icicle Creek and Wenatchee River.

Kelly Rd is unpaved and may be challenging when wet. Go 0.7 mi up Kelly Rd and park on shoulder.

STOP 7:
Basal Chumstick Formation, view of folds to east
47.5017°N, 120.4403°W

We stop here to admire conglomerate with angular to rounded clasts of biotite gneiss and vein quartz that is interbedded with feldspathic sandstone typical of the Chumstick Formation.

These rocks are part of a unit that crops out around the southeast, southwest, and northwest sides of Swakane Biotite Gneiss in the core of the northwest-plunging Eagle Creek anticline; Gresens and others (1981b) described it as their "red-bed fanglomerate" at the base of the Chumstick. Evans (1994) stated that this unit postdates the Chumstick and proposed that it is a "paleocolluvium deposit that surrounded basement blocks which were uplifted and exposed during Chumstick basin deformation." We agree with Gresens and others (1981b).

Look east, across the Wenatchee River, to see folds in the Chumstick Formation (fig. 4). Do these folds record pure northeast–southwest shortening, top-to-the-northeast transport, or top-to-the-southwest transport? What do they imply about structure at depth? It is unclear to us whether these folds are structurally above or below the gneiss in the core of the Eagle Creek anticline.

Most of the area shown in figure 4 was mapped by Whetten and Waitt (1978) and Tabor and others (1987) as sandstone of the Chumstick Formation that underlies Nahahum Canyon Member farther northeast, though locally the contact they mapped is strongly discordant to bedding evident in high-resolution LiDAR topography (https://lidarportal.dnr.wa.gov/).

Continue east on Kelly Rd. In 0.8 mi, turn left on Bardin Rd., which turns right and becomes Za-

ger Rd. 1.1 mi from stop 7, turn left on Pioneer Way, which becomes Old Monitor Rd. Continue past fruit-packing plant, turn left onto Main St., across railroad tracks, to stoplight at US 2/97, 2.1 mi from stop 7. Cross US 2/97 and continue east on Easy St. At 1.8 mi from US 2/97, turn left on American Fruit Rd., drive beneath irrigation canal trestle, and turn right on Sunridge Ln., 0.2 mi from Easy St. Parking here is difficult; it may be best to continue up Sunridge Ln., make a U-turn, and park on west shoulder of Sunridge about 100 m north of American Fruit Rd.

STOP 8:
Nahahum Canyon Member of Chumstick Formation
47.4854°N, 120.3714°W

Gresens and others (1981b) identified shaly sandstone and shale in the Chumstick Formation as the Nahahum Canyon Member. Lack of material coarser than sand suggested deposition in one or more shallow lakes. They noted that landslides are common in Nahahum terrane and exposure is poor.

All workers have mapped the Nahahum Canyon Member as restricted to the northeast side of the Eagle Creek anticline. Gresens and others (1981b, their fig. 2) placed the Nahahum Canyon at the top of the Chumstick Formation. Tabor and others (1987, their section B–B') show it as overlain by typical Chumstick sandstone. Evans (1994) and Donaghy and others (2021) show it as overlain by Evans' Deadhorse Canyon Member of the Chumstick. Cheney and Hayman (2010) assigned beds mapped by others as Nahahum Canyon to the younger Wenatchee Formation.

Tuff beds have not been recognized in the Nahahum Canyon Member of the Chumstick Formation. Eddy and others (2016) obtained an MDA of 46.902 ± 0.076 for sandstone of the Nahahum Canyon collected from the type section along Eagle Creek, 6.5 km east–northeast of Stop 5. Gilmour (2012) reported a 44.447 ± 0.027 U-Pb zircon age for rhyodacite of the Wenatchee dome (to be seen tomorrow), which intrudes(?) strata that Gresens (1983) assigned to the Nahahum Canyon.

What is the depositional environment of the beds here? Which way do they face? How might they be more precisely dated?

Go south on Sunridge Ln., turn right on American Fruit Rd., turn right on Easy St., and turn right at stoplight on US 2/97 (2 mi from stop 8). West on US 2/97 to left turn at first Cashmere stoplight, west on Cottage Ave. to roundabout, left at roundabout onto Division St., go across railroad tracks and curve to right as Division becomes Pioneer Ave. At 1.6 mi from roundabout, turn right on Wescott and left into Chelan County Expo Center.

ACKNOWLEDGMENTS

We thank Scott Bennett, Ralph Dawes, and Heather Welch for helpful reviews. Any use of trade, firm, or product names is for descriptive purposes only and does not imply endorsement by the U.S. Government.

REFERENCES CITED

Cheney, E.S., and Hayman, N.W., 2009, The Chiwaukum Structural Low: Cenozoic shortening of the central Cascade Range, Washington State, USA: Geological Society of America Bulletin, v. 121, p. 1135–1153, doi: https://doi.org/10.1130/B26446.1.

Cheney, E.S., and Hayman, N.W., 2010, The Chiwaukum Structural Low: Cenozoic shortening of the central Cascade Range, Washington State, USA: Reply: Geological Society of America Bulletin, v. 122, p. 2103–2108, doi: https://doi.org/10.1130/B30220.1.

Donaghy, E.E., Umhoefer, P.J., Eddy, M.P., Miller, R.B., and LaCasse, T., 2021, Stratigraphy, age, and provenance of the Eocene Chumstick basin, Washington Cascades: Implications for paleogeography, regional tectonics, and development of strike-slip basins: Geological Society of America Bulletin, v. 133, p. 2418–2438, doi: https://doi.org/10.1130/B35738.1.

Eddy, M.P., Bowring, S.A., Umhoefer, P.J., Miller, R.B., McLean, N.M., and Donaghy, E.E., 2016, High-resolution temporal and stratigraphic record of Siletzia's accretion and triple junction migration from nonmarine sedimentary basins in central and western Washington: Geological Society of America Bulletin, v. 128, p. 425–441, doi: https://doi.org/10.1130/B31335.1.

Enkelmann, E., Ehlers, T.A., and Merli, G., 2015, Thermal and exhumation history of the Eocene Chumstick Basin, Washington State, USA: Tectonics, v. 34, p. 951–969, doi: https://doi.org/10.1002/2014TC003767.

Evans, J.E., 1994, Depositional history of the Eocene Chumstick Formation: Implications of tectonic partitioning for the history of the Leavenworth and Entiat–Eagle Creek fault systems, Washington: Tectonics, v. 13, no. 6, p. 1425–1444, doi: https://doi.org/10.1029/94TC01321.

Evans, J.E., 1996, Reply to comment on “Depositional history of the Eocene Chumstick Formation: Implications of tectonic partitioning for the history of the Leavenworth and Entiat- Eagle Creek fault systems, Washington”: Tectonics, v. 15, p. 510–514, https://doi.org/10.1029/95TC03695.

Evans, J.E., 2010, The Chiwaukum structural low: Cenozoic shortening of the central Cascade Range, Washington State, USA: Comment: Geological Society of America Bulletin, v. 122, no. 11/12.

Gilmour, L.A., 2012, U/Pb ages of Eocene and younger rocks on the eastern flank of the central Cascade Range, Washington, USA: M.S. Thesis, Seattle, University of Washington, 50 p.

Gresens, R.L., Naeser, C.W., and Whetten, J.W., 1981a, Stratigraphy and age of the Chumstick and Wenatchee formations: Tertiary fluvial and lacustrine rocks, Chiwaukum graben, Washington: Summary: Geological Society of America Bulletin, v. 92, Part I, p. 233–236 , doi: https://doi.org/10.1130/0016-7606(1981)92<233:SAAOTC>2.0.CO;2.

Gresens, R.L., Naeser, C.W., and Whetten, J.W., 1981b, Stratigraphy and age of the Chumstick and Wenatchee formations: Tertiary fluvial and lacustrine rocks, Chiwaukum graben, Washington: Geological Society of America Bulletin, v. 92, Part II, p. 841–876.

Gresens, R.L., 1982, Early Cenozoic geology of central Washington State. II. Implications for plate tectonics and alternatives for the origin of the Chiwaukum graben: Northwest Science, v. 56, p. 259–264.

Gresens, R.L., 1983, Geology of the Wenatchee and Monitor quadrangles, Chelan and Douglas Counties, Washington: Washington Division of Geology and Earth Resources Bulletin 75, 75 p., 3 sheets, scale 1:24,000.

Haugerud, R.A., 2021, Revisiting the Leavenworth fault, southeastern North Cascade Range, Washington [abs.]: Geological Society of America Abstracts with Programs, v. 53, doi: https://doi.org/10.1130/abs/2021AM-367835.

Hauptman, J.L., 1983, The sedimentology of the Wenatchee Formation: Late Paleogene fluvial and lacustrine strata of the east-central Cascade Range, Washington State: M.S. thesis, Seattle, University of Washington, 164 p., 24 plates.

Johnson, S.Y., 1985, Eocene strike-slip faulting and nonmarine basin formation in Washington, *in* Biddle, K.T., and Christie-Blick, N., eds., Strike slip deformation, basin formation, and sedimentology: Society of Economic Paleontologists and Mineralogists, Special Publication 37, p. 283–302.

Johnson, S.Y., 1996, Comment on “Depositional history of the Eocene Chumstick Formation: Implications of tectonic partitioning for the history of the Leavenworth and Entiat–Eagle Creek fault systems, Washington”: Tectonics, v. 15, no. 2, p. 506–509, doi: https://doi.org/10.1029/95TC03694.

McAdam, S., 2013, Gravity and magnetic analysis of the Chiwaukum Basin, central Washington: M.S. thesis, Missouri State University, 97 p., available at https://bearworks.missouristate.edu/theses/2765 [Accessed June 2022].

McClincy, M.J., 1986, Tephrostratigraphy of the middle Eocene Chumstick Formation, Cascade Range, Douglas County, Washington: M.S. thesis, Portland, Ore., Portland State University, 125 p., available at https://pdxscholar.library.pdx.edu/open_access_etds/3633/ [Accessed June 2022].

MacDonald, J.H. Jr., Harper, G.D., Miller, R.B., Miller, J.S., Mlinarevic, A.N., and Schultz, C.E., 2008, The Ingalls ophiolite complex, central Cascades, Washington: Geochemistry, tectonic setting, and regional correlations, *in* Wright, J.E., and Shervais, J.W., eds., Ophiolites, arcs, and batholiths: A tribute to Cliff Hopson: Geological Society of America Special Paper 438, p. 133–159, doi: https://doi.org/10.1130/2008.2438(04).

Methner, K., Fiebig, J., Wacker, U., Umhoefer, P., Chamberlain, C.P., and Mulch, A., 2016, Eocene–

Oligocene proto-Cascades topography revealed by clumped (Δ_{47}) and oxygen isotope ($\delta^{18}O$) geochemistry (Chumstick Basin, WA, USA): Tectonics, v. 35, p. 546–564, doi: https://doi.org/10.1002/2015TC003984 .

Miller, R.B., 1985, The ophiolitic Ingalls Complex, north-central Cascade Mountains, Washington: Geological Society of America Bulletin, v. 96, p. 189–209.

Miller, R.B., Bryant, K.I., Doran, B., Eddy, M.P., Raviola, F.P., Sylva, N., and Umhoefer, P.J., 2022, Eocene dike orientations across the Washington Cascades in response to a major strike-slip faulting episode and ridge-trench interaction: Geosphere, v. 18, p. 1–29, doi: https://doi.org/10.1130/GES02387.1.

Page, B.M., 1939, Geology of the Chiwaukum quadrangle, Washington: Ph.D. thesis, Stanford University, 203 p.

Paterson, S.R., Miller, R.B., Alsleben, H., Whitney, D.L., Valley, P.M., and Hurlow, H., 2004, Driving mechanism for >40 km of exhumation during contraction and extension in a continental arc, Cascade core, Washington: Tectonics, v. 23, TC3005, doi: https://doi.org/10.1029/2002TC001440.

Russell, I.C., 1900, A preliminary paper on the geology of the Cascade Mountains of northern Washington: U.S. Geological Survey Annual Report 20, pt. 2, p. 83–210.

Silling, R.M., 1979, A gravity study of the Chiwaukum graben, Washington: M.S. thesis, Seattle, University of Washington, 100 p.

Smith, G.O., 1904, Mount Stuart folio, Washington: U.S. Geological Survey, Geologic Atlas of the United States Folio GF-106, 4 sheets, scale 1:125,000.

Tabor, R.W., Waitt, R.B., Frizzell, V.A., Swanson, D.A., Byerly, G.R., and Bentley, R.D., 1982, Geologic map of the Wenatchee 1:100,000 quadrangle, central Washington: U.S. Geological Survey Miscellaneous Investigations Series, 1–1311, 26 p., 3 sheets, scale 1:100,000.

Tabor, R.W., Frizzell, V.A. Jr., Whetten, J.R., Waitt, R.B., Swanson, D.A., Byerly, G.R., Booth, D.B., Hetherington, M.J., and Zartman, R.E., 1987, Geologic map of the Chelan 30-minute by 60-minute quadrangle, Washington: U.S. Geological Survey Miscellaneous Investigations Series I-1661, 29 p., 1 sheet, scale 1:100,000.

Taylor, S.B., Johnson, S.Y., Fraser, G.T., and Roberts, J.W., 1988, Sedimentation and tectonics of the lower and middle Eocene Swauk Formation in eastern Swauk Basin, central Cascades, central Washington: Canadian Journal of Earth Sciences, v. 25, p. 1020–1036.

Turcotte, D.L., and Schubert, G., 1982, Geodynamics, New York, John Wiley & Sons, 450 p.

Walker, C.W., 1980, Geology and energy resources of the Roslyn-Cle Elum area, Kittitas County, Washington: Washington Division of Geology and Earth Resources Open-File Report 80-1, 59 p., 5 sheets, scale 1:24,000.

Whetten, J.T., 1980a, Preliminary bedrock geologic map of the Chiwaukum 4 NW quadrangle, Chiwaukum graben, Washington: U.S. Geological Survey Open-File Report OF-80-456, 5 p., 2 sheets, scale 1:24,000.

Whetten, J.T., 1980b, Preliminary bedrock geologic map of the east half of the Chiwaukum 4 SW quadrangle, Chiwaukum graben, Washington: U.S. Geological Survey Open-File Report OF-80-616, 6 p., 1 sheet, scale 1:24,000.

Whetten, J.T., 1980c, Preliminary bedrock map of the Chiwaukum 4 SE quadrangle, Chiwaukum graben, Washington, U.S. Geological Survey Open-File Report OF-80-723, 6 p., 1 sheet, scale 1:24,000.

Whetten, J.T., and Laravie, J.A., 1976, Preliminary geologic map of the Chiwaukum 4 NE quadrangle, Chiwaukum graben, Washington: U.S. Geological Survey, Miscellaneous Field Studies Map MF-794, scale 1:24,000.

Whetten, J.T., and Waitt, R.B., 1978, Preliminary geologic map of the Cashmere quadrangle, Chiwaukum Lowland, Washington: U.S. Geological Survey Miscellaneous Field Studies Map MF-908, scale 1:24,000.

Willis, C.L., 1953, The Chiwaukum graben, a major structure of central Washington: American Journal of Science, v. 251, p. 789–797.

BIG ICE AND BIG WATER: QUESTIONING THE PLEISTOCENE GEOMORPHOLOGY OF THE OKANOGAN LOBE LANDSCAPE

Ralph L. Dawes

Wenatchee Valley College, Wenatchee, Washington

ABSTRACT

This study uses literature review, map views, and field reconnaissance to assess competing ideas about the origin of the Okanogan Lobe landscape, focusing on an unresolved controversy about the proposal that its drumlins and tunnel valleys were produced by a single, nearly lobe-wide, subglacial sheet flood. The proposal argues that a sheet flood formed the drumlin fields, collapsed into channelized flow to form the tunnel valleys and, in the landscape beyond the ice lobe, was a source of the megafloods that created the adjacent Channeled Scablands of the Pacific Northwest (Shaw and others, 1999; Lesemann and Brennand, 2009). This is the meltwater hypothesis (Shaw and Sharpe, 1987; Shaw, 2002). Recent reviews of the Channeled Scablands (e.g., Baker and others, 2016; Baker, 2020; O'Connor and others, 2020) cite the catastrophic release of subglacial meltwater from the Okanogan Lobe as a possible source of the megafloods that formed the scablands. Megaflood is taken to mean a peak discharge of at least 10^6 m^3/s.

The Okanogan Lobe landscape, because of its proximity to the Channeled Scablands, is a unique testing ground for competing ideas about the origin of subglacial landforms. Previous studies of the megaflood-formed Channeled Scablands have analyzed the sediments to determine their provenance and timing of deposition; reconstructed the sources, pathways, and volumes of the megafloods from field evidence and modeling; and established type examples of the landforms created by megaflooding.

Tunnel valleys of the Okanogan Lobe landscape, a significant aspect of the meltwater hypothesis, have overdeepenings with adverse slopes or undulating longitudinal profiles. The tunnel valleys are eroded into bedrock at elevations ranging from 340 m below sea level to 1,600 m above sea level, which would require an extremely large volume of water confined beneath the ice sheet to form according to the meltwater hypothesis. The landforms identified as tunnel valleys have a variety of forms and origins. Factors related to the formation of these valleys include erosion during multiple glaciations, erosion of valleys subparallel to the glacial margin by meltwater streams during glacial advance and retreat, erosion by impounded water through drainage divides when a main valley was filled with advancing or retreating glacial ice, and stream capture due to diversion by glacial ice or drift. The larger overdeepened valleys are along faults or zones of less resistant rock. Many of the smaller valleys follow jointing in crystalline bedrock. Glacial erosion by abrasion and plucking played a role in eroding most valleys. Although erosion and sediment removal by subglacial fluvial discharges have likely taken place in most of the valleys as well, the subglacial discharges were less than megaflood scale.

Likewise, the drumlin fields are likely not related to a single megaflood. Subglacial processes related to ice streaming formed the drumlins, which transition into more elongate landforms known as mega-scale glacial lineations in the Cordilleran Ice Sheet (Eyles and others, 2018). This study finds that the meltwater hypothesis does not fit the field evidence, modeling results, theories of the origin of subglacial landforms, and theories of the origin of megaflood landforms that are currently available. The associated field trip will examine key landforms related to the Okanogan Lobe.

INTRODUCTION

At last glacial maximum, ice in the Okanogan Lobe of the Cordilleran Ice Sheet flowed from the interior plateau of south-central British Columbia, around 52°N (Prest and others, 1968; Clague, 1989; Ryder and others, 1991) to a lobate terminus defined by the Withrow Moraine on the Columbia Plateau of north-central Washington (47.6°N; fig. 1). This study refers to the entire length of this sector of the ice sheet as the Okanogan Lobe. (The valley along the axis of the lobe is spelled Okanagan in Canada.)

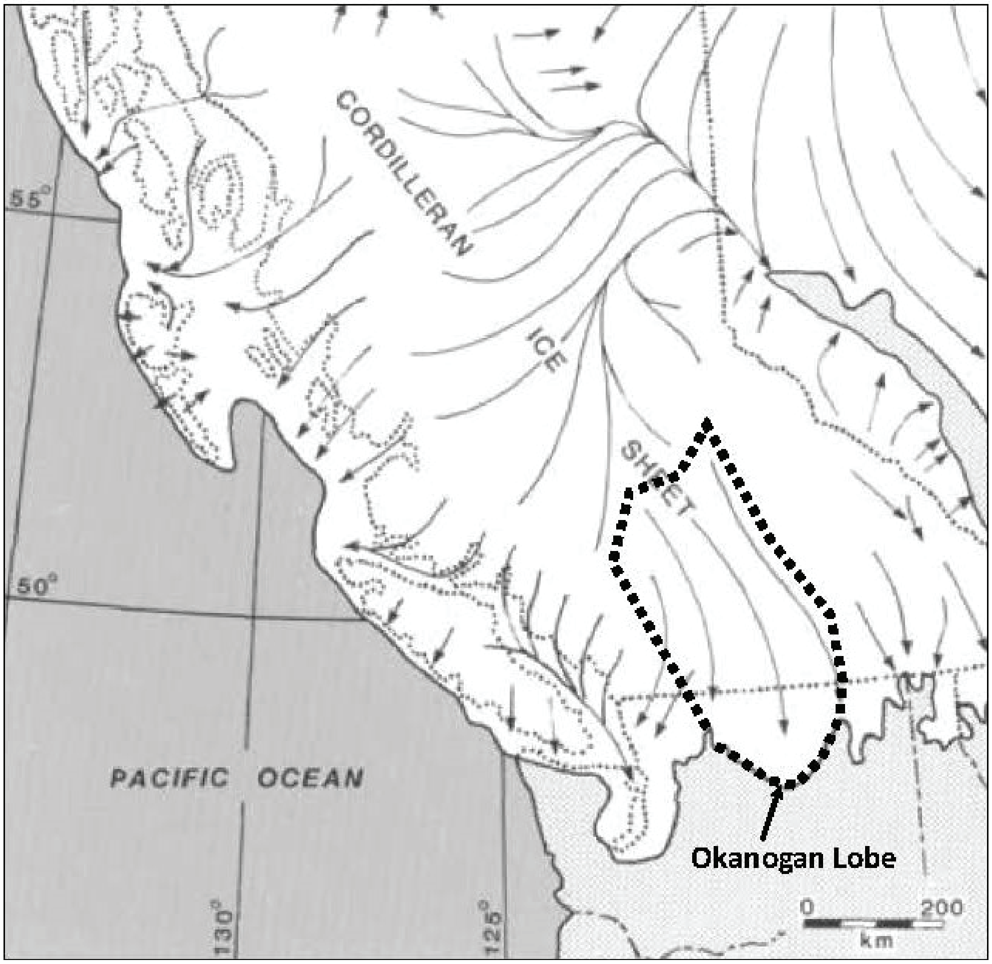

Figure 1. Map of Okanogan Lobe sector in the Cordilleran Ice Sheet (modification of map from Clague and others, 1994, p. 65).

The Cordilleran Ice Sheet is thought to have originated from alpine glaciers and ice caps in the Coast Mountains, Canadian Rockies, and other interior mountains of British Columbia and bordering provinces, which formed piedmont glaciers that coalesced in the interior plateau of British Columbia. At glacial maximum, the ice sheet flowed outward from ice divides above the interior plateau (Clague and Ward, 2011). The ice sheet surface was ~2,300 m above sea level in the Okanogan Lobe sector along the Canada/ U.S. border, according to field evidence (Prest and others, 1968; Clague, 1989). The Cordilleran Ice Sheet was similar to the Greenland Ice Sheet in size and in having mountain ranges and outlet corridors around a low-relief interior.

The Okanogan Lobe advanced south into Washington State after 20 ka, crossed and dammed the Columbia River by 18 ka, and was at its broad, lobate terminus, the Withrow Moraine, sometime between 14.5 and 16.0 ka (Clague and Ward, 2011; Balbas and others, 2017; O'Connor and others, 2020). The Withrow Moraine is on the Waterville Plateau, which is part of the larger Columbia Plateau. Retreat of the Okanogan Lobe after 14.5 ka was rapid, as indicated by ~13.5 ka Glacier Peak tephra deposited on exposed ground in the (American) Okanogan Valley, north of the Columbia River (Porter, 1978; Kuehn and others, 2009), ~12 ka moraines deposited from alpine or ice cap remnants in mountains northeast of the Okanogan Lobe landscape (Menounos and others, 2017), and ice-free exposures in the interior plateau of south-central British Columbia by ~12 ka (Souch, 1989).

The Okanogan Lobe landscape has several drumlin fields. Other glacial landforms of the Okanogan Lobe landscape include rôches moutonnées, crags-and-tails, mega-scale glacial lineations (MSGL), and eskers. Glacial outwash and kame terraces occur in many valleys. Glacial polish and glacial striations are observed on many bedrock surfaces. In some places, polish and striations are only observed where they have apparently been preserved under a veneer of regolith, which suggests that polish and striations may have weathered and eroded from many rock surfaces exposed since the Pleistocene. Glacial till and erratics are widely distributed. Lacustrine beds deposited in glacially impounded lakes during glacial recession are found in many valleys and are widespread in large, low-elevation valleys. Tunnel valleys, defined as valleys that were subglacial and have overdeepened basins, or have undulating longitudinal profiles with adverse slopes (going uphill in the downstream direction), occur in the landscape across a broad range of sizes and forms.

METHODS

This study is based on a review of published geologic literature, including papers and geologic maps, examination of digitized topography and landscapes using Google Maps and Google Earth, and field reconnaissance of selected parts of the Okanogan Lobe in

Washington. This study tests the meltwater hypothesis in the context of the Okanogan Lobe landscape by considering the evidence and theoretical grounds for a source of the meltwater, the origin of the drumlins, the origin of the tunnel valleys, and the nature of other erosional and depositional features of the glaciated landscape.

The proximity and possible genetic connection of the Okanogan Lobe to the adjacent Channeled Scablands prompts some additional ways to test the hypothesis. The Channeled Scablands originated from subaerial megaflooding (Bretz, 1923). Published studies on the provenance of sediments deposited by megafloods in the Channeled Scablands and on the Pacific Ocean floor beyond the mouth of the Columbia River are reviewed to look for signs of Okanogan Lobe provenance. Also taken into account are hydrodynamic models of megaflooding produced by Glacial Lake Missoula. The Channeled Scablands are the type area of megaflood erosional and depositional features. This study examines whether or not Channeled Scabland types of megaflood landforms are present in the Okanogan Lobe landscape.

MELTWATER SOURCE

The volume of Glacial Lake Missoula is estimated as 2,000–2,300 km^3 at maximum (Pardee, 1942; Clarke and others, 1984). The reservoir in the vicinity of the Okanogan Lobe in the Cordilleran Ice Sheet proposed for the meltwater megaflood hypothesis is many times larger (100,000 km^3; Shaw and others, 1999) or implied to be about the same magnitude as the volume of Glacial Lake Missoula (Lesemann and Brennand, 2009). According to the meltwater hypothesis, this reservoir may have been subglacial or supraglacial, or a combination.

The model of Livingstone and others (2013), which calculated possible subglacial lakes beneath the Laurentide and Cordilleran ice sheets, has been described as showing there could have been a subglacial lake in the Okanagan Valley that generated catastrophic flooding (Livingstone and others, 2013; Baker and others, 2016). However, according to the published model results (Livingstone and others, 2013, fig. 9, p. 30), the volume of the modeled lake is no more than 15 km^3, including the assumption there was no sedimentary infill on top of the overdeepened (to below sea level) bedrock floor of the valley. The model produced no subglacial lake on the scale of the meltwater hypothesis for the Okanogan Lobe.

There is no reported field evidence of an extremely large subglacial lake north of the Okanogan Valley, in the area around the ice divide (Stumpf and others, 2014). Wisconsin stage lacustrine deposits that are thick and widespread in many of the larger valleys, including the Okanagan Valley, have been generally interpreted as deposited in proglacial lakes during ice sheet advance and retreat (Eyles and Clague, 1991; Ryder and others, 1991; Brennand and others, 2014). As the ice sheet advanced into or retreated from lake-filled valleys, some of the lakes may have been subglacial, or partly subglacial. Some deposits associated with the lacustrine beds that have been interpreted as mass movement deposits in a lake, and some high-flow gravels interspersed with lacustrine sediments, may have been deposited beneath a glacier that was advancing into a valley or retreating into a floating remnant.

In the Okanagan Valley south of Lake Okanagan are bouldery deposits interpreted as representing proglacial Lake Penticton (the larger, late-glacial precursor to Lake Okanogan) eroding through an ice dam that was located at a bedrock constriction in the valley. The signs of a flood from the ice dam breach extend about 30 km to near the U.S. border (Nasmith, 1962; Roed, 2011). Leaving aside drumlins and tunnel valleys, no signs have been reported of a proglacial or subglacial lake outburst flood occurring in the U.S. Okanogan Valley south of the border. Lesemann and Brennand (2009) propose that stream terraces along valleys south of the 49th parallel, particularly along the Okanogan Valley and Columbia River Valley, could be largely composed of deposits from the waning stage of one or more subglacial megafloods. As discussed below in the Channeled Scablands and Okanogan Lobe section, the sedimentary structures and sedimentology of these terraces do not match flood bars of the subaerial megaflood type, lack the gravel dunes on their surfaces that are a prominent feature of such megaflood deposits, and have surfaces spotted with kettles and glacial erratics, consistent with recessional kame terraces deposited alongside a waning glacier in the valley.

Lesemann and Brennand (2009) suggest much of the Okanogan Valley could have been filled by a subglacial lake with a thin ice shelf floating on it, a subglacial lake orders of magnitude larger in volume than the one calculated by the model of Livingstone and others (2013). The proposed lake would provide a source for meltwater megaflooding, although an ice shelf would not greatly overpressurize the water, and much of the landscape hypothesized to have been shaped by meltwater flooding is upstream from or at higher elevations than the Okanogan Valley. The scenario suggested by Lesemann and Brennand (2009) counters previously published interpretations that the ice sheet was thickest over the deepest valleys.

Published reconstructions of the Cordilleran Ice Sheet surface in the Okanogan region have the ice thickest down the axis of the Okanogan Valley (Waitt and Thorson, 1979). A thick ice sheet across the Okanogan Valley is consistent with the evidence that, south of the Canada/U.S. border, the ice sheet covered mountains up to 2,400 m above sea level (asl) on the west side of the valley (Richard Waitt, oral commun., and personal observations). On the east side of the valley, south of the border, the ice sheet covered all peaks within 65 km of the Okanogan Valley, and deposited erratics from the north on top of at least one of them, Mount Bonaparte, 2,200 m asl (personal observations). The thickness of the ice sheet on the margins of the Okanogan Valley, the flow directions of erratics, and the ice flow directions from elongate landforms (drumlins, whalebacks, rôches moutonnées) and striations are difficult to square with the surface of the ice sheet dropping steeply from above the high sides of the valley to a thin ice shelf along the floor of the valley.

The other possibility for a meltwater megaflood source is a supraglacial lake. This would require an extremely large depression in the surface of the ice sheet in the vicinity of the Okanogan Lobe ice divide, where Okanogan ice flow originated during last glacial maximum. A depression in the ice sheet there contradicts the physics of an ice divide. A numerical model of the Cordilleran Ice Sheet by Seguinot and others (2016) produces the thickest ice in the vicinity of the field-based ice divide, and along the axis of the Okanogan Valley going south from there, consistent with the more field-based reconstruction of Waitt and Thorson (1979). The Cordilleran Ice Sheet at the north end of the Okanogan Lobe, in the vicinity of the reconstructed ice divide, left trimlines on mountains adjacent to the area up to 2,400 m asl (Prest and others, 1968; Clague, 1989). Ice flow direction indicators do not indicate ice flowing into the Okanogan Valley axis from all surrounding mountains, as would be expected if the ice were thin over the valley or over the interior plateau in the vicinity of the ice divide. Rather, some of the ice flow went towards the southern British Columbia Coast Mountains and the North Cascades in Washington State (Prest and others, 1968; Clague, 1989; Ferbey and others, 2016; Arnold and Ferbey, 2020), and ice flow brought erratics southward to the tops of peaks alongside the Okanogan Valley in Washington.

The evidence of ice age lakes in the valleys of the Okanogan Lobe landscape is consistent with proglacial lakes that formed due to temporary ice or drift dams during glacial advance and retreat (Eyles and Clague, 1991; Ryder and others, 1991). Sedimentology of deposits that may be from debris flows, slumps, melting ice blocks, and turbidity currents do not necessarily distinguish subglacial from proglacial, ice-marginal lakes, but nearly all the deposits are capped by silt or varve-like beds that record subaerial lake processes. None of the exposed evidence associated with the glacial lakes that existed in the Okanogan Lobe landscape is consistent with subglacial floods of the scale proposed by the meltwater hypothesis. In or near the Okanogan Lobe, the only reported evidence of a proglacial lake outburst flood that may have approached or exceeded megaflood level discharge is in the Fraser River Valley, which is west of the Okanogan Lobe landscape and drains through the Coast Mountains to near Vancouver (Clague and others, 2021).

During glacial retreat, the bottoms of deepest valleys had the largest, thickest, longest-lasting masses of remaining glacial ice, with sequences of kames and meltwater streams along the sides of the valleys marking the lowering of the glacial surface (Eyles and Clague, 1991; Ryder and others, 1991). A scenario involving an ice shelf floating on a large glacial lake along the length of the Okanogan Valley around the time of glacial maximum is difficult to reconcile with the ice being thickest along the axis of the valley at the end of glaciation. The same process occurred at the north end of the Okanogan Lobe region, near the ice divide, where evidence shows the ice sheet retreating to ice caps on surrounding mountain ranges and large remnant bodies of glacial ice along the axes of the valleys (Fulton, 1991; Eyles and Clague, 1991; Ryder and others, 1991). This suggests that the ice was too thick prior to retreat to contain a huge reservoir on its surface.

Thus, neither evidence nor modeling support the existence of a large body of water, either under or above the Okanogan Lobe.

DRUMLINS

Drumlins in the Okanogan Lobe landscape occur in valleys and plateaus and range from being composed of glacial drift to being composed of bedrock. Similar elongate landforms called drumlinoids are included in this study with drumlins. Most drumlins mapped in Canada are reported as consisting entirely of glacial till, with a small portion being bedrock-cored (Prest and others, 1968; Stumpf and others, 2014). Some of the drumlins of the Okanogan Lobe are bedrock-cored and some are partly bedrock-cored (Fulton, 1976; Lesemann and Brennand, 2009; Ferbey, 2013; Eyles and others, 2018; my field observations). Many bedrock-cored drumlins have a veneer of bouldery diamicton about 1 m thick. Some partly bedrock-cored drumlins appear gradational from crags-and-tails, with bedrock at the stoss end and sediment filling the tapering lee end (e.g., drumlin field south of Kamloops; Fulton, 1976; my field observations; Google Earth).

In fields of drumlins formed on plateau basalt, particularly the Columbia River Basalt flows on the Omak and Waterville plateaus, basalt is usually <1 m below the surface, overlain by a thin diamicton of angular basalt boulders, cobbles, gravel, and sand. On many of the basalt-cored drumlins, angular boulders of basalt appear to be the sole rock type. In till deposited between the basalt-cored drumlins, rounded plutonic and metamorphic rocks from further up-glacier occur, though angular clasts of basalt dominate.

The drumlin fields of the Okanogan Lobe are associated with MSGL (Eyles and others, 2018). MSGL are ridges parallel to the ice flow direction that tend to be lower, narrower, and much longer than drumlins. MSGL in the Okanogan Lobe landscape range from consisting of diamicton or boulders to being made of bedrock. Eyles and others (2018) first identified MSGL in the Okanogan Lobe and interpreted them as the result of ice streaming.

MSGL have been observed in parts of Antarctica recently uncovered by retreating glaciers, and have been observed beneath glaciers by ice-penetrating radar (King and others, 2009). The ones observed to date occur exclusively beneath ice streams (Spagnolo and others, 2014). Ice streams are flow corridors in ice sheets where ice flow is at least an order of magnitude faster than in adjacent zones, as observed on the Antarctic and Greenland ice sheets (Margold and others, 2015). It has been proposed that a continuum exists between drumlins and MSGL (Clark, 1993; Stokes and Clark, 2002; Sookhan and others, 2021) and that a transition from drumlins to MSGL represents a transition from slower to faster ice flow.

Eyles and others (2018) interpret MSGL as markers of ice streams in the Cordilleran Ice Sheet. Although some MSGL in the Okanogan Lobe are too subdued to have been observed in earlier, lower-precision mapping, earlier studies have, in some cases, referred to them as drumlins (e.g., Lesemann and Brennand, 2009; McClenagan, 2013). It may only be important to have a different name for MSGL to distinguish them from drumlins if MSGL have a distinctive origin such as ice streaming. Most MSGL in the Okanogan Lobe are on relatively flat plateaus or in wide parts of valleys, though in some places MSGL cross low mountains or bedrock hills. Eyles and others (2018) identified the axis of the Okanogan Lobe, centered along the Okanogan Valley and spreading out across the Omak and Columbia Plateaus at the southern end, as 1 of 15 ice streams in the Cordilleran Ice Sheet.

The meltwater hypothesis (Shaw and Sharpe, 1987; Shaw, 2002) proposes that the drumlins formed from subglacial megafloods up to tens of kilometers wide, hundreds of kilometers long, and at least as deep as the height of the drumlins. The meltwater hypothesis was originally conceived to explain drumlins. It is based on form analogy, with drumlins interpreted as looking like forms created by jets of ultra-high-speed water on metals and plastics and forms eroded into clay at the base of turbidity currents. A key part of the form analogy for drumlins originating from pressurized, turbulent sheet floods is the presence of furrows around the stoss or up-current end of drumlins, and along the sides. These furrows or troughs, also called hairpin erosional marks, are interpreted as being due to flow separation around the prow of the drumlin, creating vortices that erode at the base of the front and sides of the drumlin (see Shaw, 1994).

Few, if any, of the drumlins in the Withrow, Omak Plateau, Omak, or Tonasket drumlin fields have hairpin erosional marks, nor do many of the other drumlins in the British Columbia portion of the Okanogan Lobe. Some of the drumlins in drumlin fields southeast of Quilchena and Kamloops on the Thompson Plateau have depressions around their upflow ends and some along their sides, which appears to fit the hairpin erosional pattern interpreted in the meltwater hypothesis (Lesemann and Brennand, 2009). These drumlin fields grade into MSGL that continue to the southeast, which Eyles and others (2018) attribute to ice streaming, dismissing a meltwater flood origin.

In response to McClenagan (2013), who interpreted an area of drumlins in central British Columbia, north of the Okanogan Lobe landscape, in terms of the meltwater hypothesis, Stumpf and others (2014), emphasized the many decades of fieldwork and mapping previously performed on the area. They argued, among other things, that the drumlins (and what are now called MSGL) are best interpreted as resulting from glacial erosion and deposition processes. One line of support for a glacial rather than megaflood origin of the drumlins is the detailed studies of transport directions of clasts of glacial till cobbles and boulders from drumlins back to their sources (Stumpf and others, 2014). The transport directions match what are interpreted as ice-flow direction indicators, including orientations of drumlins, rôches moutonnées, crags-and-tails, and striations. The ice flow and till source indicators have been studied in enough detail to show that together they record switches in ice flow directions probably caused by migrating ice divides, which is consistent with ice-driven processes, not with subglacial flood-driven processes. Stumpf and others (2014) also raise the lack of any identifiable source for a meltwater flood, the lack of p- and s-forms, and the lack of flood-laid sediments as criticisms of the meltwater hypothesis. (P- and s-forms are discussed below under Tunnel Valleys.)

TUNNEL VALLEYS

The floors of many valleys in the Okanogan Lobe include uphill slopes in the downstream direction (adverse slopes) and in that sense qualify as tunnel valleys. The adverse slopes are commonly thought to originate from erosion and sediment evacuation by subglacial fluvial processes, with the weight of the overlying glacier forcing hydraulic flow of subglacial water. Many reviews of tunnel valleys ascribe their origin to episodic or relatively gradualistic, rather than catastrophic, discharges of subglacial meltwater, although some do not rule out catastrophic subglacial floods. Tunnel valleys are most commonly interpreted as requiring repeated abrupt subglacial discharges to form, in some cases possibly due to higher water production in summer, consistent with measurements of subglacial discharges beneath active glaciers (Ó Cofaigh, 1996; Alley and others, 2003, 2019; Kehew and others, 2012; van der Vegt and others, 2012).

Tunnel valleys form in wet-based glacial environments. Hooke (1991) and Alley and others (2003, 2019) have argued that adverse slopes in subglacial fluvial channels are limited to no more than 1.5 times the gradient of the overlying ice sheet surface because water near freezing, in contact with the glacier, will freeze due to supercooling caused by pressure loss if the slope is steeper. Alley and others (2019) also argue that glacial ice cannot remove subglacial sediment at the rate ice erodes bedrock, resulting in a shear-reducing diamicton between the ice base and the bedrock that effectively stops further erosion—unless fluvial processes at the base of the glacier remove the sediment. In zones of ablation, substantial amounts of water may exist at the base of the glacier, including the addition of supraglacial water via moulins or other pathways. If the rate at which subglacial water is produced cannot be accommodated into the ground beneath the glacier, the water pressure may rise toward equaling the pressure due to the weight of the glacier, greatly reducing the resistance to ice movement at the base of the glacier. If the rate of water production at the base of the glacier is high enough, a distributed, but possibly very thin, sheet of subglacial water may form, or the subglacial water may be channelized.

Along with having adverse slopes, which many analyses argue cannot be due to glacial erosion alone (Ó Cofaigh, 1996; Alley and others, 2003, 2019; Kehew and others, 2012; van der Vegt and others, 2012), tunnel valleys in some studies have a number of features that appear to be consistent with turbulent fluvial erosion (e.g., Shaw and others, 2020), or in some cases, it is argued, require it. This includes V-shaped profiles eroded into bedrock. In many ice-sheet or former ice-sheet settings, tunnel valleys form anastomosing (also called anabranching) channel networks that cut other glacial landforms such as drumlins, moraines, and MSGL. The pattern of anastomosing channels suggests a water drainage network. The cross-valley profile of Okanagan Lake basin, the largest overdeeped basin in the region labeled as a tunnel valley (Shaw and others, 1999; Lesemann and Brennand, 2009), has been described as V-shaped (Eyles and others, 1991; Lesemann and Brennand, 2009), although Roed (2011) interprets the profile with vertical exaggeration removed as U-shaped. The Palmer Lake valley and other parts of the Okanogan Valley, which are in the tunnel valley network of Shaw and others (1999) and Lesemann and Brennand (2009), appear possibly U-shaped as far as their bedrock sides are exposed. Lake Chelan is in a U-shaped trough (Whetten, 1967; Kendra and Singleton, 1987). Cross-valley profiles, therefore, do not conclusively support or refute erosion by turbulent fluvial flow in the Okanogan to excavate the larger trough-like valleys with overdeepenings.

A group of forms eroded into bedrock by, at least in some cases, turbulent flows of water, are called p-forms and/or s-forms, with p-forms commonly interpreted as coming from plastic-flow erosion by glacial ice and s-forms referring to forms thought in most cases to originate from fluvial erosion (Dahl, 1965; Kor and others, 1991). The origins of some of these forms in subglacial environments may be ambiguous and cannot be concluded from the label. These are mostly small-scale (centimeters to tens of meters) forms eroded into bedrock, including potholes that lack glacial polish and striations, grooves like the hairpin curves associated with the front and sides of some drumlins, scallop-shaped depressions with sharp edges on the crescent sides, and flutes (elongate grooves), including flutes with overhanging, sharp rims. s-forms occur in some tunnel valleys in other parts of the world (e.g., Shaw and others, 2020), and some types of s-forms occur in bedrock gorges recently eroded by extremely deep, fast, turbulent floods (e.g., Baker and Pickup, 1987).

In the Okanogan Lobe, depressions that have been labeled as tunnel valleys generally do not contain s-forms of the types that are most often ascribed to turbulent fluvial erosion (Stumpf and others, 2014; personal observations). A possible exception is at Squally Point alongside Lake Okanagan south of Kelowna, where elongate protruding forms, some with whaleback form, some with drumlin form, some with irregular form, have been eroded into the gneissic bedrock, and tunnel valleys with convex-upward and undulating longitudinal profiles cut from near Okanagan Lake level, across the point, and back to near lake level. Some of the elongate protruding forms have depressions at their upflow ends and along their sides. However, whether this matches the hairpin grooves around drumlins form of Shaw (1994; Shaw and others, 2020) is questionable. Most of the elongate forms at Squally Point lack grooves around their stoss ends and sides. In general, the grooves and valleys of Squally Point appear to be eroded into the jointing pattern of the bedrock. The steep downflow ends of some of the protruding, streamlined erosional forms and surfaces suggest glacial plucking. This landscape fits the glacially eroded gneiss and hardbed pattern described by Krabbendam and Glasser (2011). Krabbendam and others (2016) attribute similar landforms to glacial erosion, primarily by glacial plucking and abrasion, in landscapes interpreted by Shaw (1988) and Shaw and Kvill (1984) as due to catastrophic meltwater floods.

The Garnet Valley west of Okanagan Lake in British Columbia is described as part of an anabranching system of valleys hypothesized to have been a tunnel valley system by Lesemann and Brennand (2009). Garnet Valley is part of a system of valleys that run parallel to the Okanogan Valley along the west side of Lake Okanagan that could, at least in part, be accounted for by erosion due to glacial meltwater draining along the west side of a retreating mass of the ice sheet that filled the central Okanagan Valley floor during deglaciation.

On the Omak Plateau, where a drumlin field and MSGL occur (Elyes and others, 2018), the one tunnel valley is Soap Lake valley (fig. 2), which cuts the west side of the Omak Plateau. Along the margins of Soap Lake valley, drumlin-like glacial landforms are eroded into gneissic and granitic bedrock. Soap Lake valley is eroded along a fault (Gulick, 1990). Soap Lake valley has a U-shaped cross-profile and contains whalebacks and roche moutonnées, some with signs of glacial polish and striations on the surface. It seems possible from the evidence that the valley may have formed primarily by glacial erosion over several glacial cycles, with a possible role for sub-megaflood-scale subglacial fluvial erosion and sediment removal.

East of the Omak Plateau is the Omak Lake valley (fig. 2), an apparently overdeepened tunnel valley (Shaw and others, 1999; Lesemann and Brennand, 2009). The valley is considered likely to have previ-

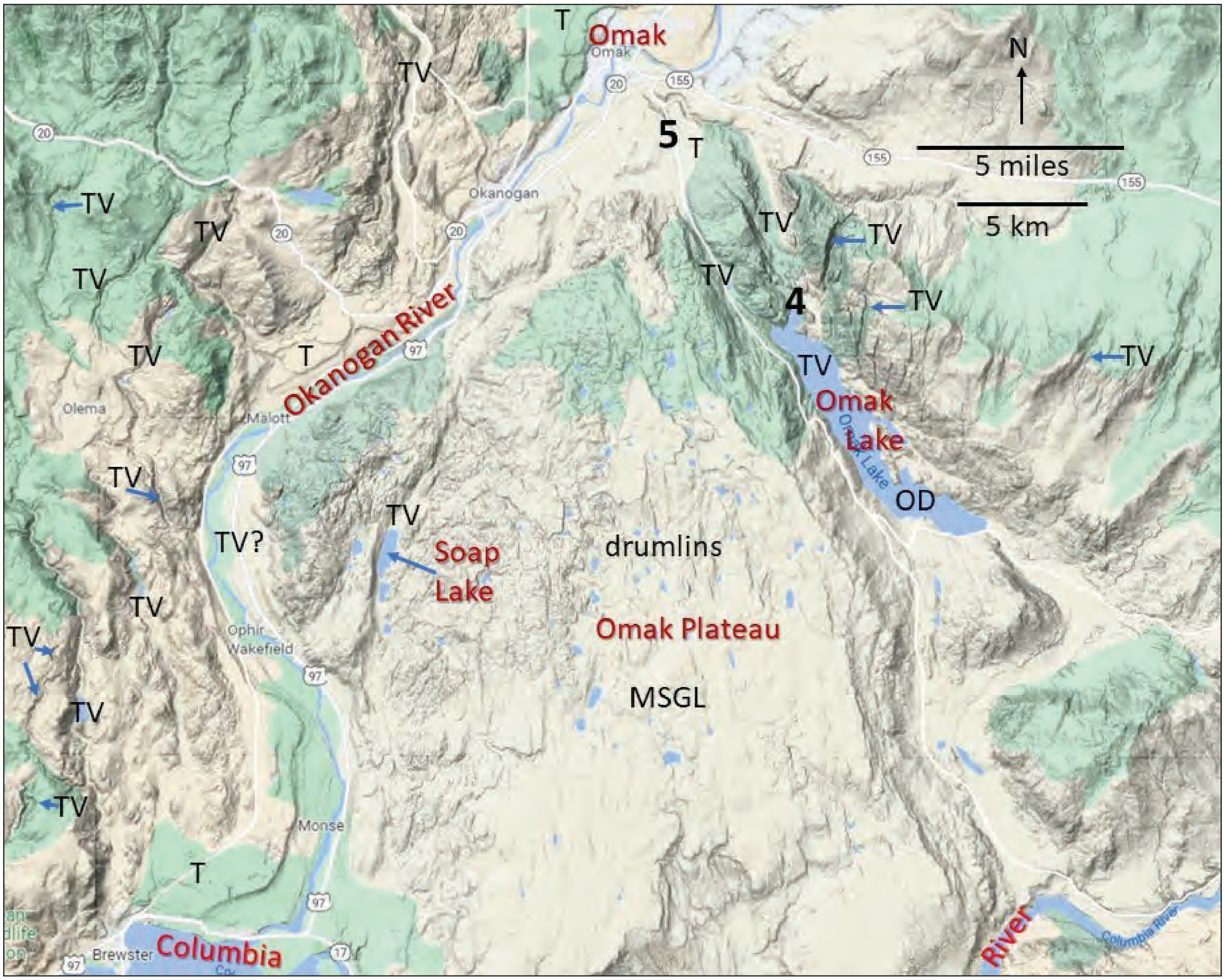

Figure 2. Google Maps terrain layer showing southern Okanogan River, Omak Plateau, and Omak Lake. Abbreviations: TV, tunnel valley; T, terrace; OD, wide, overdeepened basin with lake. Field trip stops 4 and 5 are labeled.

ously been part of the course of the Columbia River (Flint, 1935), pushed north of the Omak Plateau in the Miocene epoch by the Columbia River flood basalt. Most of the floor of the Omak Lake valley is over 100 m elevation higher than the Columbia and Okanogan rivers, with which it would have once formed a continuous channel. Therefore, the blocking of the Columbia River from the Omak Lake valley and the formation of its current channel through the Columbia River Basalt south of the Omak Plateau likely occurred during a pre-Wisconsin glaciation, if the cutoff was forced by glacial ice damming the Omak Lake valley (Flint, 1935). Like the Soap Lake valley, the overdeepened valley occupied by Omak Lake has a U-shaped cross-profile and contains whalebacks and roche moutonnées, some with glacial polish and striations on their surface. It follows a crustal-scale fault, the Okanogan detachment fault (locally called the Omak Lake Fault Zone; Goodge and Hansen, 1994), which borders the west side of the Okanogan metamorphic core complex. It is possible that the Omak Lake valley is the result of erosion by the ancestral Columbia River followed by subglacial erosion focused along the detachment fault during multiple glaciations. Sub-megaflood-scale subglacial fluvial erosion and sediment removal may have been involved in excavating its overdeepened floor.

The meltwater hypothesis (Shaw and others, 1999; Lesemann and Brennand, 2009) proposes the Lake Okanagan valley in British Columbia was scoured to bedrock by a catastrophic flood. This is supported by studies based on data from seismic lines conducted across and along the length of Lake Okanagan (Eyles and others 1990, 1991). The seismic studies interpreted the sediment now filling the valley from lake bottom to bedrock as a three-part sequence with what could be a bouldery flood deposit at bottom, subglacial mass movement and ice-proximal deposits in the middle part, and a widespread lacustrine silt bed sequence from a subaerial lake on top. This is interpreted as representing a complete scouring out of sediment from the bottom of the Okanagan Valley by a giant subglacial flood (or several such floods; Lesemann and Brennand, 2009).

However, an alternative interpretation of the basal (deepest) stratigraphic facies is that it is lodgment till (Nichol and others, 2015). The interpretation of sedimentology and sedimentary facies in the bottom and middle parts of the seismic stratigraphic sequence is tenuous, given the limited resolution of the seismic data and the lack of drill core or exposures of the strata on land. The scouring subglacial flood interpretation is not consistent with field, seismic, and drill-core studies of the valley north and south of the lake, which find a deposit of middle Pleistocene glacial till overlain by a nearly million-year-old basalt flow (Barendregt and others, 1995; Roed and others, 2014), and a late Wisconsin sequence of Fraser advance outwash overlain by till and lacustrine sediment (Nichol and others, 2015). Glacial till was deposited on lacustrine beds in the Okanagan Valley south of Lake Okanagan, a sequence interpreted as a proglacial lake being overridden by the ice during glacial advance (Nasmith, 1962).

The proposal that the bottom of the Canadian Okanagan Valley was swept clean by a catastrophic subglacial flood does not match the evidence in the U.S. Okanogan Valley, where advance outwash of the Fraser glaciation is overlain by till and proglacial lacustrine beds (with mollusk fossils in some locations; Pine, 1985; Minard, 1985). South of Lake Osoyoos at the border with Canada, the floor of the U.S. Okanogan River Valley narrows to <1.3 km wide between exposed bedrock walls at Wagon Road Coulee and Mallott. If the overdeepenings to below sea level beneath lakes in the Canadian Okanagan Valley were due to erosion by a system-wide catastrophic meltwater flood, it is not clear why the overdeepening process was restricted to the Okanagan Valley in Canada and Omak Lake basin in the U.S. More likely, glacial processes, including a confluence of glacial ice flow steered by preexisting topography, along with the existence of a detachment fault along the floor of the Okanogan and Omak Lake Valleys, contributed to the erosion of the overdeepenings.

In sum, the tunnel valleys of the Okanogan Lobe landscape are eroded into bedrock and occur in a wide range of scales and forms and over a wide range of elevations, from overdeepened troughs eroded at bottom to below sea level, to linear slot valleys cut through ridges. Some of the largest valleys appear U-shaped in cross-profile, thus implying erosion by glacial ice rather than meltwater. The largest overdeepened valleys, and some of intermediate size, are eroded along faults or zones of less resistant rock. The smallest valleys follow joint orientations in the bedrock. There are many valleys that channeled subaerial meltwater that was shed as the ice surface retreated down the sides of valleys (Dulfer and Margold, 2021; personal observations), and while some of these may have adverse slopes due to having been tunnel valleys when subglacial, some may have adverse slopes due to being formed as outlets to temporary lakes impounded alongside the retreating ice. Many valleys contain glacial striations and glacial erosional landforms such as roche moutoneeś and other smoothed surface forms ending at steep lee slopes. The valleys formed over a long history that included multiple cycles of glacial advance and retreat. Subglacial meltwater was involved in eroding many of the valleys, but a subglacial flood large enough to occupy the tunnel valleys is not needed to account for how the valleys formed and is implausible based on the elevation range such a flood would have to envelop. Additionally, tunnel valley formation by a large subglacial flood lacks support from the other tests of the hypothesis covered in this study.

THE CHANNELED SCABLANDS AND THE OKANOGAN LOBE

The Channeled Scablands provide ways to test the meltwater hypothesis, including sediment provenance (sources) for megaflood deposits in the Channeled Scablands; theoretical models calculated for flood sources, volumes, and pathways; and examples of megaflood-generated landforms.

Provenance of Late Wisconsin Sediments in the Channeled Scablands

Glacial Lake Missoula and the Purcell Trench ice dam that created it are in a geologic region dominated by the Proterozoic Belt Supergroup of sedimentary and metasedimentary rock, along with intrusions of Cretaceous to Eocene granitic rock near and downstream from the ice dam. Many of the Belt clastic rocks contain hematite and magnetite and are red in color (Hanson and others, 2015). A lithology in the Belt Supergroup that tends to survive as macroscopic clasts in megaflood deposits is quartzite derived from continental quartz arenite. Such quartzite does not occur in the Okanogan. Except for Cretaceous to Eocene plutons, bedrock of the Glacial Lake Missoula area contrasts with the bedrock of the Okanogan Lobe, which contains Late Paleozoic to Jurassic accreted oceanic and island arc crust, Cretaceous to Eocene plutonic and metamorphic rock, Eocene gneissic mylonite from metamorphic core complexes, Eocene arkosic sandstone, and Eocene volcanic rock (Stoffel and others, 1991, and references to specific map quadrangles therein; Erdmer and Cui, 2009; Okulitch, 2013; personal observations) The different geologic substrates of the Okanogan Lobe and Glacial Lake Missoula produce different signals in surficial sediments derived from the two regions.

In Glacial Lake Columbia, which formed in the Columbia River Valley behind the ice dam created when the Okanogan Lobe crossed the Columbia River, Hanson and others (2015) and Hanson and Clague (2016) conducted a sediment provenance study of beds of fine-grained sediment that they and Atwater (1986, 1987) interpret as having settled out of megafloods that entered the lake. They interpret the red color and magnetic properties of the sediment as deriving from minerals in the Belt Supergroup, consistent with the megaflood deposits originating from Glacial Lake Missoula.

Detrital zircon age spectra can also be used to attempt to distinguish Glacial Lake Missoula sediment from an Okanogan Lobe source. Studies by Gaylord and others (2007) and Anfinson and others (2009) found that in flood bed sequences from the central Channeled Scabland, including the Hanford Basin, the zircon age spectrum was dominated by a Glacial Lake Missoula signal, although an Okanogan Lobe signal may have been present in some beds. The Okanogan Lobe signal could be accounted for by Glacial Lake Missoula megafloods picking up locally sourced glacial deposits from Glacial Lake Columbia, which lapped against the margin of the Okanogan Lobe, as the floods swept through the lake. Flood beds deposited in Glacial Lake Missoula, adjacent to the terminus of the Okanogan Lobe, were found to have a strong Okanogan Lobe signal in a set of thin flood beds on top of a long sequence of thicker, Glacial Lake Missoula-sourced flood beds (Gaylord and others, 2007). This was interpreted as due to small outburst floods coming from the nearby margin of the Okanogan Lobe as it began retreating. This agrees with the interpretation of the megaflood bed sequence of Glacial Lake Columbia by Atwater (1987), which interprets the bulk of the flood sequence, consisting of the larger flood beds, as originating from Glacial Lake Missoula.

Shaw and others (1999) argued that flood deposits at a site named Sage Trig (Atwater, 1986), which was in the Sanpoil Arm embayment of Glacial Lake Columbia, are from floods that came from beneath the nearby margin of the Okanogan Lobe. There is extensive deformation and disruption of strata in the Sage sequence, including soft sediment deformation, rip-up clasts, possible remobilization of earlier silt from up-slope, and post-depositional slumping. The complexity of the disrupted bedding from high-energy floods, and the geographic position and topography of the site, make the ultimate source of floods difficult to pin down on the basis of flow direction indicators. Atwater (1986) and Waitt and others (2021) interpret the deposits as most likely due to flooding from Glacial Lake Missoula into Glacial Lake Columbia.

The Channeled Scablands megafloods deposited beds of sediment on the floor of the Pacific Ocean beyond the mouth of the Columbia River. Studies of fresh-water plankton and oxygen isotopes (Hendy, 2009; Lopes and Mix, 2009), Hf-Nd-Pb isotopes (Prytulak and others, 2006), and Nd and K-Ar isotopes plus trace element abundances (Gombiner and others, 2016) extracted from drill-core samples of the seafloor megaflood sediments, indicate that a sequence of large, Glacial Lake Missoula-sourced megafloods occurred approximately 15–20 ka, in agreement with the record on land. Some of the isotopes also show a strong signal from the Columbia River Basalt, presumably derived from the erosion of the Channeled Scablands.

The study by Lopes and Mix (2009) detected low salinity, or large inputs of fresh water, into the Pacific Ocean. They also detected freshwater diatoms of a large, deep lake habitat in 17.5–20 ka megaflood beds, consistent with Glacial Lake Missoula and inconsistent with an Okanogan Lobe reservoir. Diatoms found in seafloor megaflood deposits 23–31.5 ka are from habitats involving shallow lakes or streams and come from an unknown source or sources, prior to the existence of Glacial Lake Missoula and the Okanogan Lobe (Lopes and Mix, 2009).

Gombiner and others (2016) reported that the megaflood beds, which they measured as 19–14 ka in age by K-Ar dating, were cyclic and repetitive in nature. They point out that although their data all point to Glacial Lake Missoula (or a source on predominantly Proterozoic cratonic crust), their samples are of selected beds, not all flood beds, and that adjacent beds may have been combined in some samples. While a megaflood source located on the younger crust to the west of Glacial Lake Missoula was not clearly detected in their data, their study did not rule out other sources completely.

The evidence indicates that Glacial Lake Missoula was the predominant source of Latest Wisconsin (~15–20 ka) megafloods and that megaflood sediments in Glacial Lake Columbia, along the southeastern margin of the Okanogan Lobe, came from Glacial Lake Missoula, not the adjacent Okanogan Lobe.

The Channeled Scablands Water Volume Problem

Early modeling calculated that Glacial Lake Missoula could not supply enough water to reach the highest flood levels indicated by field evidence (Komatsu and others, 2000; Miyamoto and others, 2007). It seemed that another source of water was needed to explain the field evidence. Additional water from beneath the southern Cordilleran Ice Sheet simultaneous with draining of Glacial Lake Missoula, or else megafloods coming only from beneath the Cordilleran Ice Sheet, larger than Glacial Lake Missoula drainages, seemed possible sources to solve the "missing volume" problem of water in the Channeled Scablands.

However, the most recent hydrodynamic modeling of Glacial Lake Missoula flooding the Channeled Scablands, which applies updated information on the timing of the Okanogan Lobe damming the Columbia River and the resulting effect of possible pathways for the floods, finds that, if anything, the flood levels are slightly too high along the periphery of the Okanogan lobe (Denlinger and others, 2021). Hundreds of kilometers downstream, in south-central Washington, the modeled flood levels are still too low, though by an amount, tens of meters, which Denlinger and others suggest might be accounted for by enlargement of the flood volume by incorporation of loess eroded from the flood pathways, consistent with field evidence of erosion and transport of large volumes of loess from eastern Washington by the Channeled Scablands-forming floods. To the extent that these recent hydrodynamically modeled scenarios are accurate, they rule out a significant role for subglacial meltwater from the Okanogan Lobe in the megaflooding that created the Channeled Scablands.

Comparison of Channeled Scabland-Type and Okanogan Lobe Landforms

The Channeled Scablands adjacent to the Okanogan Lobe are the initial type-area for megaflood landforms known to be the result of turbulent flows up to hundreds of meters deep moving at speeds that may have reached mean flow velocities of >60 km/h (Baker, 1973). Examples include large, steep-walled canyons (coulees) eroded into plateau basalt, some headed by (now dry) cataracts; large (up to >100 m in diameter and >20 m deep), steep-walled potholes eroded into plateau basalt; giant flood bars of sand, gravel, and boulders deposited mainly in large, downvalley foreset beds at inside bends of main flood channels, behind flow barriers, and at the mouths of large coulees emptying into broad basins; and large, widely spaced gravel dunes ("giant current ripples," Pardee, 1942; Bretz and others, 1956) on flood bars. We can assess the hypothesis of megaflood discharge related to the Okanogan Lobe by identifying megaflood landforms in the landscape.

One possible Channeled Scablands-type landform in the Okanogan Lobe landscape is The Chasm, an 8.75-km-long coulee eroded into plateau basalt in the interior plateau of British Columbia, with a dry-cataract upper end and eskers and kettles in it (Burke and others, 2012a,b). Beneath the floor of the coulee are what may be sand-and-gravel dune structures up to ~2 m amplitude and 60 m wavelength. This is interpreted by Burke and others (2012a,b) to be a tunnel valley (tunnel channel) that was formed by subglacial discharge that exceeded bankfull stage. Two smaller valleys a few kilometers southwest of The Chasm are also eroded into plateau basalt and may have been tunnel valleys. The lack of similar coulees in glaciated areas of plateau basalt outside the vicinity of The Chasm, including in zones of drumlin fields and MSGL on the Omak and Waterville plateaus, is consistent with The Chasm representing a localized process that formed when the glacial margin was nearby during glacial retreat (Burke and others, 2012a,b), rather than resulting from a regional, Okanogan-Lobe-scale megaflood.

It is possible that there are some anastomosing valley systems in the Okanogan Lobe landscape that were eroded by water beneath the ice sheet (Lesemann and Brennand, 2009; McClenagan, 2013). Alternative explanations for these valley networks have been discussed above and in Stumpf and others (2014). The lack of evidence for megaflood-scale floods coming from the Okanogan Lobe into the Channeled Scablands suggests that any subglacial fluvial discharges that may have occurred in these valleys were local rather than regional in impact. In addition, the lack of tunnel valleys or anastomosing valleys behind the Withrow Moraine, along the terminus of the Okanogan Lobe on the Waterville Plateau, in a zone of drumlins and MSGL, and also on the Omak Plateau where drumlins and MSGL occur but neither tunnel valleys nor an associated valley network, suggests that drumlin fields and MSGL can form without tunnel valleys or anastomosing subglacial valleys forming among them or downstream from them.

Giant flood bars topped with gravel dunes on them occur in the Fraser River valley, west of the Okanogan Lobe landscape. These are interpreted as evidence of a proglacial lake outburst flood that occurred during ice sheet retreat (Clague and others, 2021), which might have approached or exceeded megaflood-level discharge.

A set of what may be giant current ripples occur in the Okanogan Valley on a terrace between the Omak Airport and the Okanogan River (Cooley, 2022). These are visible on LiDAR around latitude and longitude +48.4473, -119.4813 (Cooley, 2022; Washington Lidar Portal, 2022). They are on a bench or terrace adjacent to and above the present-day Okanogan River floodplain. The bench is inset into the side of a much broader, higher terrace, locally called Bide A Wee Flat, which is considered part of the Great Terrace (Russell, 1898; Flint, 1935; see discussion below under Other Erosional and Depositional Features). Being on a landform inset into the adjacent higher terrace makes the set of giant current ripples near Omak likely to be a very late-glacial feature, deposited when there were only last remnants of glacial ice in the Okanogan Valley, or else it is a post-glacial feature. The top of the flood which formed the gravel dunes apparently was below the level of Bide A Wee Flat, <1 km to the west. This limits the depth of the flood related to the Omak current ripples to <20 m.

The lack of documented exposures of internal bedding of the giant current ripples near Omak, and the possible partial mantling of their surface by subsequent finer sediment, which may be subduing their apparent height, along with the possibility that the ripple field once extended further but was subsequently eroded at its margins, make it problematic to apply studies of Channeled Scabland giant current ripples to their interpretation. Baker's work in the Channeled Scablands (1973,1978, 2009) showed possible correlations between the chord (wavelength) and wave height of gravel dunes on flood bars and the possible depth, surface slope, velocity, and power of the floods that formed them. However, the giant current ripples near Omak may not fit the parameters of the sets of giant current ripples in the Channeled Scablands that Baker studied. Baker had field evidence of high-water marks to estimate flood depth, cross-sectional area, and flood surface slope. The flood bars Baker studied (1973, 1978, 2009; also see Rudoy and Baker, 1993) had exposures of internal sediment clasts and sedimentary structures. He found boulders ranging from 0.5 to 1.5 m in intermediate diameter armoring the surfaces of the gravel dunes, which he attributed to waning-flow winnowing and sorting. Exposures of the deeper, internal beds of the flood bars showed them to be filled largely with open-framework gravel. A distinctive, predominant sedimentary structure in the flood bars is long (commonly >10 m) foreset beds dipping down-valley or down-flow at angles of 10–27°, with some of the lower values possibly reflecting apparent dips (Baker, 1978).

Most of the flood bars in the Channeled Scablands that Baker studied retained their entire original form. This contrasts with the giant current ripples near Omak. They appear to be a partial remnant of what was once a more extensive flood bar that was developed on a preexisting terrace, outwash plain, or floodplain. Subsequent erosion and sedimentation have obscured the shape and extent of the possible flood bar near Omak and the landscape on which it formed. Field study of the giant current ripples near Omak and their contextual landscape has not yet been performed. Although no firm conclusions can currently be drawn about the timing and magnitude of the flood that formed the Omak giant ripples, what clues there are suggest it was latest-glacial or early post-glacial and was below megaflood level. The flood was confined to a channel in the Okanogan Valley beside and below the Great Terrace. During glacial retreat, numerous temporary proglacial lakes formed in valleys in the region. An outburst from one of those lakes may have been the source.

There are some drumlinoids, forms suggestive of drumlins, eroded into Columbia River Basalt in the Channeled Scablands near Dry Falls (seen around latitude and longitude +47.5956, -119.3334 on Google Maps). Baker and Milton (1974) call elongate landforms in the scabland near Dry Falls longitudinal grooves, focusing on the depressions. They classify the type of scabland landscape in this area as butte and basin topography. Hairpin erosional marks appear to generally absent from the margins of the drumlinoids. These landforms have some properties that are not found in drumlin fields of the Okanogan Lobe, including the drumlin fields on the nearby Waterville and Omak plateaus where drumlins are cored by Columbia River Basalt. Sectors of the scabland landforms near Dry Falls are parallel but then curve, converge, diverge, or get cut off by other sectors of the elongate landforms coming in at different orientations. These apparent flow patterns are not seen in Okanogan Lobe drumlins, which are more extensively parallel.

Also in the Channeled Scablands near Dry Falls are large potholes with vertical, and in some cases overhanging, walls that were eroded into the basalt by the megafloods. Such potholes are a feature of the Channeled Scablands that have been attributed to plucking by kolks (vortices) that formed in deep, turbulent flows (Baker 1978, 2009). Such potholes are missing from the Omak and Waterville Plateau drumlin fields. In many cases, the Okanogan Lobe drumlin fields grade into parallel-aligned MSGL, which are lacking in the Channeled Scablands. The basalt drumlins of the Okanogan Lobe are smoother-sided, including on stoss ends and long sides, whereas the scabland landforms near Dry Falls tend to be eroded in steps that follow the bases of columnar-jointed layers in the basalt flows, consistent with erosion by high-energy, turbulent floods passing by (Baker, 1978, 2009; Baker and Milton, 1974). The lack of Channeled Scablands-type megaflood landform features in the basalt-floored Omak and Waterville plateau drumlin fields, including the lack of scabland-style potholes in the basalt, the lack of vertically eroded steps on the sides of drumlins along basalt colonnades, the lack of curving orientations of drumlin long axes across the drumlin fields in plan view, and the presence of MSGL in the drumlin fields but not in the Channeled Scablands, suggest that megafloods like those of the Channeled Scablands did not occur across the drumlin fields.

The lack of any megaflood erosional features along the length of the Withrow Moraine and beyond it on the Waterville Plateau, beyond where the array of drumlins and MSGL are cut off at right angles by the terminal moraine, indicates that the drumlins and MSGL on the Waterville Plateau were not formed by fluvial processes that produced detectable evidence on the landscape beyond the glacial terminus

OTHER EROSIONAL AND DEPOSITIONAL FEATURES

Glacial retreat involved downwasting in steps from high elevations, producing sets of kame terraces that are largest at low elevations alongside the largest rivers. The stepwise down-wasting of the ice sheet, in creating lakes and kame terraces in valley after valley, also created sequences of side-stream drainages that may in some cases be mistaken for, or have followed preexisting, tunnel valleys (Dulfer and Margold, 2021). The descending-elevation retreat or stagnation of the ice sheet ended with a large body of ice remaining in the largest, lowest-elevation river valleys, particularly the Okanogan and Columbia River Valleys, and created the largest set of kame deltas along the sides of those valleys (fig. 2.). This “Great Terrace” (Russell, 1898) has been proposed by the meltwater hypothesis as a possible repository of sediments transported by subglacial megaflooding (Lesemann and Brennand, 2009). However, the sedimentology, internal sedimentary structures, and morphology of the terraces indicate deposition of sediments by a combination of ice-proximal, energetic flows, side-stream alluvial fans, deltas, and channels, and temporary proglacial lakes (Waters, 1933; Flint, 1935; Pine, 1985; Minard, 1985). Ice contact features are visible in some of the exposures of bedding inside the terraces (Pine, 1985; Minard, 1985; my observations). Kettles and erratics occur on the surfaces of the terraces. Large foreset beds filled with gravel and dipping steeply down-valley are missing. Giant current ripples, with one possible late-glacial or post-glacial exception near Omak discussed above, are missing from the terrace surfaces.

CONCLUSIONS

The Okanogan Lobe landscape can be accounted for by interpretations based on many decades of fieldwork, mapping, and numeric modeling. There are problems with applying the purportedly analogous forms of the meltwater hypothesis to drumlins in the different scales and boundary conditions involved in subglacial environments, in how to measure similarity of shapes, and in agreeing on how to evaluate the hypothesis using field evidence. For the Okanogan Lobe, this study has looked at evidence other than the form analogy argument to assess the plausibility of the hypothesis, including whether there was a sufficiently large reservoir of meltwater, whether the system of tunnel valleys was occupied by a system-wide subglacial flood, and whether any significantly large bodies of meltwater-laid sediment occur down-glacier from the possible meltwater landforms and downstream from there in the Channeled Scablands.

The drumlins and tunnel valleys of the Okanogan Lobe landscape formed by a combination of glacial erosion and deposition, and glaciofluvial erosion and deposition. The drumlins have been shown to be associated with MSGL and likely are due primarily to ice flow at the base of the glacier. The tunnel valleys in the Okanogan Lobe landscape originated from a variety of processes. There were probably occasional or episodic discharges of subglacial meltwater from the Okanogan Lobe, which may have peaked in a given area during glacial retreat. However, large floods from beneath the Okanogan Lobe, comparable in volume and peak discharge to Glacial Lake Missoula, did not create the drumlins and tunnel valleys and did not contribute to Late Wisconsin Channeled Scablands megafloods.

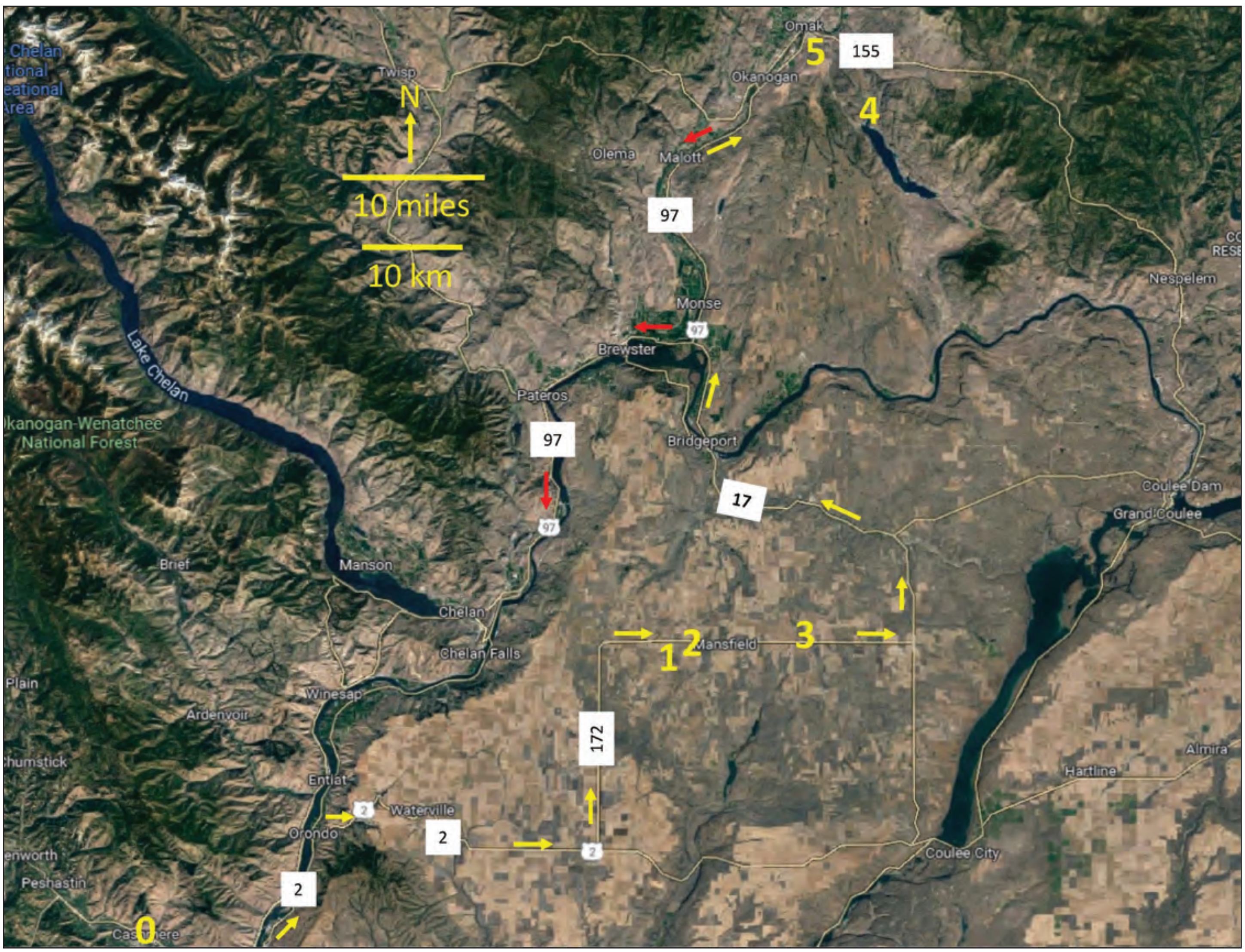

Figure 3. Numbered field trip stops on Google Maps satellite layer. Highway numbers in white boxes. Yellow arrows mark route to stops. Red arrows mark return route.

GUIDE TO FIELD STOPS IN THE SOUTHERN OKANOGAN LOBE

This field trip departs and returns to the TRGS meeting center at the Chelan County Fairgrounds and Expo Center in Cashmere, Washington (fig. 3). Latitudes, longitudes, and driving distances are taken from Google Maps.

On the way to Stop 1, you will be going up the Columbia River Valley north of Wenatchee for about 13 mi, along a relatively steep-walled stretch of the river valley known as Rocky Reach. The bedrock in Rocky Reach is the Swakane Biotite Gneiss, Cretaceous in age (Matzel and others, 2004; Sauer and others, 2017). This portion of the Columbia River Valley was swept by at least one, and possibly the largest, of the Late Wisconsin Glacial Lake Missoula megafloods, around 18.2 ± 1.3 ka (Balbas and others, 2017). Subsequently, the Okanogan Lobe crossed the Columbia River and dammed it, creating Glacial Lake Columbia, with the wall of ice holding back the river located, at last glacial maximum, about where Grand Coulee Dam is today. Glacial Lake Columbia drained around ~15.9 ± 0.7 ka (^{14}C age graphically converted to calendar age from Atwater, 1986), or ~14.0 ± 1.4 – 14.4 ± 1.3 ka (Balbas and others, 2017). Take a look at Rocky Reach and compare its megaflood-eroded sides (to elevations that were around a thousand feet above the bottom of the valley) to tunnel valleys we will see at Stop 4.

After leaving the Columbia River at Orondo we will climb up onto the Waterville Plateau on Highway 2. The land around the town of Waterville is covered by loess, wind-blown silt, most of which was blown from megaflood sediment strewn across the Channeled Scablands of eastern Washington (fig. 4). The loess mantle tells us that this landscape was neither flooded nor glaciated. As we drive through Withrow, ahead of us will loom the Withrow Moraine, the terminal moraine of the Wenatchee Lobe, a hummocky landscape studded with erratics of basalt. The Columbia River Basalt is the bedrock beneath the unconsolidated Quaternary deposits on the Waterville Plateau.

Stop 1 is 70 mi from the Chelan County Expo Center in Cashmere. Take Highway 2/97 east. Drive on Highway 2, which separates from Highway 97 in Orondo. Turn north off of Highway 2 at Farmer (some grain elevators and a small community center building) onto State Route 172. Proceed north through Withrow (and the Withrow Moraine) towards Mansfield on Route 172.

About 5 mi before Stop 1, Route 172 bends around the south end of Lone Butte. Lone Butte is one of three large masses of basalt on the Waterville Plateau proposed to have been lifted or slid from place and transported semi-intact for 0.5–2.5 mi. The other large masses of basalt are Burke Hill (Stop 1) and the Pot Hills (Stop 3).

After about 66 mi take a right and go south on C Rd NE. At 2 mi, take a right (go west) on 12th Rd. N (unpaved road). Proceed about 1 mi and park where the shoulder is wide.

STOP 1:
Drumlins on the Waterville Plateau
+47.7882, -119.7055

A set of drumlins visible here have their stoss ends positioned along 12th Rd. NE. The stoss ends are the north ends, facing the oncoming ice flow, or subglacial meltwater flood, direction. The drumlin long axes are oriented north–northwest to south–southwest. Map and satellite views show the drumlin orientation is consistent with other possible ice flow direction indicators—flutings, striations on bedrock, and MSGL—in this area of the Waterville Plateau. This consistency of orientation of possible ice flow direction indicators occurs in all zones of drumlins and MSGL in the Okanogan Lobe landscape.

The drumlins here appear to be cored by Columbia River Basalt and mantled by angular basalt boulders up to ~1 m diameter. In low areas between drumlins occasional signs of bedrock through the glacial drift suggest a thin veneer of sediment covers the bedrock in this area. Most cobbles and boulders on the low ground by the road are pieces of basalt. Also present are pebbles, cobbles, and boulders (glacial erratics) of plutonic and gneissic metamorphic rock, more rounded than the basalt clasts. The nearest bedrock exposures of plutonic and metamorphic rock are along the Columbia River ~13 mi (20 km) north of here.

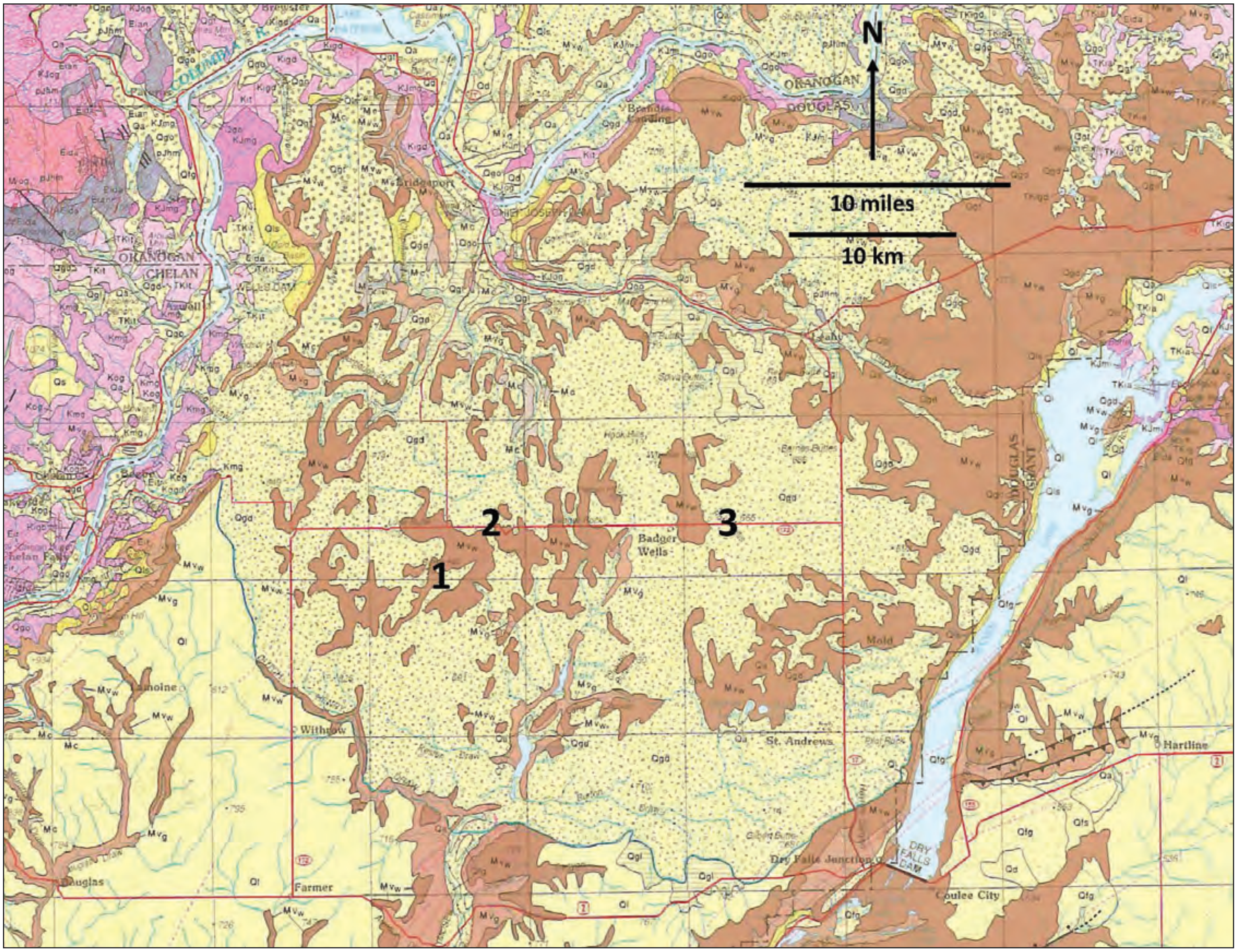

Figure 4. Numbered field trip stops 1–3 on the Waterville Plateau on an excerpt from geologic map of the NE Washington quadrant (Stoffel and others, 1991). The yellow unit with variable dot pattern is Qgd, Cordilleran Ice Sheet Quaternary glacial drift. The brown M units are Miocene Columbia River Basalt.

Waitt and others (1994) have suggested that Burke Hill, the high area rising north of this stop, may be a mass of Columbia River Basalt that was detached by the ice sheet and moved ~0.7 mi (1.2 km) south–southeast from a depression or inset in the basalt to the north–northeast, the same direction as the elongate ice flow indicators are aligned. We will more closely examine this possible form of glacial transport of large masses of rock at the Pot Hills, Stop 3.

The meltwater hypothesis (Shaw and others, 1999; Lesemann and Brennand, 2009) has the drumlins, flutings, and MSGL of the Waterville Plateau formed by turbulent flow of a catastrophic sheet flood that lifted the Okanogan Lobe while it passed and then let the glacier back down once it drained. South of the Withrow Moraine, the Waterville Plateau is mantled by loess. The only channel eroded by megaflooding south of the Withrow Moraine is Moses Coulee, 9 mi (15 km) southeast of here. However, the drumlins, flutings, and MSGL on the Waterville Plateau fan out to near the terminal Withrow Moraine.

A stream valley follows the southeastern margin of the Okanogan Lobe along the Waterville Plateau from near McNeil Canyon to Moses Coulee. The creek in the lower valley, Dutch Henry Creek, spills over Dutch Henry Falls down the side of Moses Coulee. The valley is small, shallow, meandering, and does not fit the form of a flood-eroded coulee of the Channeled Scabland. The valley follows the crease where the margin of the south-sloping Withrow Moraine meets the loess-covered, northward-sloping Waterville Plateau. The valley was formed by meltwater coming off the terminus of the Okanogan Lobe, with less flow and modification of the valley occurring during interglacial time. It contrasts with megaflood-eroded coulees of the Channeled Scablands and was clearly not a megaflood channel. There are no coulees that could have been meltwater channels from the terminal moraine to Moses Coulee, which seems to rule out the possibility that the drumlins, flutes, and MSGL on the Waterville Plateau could have been formed by catastrophic subglacial meltwater floods.

Moses Coulee has been proposed as an outlet formed by subglacial megafloods, or one such flood, from the Okanogan Lobe (Shaw and others, 1999; Lesemann and Brennand, 2009). The Withrow Moraine crosses the coulee floor, showing that the ice reached its maximum advance after Moses Coulee had formed. The origin of Moses Coulee by megafloods from Glacial Lake Missoula, which is the most commonly proposed model for how it formed, is considered questionable due to the lack of deep coulees channeling into the head of Moses Coulee from the Columbia River Valley, from which the floods would have entered Moses Coulee if Grand Coulee did not yet exist or was blocked. This is discussed by Hanson (1970) and by Waitt and others (2021), who propose scenarios accounting for the origin of Moses Coulee by floods from Glacial Lake Missoula via the Columbia River Valley. The subglacial meltwater megaflood alternative for the origin of Moses Coulee has, in my view, a more insurmountable problem accounting for the lack of obvious channels for the floods to get to the coulee.

Return to State Route 172 and proceed east towards Mansfield. In 1.5 mi the Mansfield Sportsman Club is on the north side of the highway. At 0.1 mi east of the Sportsman Club, park on the right shoulder and get out to examine the surfaces of bedrock exposed in the shoulder of the road.

STOP 2:
Glacial striations on a surface of polished bedrock
+47.8156, -119.6500

This stop is to look at possible glacial polish and striations on a smoothed surface of Columbia River Basalt along the side of the road. The striations are oriented approximately north–south. There may not be any clear unidirectional indicator of ice-flow direction on this surface, but drumlins and MSGL in the area are oriented in the same north–south direction as the striations and presumably record the ice base of the ice sheet moving south along its base. There is another set of lineations on the outcrop surface, of unknown origin, at right angles to the first.

Glacial polish and striations demonstrate that the base of the glacier was in direct contact with the substrate as the ice moved. That the striations here, and as reported in many parts of the Okanogan Lobe landscape elsewhere, are generally aligned with larger, elongate, streamlined subglacial landforms, particularly drumlins and MSGL, supports the possibility that the larger landforms may also have been formed by erosional and depositional processes in contact with the base of the glacier. The meltwater hypothesis counterargument is that the ice sheet returned to contact with its bed after the meltwater flood had drained, with the glacier then ornamenting and modifying the fluvially created bedforms.

Glacial striations are commonly best preserved where they have been beneath a veneer of regolith (personal observations), which may be the case here. It may be the case that many striations on surfaces exposed since deglaciation have weathered away.

Continue east on State Route 172 through Mansfield. Approximately 8.5 mi east of Stop 2, take a left (go north) on M Rd. NE. Within 200 ft veer right onto an unimproved road that loops around the Pot Hills. Follow the road about 1.75 mi around the north side of Pot Hills and park on the northeast side by the road, by where you can see signs of footpaths going up Pot Hills.

STOP 3:
The Pot Hills
+47.8184, -119.4536

The Pot Hills are made of Columbia River Basalt. Although the basalt is fractured, the hills may consist of a semi-coherent basalt flow, or sequence of basalt flows, that fractured and deformed during glacial transport of the entire mass. The same origin has been proposed for Burke Hill, by Stop 1, and Lone Butte, which we drove around the south end of on Highway 172 west of Mansfield (Waitt and others, 1994). Seen in satellite view in Google Maps and Google Earth, the Pot Hills consist of slightly curved ridges that are nearly transverse to the northwest–southeast outline of the hills. Drumlins and flutes (shallow linear depression) northwest of the Pot Hills track toward a possible source-area depression 2 mi (3 km) to the northwest. In a larger context, this part of the Waterville Plateau is identified as a zone of MSGL in Eyles and others (2018).

If Pot Hills is a partly disaggregated block of basalt that was moved *en masse* at the base of the glacier, it illustrates the power of the glacial ice flow to which the bed of the glacier in this area was subjected. Columbia River Basalt has sedimentary interbeds of sand, silt, and mud between some flows. A sedimentary interbed could have been saturated with water and ice during glaciation and become a surface of failure that enabled the glacier to pluck an extremely massive body of rock.

If time does not allow walking up onto the Pot Hills, check out the landscape from road level and examine the boulders moved to the side of the road during roadbuilding. How many are not basalt? What types of rock are they? Are they more rounded than the basalt erratics? (And do the basalt boulders count as erratics if basalt is the underlying bedrock?)

Continue along the Pot Hills road and reenter State Route 172, eastbound. The drive to Stop 4 totals about 72 mi. In 4.2 mi from the Pot Hills, turn left (north) on State Route 17. Proceed through Bridgeport and on to the end of Route 17 where it meets Highway 97. Go north on Highway 97 for 26 mi and get off at the first Omak Exit onto Dayton Street. In 0.3 mi turn right (east) onto State Route 155, following the signs for Grand Coulee Dam. In 4.1 mi turn right (south) onto North End Omak Lake Road. In 5.3 mi, at the Mission Creek Boat Launch, park on the right (west) side of the parking lot.

Once we are driving along the Okanogan River on Highway 97 on the way to Stop 4, we will be in a zone of tunnel valleys and what are probably a complex of glacial kame terraces. In the lower Okanogan River valley and downstream from there in the Columbia River Valley, on the west and north sides of the valleys, is the Great Terrace. We will drive past it and other terraces visible in the lower Okanogan River area. Higher up in tributary valleys, out of sight from the bottom of the valley for the most part, are smaller terraces, consistent with a sequence of glacial retreat down the sides of the valleys to a remnant glacial body in the south and east sides of the main valley.

Similarly, along with the Okanogan River valley itself qualifying as an overdeepened or tunnel valley in the meltwater hypothesis, there are a large number of tunnel valleys cutting across ridges and connecting what appear to be previously separate drainages in the Okanogan Highlands on either side of the main river valley. Once we enter North End Omak Lake road nearing Stop 4, we will be in a tunnel valley that is tributary to the larger Omak Lake basin. Landforms eroded into bedrock along the sides of the valley are of interest as a possible indicator of how the valley was eroded.

STOP 4:
Omak Creek–Omak Lake tunnel valley
+48.3221, -119.4324

The Mission Beach Boat Launch is at the north end of Omak Lake, which is in an overdeepened basin identified as a tunnel valley (Shaw and others, 1999; Lesemann and Brennand, 2009). Omak Creek valley, which we are at the south end of here, runs 5 mi (7 km) north to its junction with Mission Creek. It is one of two subparallel valleys that converge into the north end of Omak Lake.

Omak Lake basin bedrock is plutonic and metamorphic. The rock here is mapped as Mission Creek Granodiorite (Eocene or Cretaceous) of the Okanogan Metamorphic Core Complex (Goodge and Hansen, 1994). Erosional landforms in the bedrock along the sides of Omak Creek valley are similar to those in the rest of the Omak Lake basin. Many of the erosional forms are elongated in the likely direction of ice flow and include possible roche moutonnées, steepest at their southern ends, and whalebacks. Other parts of the rock walls on either side of the valley, not so protruding and elongate, tend to have smoothed surfaces facing northward ending at steep slopes facing southward, consistent with glacial abrasion on the smoothed surfaces and glacial plucking on the steep, down-flow sides.

An outcrop by the shore on the west side of the parking lot has a streamlined form and a glacially polished and striated surface. The striations are oriented south–southeast.

The Omak Lake basin was in a zone of converging glacial ice flow, according to the topography and the possible ice flow direction indicators. The valley may have been a pre-Wisconsin portion of the the Columbia River Valley, the river having been pushed to the north here by the northernmost flows of Miocene-age Columbia River Basalt, which cover the Omak Plateau west of Lake Omak (Flint, 1935; discussed in the Tunnel Valleys section above). The Omak Lake Basin is centered along the crustal-scale (Potter and others, 1986) detachment fault that borders the west side of the Okanogan Metamorphic Core Complex (Goodge and Hansen, 1994). The meltwater hypothesis suggests the Omak Lake basin is a tunnel valley that was eroded by one or more subglacial turbulent floods, with glacial features such as striations formed afterward once the glacier had recontacted its bed. The probable long history of the valley, including the detachment fault zone creating a zone of rock less resistant to erosion, the Columbia River likely eroding the valley between the Miocene and sometime in the Pleistocene, the likelihood that ice flow was channeled from the Okanogan Valley and other topographic lows east of the Okanogan Valley into the Omak Lake basin, and the evidence of glacially eroded landforms along the length of the valley, suggest that the origin of the valley is more complex than erosion by subglacial meltwater flooding and that glacial erosion contributed substantially to its form, including the erosion of the overdeepened basin occupied by Omak Lake.

The ridge east of Omak Creek valley, between Omak Lake on its south side and French Valley (along Highway 155) on its north side, is cut by numerous slot valleys. The largest is Deep Valley, 4 km long, 0.3–0.5 km wide. It is ridge-crossing and has a longitudinal profile that is concave-up with undulations and adverse slopes. Its form qualifies it as a tunnel valley analogous to Wildhorse Canyon at Squally Point, British Columbia and Soap Lake valley on the west side of the Omak Plateau. It follows the main joint system in the bedrock mapped by Goodge and Hansen (1994). Relatively small tunnel valleys of the Deep Canyon and Wildhorse Canyon type may have been at least partly eroded by water beneath the ice sheet. However, some of them have glacially striated bedrock surfaces and what are likely glacially eroded forms consistent with abrasion and plucking by moving glacial ice. Again, a polygenetic origin is suggested, including erosion over more than one glaciation and possibly both glacial and glaciofluvial erosion. Unlike the large, lake-filled, overdeepened basins such as Omak Lake, there would not have been a stream along the ones like Deep Canyon between glaciations, given their convex-upward profiles, and they are not at the convergence of broad zones of ice flow the way the larger, overdeepened basins are.

Along the east side of the Okanogan Valley, where bedrock is predominantly gneissic and granitic, valleys like Deep Valley commonly cut through uplands or across ridges that are transverse to the ice flow direction indicated by elongate landforms and striations. On a much smaller scale, linear slot valleys cut across high parts of the ridges, including the ridge east of Stop 4. (The valleys are not visible from Stop 4.) The small slot valleys are commonly parallel to the jointing of the bedrock, are parallel to moderately oblique to the likely ice flow direction, and commonly have concave-up longitudinal profiles.

The meltwater hypothesis suggests that the slot valleys were tunnel valleys formed by water forced over the ridges beneath the ice sheet. The presence of striations and other signs of glacial erosion in some of these valleys (personal observations) suggests a role for glacial erosion in forming them. In some of them, small kame terraces, which would have formed alongside remnant glacial ice, suggest the presence of glacial ice in the valleys after they had finished forming. The likelihood that the valleys were formed over multiple glaciations adds to the complexity of their origin.

Return 5.3 mi to State Route 155 and turn left (west) onto 155. In 3.1 mi take a left (turn south) *on Columbia River Road/Omak Lake Road. In about 0.4 mi park at a wide gravel area on the right (west) side of the road. The outcrop we will be looking at is on the other side of the road.*

STOP 5:
Glacial drift exposed inside of terrace in East Omak
+48.3970, -119.5052

Be careful of traffic on the road, and of rocks falling from the slopes, and of you slipping from a slope while looking at these roadcuts across the road from the East Omak sawmill (currently closed). A half mile south of here at the intersection of Columbia River Road (also called Omak Lake Road) and Moomaw Road, Minard (1985) mapped a three-part sequence of advance outwash, glacial till, and retreat outwash associated with the Fraser (Vashon) glaciation (latest Wisconsin). However, outcrops are poor up-valley from these roadcuts, so we will examine the stratigraphy visible here.

The roadcut is on the side of a terrace interpreted as a kame terrace that formed alongside a mass of glacial ice that remained in the Okanogan Valley during glacial retreat (Russell, 1898; Waters, 1933; Flint, 1935; Pine, 1985; Minard, 1985). The terrace here tops out at about 365 m asl. The more extensive Omak Flats terrace across the Okanogan River, on which Omak Airport is located, is 360–400 m asl and probably formed at the same time. There are narrower terraces at higher elevations on the sides of the Okanogan River valley and on the sides of tributary valleys. Inset into the sides of the broad, ~360–400 m asl terrace are much narrower, more discontinuous terraces at elevations 310–355 m asl.

This terrace and Omak Flats are part of the Great Terrace (Russell, 1898), which extends south along the Okanogan and Columbia River Valleys ~60 mi to Chelan Falls near the terminus of the Okanogan Lobe. It may be that the Great Terrace is contiguous from there with a tapering outwash plain surface preserved in patches alongside the Columbia River to Wenatchee, another 25 mi (Waitt, 2016). The sequence of terraces alongside the main valley is consistent with retreat of the ice sheet into the bottom of the Okanogan Valley, with pauses along the way forming side-valley kame terraces, a longer interval of melting of a large ice mass or set of ice masses in the middle of the valley, and a few more retreat-and-pause steps recorded by the lowest, smallest terraces. Kettles occur on the terraces. Sedimentology and sedimentary structures suggest they are composed largely of glacial drift including till, outwash, and lacustrine beds, along with disturbed and cross-cutting features suggesting ice contact and melting of ice blocks, and alluvial fans and deltas from side-streams interfingering with and built onto the terraces (Waters, 1933; Flint, 1935; Pine, 1985; Minard, 1985).

Lesemann and Brennand (2009) suggest that this large system of terraces in the lower Okanogan Valley could contain a large volume sediment deposited by subglacial meltwater megaflooding. This seems unlikely, given that the terraces match the form and structure of kame terraces and have no evidence of being megaflood deposits in the style of giant gravel bars as in the Channeled Scablands, which have long down-valley foreset bed sequences and gravel dunes (giant current ripples) on their surfaces.

End of field trip. Return to Route 155 and turn left (west). After 1 mi turn left on Dayton St. In 1 mi, at the stoplight, turn right onto Highway 97. Follow Highway 97 south to Cashmere.

REFERENCES

Alley, R.B., Lawson, D.E., Evenson, E.B., Larson, G.J., and Baker, G.S., 2003, Stabilizing feedbacks in glacier bed erosion: Nature, v. 424, p. 758–760.

Alley, R.B., Cuffey, K.M., and Zoet, L.K., 2019, Glacial erosion: Status and outlook: Annals of Glaciology v. 60, no. 80, p. 1–13.

Anfinson, O.A., Gaylord, D.R., Pope, M.C., and Cabbage, P.R., 2009, Detrital zircon geochronology applied to Late Quaternary megaflood deposits from the Channeled Scabland, WA: GSA Annual Meeting, Portland, Oregon, Geological Society of America Abstracts with Programs. v. 41, no. 7, p. 169.

Arnold, H., and Ferbey, T., 2020, Ice-flow indicator database, British Columbia and Yukon: British Columbia Ministry of Energy and Mines and Petroleum Resources, British Columbia Geological Survey Open File Report 2020-03.

Atwater, B.F., 1986, Pleistocene glacial lake deposits of the Sanpoil River Valley, northeastern Washington: U.S. Geological Survey Bulletin 1661.

Atwater, B.F., 1987, Status of glacial Lake Columbia during the last floods from glacial Lake Missoula: Quaternary Research, v. 27, p. 182–201.

Baker, V.R., 1973, Paleohydrology and sedimentology of Lake Missoula flooding in eastern Washington: Geological Society of America special papers, v. 144.

Baker, V.R., 1978, Paleohydraulics and hydrodynamics of scabland floods, *in* Baker, V.R., and Nummedal, D., eds., The Channeled Scabland: A guide to the geomorphology of the Columbia Basin, Washington: NASA, Proceedings of Comparative Planetary Geology Field Conference, p. 59–80.

Baker, V.R., 2009, Channeled scabland morphology, *in* Burr, D.M., Carling, P.A., and Baker, V.R., eds., Megaflooding on Earth and Mars: Cambridge University Press, p. 65–77.

Baker, V.R., 2020, Global megaflood paleohydrology, *in* Herget, J., and Fontana, A., eds., Palaeohydrology: Cham, Switzerland, Springer, p. 3–28.

Baker, V.R., and Milton, D.J., 1974, Erosion by catastrophic floods on Mars and Earth: Icarus, v. 23, p. 27–41.

Baker, V.R., and Pickup, G., 1987, Flood geomorphology of the Katherine Gorge, northern territory, Australia: Geological Society of America Bulletin, v. 98, no. 6, p. 635–646.

Baker, V.R., Bjornstad, B.N., Gaylord, D.R., Smith, G.A., Meyer, S.E., Alho, P., Breckenridge, R.M., Sweeney, M.R., and Zreda, M., 2016, Pleistocene megaflood landscapes of the Channeled Scabland, *in* Lewis, R.S., and Schmidt, K.L., eds., Exploring the geology of the Inland Northwest: Geological Society of America Field Guide, v. 41, p. 1–73.

Balbas, A.M., Barth, A.M., Clark, P.U., Clark, J., Caffee, M., O'Connor, J., Baker, V.R., Konrad, K., and Bjornstad, B., 2017, ^{10}Be dating of late Pleistocene megafloods and Cordilleran Ice Sheet retreat in the northwestern United States: Geology, v. 45, p. 583–586.

Barendregt, R.W., Layer, P.W., Huscroft, C.A., and Benowitz, J., 1995, An Early Pleistocene till, Okanagan Valley, British Columbia, Canada: Canadian Journal of Earth Sciences, v. 32, p. 2046–2056.

Brennand, T.A., Lian, O.B., and Perkins, A.J., 2014, The life and times of the Cordilleran Ice Sheet around the southern Fraser Plateau, British Columbia, *in* Trials and tribulations of life on an active subduction zone: Field trips in and around Vancouver, Canada: Geological Society of America Field Guide, New York, p. 101–124.

Bretz, J.H., 1923, The Channeled Scablands of the Columbia Plateau: The Journal of Geology, v. 31, p. 617–649.

Bretz, J.H., Smith, H.U., and Neff, G.E., 1956, Channeled Scabland of Washington: New data and interpretations: Geological Society of America Bulletin, v. 67, p. 957–1049.

Burke, M.J., Brennand, T.A., and Perkins, A.J., 2012a, Evolution of the subglacial hydrologic system beneath the rapidly decaying Cordilleran Ice Sheet caused by ice-dammed lake drainage: Implications for meltwater-induced ice acceleration: Quaternary Science Reviews, v. 50, p. 125–140.

Burke, M.J., Brennand, T.A., and Perkins, A.J., 2012b, Transient subglacial hydrology of a thin ice sheet: Insights from the Chasm esker, British Columbia, Canada: Quaternary Science Reviews, v. 58, p. 30–55.

Clague, J.J., 1989, Cordilleran Ice Sheet, *in* Fulton, R.J., ed., Quaternary geology of Canada and Greenland: Geological Survey of Canada, Geology of Canada, no. 1 (also Geological Society of America, The Geology of North America, v. K-1), v. 1, p. 40–42.

Clague, J.J., and Ward, B., 2011, Pleistocene glaciation of British Columbia, *in* Ehlers, J., Gibbard, P.L., and Hughes, P.D., eds., Quaternary glaciations-extent and chronology: A closer look: Developments in Quaternary Science: Elsevier, v. 15, ch. 44, p. 563–573.

Clague, J.J., Mathewes, R.W., and Ager, T.A., 1994, Environments of northwestern North America before the Last Glacial Maximum, *in* Madsen, D.B., ed., Entering America: Northeast Asia and Beringia before the Last Glacial Maximum: University of Utah Press, p. 63–96.

Clague, J.J., Roberts, N.J., Miller, B., Menounos, B., and Goehring, B., 2021, A huge flood in the Fraser River valley, British Columbia, near the Pleistocene Termination: Geomorphology, v. 374, p. 107473.

Clark, C.D., 1993, Mega-scale glacial lineations and cross-cutting ice-flow landforms: Earth surface processes and landforms, v. 18, p. 1–29.

Clarke, G.K.C., Mathews, W.H., and Pack, R.T., 1984, Outburst floods from glacial Lake Missoula: Quaternary Research, v. 22, p. 289–299.

Cooley, S., 2022, Giant current ripples at Omak, WA: North End Workbench blog entry, available at https://www.skyecooley.com/ [Accessed May 24, 2022].

Dahl, R., 1965, Plastically sculptured detail forms on rock surfaces in northern Nordland, Norway: Geografiska Annaler: Series A, Physical Geography, v. 47, p. 83–140.

Denlinger, R.P., George, D.L., Cannon, C.M., O'Connor, J.E., and Waitt, R.B., 2021, Diverse cataclysmic floods from Pleistocene glacial Lake Missoula: Untangling the Quaternary period—A legacy of Stephen C. Porter: Geological Society of America Special Paper 548.

Dulfer, H.E., and Margold, M., 2021, Glacial geomorphology of the central sector of the Cordilleran Ice Sheet, Northern British Columbia, Canada: Journal of Maps, v. 17, p. 413–427.

Erdmer, P., and Cui, Y., 2009, Geological map of British Columbia: British Columbia Ministry of Energy, Mines and Petroleum Resources, Geoscience Map 2009-1, scale 1:500,000.

Eyles, N., and Clague, J., 1991, Glaciolacustrine sedimentation during advance and retreat of the Cordilleran Ice Sheet in central British Colombia: Géographie physique et Quaternaire, v. 45, p. 317–331.

Eyles, N., Mullins, H.T., and Hine, A.C., 1990, Thick and fast: Sedimentation in a Pleistocene fjord lake of British Columbia, Canada: Geology, v. 18, p. 1153–1157.

Eyles, N., Mullins, H.T., and Hine, A.C., 1991, The seismic stratigraphy of Okanagan lake: A record of rapid deglaciation in a deep 'fjord lake' basin: Sedimentary Geology, v. 73, p. 13–41.

Eyles, N., Moreno, L.A., and Sookhan, S., 2018, Ice streams of the late Wisconsin Cordilleran ice sheet in western North America: Quaternary Science Reviews, v. 179, p. 87–122.

Ferbey, T., 2013, Regional to property-scale drift prospecting surveys in British Columbia: British Columbia Ministry of Energy, Mines, and Natural Gas, Victoria, BC, Open-File 2013-02, scale 1:5,000,000.

Ferbey, T., Arnold, H., and Hickin, A.S., 2016, Ice-flow indicator compilation, British Columbia: Open-File 2013-06, Ministry of Energy, Mines and Natural Gas, British Columbia Geological Survey, Victoria, BC, scale 1:1,650,000.

Flint, R.F., 1935, Glacial features of the southern Okanogan region: Bulletin of the Geological Society of America, v. 46, p. 169–194.

Fulton, R.J., 1976, Surficial geology, Kamloops Lake west of Sixth Meridian, British Columbia: Geological Survey of Canada, Map 1394A.

Fulton, R.J, 1991, A conceptual model for growth and decay of the Cordilleran Ice Sheet: Géographie physique et Quaternaire, v. 45, p. 281–286.

Gaylord, D.R., Pope, M.C., Cabbage, P.R., Glover III, J.F., Anfinson, O.A., Baar, E.E., and Vervoort, J.D., 2007, Provenance of glacial outburst flood deposits in the Channeled Scabland, WA: Influence of glacial Lake Missoula, meltwater, Snake River, and Bonneville flood sources: Geological Society of America Abstracts with Programs, v. 39, p. 82.

Gombiner, J.H., Hemming, S.R., Hendy, I.L., Bryce, J.G., and Blichert-Toft, J., 2016, Isotopic and elemental evidence for Scabland Flood sediments offshore Vancouver Island: Quaternary Science Reviews, v. 139, p. 129–137.

Goodge, J.W., and Hansen, V.L., 1994, Geologic map of the Omak Lake 15' quadrangle, Okanogan County, Washington, no. 1726.

Gulick, 1990, Geologic map of the Omak 1:100,000 quadrangle, Washington Open-File Report 90-12, U.S. Geological Survey.

Hanson, L.G., 1970, The origin and development of Moses Coulee and other scabland features on the

Waterville Plateau, Washington: Ph.D. Dissertation, University of Washington, 139 p.

Hanson, M.A., and Clague, J.J., 2016, Record of glacial lake Missoula floods in glacial lake Columbia, Washington: Quaternary Science Reviews, v. 133, p. 62–76.

Hanson, M.A., Enkin, R.J., Barendregt, R.W., and Clague, J.J., 2015, Provenance and deposition of glacial Lake Missoula lacustrine and flood sediments determined from rock magnetic properties: Quaternary Research, v. 83, p. 166–177.

Hendy, I., 2009, A fresh perspective on the Cordilleran Ice Sheet: Geology, v. 37, p. 95–96.

Hooke, R., 1991, Positive feedbacks associated with erosion of glacial cirques and overdeepenings: Geological Society of America Bulletin, v. 103, p. 1104–1108.

Kehew, A.E., Piotrowski, J.A., and Jørgensen, F., 2012, Tunnel valleys: Concepts and controversies—A review: Earth-Science Reviews, v. 113, p. 33–58.

Kendra, W., and Singleton, L.R., 1987, Morphometry of Lake Chelan: Water Quality Investigations Section, Washington State Department of Ecology., Ecology Report 87-1, 33 p.

King, E.C., Hindmarsh, R.C., and Stokes, C.R., 2009, Formation of mega-scale glacial lineations observed beneath a West Antarctic ice stream: Nature Geoscience, v. 2, p. 585–588.

Komatsu, G., Miyamoto, H., Ito, K., Tosaka, H., and Tokunaga, T., 2000, The Channeled Scabland: Back to Bretz?, Comment and Reply: Geology, v. 28, p. 573–574.

Kor, P.S.G., Shaw, J., and Sharpe, D.R., 1991, Erosion of bedrock by subglacial meltwater, Georgian Bay, Ontario: A regional view: Canadian Journal of Earth Sciences, v. 28, p. 623–642.

Krabbendam, M., and Glasser, N.F., 2011, Glacial erosion and bedrock properties in NW Scotland: Abrasion and plucking, hardness and joint spacing: Geomorphology, v. 130, p. 374–383.

Krabbendam, M., Eyles, N., Putkinen, N., Bradwell, T., and Arbelaez-Moreno, L., 2016, Streamlined hard beds formed by palaeo-ice streams: A review: Sedimentary Geology, v. 338, p. 24–50.

Kuehn, S.C., Froese, D.G., Carrara, P.E., Foit, F.F., Pearce, N.J., and Rotheisler, P., 2009, Major- and trace-element characterization, expanded distribution, and a new chronology for the latest Pleistocene Glacier Peak tephras in western North America: Quaternary Research, v. 71, p. 201–216.

Lesemann, J.E., and Brennand, T.A., 2009, Regional reconstruction of subglacial hydrology and glaciodynamic behaviour along the southern margin of the Cordilleran Ice Sheet in British Columbia, Canada and northern Washington State, USA: Quaternary Science Reviews, v. 28, p. 2420–2444.

Livingstone, S.J., Clark, C.D., and Tarasov, L., 2013, Modelling North American palaeo-subglacial lakes and their meltwater drainage pathways: Earth and Planetary Science Letters, v. 375, p. 13–33.

Lopes, C., and Mix, A.C., 2009, Pleistocene megafloods in the northeast Pacific: Geology, v. 37, p. 79–82.

Margold, M., Stokes, C.R., and Clark, C.D., 2015, Ice streams in the Laurentide Ice Sheet: Identification, characteristics and comparison to modern ice sheets: Earth-Science Reviews, v. 143, p. 117–146.

Matzel, J.E., Bowring, S.A., and Miller, R.B., 2004, Protolith age of the Swakane Gneiss, North Cascades, Washington: Evidence of rapid underthrusting of sediments beneath an arc. Tectonics, v. 23, TC6009.

McClenagan, J.D., 2013, Streamlined erosional residuals and drumlins in central British Columbia, Canada: Geomorphology, v. 189, p. 41–54.

Menounos, B., Goehring, B.M., Osborn, G., Margold, M., Ward, B., Bond, J., Clarke, G.K., Clague, J.J., Lakeman, T., Koch, J., and Caffee, M.W., 2017, Cordilleran Ice Sheet mass loss preceded climate reversals near the Pleistocene Termination: Science, v. 358, p. 781–784.

Minard, J.P., 1985, Geologic map of Quaternary deposits of the Pothole Quadrangle, Okanogan County, Washington: Miscellaneous Field Studies Map 1680, U.S. Geological Survey.

Miyamoto, H., Komatsu, G., Baker, V.R., Dohm, J.M., Ito, K., and Tosaka, H., 2007, Cataclysmic scabland flooding: Insights from a simple depth-averaged numerical model: Environmental Modelling & Software, v. 22, no. 10, p. 1400–1408.

Nasmith, H., 1962, Late glacial history and surficial deposits of the Okanagan Valley, British Columbia: Bulletin 46, British Columbia Ministry of Energy, Mines, and Petroleum Resources.

Nichol, C., Monahan, P., Fulton, R., Ping, J., Wei, X., and Thomson, S., 2015, Quaternary stratigraphy and evidence for multiple glacial episodes in the north Okanagan Valley, British Columbia: Canadian Journal of Earth Sciences, v. 52, p. 338–356.

Ó Cofaigh, C., 1996, Tunnel valley genesis: Progress in Physical Geography, v. 20, p. 1–19.

O'Connor, J.E., Baker, V.R., Waitt, R.B., Smith, L.N., Cannon, C.M., George, D.L., and Denlinger, R.P., 2020, The Missoula and Bonneville floods—A review of ice-age megafloods in the Columbia River basin: Earth-Science Reviews, v. 208, p. 103–181.

Okulitch, A.V., 2013, Geology, Okanagan Watershed, British Columbia: Geological Survey of Canada, Open File 6839, 3 sheets.

Pardee, J.T., 1942, Unusual currents in glacial lake Missoula, Montana: Bulletin of the Geological Society of America, v. 53, p. 1569–1600.

Pine, K.A., 1985, Glacial geology of the Tonasket–Spectacle lake area, Okanogan County, Washington: Master's thesis, Western Washington University, Bellingham, Washington.

Porter, S.C., 1978, Glacier Peak tephra in the North Cascade Range, Washington: Stratigraphy, distribution, and relationship to late-glacial events: Quaternary Research, v. 10, p. 30–41.

Potter, C.J., Sanford, W.E., Yoos, T.R., Prussen, E.I., Keach, R.W., Oliver, J.E., Kaufman, S., and Brown, L.D., 1986, COCORP deep seismic reflection traverse of the interior of the North American Cordillera, Washington and Idaho: Implications for orogenic evolution: Tectonics, v. 5, p. 1007–1025.

Prest, V.K., Grant, D.R., and Rampton, V.N., 1968, Glacial map of Canada: Geological Survey of Canada, Map 1253A.

Prytulak, J., Vervoort, J.D., Plank, T., and Yu, C., 2006, Astoria Fan sediments, DSDP site 174, Cascadia Basin: Hf–Nd–Pb constraints on provenance and outburst flooding: Chemical Geology, v. 233, p. 276–292.

Roed, M.A., 2011, Geologic history, *in* Roed, M.A., and Fulton, R.J., eds., Okanagan Geology South: Geologic highlights of the South Okanagan, British Columbia: Okanagan Geology Committee, Sandhill Book Marketing, Ltd., Kelowna, BC, p. 41–67.

Roed, M.A., Barendregt, R.W., Benowitz, J.A., Smith, C.A.S., Sanborn, P.T., Greenough, J.D., Huscroft, C., Layer, P.W., Mathewes, R.W., and Tessler, D., 2014, Evidence for an Early Pleistocene glaciation in the Okanagan Valley, southern British Columbia: Canadian Journal of Earth Sciences, v. 51, p. 125–141.

Rudoy, A.N., and Baker, V.R., 1993, Sedimentary effects of cataclysmic late Pleistocene glacial outburst flooding, Altay Mountains, Siberia: Sedimentary Geology, v. 85, p. 53–62.

Russell, I.C., 1898, The great terrace of the Columbia and other topographic features in the neighborhood of Lake Chelan, Washington: American Geologist, v. 22, p. 362–369.

Ryder, J., Fulton, R., and Clague, J., 1991, The Cordilleran ice sheet and the glacial geomorphology of southern and central British Colombia: Géographie physique et Quaternaire, v. 45, p. 365–377.

Sauer, K.B., Gordon, S.M., Miller, R.B., Vervoort, J.D., and Fisher, C.M., 2017, Transfer of metasupracrustal rocks to midcrustal depths in the North Cascades continental magmatic arc, Skagit Gneiss Complex, Washington: Tectonics, v. 36, no. 12, p. 3254–3276.

Seguinot, J., Rogozhina, I., Stroeven, A.P., Margold, M., and Kleman, J., 2016, Numerical simulations of the Cordilleran ice sheet through the last glacial cycle: The Cryosphere, v. 10, p. 639–664.

Shaw, J., 1988, Subglacial erosional marks, Wilton Creek, Ontario: Canadian Journal of Earth Sciences, v. 25, p. 1256–1267.

Shaw, J., 1994, Hairpin erosional marks, horseshoe vortices and subglacial erosion: Sedimentary Geology, v. 91, p. 269–283.

Shaw, J., 2002, The meltwater hypothesis for subglacial bedforms: Quaternary International, v. 90, p. 5–22.

Shaw, J., and Kvill, D., 1984, A glaciofluvial origin for drumlins of the Livingstone Lake area, Saskatchewan: Canadian Journal of Earth Sciences, v. 21, p. 1442–1459.

Shaw, J., and Sharpe, D.R., 1987, Drumlin formation by subglacial meltwater erosion: Canadian Journal of Earth Sciences, v. 24, p. 2316–2322.

Shaw, J., Munro-Stasiuk, M., Sawyer, B., Beaney, C., Lesemann, J.E., Musacchio, A., Rains, B., and Young, R.R., 1999, The channeled scabland: Back to Bretz?: Geology, v. 27, p. 605–608.

Shaw, J., Gilbert, R.G., Sharpe, D.R., Lesemann, J.E., and Young, R.R., 2020, The origins of s-forms: Form similarity, process analogy, and links to high-energy, subglacial meltwater flows: Earth-Science Reviews, v. 200, p. 102994.

Sookhan, S., Eyles, N., Bukhari, S., and Paulen, R.C., 2021, LiDAR-based quantitative assessment of drumlin to mega-scale glacial lineation continuums and flow of the paleo Seneca-Cayuga paleo-ice stream: Quaternary Science Reviews, v. 263, p. 107003.

Souch, C., 1989, New radiocarbon dates for early déglaciation from the southeastern Coast Mountains of British Columbia: Canadian Journal of Earth Sciences, v. 26, p. 2169–2171.

Spagnolo, M., Clark, C.D., Ely, J.C., Stokes, C.R., Anderson, J.B., Andreassen, K., Graham, A.G., and King, E.C., 2014, Size, shape and spatial arrangement of mega-scale glacial lineations from a large and diverse dataset: Earth Surface Processes and Landforms, v. 39, p. 1432–1448.

Stoffel, K.L., Joseph, N.L., Waggoner, S.Z., Gulick, C.W., Korosec, M.A., and Bunning, B.B., 1991, Geologic map of Washington, northeast quadrant: Washington Division of Geology and Earth Resources, Geologic Map 39.

Stokes, C.R., and Clark, C.D., 2002, Are long subglacial bedforms indicative of fast ice flow?: Boreas, v. 31. p. 239–249.

Stumpf, A.J., Ferbey, T., Plouffe, A., Clague, J.J., Ward, B.C., Paulen, R.C., and Bush, A.B., 2014, comment on: “Streamlined erosional residuals and drumlins in central British Columbia, Canada” by McClenagan, J.D., 2013, Geomorphology v. 189, p. 41–54, *in* Geomorphology, v. 209, p. 147–150.

van der Vegt, P., Janszen, A., and Moscariello, A., 2012, Tunnel valleys: Current knowledge and future perspectives: Geological Society, London, Special Publications, v. 368, p. 75–97.

Waitt, R.B., 2016, Megafloods and Clovis cache at Wenatchee, Washington: Quaternary Research, v. 85, p. 430–444.

Waitt, R.B. Jr., and Thorson, R.M., 1979, The Cordilleran ice sheet in Washington, Idaho, and Montana, *in* Wright, H., and Porter, S.C., eds., Late-Quaternary environments of the United States, v. 1, p. 53–70.

Waitt, R.B., O’Conner, J.E., and Benito, G., 1994, Scores of gigantic, successively smaller Lake Missoula floods through Channeled Scabland and Columbia Valley, *in* Swanson, D.A., and Haugerud, R.A., eds., Geologic field trips in the Pacific Northwest, Geological Society of America Annual Meeting, Seattle, p. 1K-1–1K-87.

Waitt, R.B., Atwater, B.F., Lehnigk, K., Larsen, I.J., Bjornstad, B.N., Hanson, M.A., and O’Connor, J.E., 2021, Upper Grand Coulee: New views of a channeled scabland megafloods enigma, *in* Booth, A.M., and Grunder, A.L., eds., From Terranes to terrains: Geologic field guides on the construction and destruction of the Pacific Northwest: Geological Society of America Field Guide v. 62, p. 245–300.

Washington State Lidar Portal, https://lidarportal.dnr.wa.gov/#48.44733:-119.48189:17 [Accessed May 24, 2022].

Waters, A.C., 1933, Terraces and coulees along the Columbia River near lake Chelan, Washington: Bulletin of the Geological Society of America, v. 44, p. 783–820.

Whetten, J.T., 1967, Lake Chelan, Washington: Bottom and sub-bottom topography: Limnology and Oceanography, v. 12, p. 253–259.

WENATCHEE, WASHINGTON AREA MINERALIZATION, IN CONTEXT: UNTANGLING THE CENOZOIC STRUCTURAL STORY

Kelsay M. Stanton

Washington Geological Survey, Olympia, Washington

The sedimentary Eocene Chumstick Formation shows hydrothermal alteration that hosts mineralization for historical gold mining in the Wenatchee, Washington area (figs. 1, 2; Patton and Cheney, 1971; Margolis, 1989; Ott and others, 1986). In addition to small-scale prospecting since the late 1800s, several larger mines produced over 1 million oz Au and over 2 million oz Ag, with the Cannon mine operating until the mid-1990s (Derkey and others, 1990; Derkey, 1995). Hydrothermal alteration of the Chumstick Formation occurred during the late Eocene, while the sediments were still being deposited in the Chiwaukum/Chumstick basin (Margolis, 1989). Local volcanism pre- and postdates ore-producing alteration, as well as late Eocene/early Oligocene folding of the Chumstick sandstone (Gresens, 1983; Tabor and others, 1982). Oligocene thrust faulting structurally stacks the hydrothermally altered sandstones and siltstones, resulting in repeating zones of mineralization with depth (Margolis, 1989; Patton and Cheney, 1971). This field trip identifies locations showing evidence of this complex stratigraphic and structural history.

This field trip is subsequent to the Haugerud and Stanton, Chumstick Formation field trip on Saturday, July 30th. Please see Haugerud and Stanton (this volume) for further discussion of the Chumstick Formation.

GEOLOGY OVERVIEW

Mineralization in the Wenatchee district is hosted within the Eocene Chumstick Formation, a series of arkosic sandstones, siltstones, and conglomerates filling the Chumstick basin (sometimes also called the Chiwaukum basin; Tabor and others, 1982). Dating of tuffs within the Chumstick Formation suggest rapid deposition of the sediments around 45 Ma (Tabor and others, 1982; Donaghy and others, 2021). Folding of the Chumstick Formation occurred in the late Eocene, constrained by a ~34 Ma tuff in the overlying Wenatchee Formation (Gresens and others, 1981).

The Oligocene Wenatchee Formation unconformably overlies the Chumstick Formation and consists of quartzose sandstone, shales, and conglomerates (Gresens and others, 1981; Tabor and others, 1982). In some places the flat-lying Wenatchee Formation overlies steeply dipping Chumstick Formation, but south of the town of Wenatchee, the Wenatchee Formation has also been folded and faulted (fig. 3; Gresens and others, 1981; Margolis, 1989).

Mineralization is generally strata-bound within the Chumstick Formation, probably occurring in aquifers within the sandstone/conglomerate and bounded by mudstones (Margolis, 1989; Ott and others, 1986). Location of mineralization is restricted below the “Compton” tuff, which appears to be associated with the Norco volcanic complex south of Wenatchee (Patton and Cheney, 1971; Margolis, 1989). The location of mineralization constrains the age to post-Compton deposition (K-Ar age 46.2 ± 1.8 Ma, biotite), leading Margolis (1989) to suggest that the hydrothermal activity that caused mineralization was not associated with the Compton/Norco volcanics.

The district is characterized by an Oligocene, post-mineralization, northeast-verging thrust belt, approximately 6 km wide by 15 km along strike, with three major southwest-dipping faults. The faulting appears to be accommodated on the relatively weak mudstones. The thrust belt occurs after an Eocene folding event restricted to the Chumstick Formation, with the easternmost thrust fault coinciding with a fold axis from the Eocene event (Margolis, 1989). An Oligocene andesite intrusion (29 m.y.; Gresens, 1983; Margolis, 1989) apparently constrains the thrust faulting, potentially making it coeval with Wenatchee Formation deposition, although the faults place Chumstick Formation over Wenatchee Formation. The reverse faults and the folds from the Oligocene deformation are offset dextrally.

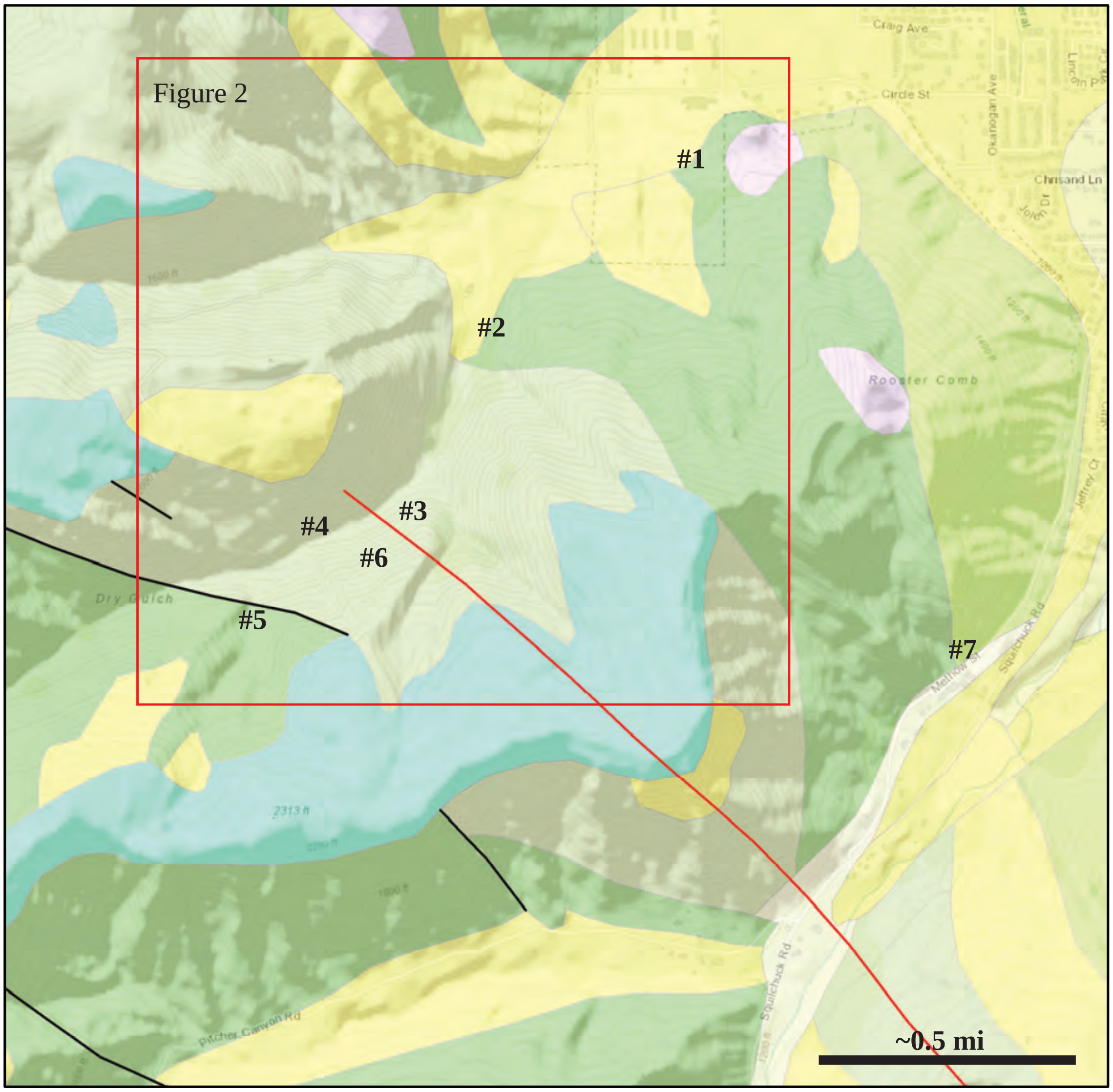

N

Quaternary alluvium, talus and landslide deposits

Pliocene–Miocene mass wasting deposits

Oligocene sedimentary rocks, Wenatchee Formation

Oligocene–Eocene volcanic rocks

Eocene sedimentary rocks, Nahahum Cyn Member, Chumstick Formation

Eocene sedimentary rocks, Chumstick Formation

Fault

Fold axis

#5 Field trip stop

Figure 1. 1:100k geologic map of the region south of Wenatchee, Washington with numbered field trip stops. Geologic map overlies ESRI topographic base map.

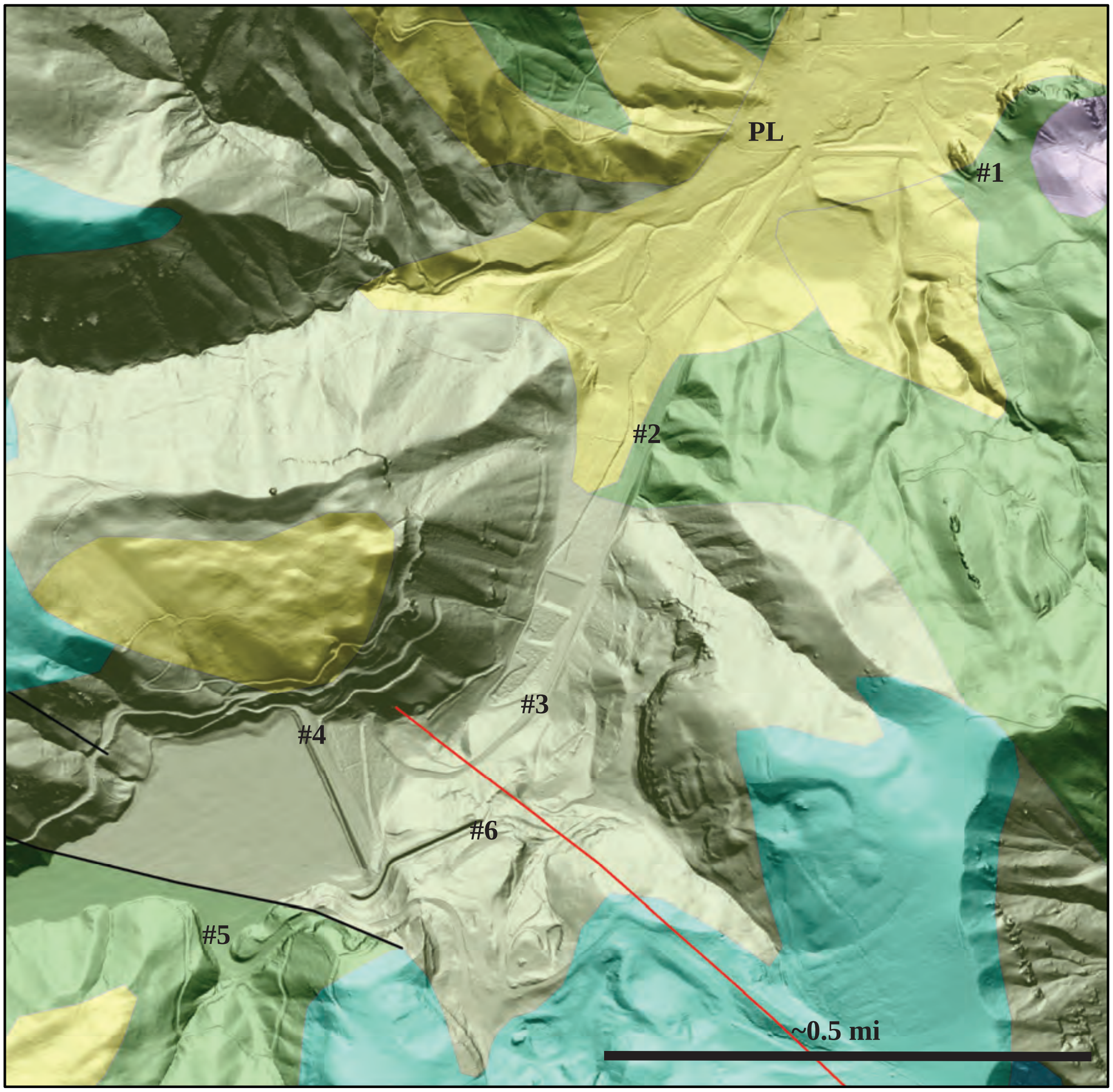

Quaternary alluvium and landslide deposits

Pliocene–Miocene mass wasting deposits

Oligocene sedimentary rocks, Wenatchee Formation

Oligocene–Eocene volcanic rocks

Eocene sedimentary rocks, Chumstick Formation

Fault

Fold axis

PL Dry Gulch Trailhead parking lot

#5 Field trip stop

N

Figure 2. Inset from figure 1 of the 1:100k geologic map of Dry Gulch, in south Wenatchee, Washington with numbered field trip stops. Geologic map overlies LiDAR.

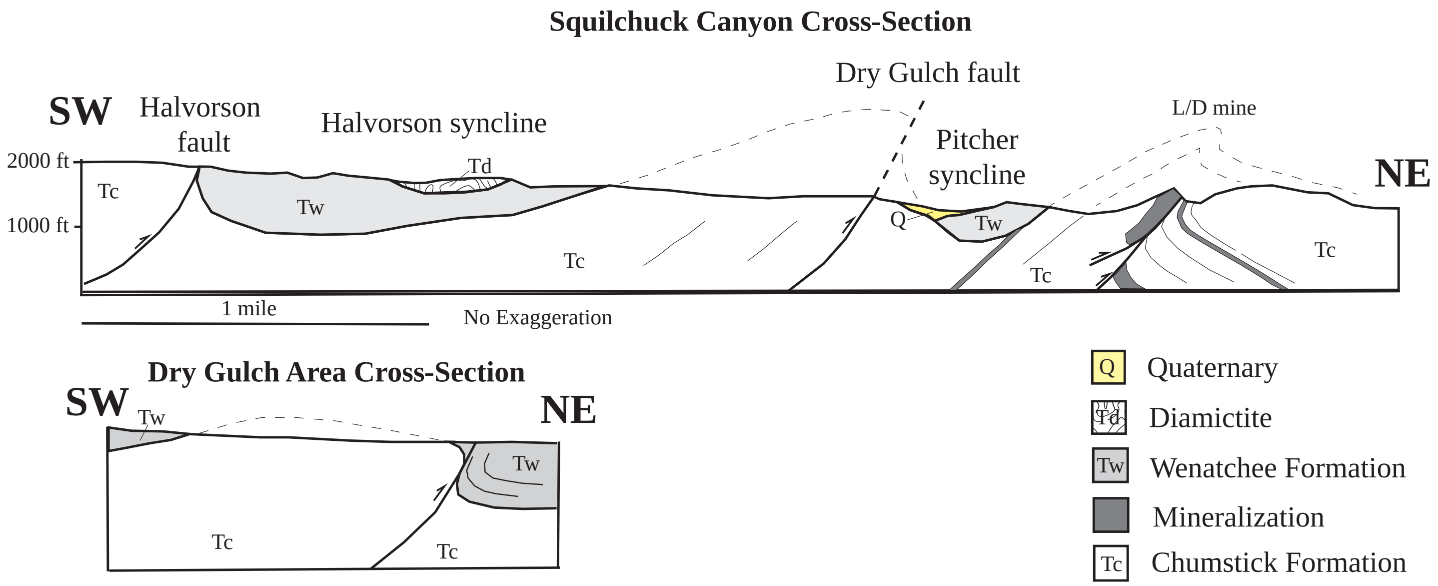

Figure 3. Schematic cross-sections across mineralized portions of the Chumstick and Wenatchee Formations along Squilchuck Canyon and Dry Gulch. After Margolis, 1989.

The Chumstick Formation, Wenatchee Formation, and all Oligocene thrust faulting is capped by locally extensive Pliocene basaltic diamictites as well as Pliocene to early Quaternary mass-wasting deposits (Gresens, 1983; Tabor and others, 1982).

Ore minerals in the Wenatchee district are pyrite, electrum, pyrargyrite, tetrahedrite, chalcopyrite, and acanthite. Gangue minerals are quartz, calcite, adularia, and clays (Klisch, 1989). The Lovitt Mine (Stop 7) had sporadic production between 1894 and 1946, then continuous production between 1949 and 1967, with a yield of 410,482 oz Au (0.396 oz/ton) and 625,849 oz Ag (0.60 oz/ton; Derkey and others, 1990). The Cannon mine (Stop 1) was in continuous production from 1985 to 1994, yielding more than 1.25 million oz Au and ~2 million oz Ag (Derkey, 1995). The Cannon mine was one of the largest underground gold mines in the nation when it closed, with more than 6 mi of tunnels that reached ~1,100 ft below the surface (Derkey, 1995).

FIELD TRIP LOG

Start at the Chelan County Fairgrounds, 5700 Wescott Drive, Cashmere, WA. Drive north on Wescott Drive 0.3 mi, turning right onto Sunset Hwy. Drive east for 1.3 mi, turning left onto S. Division St. Drive approximately 0.1 mi to the traffic circle, taking the right exit to drive east on Cottage Ave for 0.7 mi. Turn right onto US Hwy 2, driving east toward Wenatchee for approximately 7 mi. Hwy 2 will turn into N. Wenatchee Ave. Continue on N. Wenatchee Ave., now driving south, for 2 mi, where it will turn slightly right and turn into N. Miller St. Continue on Miller St. for approximately 3 mi to where it "T"s into Circle St. Take a right onto Circle St. to where it ends at the Dry Gulch/Saddle Rock trailhead in approximately 0.2 mi.

Dry Gulch/Cannon Mine—Hike with six stops

Start at the Dry Gulch/Saddle Rock Trailhead (47.3956, -120.3298). This trailhead has two porta-potties and shaded picnic tables but no water or other amenities.

From the parking lot, take the eastern trail toward Dry Gulch. Take the first trail to the left (east) and head toward the prominent outcrop, about 0.3 mi to the east of the trailhead parking area.

STOP 1:
Wenatchee "Dome"
47.3948, -120.3258

Two bedrock outcrops make up Wenatchee "Dome," called such because of its general shape. Both outcrops are north of the trail/road, with the smaller but more prominent outcrop closer to the trailhead. The larger outcrop makes the top of the hill or "dome" located at the intersection of Circle St. and Miller St. The main horizontal shaft to the Cannon mine, now sealed, is at the northern side of the larger outcrop. This is now the Wenatchee School District maintenance facility.

The rock is biotitic rhyodacite porphyry with a platy structure that may be flow banding (fig. 4; Gresens, 1983) but has also been called exfoliation weathering with flow banding parallel to jointing, dipping 25–55° from a common center (Patton and Cheney, 1971). Gresens (1983) stresses that the flow banding doesn't bend around the eastern side of the dome as would be expected with weathering exfoliation, and indeed, seems truncated, although he also suggests this truncation may result from right-lateral displacement of Wenatchee Dome from outcrops further south. Gresens (1983) indicates that this displacement supports right-lateral movement on the Entiat–Eagle Creek faults, roughly on strike to the north. Both Gresens (1983) and Tabor and others (1982) describe these rocks as intrusive.

Perlitic texture occurs at the border of the dome, extending out at least 50 ft west. The perlitic texture is friable and difficult to get in hand sample, but according to Gresens (1983) it is: "light-gray colored with whitish to yellowish specks that apparently represent an alteration product. Biotite flakes occur in the glass matrix." The rhyodacite itself is light gray with quartz and plagioclase phenocrysts in a fine-grained matrix, and occasional mafic minerals in hand sample. See Gresens (1983) for a more in-depth discussion of the petrology.

Gresens (1983) reports K-Ar ages of 43.2 ± 0.4 Ma and 43.5 ± 1.6 Ma for biotite in the rhyodacite and the perlite, respectively. Zircon fission-track ages are slightly older at 51.4 ± 2.8 Ma and 47.0 ± 2.7 Ma. Evans (1994) uses the younger age for the Wenatchee Dome, along with the right-lateral displacement from nearby similar rocks, to provide a control on the opening of a proposed eastern Chumstick subbasin by oblique motion on the Entiat–Eagle Creek fault system as well as constraint on the subsequent deposition of the Nahahum Cyn Member of the Chumstick Formation, which Evans (1994) claims was limited to the eastern subbasin. The younger age would also make the Wenatchee

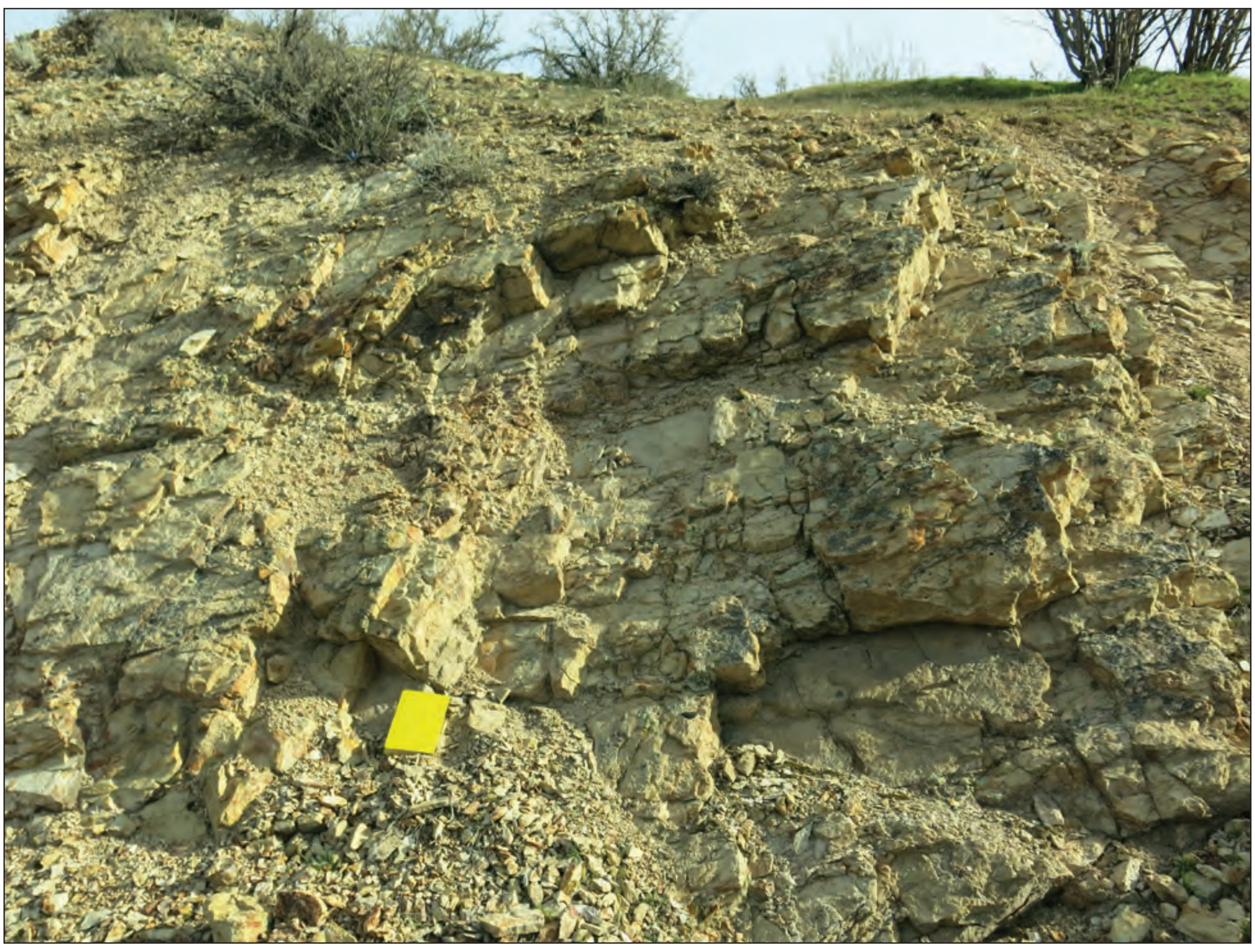

Figure 4. Rhyodacite of "Wenatchee Dome" showing either exfoliation weathering or flow banding at Stop #1. Photo by Kelsay Stanton.

Dome rocks coeval with the tuff in the upper Clark Cyn Member of the Chumstick Formation, with the Compton tuff, and with the Norco volcanics, and would suggest widespread local volcanism and faulting during the late Eocene. If older, the Wenatchee Dome rocks may be related to older tuffs in the Clark Cyn Member and were faulted later. There is no observable relationship between the Wenatchee Dome rocks and the mineralization associated with metal production, although the Wenatchee Dome rocks are presumed to be post-mineralization due to lack of alteration (Margolis, 1989).

Field stop discussion will focus on evidence supporting flow-banding and/or exfoliation weathering and its possible truncation on the eastern side of the dome, as well as evidence supporting or refuting an intrusive cooling.

Backtrack west to the main Dry Gulch trail and proceed south approximately 0.4 mi, where there are exposures east of the trail.

STOP 2:
Roadcut near mouth of Dry Gulch
47.3914, -120.329

The roadcut exposes conglomerate-bearing gneiss and granodiorite clasts with a volcanic dike crosscutting the conglomerate. Nearby sandstone is friable and feldspar rich, with possible silicification. The conglomerate and sandstone are part of the Chumstick Formation. The dike may be an andesitic intrusion noted in Patton and Cheney (1971). They describe the intrusions as having steeply dipping joints parallel to the bedding of the Chumstick sandstone, which they suggest indicates the intrusions may have been emplaced during the last stages of folding and faulting. This could also be the ~29 Ma andesite noted by Gresens (1983) and Margolis (1989) that intrudes one of the thrust faults that places Chumstick Formation over the Wenatchee Formation.

Field stop discussion will focus on distinguishing features of the Chumstick Formation as well as evidence for or against the dike being coeval with folding.

Proceed south along the trail. On the left (east) is a coal tailings pile in the mouth of a small drainage.

The Washington Division of Geology reports a mine in Dry Gulch operating prior to 1934 within a 4 ft bed of "bony coal, bone, and carbonaceous shale." About 362 tons were produced, with an "at mine" value of $3.41 in 1933 (Glover, 1936).

Approximately 0.4 mi from stop 2 is a large exposure in a quarry on the southeast side of Dry Gulch.

STOP 3:
Wenatchee Formation in old silica mine
47.3865, -120.3359

The silica mine in Dry Gulch is one of the reference sections for the Wenatchee Formation (Gresens and others, 1981). This mine continued at least until 1983, when Wenatchee Silica Products, Inc. reported 60,000 tons of silica sand and alumina clay, which they called "a very slow year" (Bunning, 1983). The Wenatchee Formation consists of quartzose sandstones, conglomerates, shales, and clay beds. At this exposure it is dipping to the southwest.

Field discussion will focus on the characteristics of the Wenatchee Formation, which include leaf fossils commonly found in boulders along the trail.

Continue along the trail through switchbacks to the western side of the tailings dam, approximately 0.5 mi.

STOP 4:
Folded Wenatchee Formation
47.3859, -120.3415

The Wenatchee Formation is exposed on the southern side of Dry Gulch, where it is nearly vertical (fig. 5). This exposure is in the footwall of a thrust fault, placing Chumstick Formation over the Wenatchee Formation.

The tailings dam is part of the Cannon mine. According to Caldwell and others (1986), the dam contains a clayey sandy silt core from material obtained locally. Weathered and decomposed basalt make the compacted shell of the embankment. Seepage is controlled by filter drains within the impoundment and down-valley of the dam as well as a grout curtain upstream of the dam.

Figure 5. Nearly vertical Wenatchee Formation in Dry Gulch at Stop #4. View to the east. Photo by Kelsay Stanton.

Field discussion will focus on the structure of the Wenatchee Formation.

Proceed across the impoundment toward the south–southwest approximately 0.2 mi to exposures of light-colored sedimentary rock in a bank.

STOP 5:
Bank exposure southwest of tailings dam
47.3832, -120.341

The sedimentary rock exposed in the bank is rich in felspars and shows silicic alteration. This is the Chumstick Formation, here thrust over the Wenatchee Formation.

Field discussion will focus on constraining the location of the fault.

Proceed approximately 0.3 mi northeast along the base of the southeastern slopes of Dry Gulch to the northern end of the berm southeast of the tailings dam.

STOP 6:
View of silica mine, diamictite
47.3844, -120.3375

The Pliocene diamictite of Gresens (1983) and Tabor and others (1981) is visible to the northeast across the silica mine (fig. 6). These have clasts of Columbia River Basalt and are not folded or faulted.

Return to trailhead. After bathroom break, drive east on Circle St. for 0.7 mi. Turn right on Okanogan Ave for 0.2 mi. Turn left on Chrisand Ln. for 0.3 mi. Turn right on Methow St. for 1.1mi.

Lovitt/L-D/Gold King Mine
47.3807, -120.3162

Please be aware that the mine is on private property. Permission for access was granted for the 2022 TRGS field trip.

Figure 6. Wenatchee Formation north of the Dry Gulch fault as seen from Stop #6. View to the north–northeast. Basalt diamictite caps the Wenatchee Formation in the upper right of the photo. Photo by Kelsay Stanton.

STOP 7:
Silicified sandstone at southeast corner of property
47.3807, -120.3162

The roadcut exposes altered and silicified Chumstick sandstone with extensive silicic veining and minor faulting/shearing. Propylitic alteration is evident by dark-colored, altered sandstone with alteration of biotite to pyrite (fig. 7). Gresens (1983) actually mistook the propylitic alteration to be a different unit, calling these outcrops Swauk(?) sandstone rather than Chumstick Fm. At this outcrop, the propylitic alteration is less coherent, weathering out and almost looking like fault gouge. The propylitic alteration is overprinted by argillic alteration, called such because of the presence of kaolinite (Margolis, 1989). Some sulfide stringers are visible in hand samples (acanthite?) and possibly electrum (?). At this outcrop the quartz stockwork is also apparent, indicating nearness to or overprinting by the silicic alteration (fig. 8). The quartz stockwork likely needs the argillic and silicic alteration to first create a brittle host, with fracturing allowing the vein emplacement. Where present, the stockwork is the most enriched in Au and Ag, occurring as electrum and sulfides (Margolis, 1989; Klisch, 1989).

Field discussion will focus on identifying minerals in hand samples as well as location of propylitic, argillic, and silicic alteration. We will also look at the mine works.

Figure 7. Propylitic alteration near the L/D mine at outcrop on west side of Methow St. View to the west. Photo by Kelsay Stanton.

Figure 8. Quartz stockwork near the L/D mine at outcrop on west side of Methow St. View to the west. Photo by Kelsay Stanton.

REFERENCES

Bunning, B., 1983, New developments in minerals and energy in Washington, 1982, Washington Geologic Newsletter: Washington Division of Geology and Earth Resources, vol. 11, p.1–10.

Caldwell, J.A., Thatcher, J., and Keil, J., 1986, Environmental geotechnological considerations in the design of the Cannon mine tailing impoundment: International Symposium on Environmental Geotechnology, p. 312–321.

Derkey, R., 1995, A brief history of the Cannon mine, Washington Geology, v. 23, p. 21–23.

Derkey, R., Joseph, N., and Lasmanis, R., 1990, Metal mines of Washington—Preliminary report: Washington Department of Natural Resources, Washington Division of Geology and Earth Resources Open File Report 90-18, p. 277.

Donaghy, E.E., Umhoefer, P.J., Eddy, M.P., Miller, R.B., and LaCasse, T., 2021, Stratigraphy, age, and provenance of the Eocene Chumstick basin, Washington Cascades: Implications for paleogeography, regional tectonics, and development of strike-slip basins: Geological Society of America Bulletin, v. 133, p. 2418–2438.

Evans, J.E., 1994, Depositional history of the Eocene Chumstick Formation: Implications of tectonic partitioning for the history of the Leavenworth and Entiat–Eagle Creek fault systems, Washington: Tectonics, v. 13, p. 1425–1444.

Glover, S.L., 1936, Nonmetallic mineral resources of Washington with statistics for 1933: Washington Division of Geology Bulletin 33, p. 30–35.

Gresens, R.L., 1983, Geology of the Wenatchee and Monitor quadrangles, Chelan and Douglas Counties, Washington: Washington Department of Natural Resources Division of Geology and Earth Resources, Bulletin 75, p. 90.

Gresens, R.L., Naeser, C.W., and Whetten, J.W., 1981, Stratigraphy and age of the Chumstick and Wenatchee Formations: Tertiary fluvial and lacustrine rocks, Chiwaukum graben, Washington: Geological Society of America Bulletin Part II, v. 92, p. 841–876.

Klisch, M.P., 1989, A study of fluid inclusions and geochemical mechanisms for gold deposition, Canon Mine, Wenatchee, Washington: MS Thesis, Western Washington University Graduate School Collection, no. 668.

Margolis, J., 1989, Arkose-hosted, aquifer-controlled, epithermal Au-Ag mineralization, Wenatchee, Washington: Economic Geology, v. 84, p. 1891–1902.

Ott, L.E., Groody, D., Follis, E.L., and Siems, R.L., 1986, Stratigraphy, structural geology, ore mineralogy, and hydrothermal alteration at the Cannon mine, Chelan County, Washington, *in* Macdonald, A.J., ed., Gold ’86: Willowdale, Ontario, Konsult International Inc., p. 425–435.

Patton, T.C., and Cheney, E.S., 1971, L-D gold mine, Wenatchee, Wash: New structural interpretation and its utilization in the future exploration, Transactions of the Society of Mining Engineers, v. 250, p. 6–11.

Tabor, R.W., Waitt, R.B., Frizzell, V.A. Jr., Swanson, D.A., Byerly, G.R., and Bentley, R.D., 1982, Geologic map of the Wenatchee 1:100,000 quadrangle, Central Washington: U.S. Geological Survey, Map I-1311.

FIELD GEOLOGY OF THE HICKS BUTTE COMPLEX AND EASTON METAMORPHIC SUITE: A RECORD OF JURASSIC AND CENOZOIC TECTONISM IN THE CENTRAL CASCADES, WASHINGTON

James H. MacDonald, Jr.,[1] Peter B. Davis,[2] Joe D. Dragovich,[3] B. Michelle Mayes,[1] Annalisa Incorvaia,[1] Glenn T. Thompson,[1] Shanna C. Stingu,[1] and Alex D. Maruszczak[1]

[1]*Environmental Geology Program, Florida Gulf Coast University, Fort Myers, Florida*
[2]*Department of Geosciences, Pacific Lutheran University, Tacoma, Washington*
[3]*Dragovich Geo-Consulting. Olympia, Washington*

INTRODUCTION

Numerous oceanic Mesozoic terranes occur in Washington State (fig. 1; e.g., Misch, 1966; Brown, 1987; Brandon and others, 1988; Miller and others, 1993; MacDonald and others, 2008; MacDonald and Schoonmaker, 2017). These terranes originated outboard of the Mesozoic Cordilleran margin and accreted during the Late Jurassic or Cretaceous (Saleeby, 1992; Brown and Gehrels, 2007; MacDonald and Dragovich, 2015; Sauer and others, 2017). Washington State Mesozoic terranes are usually omitted from regional tectonic synthesis (e.g., Saleeby and Busby-Spera, 1992; Wyld and others, 2006). This is due to several factors, including a paucity of data compared to other Mesozoic terranes of the Cordillera, and their involvement in Early Cretaceous translation and Late Cretaceous thrust fault emplacement [i.e., the Baja British Columbia (BC) hypothesis; Cowan and others, 1997]. Another important factor is the extreme structural dislocation of pre-Tertiary terranes and microterranes in Washington due to a long and complex history of accretion and structural dismemberment (including the formation

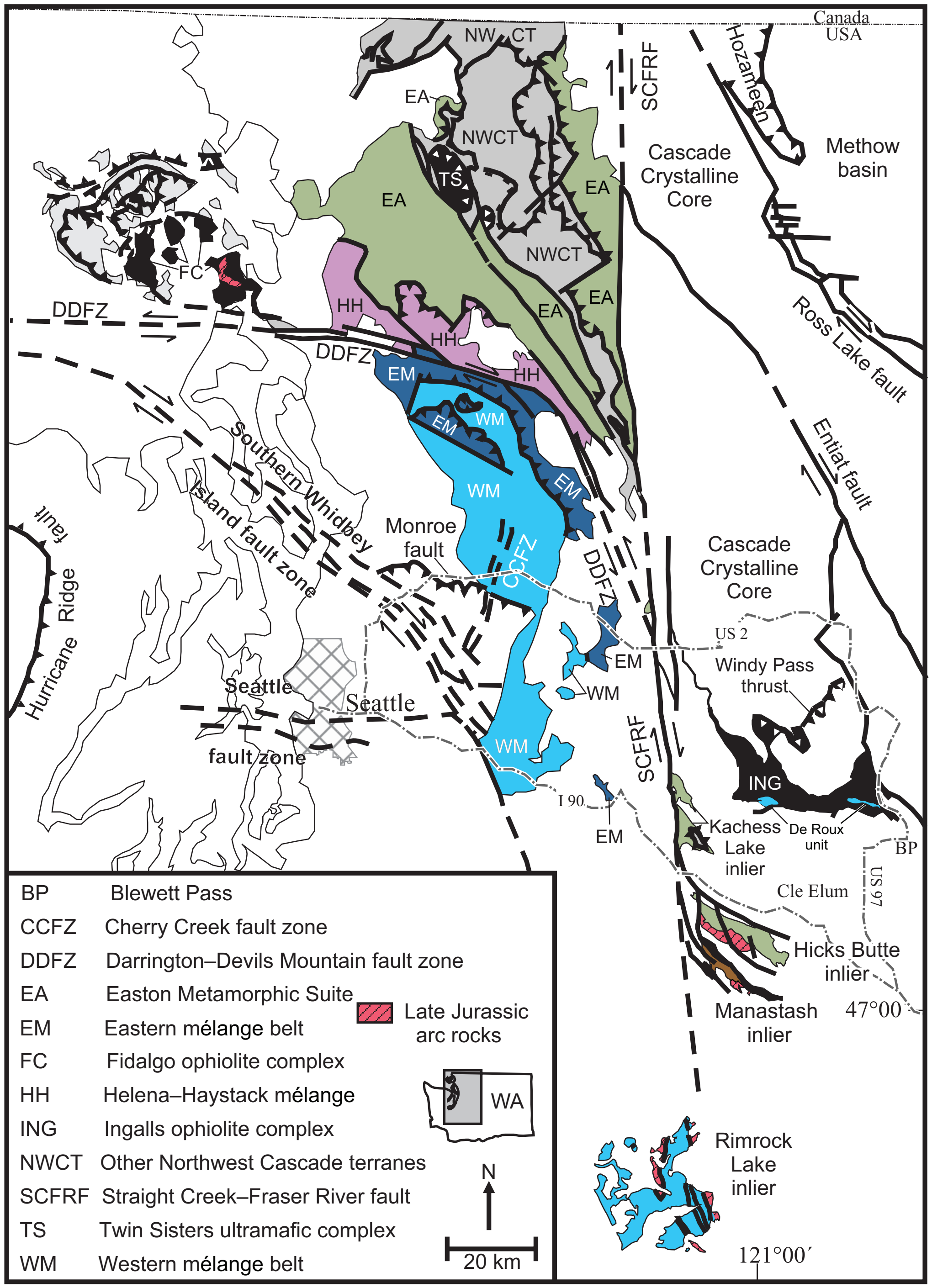

Figure 1. Simplified geologic map displaying pre-Cenozoic tectonic elements of the central and northwest Cascades, modified from Miller and others (1993) and MacDonald and Schoonmaker (2017). Ophiolitic and ultramafic rocks are black.

of several mélange belts) with further dismemberment during coastwise translation.

In the central Cascades, Washington, one of the largest of the accreted oceanic terranes is the polygenetic Jurassic Ingalls ophiolite complex (fig. 1) (Miller, 1985; Miller and others, 1993; MacDonald and others, a or b? 2008). The De Roux unit is faulted against the Ingalls ophiolite complex (fig. 1); however, the relationship between these two terranes is not fully understood (Miller, 1985; Miller and others, 1993; Harper and others, 2003). The Manastash inlier (fig. 1) consists of mostly Jurassic age arc rocks, including the 157 Ma Quartz Mountain stock (Miller and others, 1993; MacDonald and Schoonmaker, 2017). This field guide will focus on the Mesozoic rocks within Hicks Butte and Kachess Lake inliers, 117.5 km (73 mi) southwest of Wenatchee, WA (fig. 1). The units within these inliers are the Hicks Butte complex and correlative high-strain tectonics zone (fig. 2) and the Easton Metamorphic Suite (figs. 2, 3).

The pre-Cenozoic rocks of the Hicks Butte and Kachess Lake inliers are exposed as a result of the folding and faulting of younger Cenozoic rocks (figs. 2, 3; Eddy and others, 2016; Miller and others, 2022,

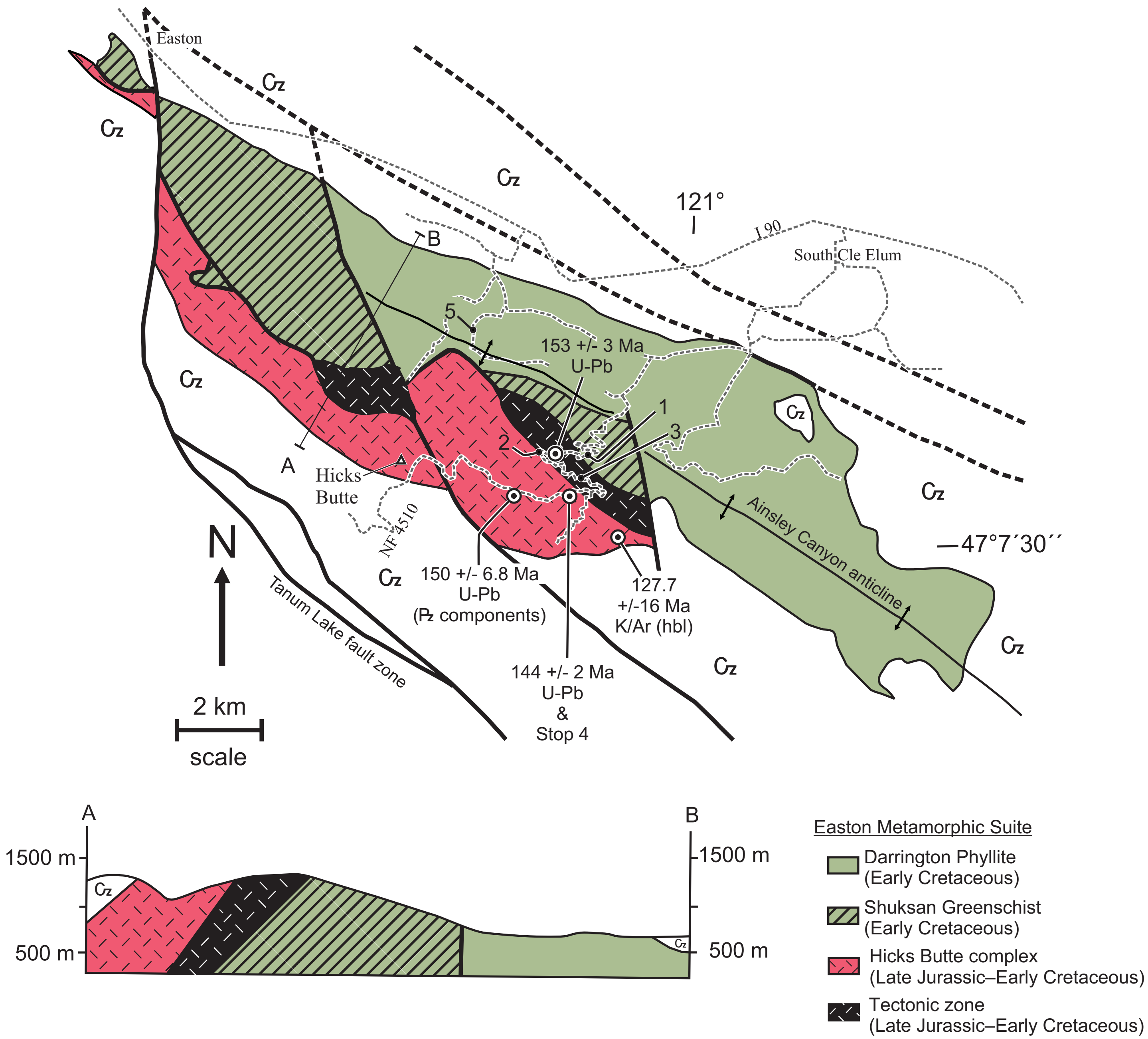

Figure 2. Simplified geologic map of the Hicks Butte inlier. Modified from Treat (1987), Miller and others (1993), and Tabor and others (2000). The eastern position of the Ainsley Canyon anticline is modified from Cheney and Hayman (2009). Note the locations of stops 1 to 5 on this figure. Cross-section A–B is shown on the map. Pz, Paleozoic; Cz, Cenozoic.

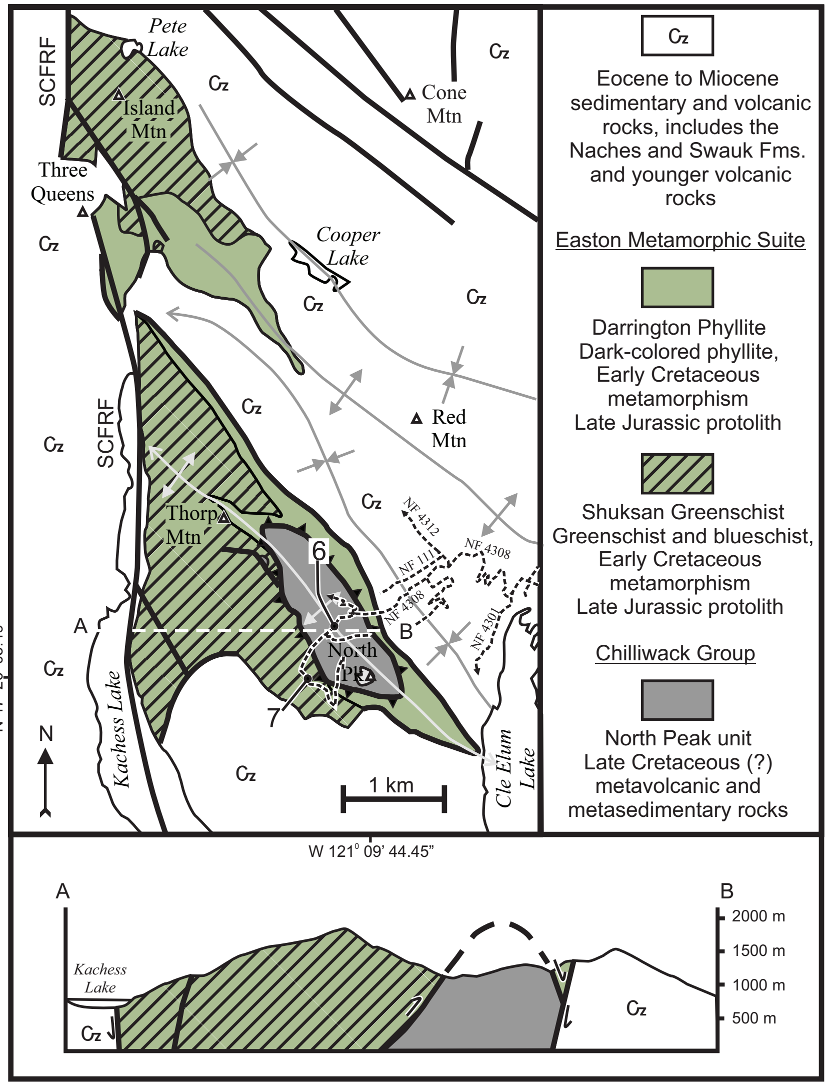

Figure 3. Simplified geologic map of the Kachess Lake inlier. Modified from Lofgren (1974), Ashleman (1979), and Tabor and others (2000). Note the locations of Stops 6 and 7 on this figure. Cross-section A–B is shown on the map.

and references therein). The Hicks Butte inlier consists of the Hicks Butte complex, its high-strained tectonic zone equivalent, and the Easton Metamorphic Suite (fig. 2). The Early Eocene Manastash Formation is deposited on the Hicks Butte inlier to its south (fig. 2). The Hicks Butte inlier is in fault contact with the Oligocene to Eocene Naches Formation to the west and is covered by the Ellensburg Formation and Miocene Grande Ronde Basalt of the Columbia River Basalt Group to the east (fig. 2; Tabor and others, 1984, 2000; Cheney and Hayman, 2009; Eddy and others, 2016). Alluvium from the Yakima River and glacial deposits obscure the inferred fault contacts of the Hicks Butte inlier to the north with the Eocene Teanaway Formation (fig. 2).

The Kachess Lake inlier consists of the Easton Metamorphic Suite and the North Peak unit—a correlative to the Chilliwack Group (fig. 3; Tabor and others, 2000; Tabor and Haugerud, 2016). The Paleocene to Eocene Swauk Formation, including the felsic Silver Pass Volcanic member, are deposited and faulted against the Kachess Lake inlier (fig. 3; Tabor and others, 1984, 2000; Tabor and Haugerud, 2016; Eddy and others, 2016). This inlier is faulted against the Oligocene to Eocene Naches Formation to the west along the Straight Creek–Fraser River fault (SCFRF; fig. 3). In addition to the Swauk Formation, the northern portion of the Kachess Lake inlier is in depositional contact with Miocene Volcaniclastic rocks of Cooper Pass and is intruded by the northern phase of the Miocene to Oligocene Snoqualmie batholith in the Three Queens area (fig. 3; Tabor and others, 2000; Tabor and Haugerud, 2016). A small occurrence of the Miocene Howson Andesite occurs at North Peak proper in the southern portion of the Kachess Lake inlier (fig. 3; Tabor and others, 2000).

HICKS BUTTE COMPLEX AND TECTONIC ZONE

Petrography

The Hicks Butte complex and its high-strained tectonic zone equivalent (fig. 2) were first recognized by Smith and Calkins (1906), initially subdivided by Stout (1964), and formalized by Treat (1987), Miller and others (1993), and Tabor and others (2000). The Hicks Butte complex consists of variably deformed hornblende tonalite and hornblende quartz diorite. Lesser hornblende gabbro, diabase, dacite, and rare hornblendite, trondhjemite, hornblende olivine gabbro, and rhyolite are also present. Diabase, dacite, hornblendite, rhyolite, and trondhjemite cut other lithologies as small 1 cm–0.5 m dikes. Lithologies are predominantly hypidiomorphic-granular. However, the dacite is allotriomorphic-granular and the hornblende olivine gabbro—which can only be found close to the main body of the Hicks Butte complex—has a symplectic and corona texture (fig. 4). A low-grade greenschist metamorphic facies overprints these rocks.

The Hicks Butte complex transitions into an approximately 500-m-wide high-strain tectonic zone by

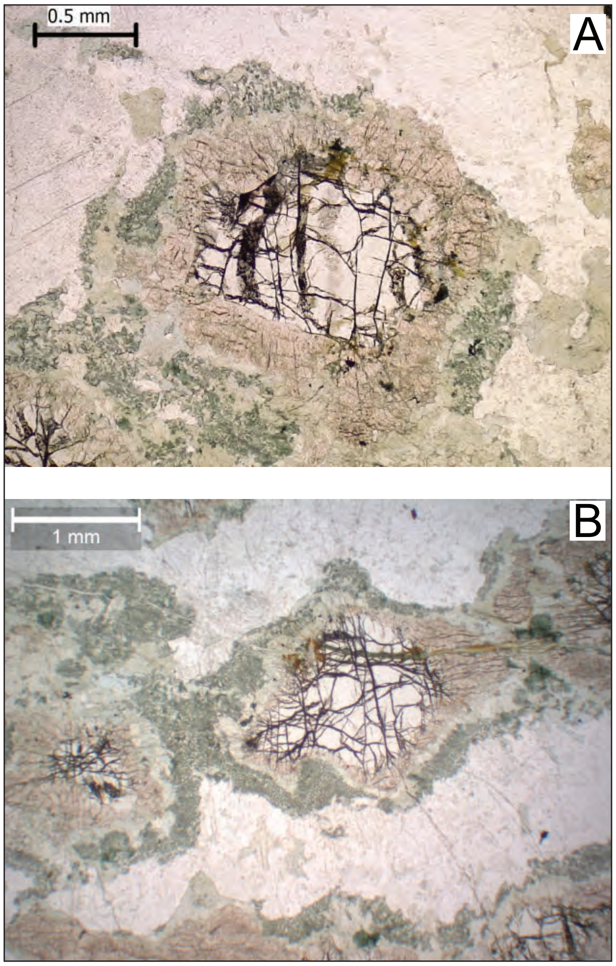

Figure 4. (A and B) Symplectic hornblende olivine gabbro from the Hicks Butte complex at stop 2. Note the corona of enstatite around the olivine. The symplectic melt can be seen as green-colored material mantling the enstatite. Also displayed are light green amphibole, clear plagioclase, and lesser oxides.

an increase in tectonic fabric development and general mylonitization or grain size reduction. The strong deformational character of this belt is distinctive enough that it has been mapped as a “tectonic zone” by several workers (Stout, 1964; Treat, 1987; Miller and others, 1993; Tabor and others, 2000). This tectonic zone consists of well-foliated and lineated tonalitic orthogneiss, amphibolite, gabbroic orthogneiss, and dacitic orthogneiss. In small meter-thick sections, the texture is mylonitic, especially in hornblende-bearing amphibolite. Epidote is a common mineral associated with orthogneiss and amphibolite. The orthogneiss is porphyroclastic and granoblastic in texture. The amphibolite is fine-grained and mostly nematoblastic. A thin 1 to 2 cm mylonite cuts through the orthogneiss at various localities.

Structure of the Hicks Butte Complex and Tectonic Zone

Foliations within the Hicks Butte complex and the tectonic zone predominantly strike northwest–southeast and dip steeply to moderately to the southwest. Igneous dikes in the Hicks Butte complex are folded within strongly lineated shear zones. Stretching lineations are common in the orthogneiss and amphibolite and trend northwest and plunge shallowly to moderately to the west–southwest. Some of the amphibolite and orthogneiss are L-tectonites, which suggests localized constrictional strain regimes. The variability of the mineral lineation orientations within the pluton decreases, defined by an increase in shape preferred orientations of hornblende and plagioclase towards, and within, the tectonic zone (fig. 2).

Ductile shear indicators show a northeast-verging (top to the northeast) shear sense of motion within the orthogneiss, in both the pluton and host rock. Boudins in the Hicks Butte complex and tectonic zone indicate general layer-parallel stretching. Davis and Stubbs (2017) conducted an Rf/Phi strain analysis of rigid clast rotation in hornblende and plagioclase through several transects from the Hicks Butte complex into the tectonic zone. Their data suggested a finite strain ratio between 1.4 and 2.1 for all samples, with increasing strain toward and into the tectonic zone. The data also suggests that only one deformation event is needed to explain the fabrics for the Hicks Butte complex and the tectonic zone (Davis and Stubbs, 2017). This is supported by the consistency of the foliations and mineral lineations between the Hicks Butte complex and the tectonic zone. Electron backscatter diffraction (EBSD) of plagioclase and quartz suggests the deformation in the tectonic zone was a result of simple shear (Davis and MacDonald, 2021). EBSD data also show a drop in temperature from ~900˚C—interpreted from the lack of crystallographic preferred orientations in plagioclase within tonalite orthogneiss near the pluton margin—through to 300–400˚C interpreted from basal <a> slip in quartz within the tectonic zone near contact with the Easton Suite.

Ages from the Hicks Butte Complex and Tectonic Zone

Miller and others (1993) reported a multigrain zircon age of 153 ± 3 Ma from a tonalite orthogneiss in the tectonic zone (fig. 2). MacDonald and Pecha (2011) and MacDonald and others (2019) reported laser-ablation inductively coupled plasma-mass spectrometry (LA-ICP-MS) U-Pb zircon ages from a hornblende quartz diorite, a hornblende olivine gabbro, and two dacites from the Hicks Butte complex. Both rims and cores were analyzed. With a few exceptions, zircons have igneous Th/U ratios indicating intrusive age estimates (MacDonald and Pecha, 2011; MacDonald and others, 2019). Eleven zircons from the hornblende quartz diorite yielded a mean intrusive age of 150.0 ± 6 Ma (2σ; MSWD = 0.2). Three additional zircons from the hornblende quartz diorite have early to middle Paleozoic intrusive ages. Forty-one zircons from the hornblende olivine gabbro yield an intrusive mean age of 153.6 ± 2.0 Ma (2σ; MSWD = 1.00). One zircon outlier from the hornblende olivine gabbro provided a Late Triassic intrusive age.

Twenty-one zircons from a dacite dike that cuts hornblende tonalite yielded a mean age of 144.0 ± 2.4 Ma (2σ; MSWD = 1.1). Five zircons from this dacite sample that have igneous Th/U ratios have Late Jurassic U-Pb ages, and two have Middle Jurassic U-Pb ages. A second dacite, which was associated with the hornblende olivine gabbro, has a complex LA-ICP-MS U-Pb age (MacDonald and others, 2019). All zircons from this dacite have igneous Th/U ratios that indicate probable intrusive ages, including: (1) 21 zircons yield a mean age of 144.5 ± 2.1 (2σ; MSWD = 1.5); (2) the 9 youngest zircons from this sample yield a mean age of 137.3 ± 2.4 MA (2σ; MSWD = 1.04); and (3) the 11 oldest zircons from this sample yield a mean age of 152.07 ± 1.0 Ma (2σ; MSWD = 1.2).

Tabor and others (2000) obtained a hornblende K-Ar age of 127.7 ± 16 Ma from an amphibolite near the tectonic zone. Tabor and others (2000) suggested that this age may be a minimum age for the amphibolite. Their conclusion was a result of the radiometric age having a large error, and the age's discrepancy from other igneous and metamorphic ages associated with the Hicks Butte complex or Easton Metamorphic Suite—which is in fault contact with the Hicks Butte complex (fig. 2).

Rock Geochemistry

Nineteen samples from the Hicks Butte complex and tectonic zone have been analyzed for whole-rock major and trace element geochemistry (figs. 5, 6; Stingu and others, 2015). The samples can be divided into two groups based on their Sr/Y ratios (fig. 5). The dacite and rhyolite all have very high Sr/Y ratios and meet all of the chemical classifications for adakites (fig. 5; Stingu and others, 2015). One hornblende tonalite and one trondhjemite also have high Sr/Y ratios and can be geochemically classified as adakites (fig. 5). All other Hicks Butte intrusive samples and all metamorphic samples from the tectonic zone have much lower Sr/Y ratios and plot within the field of island arcs (fig. 5; Stingu and others, 2015). The high

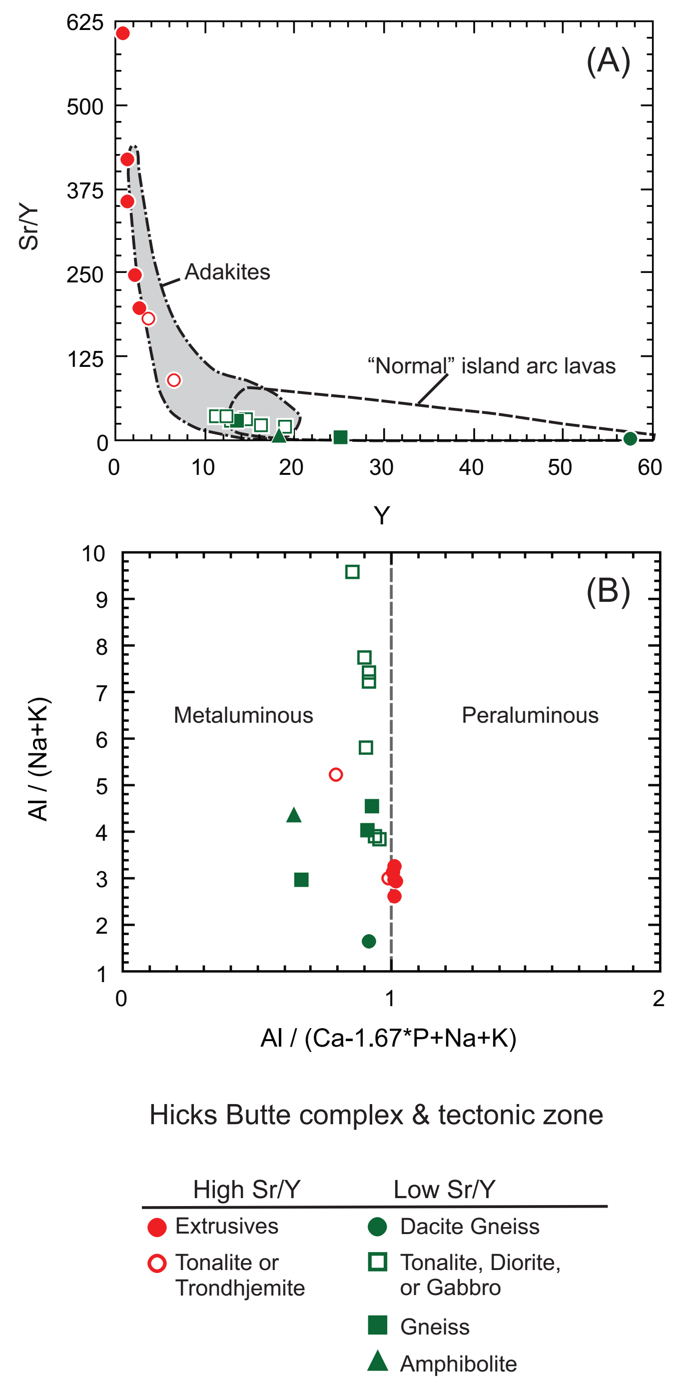

Figure 5. (A) Hicks Butte complex and tectonic zone samples plotted on the Sr/Y vs. Y diagram of Defant and Drummond (1990). (B) Molar aluminum saturation index Al/(Ca-1.67*P+Na+K) vs. molar Al/(Na+K) plot for Hicks Butte and tectonic zone samples. Metaluminous and peraluminous divisions are from Frost and others (2001).

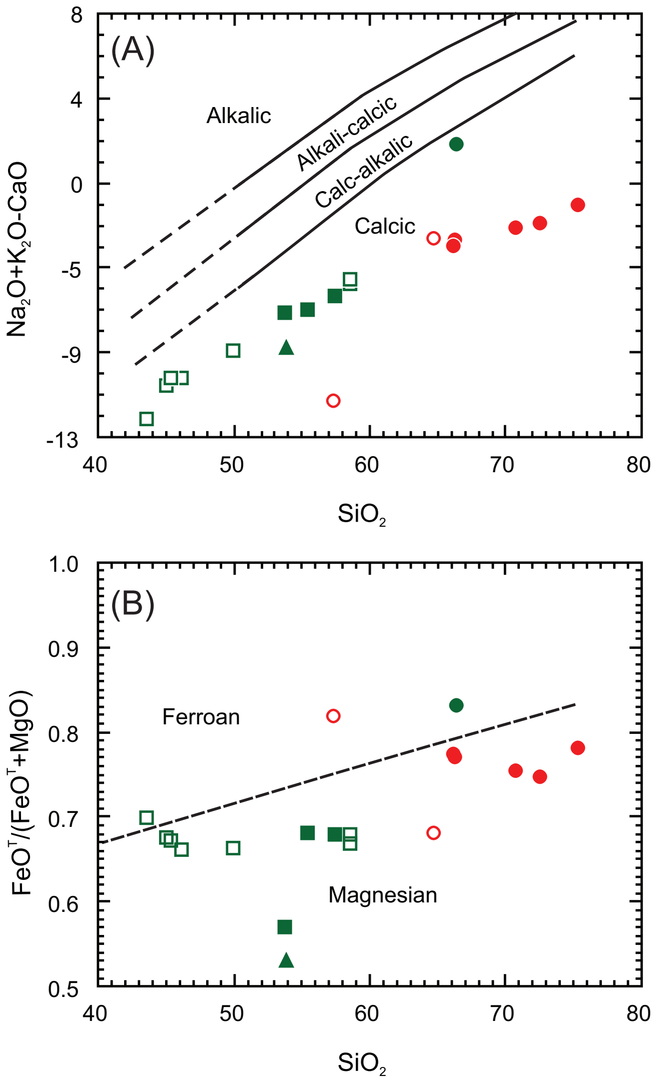

Figure 6. (A) SiO2 vs. Na2O+K2O-CaO weight percentage plot for Hicks Butte complex and tectonic zone samples. Magmatic series divisions are from Frost and others (2001). (B) SiO2 vs. FeOT/(FeOT+MgO) weight percentage plot for Hicks Butte complex and tectonic zone samples. Ferroan and magnesian division from Frost and others (2001). FeOT, all iron expressed at Fe2+. Symbols are the same as in figure 5.

Sr/Y ratio dacites and the rhyolite are peraluminous while the low Sr/Y intrusive and metamorphic samples are metaluminous (fig. 5). The high Sr/Y samples are mostly felsic (SiO_2 weight % > 63%; fig. 6). The low Sr/Y samples are predominantly mafic to intermediate (fig. 6). All samples are predominantly subalkaline, calcic, low-K, and magnesian (fig. 6; Stingu and others, 2015). The high Sr/Y ratio adakites have low $Mg^{\#}$, Ni, and Cr (Stingu and others, 2015).

Mineral Geochemistry

Treat (1987), Thompson and others (2015), and Mayes and others (2021) conducted mineral geochemistry of the Hicks Butte complex via electron probe microanalyzer (EPMA). The mineral geochemistry provides data that will support petrogenetic information of the whole-rock geochemistry. Mineral data can also be utilized to estimate pressure and temperatures of magmatic crystallization.

Plagioclase

Plagioclase from the low Sr/Y hornblende olivine gabbro are anorthite (fig.7; Mayes and others, 2021). Plagioclase from all other low Sr/Y intrusive samples are bytownite with lesser labradorite (fig. 7; Treat, 1987; Thompson and others, 2015). Plagioclase from the high Sr/Y ratio extrusive and intrusive samples are labradorite to andesine (fig. 7; Thompson and others, 2015). Although not plotted on figure 7, Treat (1987) reported that plagioclase from the tectonic zone is oligoclase.

Amphibole

Thompson and others (2015) and Mayes and others (2021) conducted EPMA analysis of amphibole from the Hicks Butte complex (fig. 8A). They used the amphibole classification scheme of Hathorne and others (2012). All amphiboles are calcium-rich. Amphiboles in the low Sr/Y intrusive Hicks Butte samples are largely magnesio-ferri-hornblende (fig. 8A). Amphiboles from the high Sr/Y ratio dacites are ferri-tschermakite, while amphibole from the high Sr/Y intrusive samples are magnesio-ferri-hornblende (fig. 8A).

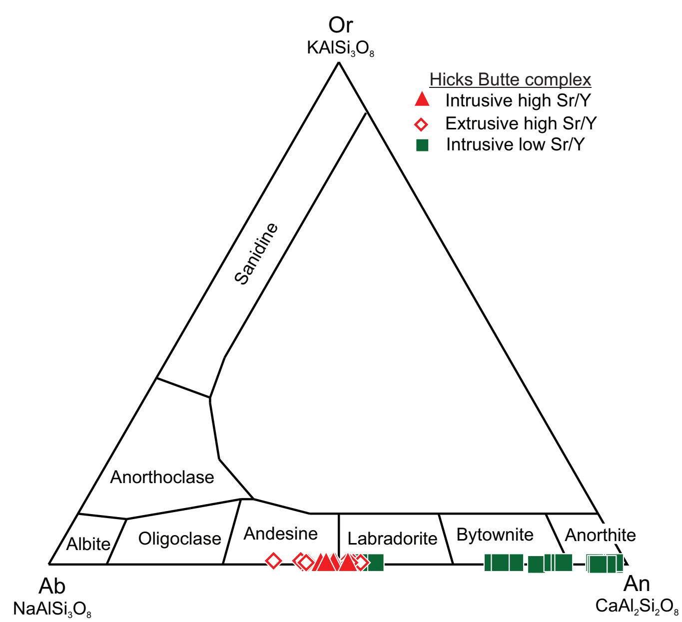

Figure 7. Hicks Butte complex plagioclase plotted on the plagioclase classification diagram.

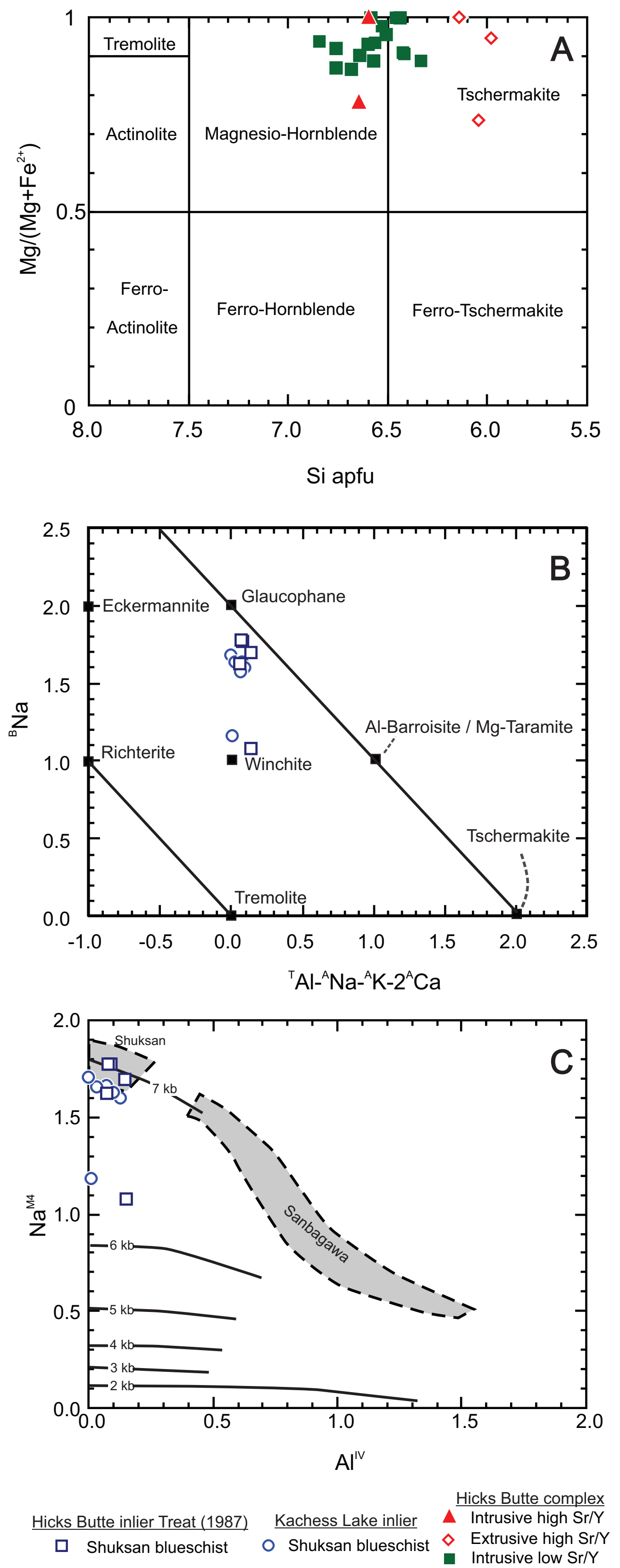

Figure 8. (A) Hicks Butte complex Ca-amphiboles plotted on the classification diagram modified from Hawthorne and Oberti (2007). apfu, atoms per formula unit. (B) Na-amphiboles from Shuksan blueschist plotted on the classification diagram of Schumacher (2007). The black squares represent the compositions of the adjacent amphibole names. (C) Na-amphiboles from Shuksan blueschist plotted on the NaM4 vs. AlIV amphibole diagram of Brown (1977).

Treat (1987) also analyzed amphibole from the Hicks Butte complex with EPMA. She reported magnesio-hornblende to tschermakite with minor cummingtonite (Treat, 1987). However, Treat did not know the high Sr/Y versus the low Sr/Y geochemical affinities of the complex and did not provide sufficient sample descriptions to infer the geochemical group of her amphiboles and thus these amphiboles are not plotted on figure 8A. Treat (1987) also analyzed amphiboles from the tectonic zone. These are magnesio-hornblende to ferro-tschermakite, overlapping the compositions of the lesser deformed complex (Treat, 1987; Thompson and others, 2015; Mayes and others, 2021).

Olivine and Pyroxene

Mayes and others (2021) analyzed olivine and pyroxene from two symplectite hornblende olivine gabbro (figs. 4, 9, 10A). The forsterite content of the olivine ranges from Fo_{67} to Fo_{74} (fig. 9). The pyroxene is enstatite and ranges from En_{74} to En_{78} (fig. 10A). The symplectite hornblende olivine gabbro has olivine, forsterite, and anorthite percentages that plot in the field defined by modern island arcs (fig. 9; Mayes and others, 2021). The gabbro also has anorthite and enstatite percentages that plot near modern island arcs and display little mineral fractionation (fig. 10A; Mayes and others, 2021). The enstatite plots away from the field defined by high-pressure magmatic settings, and along the low-pressure Skaergaard intrusion trend (fig. 10B; Mayes and others, 2021).

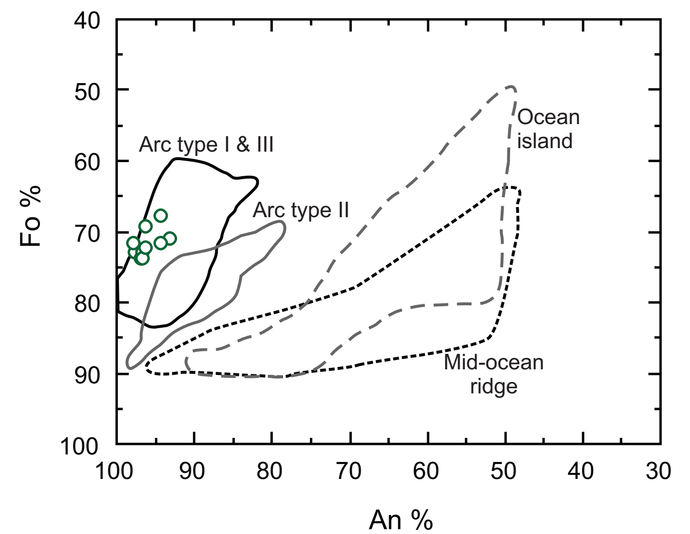

Figure 9. Forsterite (Fo) percentage vs. anorthite (An) percentage for olivine from the Hicks Butte complex hornblende olivine gabbro. Magmatic fields are from Beard (1986).

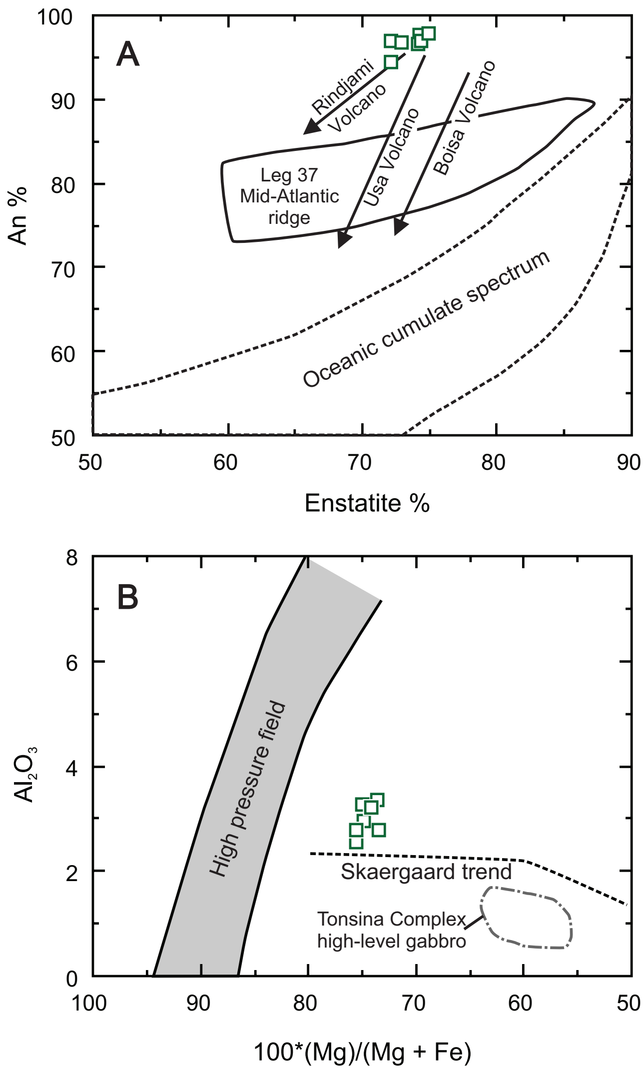

Figure 10. (A) Anorthite (An) percentage vs. enstatite percentage for pyroxene from the Hicks Butte complex hornblende olivine gabbro. Fractionation trends and magmatic fields are from Burns (1985) and Bağci and others (2006). (B) Al_2O_3 vs. magnesium number for pyroxene from the Hicks Butte complex hornblende olivine gabbro. Magmatic trends from DeBari and Coleman (1989).

Crystallization Pressure and Temperature Estimates

Thompson and others (2015) and Mayes and others (2021) estimated the temperatures of the Hicks Butte complex utilizing the amphibole geothermometer of Ridolfi and others (2010). High Sr/Y dacites yielded temperature estimates of 934°–945°C and high Sr/Y hornblende tonalite yielded a temperature of 847° ± 56°C (Thompson and others, 2015). Amphibole from the low Sr/Y samples yields temperature estimates of 828°–864°C, with the symplectite hornblende olivine gabbro yielding a temperature estimate of 896º ± 29ºC (Thompson and others, 2015; Mayes and others, 2021).

Thompson and others (2015) conducted pressure estimates utilizing the geobarometers of both Ridolfi and others (2010) and Anderson and Smith (1995); however, the Hicks Butte complex samples lack the mineral buffer assemblage required for the Anderson and Smith (1995) pressure calibration. Utilizing the amphibole geobarometer of Ridolfi and others (2010), the high Sr/Y dacite yields a pressure of 5.67 ± 1.42 kbar. The low Sr/Y ratio intrusive samples yield pressures ranging from 1.33 to 2.31 kbar (Thompson and others, 2015). The geobarometer of Anderson and Smith (1995) yielded much lower pressures (Thompson and others, 2015). Mayes and others (2021) only conducted the amphibole geobarometer of Ridolfi and others (2010) on the symplectite hornblende olivine gabbro due to the lack of the required mineral buffer assemblage. They estimated a pressure of 2.61 ± 0.12 kbar.

EASTON METAMORPHIC SUITE

Smith (1904) and Smith and Calkins (1906) first recognized the Easton Metamorphic Suite, named for the phyllite that occurs near the town of Easton within the Hicks Butte inlier (fig. 2). This metamorphic suite has been correlated to outcrops that lie across the Straight Creek Fault 100 km to the north (fig. 1). The Easton Metamorphic Suite consists of the Shuksan Greenschist, Darrington Phyllite, semischist and phyllite of Mount Josephine, and minor amphibolite with rare eclogite (figs. 1–3; Misch, 1966; Brown, 1986; Tabor and others, 1993). The Easton Metamorphic Suite to the north is thrust over terranes within the Excelsior and Welker Peak nappes along the Shuksan thrust (figs. 1, 3; Misch, 1966; Brown, 2012; Tabor and Haugerud, 2016). Haugerud and others (1981) and Brown (1986) interpreted the type localities of the Shuksan Greenschist to stratigraphically underlie the Darrington Phyllite; however, Cordova and others (2018) suggested they were always in fault contact.

The Easton Metamorphic Suite has been extensively studied west of the SCFRF (fig. 1); however, the Easton Metamorphic Suite has received mostly field-based studies within the Hicks Butte and Kachess Lake inliers east of the SCFRF. The Easton Metamorphic Suite in the Hicks Butte and Kachess Lake inliers (figs. 2, 3) only include rocks that correlate to the Shuksan Greenschist and Darrington Phyllite. In the Kachess Lake inlier, the Easton Metamorphic Suite is in thrust contact with the North Peak unit (fig. 3), which has been correlated with the Chilliwack Group based on lithology and metamorphic grade (Ashleman, 1979; Tabor and others, 2000; Tabor and Haugerud, 2016). Ubiquitous epidote-bearing blueschist—which interlayers with greenschist on a centimeter scale—is found throughout the Easton Metamorphic Suite (Brown, 1977, 1986). Brown (1977) suggested that the bulk composition of the protolith, particularly the Fe^{3+} content, may have determined if blueschist or greenschist mineral assemblages were stable and preserved. Blueschist are more commonly preserved in the Kachess Lake inlier than in the Hicks Butte inlier (Lofgren, 1974; Ashleman, 1979; Treat, 1987; Miller and others, 1993).

Petrology and Metamorphic Mineral Assemblages

The Shuksan Greenschist in the Hicks Butte and Kachess Lake inliers is interlayered centimeter-wide bands of greenschist and epidote blueschist. Thin section textures are mostly lepidoblastic to nematoblastic. The mineral assemblage of the greenschist facies of the Shuksan in the Hicks Butte and Kachess Lake inliers consists of albite–epidote–chlorite–actinolite–quartz (Lofgren, 1974; Ashleman, 1979; Treat, 1987; Miller and others, 1993; Tabor and others, 2000; Maruszczak and others, 2016; Davis and Lindmark, 2015; Davis and Stubbs, 2017). The mineral assemblage of the blueschist facies consists of epidote–Na–amphibole–quartz–albite with lesser muscovite and chlorite (Lofgren, 1974; Ashleman, 1979; Treat, 1987; Miller and others, 1993; Tabor and others, 2000; Maruszczak and others, 2016; Davis and Stubbs, 2017). Maruszczak and others (2016) and Davis and Stubbs (2017) observed retrograde greenschist-facies metamorphism overprinting the blueschist mineral assemblages locally, with zoisitic overgrowths on epidote (fig. 11) and secondary chlorite–albite–quartz. Relic igneous textures are commonly reported in the Shuksan Greenschist west of the SCFRF (fig. 1) (e.g., relict pillows, volcanic breccia, and amygdules) (Haugerud and others, 1981; Brown, 1986). However, only rare relic igneous textures in the Kachess Lake inlier have been observed east of the SCFRF in the Shuksan Greenschist (see Ashleman, 1979).

The Darrington Phyllite in the Hicks Butte and Kachess Lake inliers consists of quartzose phyllite and muscovite–chlorite–albite–quartz ± lawsonite schist that was originally a mudstone (Lofgren, 1974; Ashleman, 1979; Treat, 1987; Miller and others, 1993). Relic primary sedimentary structures are locally preserved in the Darrington Phyllite west of the SCFRF (Dungan and others, 1983). However, no relic sedimentary structures have been observed in the Hicks Butte or Kachess Lake inliers.

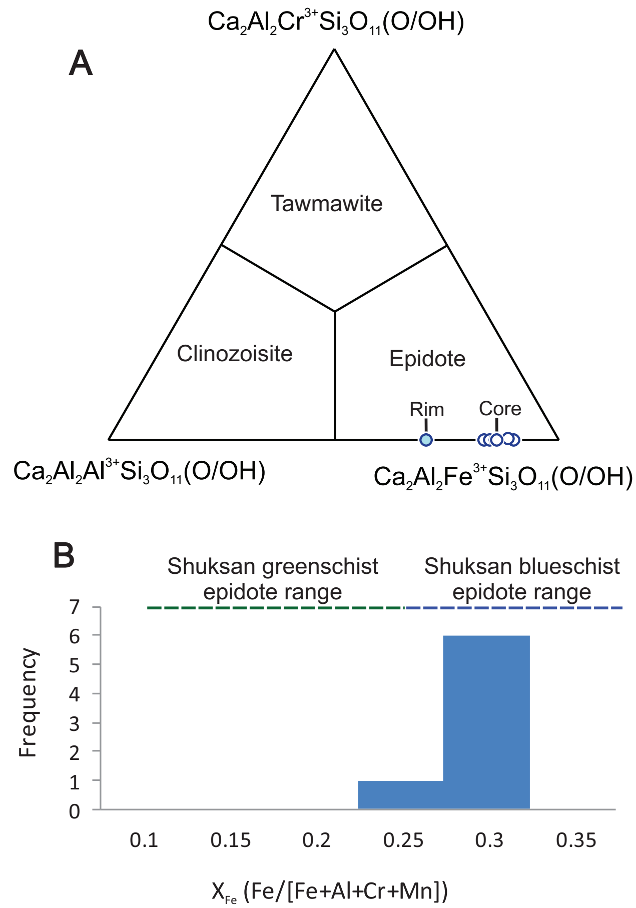

Figure 11 (A) Kachess Lake inlier Shuksan blueschist epidote plotted on the epidote group classification diagram. (B) XFe (Fe/[Fe+Al+Cr+Mn]) frequency histogram for epidote from the Kachess Lake inlier Shuksan blueschist. Lines for Shuksan greenschist-facies and blueschist-facies epidote compositions are from Brown (1986).

Structure

Foliation in the Easton Metamorphic Suite in both inliers follows the anti- and synformal structures that deform the overlying Eocene strata (figs. 2, 3). Foliations of the Easton Metamorphic Suite in the Kachess Lake inlier trend northwest–southeast and dip to the southwest (Lofgren, 1974; Ashleman, 1979; Tabor and others, 2000). Easton Metamorphic Suite foliations in the Hicks Butte inlier also trend northwest–southeast and dip to the southwest (Treat, 1987; Miller and others, 1993; Tabor and others, 2000; Davis and Stubbs, 2017).

Synmetamorphic mineral lineations in the Shuksan Greenschist in the Hicks Butte inlier lie on the dominant foliation. Synmetamorphic folds, crenulations, and crosscutting shear zones deform the Shuksan

Greenschist foliation in the Hicks Butte inlier. Additionally, small folds in the Darrington Phyllite located in the Hicks Butte inlier deform the foliation and create a crenulation cleavage. Early fold axis orientations between crenulation surfaces are coplanar with the crenulation cleavage. In addition, EBSD analysis of quartz suggests the deformation in the Darrington Phyllite was a result of a pure shear bulk strain environment (Davis and MacDonald, 2021). Open folds deform the original fabric of the Darrington Phyllite. Some local cataclasites occur in the Darrington Phyllite in the Hicks Butte inlier.

Age of the Easton Metamorphic Suite

No age data for either the Shuksan Greenschist or Darrington Phyllite east of the SCFRF exists (fig. 1). However, numerous studies on the age of these units west of the SCFRF have been conducted. We will review these "western" ages with the assumption that they apply to the Easton Metamorphic Suite in our field area due to their lithological similarities. The Easton Metamorphic Suite in the northwest Cascades (fig. 1) has 163–150 Ma Jurassic protolith ages, 160–144 Ma higher-grade metamorphic ages, and 148–120 Ma regional blueschist metamorphic ages (Armstrong, 1980; Armstrong and Misch, 1987; Gallagher and others, 1988; Dragovich and others, 1998; Brown and Gehrels, 2007; Cordova and others, 2018). Cordova and others (2018) reported amphibolite ages between 168 and 163 Ma. They suggested these amphibolite ages represented lower pressure metamorphism associated with the onset of subduction prior to the later higher-pressure metamorphism of the Shuksan Greenschists and Darrington Phyllite later in the subduction cycle (Cordova and others, 2018).

Mineral Geochemistry

Amphiboles

Treat (1987) and Maruszczak and others (2016) conducted EPMA analysis of amphiboles from blueschists in the Hicks Butte and Kachess Lake inliers, respectively (figs. 8B, 8C). Utilizing Hawthorne and others' (2012) amphibole classification scheme, these amphiboles are Na-rich and predominantly glaucophane with rare winchite (fig. 8B). The amphiboles from the blueschists are high in Na^{M4} (figs. 8B, 8C) and low in Ti (Treat, 1987; Maruszczak and others, 2016). These are identical compositions to blueschist amphiboles from west of the SCFRF (fig. 8C; e.g., Brown, 1977; Cordova and others, 2018). Treat (1987) also analyzed amphiboles from greenschists in the Hicks Butte inlier (not plotted on fig.8). These greenschist facies amphiboles are Ca-rich and range in composition from actinolitic hornblende to magnesiohornblende (Treat, 1987).

Epidote

Maruszczak and others (2016) also conducted EPMA analysis of epidote from blueschist in the Kachess Lake inlier. These epidotes have high X_{Ep} ($\geq$0.83; $Fe^{3+}/[Fe^{3+}+Al+Cr-2]$) and plot in the field defined by epidotes on the epidote group mineral triangle (fig. 11A). The X_{Fe} ($Fe^{3+}/[Fe^{3+}+Al+Cr+Mn]$) of these epidotes average 0.28 (fig. 11B), which is similar to epidote compositions in blueschists from west of the SCFRF (Brown, 1986). An epidote overgrowth has an X_{Ep} of 0.70, indicating substitution of Al^{3+} for Fe^{3+} (fig. 11A). This epidote also has a lower X_{Fe} and is more typical of epidote compositions from greenschist facies west of the SCFRF (fig. 11B; Brown, 1986).

North Peak Unit

The North Peak unit currently underlies the Shuksan greenschist–blueschist in the Kachess Lake inlier in an Eocene-aged anticlinal structure (fig. 3). The depth extent of the North Peak unit is unknown. This unit consists of a very fine-grained strongly foliated nematoblastic chlorite–epidote–muscovite–titanite–quartz with rare texturally late albite (fig. 12). Notably, there are large phenocrysts of diopside that have been stretched and partially reacted to aegirine (Fe^{+3}-rich high-pressure sodic-pyroxene). The cracks in the grains are infilled with glaucophane and quartz (no albite). Texturally and structurally late large cracks in the outcrop and thin section in figure 12 are filled with calcite and are interpreted to be Eocene tension gashes around regional folding. Other minor volumes of the North peak unit include a more massive greenschist unit that displays rosettes of pumpellyite in a very fine-grained decussate texture with chlorite–albite–quartz.

DISCUSSION

The low Sr/Y rocks of the Hicks Butte complex crystallized between 154 and 150 Ma. The low Sr/Y ratios, metaluminous, calcic, and magnesian geochemical affinities of the 154–150 Ma Hicks Butte complex rocks are indicative of an original island arc intrusive setting (figs. 5, 6; Defant and Drummond, 1990; Frost and others, 2001). This is supported by the olivine, plagioclase, and pyroxene geochemical affinities from the symplectite hornblende olivine gabbro (figs. 9, 10; Burns, 1985; Beard, 1986; DeBari and Coleman, 1989; Bağci and others, 2006). This late Jurassic island arc may have been built on older crust possibly rifted off of the North American continental margin. This is suggested by the older exotic igneous zircons that are preserved within these rocks. Assuming a barometric gradient of 0.33 kbar/km, the 154–150 Ma, Hicks Butte complex rocks crystallized between 4 and 7 km below the surface. The estimated pressure and temperatures for the 154–150 Ma Hicks Butte complex rocks are within the expected range of modern island arcs (Stern, 2002). The higher temperature and pressure estimate for the symplectite hornblende olivine gabbro are consistent with it representing the base of the arc crust for the late Jurassic Hicks Butte complex.

As suggested by Claeson (1998), the mineral assemblage of orthopyroxene + hornblende ± hercynite + magnetite on igneous olivine + plagioclase in the symplectite hornblende olivine gabbro (fig. 4) represents rapid cooling from 1100ºC to 700–800ºC between 8 and 6 kbar. The amphibole in the symplectite hornblende olivine gabbro is a late crystallizing mineral phase (fig. 4). The lower pressure yielded by this amphibole might have recorded late crystallization in this symplectite rock as it prograded from higher temperatures and pressures.

The high Sr/Y ratio of dacite and rhyolite are ca. 145–144 Ma (Early Cretaceous). Currently, there are no other Early Cretaceous igneous rocks identified within Washington State. The complex age sample, which is associated with the symplectite hornblende olivine gabbro, yields a Late Jurassic age of ca. 152 Ma along with Early Cretaceous ages of ca. 137 Ma, ca. 144.5 Ma. The high Sr/Y ratios and peraluminous geochemical affinities (fig. 5) indicate these Early Cretaceous dacite are adakites, i.e., results of partial melting of a mafic protolith (Defant and Drummond, 1990). This is supported by the low Cr, Ni, and $Mg^{\#}$ composition of the adakites, which suggests they were derived from the melting of lower arc crust (Stingu and others, 2015). Both adakitic dacite samples contained inherited restitic Late Jurassic igneous zircons. The ca. 154 Ma age group from the hornblende olivine gabbro, its field association with the dacite, and symplectite texture (fig. 4) suggest the hornblende olivine gabbro may have produced the partial melt to generate the Early Cretaceous adakites. The relationship of the ca. 137 Ma age from the dacite to the Easton Metamorphic Suite is not clear. This ca. 137 Ma age does overlap regional blueschist facies ages (e.g., Cordova and others, 2018).

The transition between the Hicks Butte complex into the tectonic zone, and then into the Easton Metamorphic Suite, has been interpreted in different ways (Treat, 1987; Miller and others, 1993; Tabor and others, 2000). The Late Jurassic similar U-Pb zircon unit ages, consistency of the geochemistry (figs. 5, 6), and general lithologic compositions suggest the tectonic zone is a high-strain equivalent of the Hicks Butte complex. The contact of the tectonic zone with the Easton Metamorphic Suite is mostly obscured. However, the consistency of the metamorphic fabrics, incremental increase of deformation as the Easton Metamorphic Suite is approached, and the overlap in regional ages between the Hicks Butte complex and the Easton Metamorphic Suite suggest their petrogenesis are most likely related.

West of the SCFRF, the Easton Metamorphic Suite crystallized at temperatures between 320°C and 400°C and at pressures between 7 and 9 kbar (Haugerud and others, 1981; Brown, 1986; Cordova and others, 2018). In the Kachess Lake inlier, Maruszczak and others (2016), using Na-amphibolite, epidote compositions (figs. 8, 11), and mineral assemblages, applied the methodology of Brown (1977) and Evans (1990) to estimate the blueschist in the Kachess Lake inlier crystallized between 300º and 400°C and 6–7 kbar. In the Hicks Butte inlier, Treat (1987) and Davis and Lindmark (2015) suggested the blueschists crystallized between 400ºC and 450ºC, and 8 to 9 kbars. They estimated the greenschist crystallized around 500ºC and 5–7 kbar (Treat, 1987; Davis and Lindmark, 2015).

The Darrington Phyllite as well as Shuksan blueschist and greenschist ages range from 148 to 142 Ma and 140 to 136 Ma generated by Cordova and others (2018). These ages generally fit within the multiple ages for the complex dacite located at the symplectite hornblende olivine gabbro site (see Stop 2 below). The subducting plate on which the Darrington Phyllite was deposited between 148 and 142 Ma (Cordova and others, 2018) could have caused the 145–144 Ma partial melting of the symplectite hornblende olivine gabbro to generate the high Sr/Y adakites.

ROAD LOG

Latitude and longitude coordinates for field trip stops are reported in World Geodetic System 1984 datum (WGS84). They are presented for each field stop in decimal degrees (hddd.dddd°**).** Google Earth and other web mapping applications use the WGS84 datum and can easily plot decimal degrees. All of the stops are on National Forest Service Roads (NFSR), which are classified by the U.S. Forest Service as "improved gravel roads." They are passable for any type of vehicle; however, vehicles with high clearance are recommended.

Driving west from the Chelan Expo Center in Cashmere, WA, turn south down highway 97, crossing over Blewett Pass. Approximately 14.3 mi south of Blewett Pass turn west off of highway 97 towards the towns of Cle Elum and South Cle Elum. Driving south out of South Cle Elum, 6th Street becomes Westside Road. Drive west on Westside Road until you reach Woods and Steele Road on your left (south). At the intersection of Westside Road and Woods and Steele Road, set your odometer to zero (0). Proceed southwest on Woods and Steele Road. At mile 0.7 turn left onto NFSR 4510. A local developer has renamed the paved section of NFSR 4510 All Seasons Drive. At mile 1.3 NFSR 4510 forks with Snow Ridge Drive. Stay to the right at the fork to continue on NFSR 4510. This fork can be confusing due to the cul-de-sac-like nature of the termination of the pavement. Soon after the fork, NFSR turns into a gravel road. Continue on NFSR 4510 until Stop 1 at mile 3. Stop 1 is within the Hicks Butte inlier.

STOP 1:
Shuksan Greenschist
N47.1445°, W121.0332°

Stop 1, at mile 3, is an outcrop of Shuksan Greenschist (fig. 2), located along the left. Here, epidote- and chlorite-bearing greenschist is strongly foliated; it displays 5- to 10-mm-thick compositional layering and is lineated. Foliation strikes northwest–southeast and dips moderately to the southwest. *Continue to Stop 2.*

STOP 2:
Dacite and symplectite gabbro of the Hicks Butte complex
N47.1452º, W121.0489º

Stop 2, at mile 3.9, is the location of high Sr/Y ratio dacite with the complex U-Pb zircon age of ca. 137 Ma, ca. 144.5 Ma, and ca. 152 Ma. The low Sr/Y symplectite hornblende olivine gabbro (fig. 4) from this stop has a U-Pb zircon age of ca. 154 Ma. See above for the discussion of the mineral geochemistry (figs. 4, 8A, 9, 10), and P-T estimates from amphibolite from this gabbro. This is also the approximate locality of the U-Pb zircon age of 153 Ma reported by Miller and others (1993), which was originally collected by Cliff Hopson and Jim Mattinson in the 1970s. *Continue to Stop 3.*

STOP 3:
Tectonic zone
N47.1394°, W121.0360°

Stop 3, at mile 4.8, is the tectonic zone—the high strain equivalent of the Hicks Butte complex. Located here are strongly foliated and lineated rocks of the tectonic zone (fig. 3). Coarse- to fine-grained tonalitic to gabbroic gneiss, amphibolite, and rare mylonite can be seen in the outcrop. Porphyroclastic textures are common. Strong planar foliation here strikes northwest–southeast and dips moderately to the southwest. Mineral and stretching lineations trend northwest here and have a shallow plunge. This is consistent with the Shuksan Greenschist at Stop 1. Open rootless folds and shear structures (e.g., rotated mineral grains) are common. A very large (>1.5 m) boudin of amphibolite occurs here. *Continue to Stop 4.*

STOP 4:
Hicks Butte complex
N47.1357°, W121.0424°

Stop 4, mile 6.3. Park along NFSR 4510 and walk uphill to the south to observe excellent outcrops of almost all lithologies of the Hicks Butte complex. Hornblende gabbro and rare hornblendite occur here as dikes cutting hornblende tonalite, hornblende quartz diorite, and hornblende diorite. Dikes range in thickness from 1 cm to ~30 cm. Dacite and rhyolite occur as <1-cm-thick to >30-cm-thick dikes cutting all other lithologies.

Enclaves occur in the granitoid lithologies, suggesting magma mixing may have occurred. Dikes are commonly folded, faulted (extensionally), or stretched into boudinage. Weak foliation and lineation here have the same general direction as at previous stops. High Sr/Y dacite at this site provided the ca. 144 Ma U-Pb zircon age. A low Sr/Y ratio hornblende quartz diorite at this site yield the ca. 150 Ma U-Pb zircon age. See the above discussion for rock and mineral geochemistry from this site as well as P-T interpretations.

Continue on NFSR 4510 until a turnaround at mile 7.8.

This turnaround provides excellent vistas of the Wenatchee Mountains and Stuart Range to the north. These consist of the Cretaceous Mount Stuart batholith, Jurassic Ingalls ophiolite complex, and younger Eocene sedimentary and volcanic rocks.

After the turnaround, continue until mile 14.2 to turn right back onto Woods and Steele Road. At mile 14.9 turn left back onto Westside Road. Continue on Westside Road until mile 18, where you will turn left onto Fowler Creek Road. Continue on Fowler Creek Road until Stop 5.

STOP 5:
Darrington Phyllite
N47.1704°, W121.0714°

Stop 5, at mile 18.8, is an outcrop of the Darrington Phyllite. Park at the intersection of Fowler Creek Road and NFSR 4517 and walk across the street to the outcrop. A tight upright F_2 fold deforms the S_1 foliation. This is associated with a steep S_2 spaced foliation. L_2 crenulation, lineation, and S_1 foliation have the same northwest–southeast-striking, southwest-dipping fabric as the rest of the Hicks Butte inlier. Well-foliated and folded, dark-colored Darrington Phyllite with quartz segregations occur along Fowler Creek Road as you go to the northwest toward Westside Road.

CAUTION—do not visit the outcrop on the north side of Fowler Creek Road and Westside Road. This is a hairpin turn and can be very dangerous. The same structures at this dangerous outcrop can be seen on Fowler Creek Road.

Turn around at Stop 5 and drive back towards Westside Road. At mile 19.6, turn left onto Westside Road. Then at mile 21.3, turn right onto Golf Course Road. At mile 21.5 turn right to merge onto Interstate 90 East (I-90 E). At mile 23.5 take exit 8 off of I-90 E towards Salmon La Sac/Roslyn. At mile 25.6 turn left onto Bullfrog Road. At mile 27.8, at the second traffic circle, continue straight onto WA-903 North. WA-903 will become Salmon La Sac Road. At mile 39.5 turn left off of WA-903/ Salmon La Sac Road onto NFSR 4308. Continue on NFSR 4308 until Stop 6.

STOP 6:
North Peak unit
N47.3430°, W121.1739°

Stop 6, at mile 44.9, is the Kachess Lake inlier. This stop is the fine-grained, dark- to light-green meta-volcaniclastic rocks of the North Peak unit (Ashleman, 1979). Ashelman (1979) reported lawsonite from the North Peak unit. Tabor and Haugerud (2016) suggested the North Peak unit is in the Excelsior Nappe of the Northwest Cascade System and correlated with the Chilliwack Group based on lithologies and metamorphic mineral assemblage. Figure 12 displays a thin section image of a greenschist-facies metatuff from the North Peak unit. The clinopyroxene in this sample has experienced brittle deformation and is prograding into higher metamorphic-grade aegirine (fig. 12). Glaucophane occurs in the large cracks within the mineral grain (fig. 12).

As you drive southwest from this stop, you will cross the folded thrust fault contact between the Easton Metamorphic Suite and the North Peak unit (fig. 2). The Darrington Phyllite, just southwest of this stop, is remarkably similar, both lithologically and structurally, to the rocks at Stop 5. *Continue along NFSR 4308 until Stop 7.*

STOP 7:
Shuksan blueschist
N47.3346°, W121.1832°

Stop 7, at mile 51.3, consists of epidote blueschist in millimeter- to centimeter-thick compositional layers. Open to tight folds are deforming the northwest–southeast-striking foliation, which is dipping moderately to steeply to the southwest. This has been consistent between both inliers. This out-

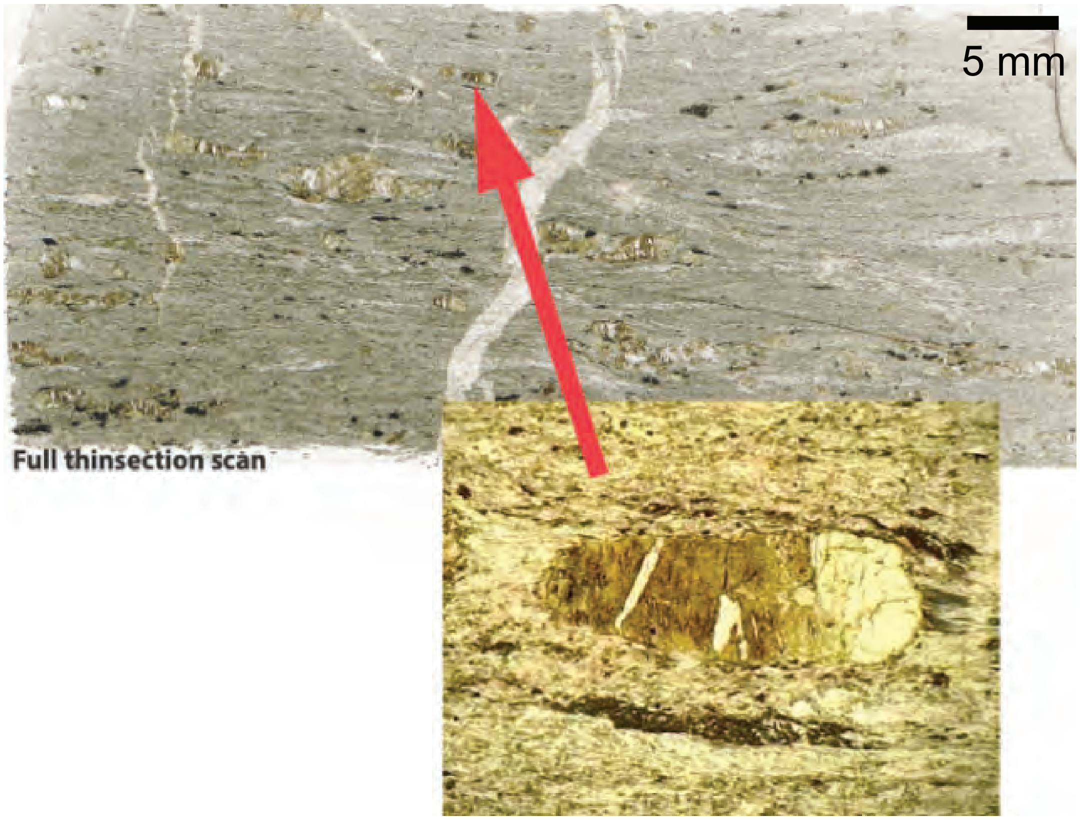

Figure 12. Thin section of a metatuff from the North Peak unit.

crop is the location of Na-amphibole and epidote discussed above. In this area, the metamorphic grade of the rock depends on your position within crenulations. In thin section, the hinges are predominantly actinolite while the limbs are rich in glaucophane. We interpret this to record prograde blueschist facies overprinting greenschist facies metamorphism.

From this stop, you can continue up NFSR 4308 to about mile 60, where you can turn around and head back to civilization.

ACKNOWLEDGMENTS

This field guide is dedicated to Rowland Tabor, whose geologic mapping of the Cascades created a lasting legacy of excellent knowledge and scientific contributions for generations to marvel at. We thank Kelsay Stanton for editing this field guide. The mineral geochemistry data discussed in this chapter were the result of course-based undergraduate research projects conducted by Florida Gulf Coast University students and funded by the NSF TUES grant 1323354 to MacDonald. Additional funding by the Florida Gulf Coast University Office of Research and Graduate Studies to MacDonald.

REFERENCES

Anderson, J.L., and Smith, D.R., 1995, The effects of temperature and fO_2 on the Al-in-hornblende barometer: The American Mineralogist, v. 80, p. 549–559.

Armstrong, R.L., 1980, Geochronometry of the Shuksan Metamorphic Suite, North Cascades, Washington: Geological Society of America Abstracts with Programs, v. 12, no. 3, p. 94.

Armstrong, R.L., and Misch, P., 1987, Rb-Sr and K-Ar dating of mid-Mesozoic blueschist and Late Paleozoic albite-epidote amphibolite and blueschist metamorphism in the North Cascades, Washington and British Columbia, and Sr isotope fingerprinting of eugeosynclinal rock assemblages: Washington Division of Geology and Earth Resources Bulletin, v. 77, p. 85–105.

Ashleman, J.C., 1979, The geology of the western part of the Kachess Lake quadrangle, Washington: M.S. thesis, University of Washington, Seattle, 88 p.

Bağci, U., Parlak, O., and Höck, V., 2006, Geochemical character and tectonic environment of ultramafic to mafic cumulate rocks from the Tekirova

(Antalya) ophiolite (southern Turkey): Geological Journal, v. 41, p. 193–219.

Beard, J.S., 1986, Characteristic mineralogy of arc-related cumulate gabbros: Implications for the tectonic setting of gabbroic plutons and for andesite genesis: Geology, v. 14, p. 848–851.

Brandon, M.T., Cowan, D.S., and Vance, J.A., 1988, The Late Cretaceous San Juan thrust system, San Juan Islands, Washington: A case history of terrane accretion in the western Cordillera: Geological Society of America Special Paper 221, 81 p.

Brown, E.H., 1977, The crossite content of Ca-amphibole as a guide to pressure of metamorphism: Journal of Petrology, v. 18, p. 53–72.

Brown, E.H., 1986, Geology of the Shuksan Suite, North Cascades, Washington, U.S.A., *in* Evans, B.W., and Brown, E.H., eds., Blueschists and Eclogites: Geological Society of America Memoir 164, p. 143–154.

Brown, E.H., 1987, Structural geology and accretionary history of the Northwest Cascades system, Washington and British Columbia: Geological Society of America Bulletin, v. 99, p. 201–214.

Brown, E.H., 2012, Obducted nappe sequences in the San Juan Island–northwest Cascades thrust system, Washington and British Columbia: Canadian Journal of Earth Sciences, v. 49, p. 796–817.

Brown, E.H., and Gehrels, G.E., 2007, Detrital zircon constraints on terrane ages and affinities and timing of orogenic events in the San Juan Islands and North Cascades, Washington: Canadian Journal of Earth Science, v. 44, p. 1375–1396.

Burns, L.E., 1985, The Border Ranges ultramafic and mafic complex, south-central Alaska: Cumulate fractionates of island-arc volcanics: Canadian Journal of Earth Sciences, v. 22, p. 1020–1038.

Cheney, E.S., and Hayman, N.W., 2009, The Chiwaukum structural low: Cenozoic shortening of the central Cascade Range, Washington State, USA: Geological Society of America Bulletin, v. 121, p. 1135–1153.

Claeson, D.T., 1998, Coronas, reaction rims, symplectites and emplacement depth of the Rymmen gabbro, Transscandinavian Igneous Belt, southern Sweden: Mineralogical Magazine, v. 62, p. 743–757.

Cordova, J.L., Mulchy, S.R., Schermer, E.R., and Webb, L.E., 2018, Subduction imitation and early evolution of the Easton metamorphic suite, northwest Cascades, Washington: Lithosphere, v. 11, p. 44–58.

Cowan, D.S., Brandon, M.T., and Garver, J.I., 1997, Geologic tests of hypotheses for large coastwise displacements: A critique illustrated by the Baja British Columbia controversy: American Journal of Science, v. 297, p. 117–173.

Davis, P., and Lindmark, M., 2015, Evidence for lower crustal syntectonic forearc emplacement of the Hicks Butte pluton breaking the correlation of HP-LT rocks across the Cascades of Washington State: Geological Society of America Abstracts with Programs, v. 47, no. 7, p. 766.

Davis, P., and Stubbs, M., 2017, Perspective on lateral terrane translation from syntectonic emplacement of the Hicks Butte pluton in the central Cascades of Washington State: Geological Society of America Abstracts with Programs. v. 49, no. 6, doi: 10.1130/abs/2017AM-306311.

Davis, P., and, MacDonald, J.H. Jr., 2021, A view into changing magmatic and deformational styles during island arc emplacement (and assembly?): Hicks Butte, central Cascades of Washington State: Geological Society of America Abstracts with Programs, v. 53, no. 4, doi: 10.1130/abs/2021CD-363218.

DeBari, S.M., and Coleman, R.G., 1989, Examination of the deep levels of an island arc: Evidence from the Tonsina ultramafic-mafic assemblage, Tonsina, Alaska: Journal of Geophysical Research: Solid Earth, v. 94, p. 4373–4391.

Defant, M.J., and Drummond, M.S., 1990, Derivation of some modern arc magmas by melting of young subducted lithosphere: Nature, v. 347, p. 662–665.

Dragovich, J.D., Norman, D.K., Grisamer, C.L., Logan, R.L., and Anderson, G., 1998, Geologic map and interpreted geologic history of the Bow and Alger 7.5 minute quadrangles, Western Skagit County, Washington: Washington Division of Geology and Earth Resources Open File Report 98-5, 80 p., 3 plates.

Dungan, M.A., Vance, J.A., and Blanchard, D.P., 1983, Geochemistry of the Shuksan greenschists and blueschists, North Cascades, Washington: Variably fractionated and altered metabasalts of oceanic affinity: Contributions to Mineralogy and Petrology, v. 82, p. 131–146.

Eddy, M.P., Bowring, S.A., Umhoefer, P.J., Miller, R.B., McLean, N.M., and Donaghy, E.E., 2016, High-resolution temporal and stratigraphic record of microplate accretion and ridge-trench interaction preserved in non-marine sedimentary basins in central and western Washington: Geological Society of America Bulletin, v. 128, p. 425–441.

Evans, B.W., 1990, Phase relations of epidote-blueschists: Lithos, v. 25, p. 3–23.

Gallagher, M.P., Brown, E.H., and Walker, N.W., 1988, A new structural and tectonic interpretation of the western part of the Shuksan blueschist terrane, northwestern Washington: Geological Society of America Bulletin, v. 100, p. 1415–1422.

Harper, G.D., Miller, R.B., MacDonald, J.H. Jr., Miller, J.S., and Mlinarevic, A.N., 2003, Evolution of a polygenetic ophiolite: The Jurassic Ingalls ophiolite, Washington Cascades, *in* Swanson, T.W., ed., Western Cordillera and adjacent areas: Geological Society of America Field Guide 4, p. 251–265.

Haugerud, R.A., Morrison, M.L., and Brown, E.H., 1981, Structural and metamorphic history of the Shuksan Metamorphic Suite in the Mount Watson and Gee Point areas, North Cascades, Washington: Geological Society of America Bulletin, v. 92, p. 374–383.

Hawthorne, F.C., and Oberti, R., 2007, Classification of the amphiboles: Reviews in Mineralogy and Geochemistry, v. 67, p. 55–88.

Hawthorne, F.C., Oberti, R., Harlow, G.E., Maresch, W.V., Martin, R.F., Schumacher, J.C., and Welch, M.D., 2012, Nomenclature of the amphibole supergroup: The American Mineralogist, v. 97, p. 2031–2048.

Lofgren, D.C., 1974, The bedrock geology of the southwestern part of the Kachess Lake quadrangle, Washington: M.S. thesis, Portland, Ore., Portland State University, 73 p.

MacDonald, J.H. Jr., and Dragovich, J.D., 2015, Sedimentary geochemistry of the Peshastin Formation and Darrington Phyllite, Cascade Mountains, Washington State: Provenance, tectonic setting, and regional implications, *in* Anderson, T.H., Didenko, A.N., Johnson, C.L., Khanchuk, A.I., and MacDonald, J.H. Jr., eds., Late Jurassic Margin of Laurasia—A record of faulting accommodating plate rotation: Geological Society of America Special Paper 513, p. 441–460.

MacDonald, J.H. Jr., and Pecha, M., 2011, Preliminary geochronology and geochemistry of the Hicks Butte complex, central Cascades, Washington: Possible links between polygenetic Mesozoic arc rocks of the central Cascades and the Blue Mountains Province: Geological Society of America Abstracts with Programs, v. 43, no. 5, p. 647.

MacDonald, J.H. Jr., and, Schoonmaker, A., 2017, Evidence of a Late Jurassic ridge subduction event: Geochemistry and age of the Quartz Mountain stock, Manastash inlier, central Cascades, Washington: Journal of Geology, v. 125, p. 423–438.

MacDonald, J.H. Jr., Harper, G.D., Miller, R.B., Miller, J.S., Mlinarevic, A.N., and Schultz, C.E., 2008, The Ingalls ophiolite complex, central Cascades, Washington: Geochemistry, tectonic setting, and regional correlations, *in* Wright, J.E., and Shervais, J.W., eds., Ophiolites, arcs, and batholiths: A tribute to Cliff Hopson: Geological Society of America Special Paper 438, p. 133–159.

MacDonald, J.H. Jr., Davis, P.B., and, Pecha, M., 2019, Hicks Butte complex, central Cascades, Washington: A record of Late Jurassic island arc formation and subsequent Cretaceous adakite generation from arc root melting: Geological Society of America Abstracts with Programs, v. 51, no. 5, doi: 10.1130/abs/2019AM-340818.

Maruszczak, A.D., Thompson, G.T., Zalud, K.M., Stingu, S.C., Fernandez, C.R., Jaeger, B.C., Reed, G.J., and MacDonald, J.H. Jr., 2016, Mineralogy and metamorphism of Shuksan blueschist, Easton Metamorphic Suite, Kachess Lake inlier, central Cascades, Washington: Geological Society of America Abstracts with Programs, v. 48, no. 7, doi:10.1130/abs/2016AM-277240.

Mayes, B.M., Incorvaia, A., MacDonald, J.H. Jr., and, Davis, P.B., 2021, Investigating the mineralogy of symplectic gabbro from the Hicks Butte complex, central Cascades, Washington, supports a formation in an island arc setting: Geological Society of America Abstracts with Programs. v. 53, no. 6, doi: 10.1130/abs/2021AM-365481.

Miller, R.B., 1985, The ophiolitic Ingalls Complex, north-central Cascade Mountains, Washington: Geological Society of America Bulletin, v. 96, p. 27–42.

Miller, R.B., Mattinson, J.M., Funk, S.G., Hopson, C.A., and Treat, C.L., 1993, Tectonic evolution of Mesozoic rocks in the southern and central Washington Cascades, *in* Dunn, G., and McDougall, K., eds., Mesozoic paleogeography of the western United States II, Book 71: Pacific Section Society of Economic Paleontologists and Mineralogists, p. 81–98.

Miller, R.B., Bryant, K.I., Doran, B., Eddy, M.P., Raviola, F.P., Sylva, N., and Umhoefer, P.J., 2022, Eocene dike orientations across the Washington Cascades in response to a major strike-slip faulting episode and ridge-trench interaction: Geosphere, v. 18, no. X, p. 1–29.

Misch, P., 1966, Tectonic evolution of the northern Cascades of Washington State; a west-Cordilleran case history: Canadian Institute of Mining and Metallurgy, v. 8, Special issue of the Canadian Institute of Mining and Metallurgy, p. 101–148.

Ridolfi, F., Renzulli, A., and Puerini, M., 2010, Stability and chemical equilibrium of amphibole in calc-alkaline magmas: An overview, new thermobarometric formulations and application to subduction-related volcanoes: Contributions to Mineralogy and Petrology, v. 160, p. 45–66.

Saleeby, J.B., 1992, Petrotectonic and paleogeographic settings of the U.S. Cordilleran ophiolites, *in* Burchfiel, B.C., Lipman, P.W., and Zoback, M.L., eds., The Cordilleran Orogen: Conterminous U.S.: Boulder, Colo., Geological Society of America, Geology of North America, v. G-3, p. 653–683.

Saleeby, J.B., and Busby-Spera, X., 1992, Early Mesozoic tectonic evolution of the western U.S. Cordillera, *in* Burchfiel, B.C., Lipman, P. W., and Zoback, M.L., eds., The Cordilleran Orogen (Geology of North America, Vol. G-3): Boulder, Colo., Geological Society of America, p. 107–168.

Sauer, K.B., Gordon, S.M., Miller, R.B., Vervoort, J.D., and Fisher, C.M., 2017, Evolution of the Jura-Cretaceous North American Cordillera margin: Insights from detrital-zircon U-Pb and Hf isotopes of sedimentary units of the North Cascade Range, Washington: Geosphere, v. 13, p. 2094–2118.

Schumacher, J.C., 2007, Metamorphic amphiboles: Composition and coexistence: Reviews in Mineralogy and Geochemistry, v. 67, p. 359–416.

Smith, G.O., 1904, Description of the Mount Stuart quadrangle: U.S. Geological Survey Atlas, Mount Stuart folio, no. 106, 10 p.

Smith, G.O., and Calkins, F.C., 1906, Description of the Snoqualmie quadrangle, Washington: U. S. Geological Survey Geological Atlas Folio, GF-0139, 14 p.

Stern, R.J., 2002, Subduction zones: Reviews of Geophysics, v. 40, doi: 10.1029/2001RG000108.

Stingu, S.C., MacDonald, J.H. Jr., and Pecha, M., 2015, Geochemistry of the Hicks Butte complex, central Cascades, Washington: Remnants of a Late Jurassic volcanic island arc with intruding early Cretaceous adakites: Geological Society of America Abstracts with Programs, v. 47, no. 7, p. 530.

Stout, M.L., 1964, Geology of a part of the south-central Cascade Mountains, Washington: Geological Society of America Bulletin, v. 75, p. 317–334.

Tabor, R.W., and Haugerud, R.A., 2016, Geology of the North Cascades, *in* Cheney, E.S., ed., The Geology of Washington and Beyond: From Laurentia to Cascadia: University of Washington Press, Seattle, p. 131–155.

Tabor, R.W., Frizzell, V.A. Jr., Vance, J.A., and Naeser, C.W., 1984, Ages and stratigraphy of lower and middle Tertiary sedimentary and volcanic rocks of the Central Cascades, Washington: Applications to the tectonic history of the Straight Creek fault: Geological Society of America Bulletin, v. 95, p. 26–44.

Tabor, R.W., Frizzell, V.A. Jr., Booth, D.B., Waitt, R.B., Whetten, J.T., and Zartman, R.E., 1993, Geologic map of the Skykomish 60′ × 30′ quadrangle, Washington: U.S. Geological Survey Miscellaneous Investigations Map I-1963, scale 1:100,000, 42 p.

Tabor, R.W., Frizzell, V.A. Jr., Booth, D.B., and Waitt, R.B., 2000, Geologic map of the Snoqualmie Pass

30 × 60-minute quadrangle, Washington: U.S. Geological Survey Geologic Investigations Map MI-2538, scale 1:100,000, 1 sheet, 57 p.

Treat, C.H., 1987, Metamorphic and structural history of the Hicks Butte inlier south-central Cascades, Washington: M.S. thesis, San Jose State University, San Jose, Calif., 93 p.

Wyld, S.J., Umhoefer, P., and Wright, J.E., 2006, Reconstructing northern Cordilleran terranes along known Cretaceous and Cenozoic strike-slip faults: Implications for the Baja B.C. hypothesis and other models, *in* Monger, J., Enkin, R., and Haggert, J., eds., Paleogeography of the North American Cordillera: Evidence for and against large-scale displacements: Geological Association of Canada Special Paper, v. 46, p. 277–298.